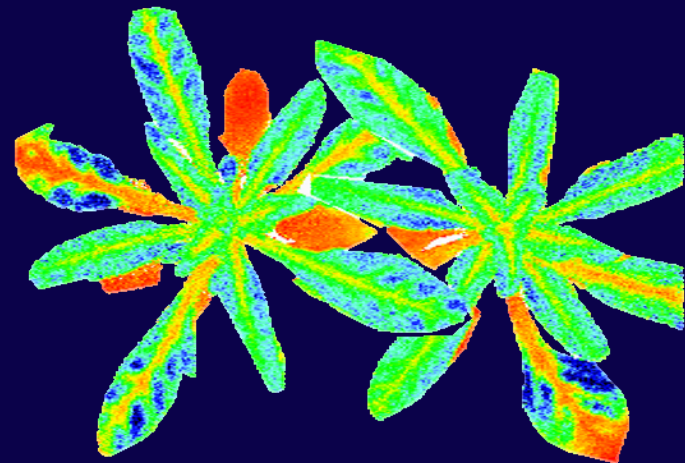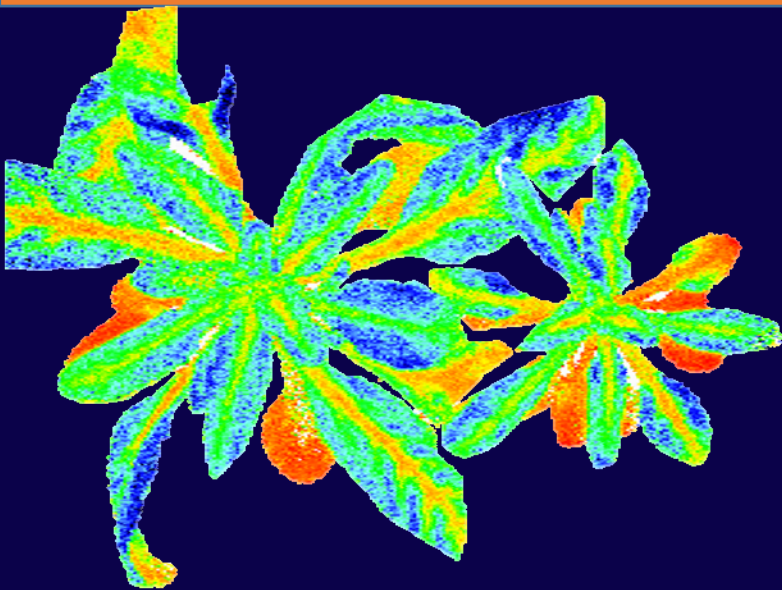# *Arabidopsis thaliana* COPT transporters function in hormone metabolism and in metal stress.

TESIS DOCTORAL
Presentada por:
Àngela Carrió Seguí

Abril 2017

Dirigida por:
Lola Peñarrubia Blasco

VNIVERSITAT DE VALÈNCIA

DEPARTAMENTO DE BIOQUÍMICA Y BIOLOGÍA MOLECULAR

Programa Oficial de Postgrado en Biotecnología

Arabidopsis thaliana COPT transporters function in hormone metabolism and in metal stress.

Memoria presentada por

Àngela Carrió Seguí

Para optar al título de Doctora por la Universidad de Valencia

Directora: Lola Peñarrubia Blasco

Burjassot, 5 abril del 2017

LOLA PEÑARRUBIA BLASCO, Doctora en Ciencias Biológicas y Catedrática de Universidad del Departamento de Bioquímica y Biología Molecular de la Universitat de València,

CERTIFICA: que la Licenciada en Biología ÀNGELA CARRIÓ SEGUÍ ha realizado, bajo su dirección y en el Laboratorio de Plantas del mencionado departamento, el trabajo titulado "*ARABIDOPSIS THALIANA* COPT TRANSPORTERS FUNCTION IN HORMONE METABOLISM AND IN METAL STRESS."

Y para que así conste, firmo la presente.

Fdo. Lola Peñarrubia Blasco

"Como no estás experimentado en las cosas de este mundo, todas las cosas te parecen imposibles; confía en el tiempo que suele dar dulces salidas a muchas amargas dificultades"

Don Quijote de la Mancha

Miguel de Cervantes

AGRADECIMIENTOS

RESUMEN

La homeostasis del cobre (Cu) es necesaria para que los organismos vivos mantengan las funciones celulares esenciales. En esta tesis utilizamos la planta modelo *Arabidopsis thaliana* como sistema de estudio para obtener información sobre el papel del transporte de Cu^+ en diversos procesos hormonales y relacionados con otros metales.

En *Arabidopsis*, el transporte de Cu^+ se realiza mediante una familia de transportadores de alta afinidad, conocidos como COPTs. Esta familia está integrada por 6 miembros que se agrupan según su localización subcelular. Por una parte, los transportadores COPT1, COPT2 y COPT6 se localizan en la membrana plasmática (pmCOPT), mientras que los transportadores COPT3 y COPT5 están localizados en membranas internas (imCOPT). A nivel funcional, los pmCOPT transportan el Cu^+ desde el espacio extracelular al citosol. Una vez el Cu entra en el citosol, se une a las chaperonas que lo distribuyen a las diferentes proteínas diana que necesitan el Cu como cofactor para poder realizar su función. Los transportadores pmCOPT son regulados a nivel transcripcional por el factor de transcripción SPL7 (SQUAMOSA Binding Protein-Like 7). En deficiencia de Cu, SPL7 se une a los elementos reguladores GTAC de los promotores de los genes de los pmCOPT induciendo su expresión. De los tres transportadores, *COPT2* es el miembro que tiene una mayor inducción en deficiencia de Cu y, en este sentido, se puede utilizar como marcador molecular de la deficiencia de este metal. Por otro lado, los transportadores imCOPT funcionan en el tráfico de Cu intracelular, adquiriendo mayor relevancia en las condiciones de deficiencia del metal prolongada en el tiempo. De este grupo, COPT5 es el miembro del que se tiene más información. Este transportador se localiza en la membrana del tonoplasto y su función es transportar el Cu^+ desde el lumen vacuolar hacia el citosol. Los imCOPT no están regulados por SPL7, ya que no tienen elementos GTAC en sus promotores y, por lo tanto, sus niveles de expresión no responden a la deficiencia de Cu. Así pues, en esta tesis nos hemos centrado en el estudio de la homeostasis del Cu a través de los mutantes *copt2* y *copt5*. Estos mutantes nos han servido como herramienta para caracterizar otros procesos biológicos que pueden estar potencialmente afectados como consecuencia de un transporte de Cu alterado.

El papel del Cu en la biosíntesis y señalización hormonal es bien conocido, siendo necesario para producir ácido abscísico (ABA) a través de la formación del cofactor de molibdeno (MoCo) y para la señalización del etileno, ya que el Cu forma parte estructural de los receptores de esta hormona. Como primera aproximación sobre la posible regulación hormonal del transporte de Cu, se realizó un estudio *in silico* de los elementos reguladores en *cis* presentes en los promotores de los genes de la familia *COPT* relacionados con hormonas. Como resultado, un total de 159 elementos reguladores fueron identificados, estando los elementos relacionados con ABA entre los más representados. Por lo tanto, uno de los objetivos planteados en esta tesis es la caracterización de

la interacción entre el transporte de Cu y el metabolismo de ABA. En primer lugar, nos planteamos estudiar el efecto de la alteración del transporte de Cu en el metabolismo de ABA. Para ello, se utilizaron los mutantes *copt2*, *copt1copt2copt6* y *COPT1^{oe}* que tienen el transporte de Cu alterado. Sobre ellos se realizó un análisis a nivel fisiológico, bioquímico y molecular del efecto del tratamiento con ABA en diferentes condiciones de Cu: deficiencia, suficiencia y exceso. Como medidas fisiológicas se utilizaron, tanto la longitud de la raíz de plántulas de 7 días, como la tasa de germinación en verde (que determina el establecimiento de la planta), para evaluar la respuesta al tratamiento de ABA en los diferentes mutantes. Mediante el análisis de estas medidas fisiológicas, observamos una mayor sensibilidad de los mutantes *copt2* y *copt1copt2copt6* respecto, a *COPT1^{oe}* y el silvestre, al tratamiento de ABA en todas la condiciones de Cu. Sin embargo, la respuesta de los mutantes al tratamiento fue menor en deficiencia de Cu. Este resultado puso de manifiesto que el estado nutricional del Cu puede afectar a la respuesta del tratamiento con ABA. A nivel bioquímico, se cuantificó mediante HPLC (cromatografía líquida de alta resolución) el contenido de ABA de los diferentes genotipos en condiciones de deficiencia, suficiencia y exceso de Cu. El contenido de ABA en el silvestre fue menor en deficiencia y exceso que en suficiencia de Cu. Los diferentes mutantes no mostraron diferencias en el contenido de ABA en deficiencia del metal. Sin embargo, en la condición de suficiencia, *copt2* y *copt1copt2copt6* tuvieron un contenido menor de la hormona respecto al silvestre. Complementariamente, se midió la cantidad de Cu en los cuatro genotipos por ICP-MS (espectrometría de masas por plasma de acoplamiento inductivo). El fin de esta medida es saber si el tratamiento de ABA afecta a la incorporación del metal. En condiciones de suficiencia, el contenido de Cu en el silvestre y *COPT1^{oe}* disminuyó cuando fueron tratadas con ABA. Sin embargo, en los otros mutantes, a pesar de tener un menor contenido del metal, éste no varió con el tratamiento de ABA. Ante estos resultados, se decidió proceder al análisis molecular de la expresión génica mediante qRT-PCR (PCR cuantitativa a tiempo real) para esclarecer si existe regulación por ABA de los *pmCOPTs.* Por otro lado, se realizó un análisis de genes relacionados con la homeostasis de ABA en los mutantes *copt2* y *COPT1^{oe}*, con el objetivo de estudiar cómo afecta la alteración del transporte del metal a la hormona. La inducción de la expresión de genes de biosíntesis de la hormona, tanto en condiciones de deficiencia como de suficiencia de Cu fue mayor en los mutantes que en el silvestre cuando se les añadió ABA. No obstante, en deficiencia de Cu los niveles de expresión fueron inferiores en los mutantes respecto del silvestre. Además, se analizó la expresión de genes de señalización de ABA, expresándose de manera diferente según el mutante y se correspondió con el fenotipo observado en el estudio fisiológico.

En segundo lugar, dentro del objetivo inicial, realizamos un estudio molecular y bioquímico de cómo el tratamiento con ABA puede afectar a la homeostasis del Cu. Inicialmente, se realizó un estudio *in silico* de los promotores de un set de genes relacionados con la homeostasis del Cu

(*COPT1*, *COPT2*, *COPT6*, *ZIP2*, *YSL2*, *SPL7* y *HY5*) y del ABA (*NCDE3*, *WRKY40* y *ABI5*) para localizar la posición de estos elementos reguladores en dichos promotores. Este análisis nos permitió determinar la posición relativa de los elementos reguladores del Cu y del ABA en el promotor, y si puede existir competencia de los factores de transcripción para unirse al DNA y regular su expresión. Seguidamente, se utilizó el mutante de perdida de función del factor de transcripción SPL7 (*spl7*) para averiguar si la respuesta al tratamiento con la hormona era debida o no a una posible competencia de los diferentes factores de transcripción. Se analizó la respuesta transcripcional al tratamiento con ABA de genes relacionados con la homeostasis del Cu en el mutante *spl7*. Los niveles de expresión de los genes de respuesta a deficiencia de Cu fueron estudiados tanto en deficiencia como en suficiencia del metal, tratados o no con ABA. En condiciones de suficiencia, los niveles de expresión de dichos genes fueron reprimidos en el silvestre y en *spl7* cuando fueron tratados con ABA. Sin embargo, en deficiencia de Cu no se apreció represión de los niveles de expresión.

Por otro lado, se utilizaron plantas *pCOPT2::GUS* y *pCOPT2::LUC* para analizar los efectos del ABA a nivel de localización tisular y de la oscilación temporal de expresión de *COPT2*, respectivamente. El tratamiento con ABA mostró un cambio en el patrón de expresión de *COPT2* en la raíz, mientras que este tratamiento no tuvo ningún efecto sobre la oscilación de la expresión.

En tercer lugar, para completar el estudio de la interacción entre ABA y Cu nos planteamos analizar los efectos de la disponibilidad del Cu sobre el metabolismo de ABA. Para ello, se utilizaron los mutantes *aba2* y *hab1-1abi1-2*, que tienen alterada la biosíntesis y la señalización del ABA, respectivamente. Fueron caracterizados a nivel fisiológico, bioquímico y molecular, para analizar su respuesta a las diferentes condiciones de Cu. Estos mutantes crecieron con o sin ABA en los medios con deficiencia, suficiencia y exceso de Cu. Mediante un estudio de la longitud de la raíz se observó que, dependiendo de la condición de Cu, los mutantes respondieron a la presencia de ABA en el medio. De hecho, el mutante de señalización de ABA fue hipersensible al ABA cuando había Cu en el medio. A continuación, se midió el contenido de Cu en estos mutantes observando que, en exceso del metal, sin presencia de ABA, tenían un mayor contenido de Cu que el silvestre. Estos resultados nos indicaron que la disponibilidad de Cu afectaba las respuestas de ABA. Por consiguiente, realizamos un estudio molecular para saber si había cambios en la expresión de los genes relacionados con la homeostasis del Cu en los mutantes *aba2* y *hab1-1abi1-2*. En condición de deficiencia de Cu, ambos mutantes tuvieron niveles más altos de expresión de los genes que el silvestre. Estos genes tuvieron niveles de expresión más bajos en suficiencia y exceso de Cu. Sin embargo, en presencia de ABA, la expresión de los genes cambió según el gen y la condición de Cu. Estos resultados nos indicaron que estamos en un escenario complejo donde el estado

nutricional de Cu afecta al ABA a múltiples niveles y, por otro lado, alteraciones en la señalización de la hormona generan cambios en la homeostasis del Cu.

El cadmio (Cd) es un metal de transición presente en la corteza terrestre. Este metal no tiene función biológica conocida y es considerado tóxico para los seres vivos. El principal efecto tóxico del Cd es debido a su capacidad para interferir en la homeostasis de otros metales esenciales. Las plantas expuestas a este metal muestran síntomas de toxicidad a nivel de la raíz, donde es secuestrado en las vacuolas. El transporte a través del xilema está limitado en muchas plantas, por lo que tiende a acumularse en raíces. Además, la toxicidad del Cd va asociada a alteraciones en la entrada de macro y micronutrientes, ya que compite con otros metales en los sitios de unión a proteínas y transportadores. El estudio de la toxicidad del Cd asociada a deficiencias nutricionales es de interés biotecnológico, ya que permitirá buscar herramientas para la biofortificación de alimentos en suelos potencialmente contaminados por este metal. Por lo tanto, uno de los objetivos planteados en esta tesis ha sido el estudio del efecto de la toxicidad del Cd en la homeostasis del Cu. Específicamente, se ha realizado una aproximación fisiológica, bioquímica y molecular de la respuesta del mutante *copt5* a la presencia de Cd en el medio. En primer lugar, se analizó el efecto del Cd en plántulas de 7 días. Una de las medidas utilizadas para observar la sensibilidad de las plántulas al tratamiento, fue el crecimiento de la raíz. Estudios previos, realizados en nuestro grupo de investigación, indicaron que el mutante *copt5* era muy sensible al Cd en medio con severa deficiencia de Cu, tras la adición de un quelante de Cu al medio de crecimiento. Así pues, nos planteamos estudiar la sensibilidad de *copt5* al Cd en unos niveles de Cu menos severos. Por lo tanto, los experimentos fueron llevados a cabo en medio ½ MS, considerado un medio ligeramente deficiente en Cu. Se testaron diferentes concentraciones de Cd en medio ½ MS con el objetivo de encontrar la mínima cantidad de Cd (CdCl$_2$ 30 μM) a la que el mutante muestra sensibilidad, evitando así el efecto tóxico en las plantas. Establecidas las condiciones experimentales, decidimos estudiar si la causa de la sensibilidad del mutante al Cd estaba relacionada con una posible interacción con el Cu. Para ello, las plántulas crecieron en medio ½ MS, al que se le añadió 1 μM de Cu para tener unas condiciones de suficiencia del metal. Entre las condiciones de leve deficiencia de Cu y suficiencia no hubo diferencias de crecimiento entre el mutante y el silvestre. Sin embargo, cuando las plantas crecieron en estos dos medios a los que se les añadió 30 μM de Cd, se observaron diferencias. En la condición de deficiencia de Cu, *copt5* fue más sensible que el silvestre al tratamiento de Cd. Sin embargo, en la condición de suficiencia de Cu, la sensibilidad del mutante al tratamiento fue menor que en la condición anteriormente mencionada. Este mismo experimento fue repetido pero añadiendo al medio Fe en lugar de Cu, para comprobar si el efecto observado era debido al Cu y no a otros factores. Dado que la sensibilidad de *copt5* al tratamiento con Cd no se vio disminuida con el suplemento de Fe, y si con el Cu, este resultado confirmó que la sensibilidad del mutante al Cd está relacionado con

la homeostasis del Cu. Una vez establecida esta relación, analizamos todos los mutantes COPTs disponibles en el laboratorio, para averiguar si esta sensibilidad era específica de la ausencia del transportador COPT5. Los mutantes *copt1*, *copt2* y *copt6* se crecieron en medio ½ MS con 30 µM de Cd y respondieron al tratamiento de la misma manera que el silvestre. Por lo tanto, este resultado indicó que el transportador vacuolar COPT5 tiene un papel específico en la tolerancia al Cd.

Como ya hemos comentado previamente, el Cu es necesario para la señalización del etileno, hormona implicada en respuestas de estrés por metales en plantas. Con esta premisa, nos planteamos la posibilidad de que el etileno estuviese mediando la respuesta de *copt5* al tratamiento con Cd. Así pues, analizamos el efecto del tratamiento en plántulas etioladas de *copt5*, ya que el etileno promueve el acortamiento del hipocótilo. Las plántulas crecieron en medios de deficiencia y suficiencia de Cu, mencionadas en el párrafo anterior, tratadas o no con Cd en condiciones de oscuridad continua. A los 7 días, se midió la longitud del hipocótilo y de la raíz de las plántulas en las cuatro condiciones. El tratamiento con Cd afectó a la longitud de los hipocótilos, tanto en suficiencia como en deficiencia de Cu. Además, no se observaron diferencias entre el mutante y el silvestre. Sin embargo, la longitud de la raíz de las plántulas *copt5* etioladas respondieron al tratamiento con Cd en deficiencia de Cu. De hecho, el efecto del tratamiento con Cu, mostrado a través de la longitud de la raíz de *copt5*, fue mayor en plántulas etioladas que en plántulas crecidas con ciclos de luz/oscuridad. Estos resultados nos llevaron a analizar los efectos del tratamiento de Cd sobre la percepción de etileno. Para llevar a cabo este estudio, las plantas crecieron en condiciones de oscuridad en recipientes de cristal que contenían los diferentes medios de crecimiento (½ MS ± Cd), los cuales permanecieron cerrados herméticamente durante 7 días. Se inyectó 1ml/l de etileno en los recipientes, donde después se analizaron los efectos del medio de crecimiento sobre la percepción de la hormona. El efecto del tratamiento de Cd sobre la longitud de los hipocótilos fue mayor en *copt5* que en el silvestre, incluso en presencia de etileno. Estos resultados nos indicaron que *copt5* tiene la percepción de etileno exacerbada en presencia de Cd.

El estudio del efecto del Cd se abordó también a nivel molecular. A través de un análisis de expresión génica mediante qRT-PCR, se analizó la expresión de *COPT1*, *COPT2* Y *COPT5* en plantas silvestres tratadas con Cd. Como hemos comentado previamente, *COPT1* y *COPT2* responden a la deficiencia de Cu, mientras que *COPT5* no lo hace. Cuando se analizó su expresión en presencia de Cd, *COPT5* no varió mientras que la de *COPT2* se redujo y la de *COPT1* se mantuvo respecto de la misma condición sin Cd. Ante estos resultados, decidimos analizar otra diana regulada por la deficiencia de Cu, como es la *FSD1*. En condiciones de deficiencia de Cu, el mutante *copt5* tuvo unos niveles de expresión de este gen más bajos que el silvestre. El tratamiento con Cd en

deficiencia de Cu, disminuyó la expresión del gen tanto en el silvestre como en *copt5*. No obstante, la expresión de la *FSD1* en el mutante siguió siendo menor que el silvestre. Por otro lado, también se analizó la expresión de la *CSD1*, ya que su expresión está regulada a nivel postranscripcional por el *MIR398*. En deficiencia de Cu, los niveles de expresión de la *CSD1* fueron menores que en el silvestre. En la condición de deficiencia de Cu, con tratamiento de Cd, a pesar de que se mantuvo esa diferencia de expresión, los niveles del gen aumentaron en ambos genotipos. Además, añadimos el análisis de expresión del gen *RBOHD*, que fue usado como control de la generación de ROS en niveles tóxicos de Cd. En condiciones de deficiencia, el silvestre tuvo la mitad del nivel de expresión del gen respecto a la condición de suficiencia de Cu. El mismo efecto fue observado en las condiciones con Cd en el medio, donde los niveles de expresión del gen fueron mayores en suficiencia que en deficiencia de Cu. Por otro lado, la expresión de este gen en el mutante *copt5*, permaneció más o menos constante en las cuatro condiciones ensayadas. La expresión de estos tres genes se analizó en el mutante *spl7* para averiguar si las respuestas alteradas de la deficiencia de Cu están reguladas o no por SPL7. La expresión de la *FSD1* en presencia de Cd disminuyó y la *CSD1* se indujo en el mutante *spl7*. Como contrapunto, la expresión del gen *RBOHD* en *spl7* respondió al tratamiento de Cd aumentando su expresión en suficiencia de Cu. Sin embargo, sus niveles no variaron en deficiencia de Cu, pese a la presencia o ausencia de Cd.

Atendiendo a que los efectos del Cd sobre el mutante *copt5* se pusieron de manifiesto afectando preferencialmente a la raíz frente a la parte aérea de la planta, nos planteamos estudiar los distintos efectos del Cd en raíces y parte aérea. Para ello, las plantas crecieron en medios hidropónicos durante 31 días en una solución de riego Hoagland modificada. Se eliminó el Cu de la solución para generar la condición de deficiencia del metal. Una vez completado el periodo de crecimiento, las plantas fueron tratadas durante 16 días con la misma solución de riego pero adicionando concentraciones crecientes Cd al medio para cultivos independientes. Al final de los 16 días de tratamiento, se midió la tasa absoluta de crecimiento de la raíz y la parte aérea por separado. La raíz fue sensible a la presencia de Cd en el medio, siendo un 16% más pequeña en el mutante frente a su control. El peso fresco de la parte aérea disminuyó a medida que aumentó la concentración de Cd en el medio. Sólo se observaron diferencias significativas entre el mutante y el silvestre en la condición de 5 µM de Cd. Para investigar el papel del COPT5 en la translocación de Cd desde las raíces a la parte aérea, se utilizó la medida de la peroxidación lipídica, a través del contenido de MDA, como parámetro indirecto del estrés oxidativo generado por el transporte de Cd. Los valores de MDA en las hojas de plantas silvestres aumentaron con el tratamiento de Cd, mientras que en plantas mutantes estos valores permanecieron constantes. El contenido en las raíces de plantas silvestres no mostró cambios por el tratamiento con Cd. Sin embargo *copt5* mostró un aumento del contenido de MDA en plantas tratadas con Cd. Así pues, el patrón de peroxidación lipídica en plantas silvestres y mutantes en presencia de Cd fue opuesto. Como el

mayor contenido de MDA en el mutante se localizó en la raíz, se decidió estudiar el daño oxidativo a nivel histológico. Para ello, se realizaron secciones transversales a partir de raíces obtenidas en cultivos hidropónicos, tanto en presencia como en ausencia de Cd en el medio. Estas secciones histológicas fueron teñidas con el colorante azul de toluidina, que permite la obtención de una tinción metacromática atendiendo a las diferentes reacciones que el colorante experimenta según la composición de paredes y membranas celulares, así como el contenido citoplasmático. Mediante el uso de esta técnica, fue posible observar que los haces vasculares de las raíces del mutante *copt5* tratadas con Cd están más afectados que los del silvestre. De manera complementaria, la separación de parte aérea y radicular en cultivos hidropónicos permitió el análisis del contenido de metales. El Cd y el Cu fueron medidos mediante ICP-MS, mostrando de nuevo diferencias de contenido entre la raíz y la parte aérea. El contenido de Cd se midió en plantas crecidas, tanto en deficiencia como en suficiencia de Cu. En raíces, el contenido de Cd se mantuvo en niveles similares en las dos condiciones de Cu, no habiendo diferencias entre el silvestre y *copt5*. Por otro lado, en la parte aérea, el contenido de Cd era mayor en las plantas crecidas en suficiencia de Cu y, además, el mutante mostró en ambos casos un menor contenido del metal en comparación con el silvestre.

En plántulas de 7 días se analizaron los efectos del Cd en la percepción de etileno. El cultivo de plantas en medio hidropónico nos permitió realizar medidas de emisión de etileno mediante cromatografía de gases. Las plantas fueron transferidas del cultivo hidropónico a botes de cristal que contenían 2 ml de la misma solución de riego en la que habían crecido. Se cerró herméticamente el bote y después de 24 horas en oscuridad se tomaron las medidas de etileno. Como resultado, obtuvimos que la condición de Cu afecta a la emisión de etileno, siendo menor en deficiencia del metal. Por otro lado, en las plantas tratadas con Cd la emisión de la hormona fue menor y no respondía a la disponibilidad de Cu en el medio. Además, en condiciones de deficiencia de Cu, *copt5* tuvo valores de emisión de etileno menores que el silvestre y cuando se trató con Cd, estos valores aún fueron menores. Por lo tanto, el tratamiento con Cd en *copt5* afectó de manera negativa a la biosíntesis de etileno y, al mismo tiempo, incrementó la percepción de la hormona. Estos resultados aportaron nueva información sobre el efecto del Cd sobre el metabolismo del etileno en plantas con la homeostasis del Cu alterada.

La homeostasis del Cu es necesaria para el metabolismo del hierro (Fe) en mamíferos. Estudios previos en nuestro laboratorio, establecieron una relación entre las homeostasis del Cu y del Fe en *Arabidopsis*, mediante el estudio del transportador COPT2, que muestra mayor resistencia a la clorosis férrica. Continuando con la caracterización de la interacción Cu-Fe, en esta tesis hemos analizado el mutante *copt5* con el objetivo de caracterizar el papel funcional del transportador en el metabolismo del Fe. En primer lugar, se realizó un estudio transcriptómico mediante

micromatrices de DNA, con el fin de detectar procesos diferenciales entre el mutante *copt5* y las plantas silvestres crecidas en condiciones de deficiencia y suficiencia de Cu. Un análisis de agrupaciones jerárquicas dividió los genes en 8 patrones de expresión. Entre los patrones, observamos que los procesos biológicos relacionados con la unión a Fe estaban presentes en 3 de los 8 patrones. A partir de estos datos, analizamos la respuesta de *copt5* a la deficiencia de Fe. Mediante la medida fisiológica de la longitud de la raíz de *copt5*, crecido en diferentes medios con combinaciones de Cu y Fe que iban desde la deficiencia hasta la suficiencia de los metales, se observó que el mutante era más sensible que las plántulas silvestres a la deficiencia de Fe. Seguidamente, se planteó el análisis bioquímico de esta sensibilidad de *copt5* a la deficiencia de Fe. Este estudio se llevó a cabo mediante un ensayo GUS, usando plantas *pCOPT5::GUS* que crecieron en condiciones control, de deficiencia de Cu y de deficiencia de Fe. Como resultado a destacar, la localización del transportador en la raíz desapareció en la condición de deficiencia de Fe. Ante este sorprendente resultado, analizamos los niveles de expresión de *COPT5* en plantas silvestres crecidas en las mismas condiciones utilizadas en el ensayo GUS. La expresión de *COPT5* no se modificó por la presencia o ausencia de Cu. Sin embargo, en deficiencia de Fe, la expresión del transportador disminuyó a la mitad respecto del control, confirmando los datos obtenidos previamente en el ensayo GUS, indicando una posible regulación del transportador por Fe. Entonces, estudiamos la expresión de factores de transcripción relacionados con el Fe (*FIT*, *bHLH38*, *bHLH39*, *BRUTUS*, *bHLH100*, *bHLH101*) en el mutante *copt5.* Estos genes fueron estudiados en condiciones control, de deficiencia de Cu y de deficiencia de Fe. En condiciones de deficiencia de Cu, todos estos genes estaban inducidos en el mutante *copt5*, excepto *FIT*. Por otro lado, en deficiencia de Fe, la expresión de los factores de transcripción disminuyó en *copt5*. Solo *FIT* y *bHLH38* estuvieron inducidos. Estos resultados nos indicaron que COPT5 puede interferir en la señalización por Fe. Poniendo en común estos datos y los obtenidos en el análisis de micromatrices, podemos concluir que la homeostasis del Fe en *copt5* está alterada cuando es sometido a deficiencia de Cu. Por lo tanto, para entender mejor estos resultados, realizamos un estudio bioquímico en más profundidad. Mediante MP-AES (espectroscopía de microondas de emisión de plasma atómico), se midió el contenido de Cu y Fe en semillas y cotiledones de plantas crecidas en condiciones control y de deficiencia de Cu. Como era de esperar según la bibliografía, el contenido de Cu en semillas de *copt5* fue menor que en el silvestre en ambas condiciones. Sin embargo, el contenido de Fe en esas mismas semillas fue ligeramente mayor en el mutante. Además, el contenido de Cu en cotiledones de plántulas de 7 días, crecidas en deficiencia de Cu, fue menor en *copt5*, mientras que el contenido de Fe fue mayor frente al silvestre. Estos resultados nos indicaron que, pese a ser más sensible a la deficiencia de Fe, *copt5* mostró un mayor contenido en este metal. A continuación, se realizó la tinción de Perls/DAB, que permite visualizar la localización del Fe en la planta, dándole una coloración negra a las acumulaciones del

metal. Esta tinción se realizó en plántulas de 3 días, donde el mutante *copt5* no tenía apenas Fe en los cotiledones respecto al silvestre. Este resultado, junto con el contenido de Fe, nos indicó que *copt5*, a pesar de tener más Fe en las semillas, se moviliza más rápido, debido a problemas en la señalización de Fe. Por lo tanto, en plántulas de 7 días, la respuesta a deficiencia de Fe estaba exacerbada. Prueba de ello fue que la expresión del transportador de Fe, *NRAMP4* localizado en la vacuola, se indujo en *copt5* en condiciones de deficiencia de Cu.

Otro aspecto a considerar en este estudio sobre la interacción Cu-Fe, fue la sustitución metálica que tiene lugar, principalmente, en el cloroplasto, a través de las superóxido dismutasas del Cu (Cu/ZnSOD) y del Fe (FeSOD). Por lo tanto, analizamos la sustitución metálica en *copt5* a nivel molecular y bioquímico en condiciones control, en deficiencia de Cu y en deficiencia de Fe. Se analizó la expresión de los genes *FSD1* y *CSD2* que codifican para la FeSOD y la Cu/ZnSOD cloroplásticas, respectivamente. En condiciones control, *copt5* tuvo niveles de expresión de la *CSD2* más bajos que el silvestre, mientras que no hubo diferencias de expresión en deficiencia de Fe. Por otro lado, en deficiencia de Cu, *copt5* no fue capaz de inducir la expresión de la *FSD1* a los niveles del silvestre. Estos resultados nos indicaron que *copt5* podría tener problemas en la actividad SOD, y por lo tanto, realizamos geles de actividad enzimática SOD. Efectivamente, los geles de actividad revelaron el mismo resultado que el análisis de expresión. No obstante, es evidente que *copt5* tiene problemas para llevar a cabo una correcta sustitución metálica.

Para finalizar este estudio, se abordó la relación Cu-Fe desde el punto de vista del Fe. Utilizamos el doble mutante *nramp3nramp4* como herramienta de estudio, para analizar los efectos de la deficiencia de Cu en un mutante que tiene el transporte de Fe vacuolar alterado. Este doble mutante resultó ser muy sensible a la deficiencia de Cu, con un fenotipo muy similar al mostrado ante la deficiencia de Fe. Se analizó la expresión de genes relacionados con la homeostasis del Cu y observamos que *COPT5* estaba sobreexpresado en el doble mutante, tanto en condiciones control como en deficiencia de Cu. Además, al igual que hicimos con *copt5*, analizamos la expresión y la actividad de las SODs. En condiciones control, *nramp3nramp4* tenía niveles más bajos de *FSD1* y *CSD2* que el silvestre. A nivel de actividad, nos llamó la atención que, en condiciones control, este doble mutante no tenía actividad Cu/ZnSOD. Estos resultados, junto con los obtenidos con el mutante *copt5*, pusieron de manifiesto que el transporte de ambos metales a nivel vacuolar es necesario para una correcta sustitución metálica.

Finalmente, tomando conjuntamente todos estos resultados obtenidos en los diferentes objetivos planteados en esta tesis, podemos decir que el estado nutricional del Cu en las plantas influye en muchos otros procesos biológicos que afectan al desarrollo normal. Además, dentro del transporte de Cu en la planta, podemos diferenciar dos niveles, uno centrado en la incorporación del metal a la célula, donde los transportadores pmCOPTs tienen un papel importante, y otro

involucrado en la redistribución interna del Cu, que es llevado a cabo por los imCOPT. Por lo tanto, en primer lugar, centrándonos en los resultados obtenidos en la tesis con respecto al transporte celular, podemos concluir que la presencia de elementos reguladores relacionados con hormonas en los promotores de los transportadores *COPT* indica una posible regulación hormonal del transporte de Cu. Además, los mutantes *copt2* y *copt2copt2copt6* son más sensibles al tratamiento con ABA exógeno que otros mutantes *copt*. Asimismo, la respuesta al tratamiento de ABA de *copt2* está atenuada en condiciones de deficiencia de Cu y este tratamiento hormonal modifica la localización del transportador en las raíces alterando el transporte de Cu. Por lo tanto, la regulación de las respuestas a deficiencia de Cu se ven afectadas por el tratamiento con ABA y, al mismo tiempo, la disponibilidad de Cu altera tanto la biosíntesis como la señalización de ABA. Por otro lado, los resultados obtenidos a partir del estudio del transporte del Cu desde la vacuola al citosol nos indican que es un punto clave para la distribución de otros metales. Así pues, podemos concluir que el desequilibrio en la distribución celular en *copt5* lo hace más sensible a la exposición de Cd. Además, el Cd altera la respuesta de la deficiencia de Cu mediada por SPL7 y la señalización del estrés oxidativo en *copt5*. En tratamientos prolongados con Cd, este metal afecta la biosíntesis de etileno en *copt5*. Sin embargo, en tratamientos cortos, la percepción de esta hormona en el mutante está exacerbada. COPT5 posiblemente tenga un papel en la tolerancia y translocación de Cd a lo largo de la planta. Continuando con *copt5*, en esta tesis hemos enfatizado que la localización del transportador de Cu es importante en la interacción entre el Cu y el Fe. El mutante *copt5* es sensible a la deficiencia de Fe, mientras que *copt2* es más resistente. Además, aportamos nueva información sobre la regulación transcripcional de *copt5* ya que, a pesar de no estar regulada por Cu, su expresión está reprimida por la deficiencia de Fe. Por otro lado, en condiciones de deficiencia de Cu, *copt5* tiene alterada la homeostasis del Fe. Las dianas de respuesta a deficiencia de Fe están inducidas y la localización de Fe a nivel tisular está alterada. Por lo tanto, una alteración en la removilización del Cu vacuolar afecta la homeostasis del Fe, poniendo de manifiesto la importancia del reciclado de metales para un correcto funcionamiento de los procesos dependientes de estos metales.

TABLE OF CONTENTS

LIST OF FIGURES AND TABLES

Chapter 3: The high affinity internal copper transporter COPT5 participates in iron mobilization in *Arabidopsis thaliana*.

TABLES

MATERIALS AND METHODS

Table M.1. Transgenic lines used in the present work.

Table M.2. Selected genes and primers used for PCR and qRT-PCR analyses.

RESULTS

Table P.1. Analysis of the putative hormone-responsive cis-elements in the COPTs promoters.

Table R.3.1. Biological processes overrepresented (FatiGo, P<0.05) in the DEG included in the Heatmap and Hierarchical Cluster Analysis.

Table R.3.2. Genes belonging to the Fe-related biological processes overrepresented (FatiGO, P<0.05) in the expression patterns described in the Hierarchical Cluster Analysis.

ANNEX

Table A.1. Overrepresented biological processes in the *copt5* microarray.

Table A.2. Genes belonging to the biological processes overrepresented (FatiGO, P<0.05) in the microarray previous Z score transformation.

ABBREVIATIONS

A. thaliana	*Arabidopsis thaliana*
a.u.	arbitrary units
AAO1	aldehyde oxidase1
ABA	abscisic acid
ABA3	ABA deficient 3
ABF	ABA-responsive element binding factor
ABI	ABA insensitive
ABRE	ABA-responsive element
ACC	1-aminocyclopropane-1-carboxylic acid
ACO	1-aminocyclopropane-1-carboxylic acid oxidase
ACS	1-aminocyclopropane-1-carboxylic acid synthase
AGR	absolute growth rate
AHA	*Arabidopsis* H^+-ATPase
ATX1	antioxidant 1
BCS	bathocuproinedisulfonic acid disodium
bHLH	basic helix-loop-helix type transcription factor
BTS	*BRUTUS*
bZIP	basic leucine zipper protein
C	control
CCH	copper chaperone
CCI	chlorophyll content index
CCS	cuprochaperone
cDNA	complementary DNA
Compl	complemented
COX	cytochrome c oxidase
CRT/COPT	copper transporter
Cu/ZnSOD	copper and zinc superoxide dismutase
CuRE	Cu-responsive element
DAB	3–3'-diaminobenzidine
DEG	differential expressed genes
dNTP	desoxinucleotide triphosphate
DPBF	Dc-3-promoter binding factor
DREB	dehydratation responsive element binding
DTT	dithiothreitol
DW	dry weight
EDTA	ethylenediaminetetraacetic acid
EIN	ethylene-insensitive protein
ER	endoplasmatic reticulum
ERF	ethylene responsive factor
ETRs	ethylene receptors
FC	fold change
FDR	false discovery rate
FeSOD	iron superoxide dismutase
FRO	plasma membrane ferric reductase oxidase
FW	fresh weight
GA	gibberellic acid

GARE	gibberellic acid response element
GCR	green cotyledon rate
GSH	glutathione
GUS	beta-glucuronidase
HMA5	heavy metal P-type ATPase
HY5	elongated hypocotyl 5
IAA	indol-3-acetic acid
IBMCP	instituto de biología molecular y celular de plantas
ICP-MS	inductively coupled plasma- mass spectrometry
imCOPT	intracelular membrane COPT transporter
INRA	institut national de la recherche agronomique
JA	jasmonic acid
KIN17	DNA/RNA-binding protein Kin 17
LAC	laccase
LDHC	light dark hot cold
LLHH	light light hot hot
LUC	luciferase
MCO	multicopper oxidase
MDA	malondialdehyde
MES	4-morpholin-ethano-sulphonic acid
miRNAs	microRNAs
MoCo	molibdenum cofactor
MOPS	3-morpholin-propaned-sulfuronic acid
MP-AES	microwave plasma-atomic emission spectroscopy
MS	Murashige and Skoog basal salt mixture
N.D.	no data
NA	nicotianamine
NBT	nitroblue tetrazolium
NRAMP	natural resistance-associated macrophage protein
PA	polyamine
PAA1	P-type ATPase
PC	plastocyanin
pmCOPT	plasma membrane COPT transporter
PP2C	protein phosphatase 2C
PPOs	chloroplastic poliphenol oxidases
PSI	photosystem I
qRT-PCR	quantitative (real-time) PCR
RAN1	response to antagonist 1
ROS	reactive oxygen species
RT	retrotranscriptase
RT-PCR	reverse transcription PCR
SD	standard deviation
SE	standard error
SA	salicylic acid
SAM	S-adenosylmethionine
SBP	SQUAMOSA-promoter binding protein
SCSIE	servicio central de soporte a la investigación experimental
SDS	sodium dodecyl sulphate

SnRK2	SNF1-related protein kinase 2
SOD	superoxide dismutase
SPL7	SQUAMOSA-promoter binding-like protein 7
TBS	Tris-buffer
TEMED	N, N,N',N'-tetrametilelylendiamine
TMD	transmembrane domain
UBQ	ubiquitin
VB	vascular bundle
VIT	vacuolar iron transporter
VRO	vacuolar-related organelle
WRKY	W-box
WT	wild type
YSL	yellow stripe-like transporter
ZIP	ZRT/IRT related protein

INTRODUCTION

1. BIOCHEMISTRY OF COPPER

1.1. The element copper

Mineral nutrition is an important environmental signal that regulates diverse developmental processes in plants. Both deficient and excess nutrient availability are considered abiotic stresses that can cause deleterious effects on both plant physiology and metabolism.

Copper (Cu) is the 29th element of the periodic table. Its electronic configuration is $3d^{10}4s^1$. Cuprous ion [Cu (I), Cu^+] has completely filled d-orbitals with 10 electrons ($3d^{10}$), whereas the cupric ion [Cu (II), Cu^{2+}] has only 9 electrons in the d-orbitals, ($3d^9$) with one electron being unpaired. Consequently, bivalent copper (Cu^{2+}) is paramagnetic and represents the most stable oxidation state of Cu (Valko *et al.*, 2005).

Cu belongs to the transition metals group which includes iron (Fe), zinc (Zn), cadmium (Cd), manganese (Mn) and molybdenum (Mo), among others. Cu forms part of the earth crust's composition and can be found in mineral form as sulphates ($CuFeS_2$, Cu_5FeS_4, CuS and Cu_2S), carbonates ($Cu_3(CO_3)_2(OH)_2$ and $Cu_2CO_3(OH)_2$) and oxide (Cu_2O). Cu concentration in the soils range between 3 and 100 mg kg^{-1} (ppm), but only 1–20% exists as free, readily bioavailable Cu^{2+}. The majority is bound to organic material and present as salts, such as $CuCl_2$, $CuSO_4$, and $Cu_3(PO_4)_2$ (Burkhead *et al.*, 2009; Hawkesford and Barraclough, 2011).

Cu malleability and ductility properties conferred it a great value in the human history. Since the prehistory, Copper Age and Bronze Age (Eneolithic), until nowadays, humans have been dedicated to metal exploitation and use (www.copper.org). Due to its high conductivity, Cu is used to manufacture electrical wiring. Cu also forms part of anti-rust substances for pipes located in marine environments, for facing of buildings, as a component in the manufacture of coins, household utensils, costume jewellery, ceramic stain and art crafts. The Cu antimicrobial properties are greatly appreciated in the cosmetic industry, in the production of aseptically products for hospitals as well as in fish farms. In addition, Cu is widely employed as a fungicide (Bordeaux mix) in the agricultural sector and it is also used as a growing factor (www.copper.org).

Cu exploitation in mining industry has progressively increased during the last 20 years until a total production of 17.5 million tonne. Cu mining activity is led by Chile with an extraction of approximately 6 million tonne during 2009. Other countries important in Cu extraction are: Zambia, Australia, China and Indochina (one million tonne) and Poland (half million tonne) (www.copper.org).

However, the continued Cu use and its abuse have a negative impact in the environment, from soil and trophic chains pollution. The principal causes of Cu pollution are two: industry activities and the use of fungicides in agriculture (Marschner, 2012).

1.2. Evolutionary considerations in copper availability

About 2.7 billion years ago, when oxygen levels in the atmosphere were still extremely low, Cu was thought to have mainly existed as insoluble cuprous sulphide, therefore limiting its use as a nutrient for primitive living beings. In contrast, anoxic conditions favoured the existence of the highly bioavailable ferrous form of Fe (Fe^{2+}), and consequently, Fe-containing proteins evolved (Crichton and Pierre, 2001). With the onset of photosynthesis and after the oxygenation of the atmosphere, as a result of oxygenic photosynthesis, the availability of both metals, Cu and Fe, was reversed. This oxidative atmosphere led to decrease in solubility of the Fe by the formation of the Fe oxides and the progressive liberation of soluble Cu^{2+} from insoluble Cu sulphate salts (Burkhead *et al.*, 2009). These events drove to the utilization of Cu as a micronutrient and the evolution of cuproproteins in organisms, sometimes substituting Fe-containing proteins (Burkhead *et al.*, 2009). The interrelationship between Cu and Fe homeostasis can still be seen in a variety of metalloenzymes with seemingly redundant functions, such as Fe superoxide dismutases (FeSOD) and Cu and Zn superoxide dismutases (Cu/ZnSOD) (Abdel-Ghany *et al.*, 2005). The hypothesis of Cu cofactor evolution as a consequence of biosphere oxygenation is supported by the observation that most aerobic organisms use Cu, while the majority of anaerobic organisms do not (Ridge *et al.*, 2008).

2. COPPER IN LIVING BEINGS

2.1. Essentiality of copper

Cu is part of the whole set of metal ions in cells that constitute the "metallome", determined as a component of metalloproteins and of any other metal-containing biomolecules present in organisms (Haraguchi, 2004). Metallome studies, often referred as metallomics, is a growing research area that is focused on the understanding of the utilization and the roles played by biometals and metal-containing molecules in living beings. Except for sodium (Na), potassium (K), calcium (Ca) and magnesium (Mg), that are required in large quantities and are considered macronutrient, other metals belongs to the group of the trace elements, such as Zn, Fe, Cu, Mn and Mo. Although these metals are required in small amounts, they are involved in critical enzymatic activities and physiological mechanisms (Haraguchi, 2004; Goldhaber, 2003). Their deficiencies, excess and alterations in metal homeostasis may result in metabolic and physiological abnormalities or even death (Mertz, 1998; Van Gossum and Neve, 1998).

Equipped with a high redox potential, Cu acts as a cofactor for proteins involved in a wide variety of biological processes, such as photosynthetic and mitochondrial electron transport chains, connective tissue formation, Fe metabolism, free radical elimination, hormone perception and neurological function (Kuo *et al.*, 2001; Peña *et al.,* 1999).

Comparative genomic analyses have been conducted to characterize key features of Cu utilization and in a variety of organisms. Recent analyses revealed the distribution of Cu-dependent and Cu-independent organisms in the three domains of life (Ridge *et al.*, 2008; Zhang and Gladyshev, 2010). Based on bioinformatic data banks studies of metalloproteins metal-binding domains, the majority of cuproteins are involved in Cu homeostasis (Andreini *et al.*, 2004). Only half of the archaea organisms appeared to utilize Cu, approximately 80% of bacteria, whereas in eukaryotes, almost all organisms use Cu (Zhang and Gladyshev, 2010). According to this information, the speciation of prokaryotic organisms appeared to only slightly affect the ancestral cuproproteome, whereas eukaryotes may have expanded their ancestral cuproproteome by either evolving new Cu domains or reusing old domains for new functions (Ellis *et al.*, 2007). With regard to the cuproteins, almost half of prokaryotic cuproteins are not present in eukaryotes. Additional cuproteins have evolved in eukaryotes, being the largest cuproteomes present in land plants (62 and 78 cuproteins in *Arabidopsis thaliana* and *Oryza sativa*, respectively) (Zhang and Gladyshev, 2010).

2.2. Plant cuproteins

Cu essentiality in living beings is mostly due to its function as cofactor in multiple cuproteins. Thus, in plants there are other different cuproteins such as plastocyanin (PC), cytochrome c oxidase (COX) and the ethylene receptors (ETRs). Plant cuproteins can be found in almost every cell compartment. Thus, other abundant cuproteins include chloroplastic polyphenol oxidases (PPOs), Cu/ZnSODs located in different subcellular compartments, and a large group of apoplastic Cu proteins, including ascorbate oxidases, amine oxidases, laccases, and plantacyanins. Apoplastic Cu proteins are involved in cell wall remodeling and lignification (Cohu and Pilon, 2007). However, it must be mentioned that the specific biological roles of most cuproteins remain unclear (Burkhead *et al.*, 2009).

Superoxide radical ($O_2^{.-}$) is mainly produced in the light-dependent reactions of the chloroplast through the reduction of O_2 at photosystem I (PSI), but it can also be the by-product of other oxygenic reactions and the mitochondrial respiration (Asada, 2006). Lipids and DNA can be rapidly affected by the superoxide ion that, therefore, must be removed to avoid the spread damage. The SODs have been extensively studied in yeast and humans (Abreu and Cabelli, 2010). The SODs function as homodimers, undergoing disproportionation of the toxic $O_2^{.-}$ to hydrogen peroxide (H_2O_2) and water. The Cu/ZnSODs have been involved in oxidative stress protection, being the Cu/ZnSOD1 (cytosolic) and the Cu/ZnSOD2 (chloroplastic) the most abundant forms. When Cu is deficient, the Fe counterpart (FeSOD) is used as an alternative to Cu/ZnSOD in plants (Abdel-Ghany *et al.*, 2005b) (see also section 4.4).

The first Cu enzyme discovered in plant plastids was PPO (Arnon, 1949). PPO is found in the thylakoid's lumen and contains a dinuclear Cu centre. Plant PPOs catalyse the conversion of monophenols to ortho-diphenols and ortho-dihydroxyphenols to ortho-quinones, resulting in black or brown pigment deposits (Mayer, 2006).

Plantacyanin is an apoplastic small blue Cu protein of the phytocyanin protein family (Nersissian *et al.*, 1998). The biological role of plantacyanin remains unclear. In *Arabidopsis*, it is highly expressed in flowers, although also found in the roots (Abdel-Ghany and Pilon, 2008).

PC, another small blue Cu protein, is essential for the light-dependent reactions of photosynthesis in higher plants (Weigel *et al.*, 2003). PC is the most abundant cuproprotein in the thylakoid lumen (Kieselbach *et al.*, 1998). It transports one electron at a time from the cytochrome b_6f complex to P700, the reaction centre of PSI, in the z-scheme of photosynthesis. In several photosynthetic organisms (e.g., in *Chlamydomonas*), but not in higher plants, the PC can be replaced by a Fe-containing cytochrome-c_6 when Cu becomes scarce (Wastl *et al.*, 2002).

Laccases are multicopper oxidases (MCOs), which contain four Cu ions per polypeptide. Laccases use oxygen to catalyse the oxidation of a wide variety of aromatic or phenolic substrate molecules to reactive radicals with the production of water and oligomers (Riva, 2006). Proposed biological functions for plant laccases include roles in lignin synthesis, wound healing, Fe acquisition, stress response, maintenance of cell wall structure and integrity, and flavonoid-derived pigment formation (Pourcel *et al.*, 2005). Lignin is an important structural component of plant cell walls, being the second most abundant component after cellulose (Davin and Lewis, 2005; Weng and Chapple, 2010). Several reports link Cu deficiency to defects in lignification. Problems in lignification explain the deformation of pine trees, the rolling, desiccation, and wilting of young leaves owing to the improper xylem vessel structure and lodging susceptibility of cereals (Marschner, 2012; Oldenkamp and Smilde, 1966).

2.3. Copper toxicity

Whilst Cu is an essential element, it is a potentially toxic agent when in excess. The most accepted explanation for Cu-induced cellular toxicity comes from the fact that Cu ions are prone to participate in the reactive oxygen species (ROS) formation, via Fenton and Haber-Weiss reactions, which cause severe oxidative damage to cells (Halliwell and Gutteridget, 1984) (Figure I1). Cu is also at the top of the Irving-Williams series and tightly binds to target sites in polypeptides (Lippard and Berg, 1994). Cu^{2+} and Cu^+ ions can act in oxidation and reduction reactions. Cu^{2+}, in the presence of biological reductants, such as ascorbic acid or glutathione (GSH), can be reduced to Cu^+ which catalyse the formation of the highly reactive hydroxyl radicals ($\cdot$OH), through the decomposition of H_2O_2 via the Fenton reaction (Lloyd *et al.*, 1997).

$$Eq\ 1 \quad Cu^+ + H_2O_2 \longrightarrow Cu^{2+} + \bullet OH + OH^-$$

$$Eq\ 2 \quad Cu^{2+} + \bullet O_2^- \longrightarrow Cu^+ + O_2$$

$$\overline{\bullet O_2^- + H_2O_2 \longrightarrow \bullet OH + O_2 + OH^-}$$
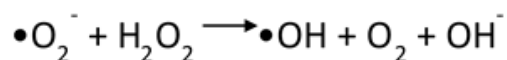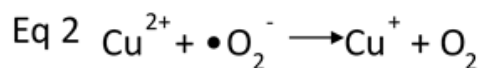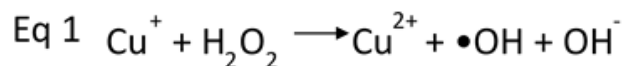
Figure I.1. Fenton and Haber-Weiss reactions. Cu^+ is oxidized to Cu^{2+} by hydrogen peroxide in the Fenton reaction (Eq 1), forming hydroxyl radicals ($\cdot OH$) as a product. In the presence of the superoxide radical ($O_2^{\cdot -}$), Cu^{2+} is reduced to Cu^+ in the Haber-Weiss reaction (Eq 2).

Cu excess mediates free radical production and direct oxidation of lipids, proteins and DNA. Cu-induced ROS may cause damage to organic molecules, but they can also act as internal signals and interact with hormonal networks, affecting plant growth and development. The balance between intracellular and extracellular Cu contents is driven by cellular transport systems that regulate uptake, export and intracellular compartmentalization (Harris, 1991). The equilibrium between Cu essentiality and toxicity is globally achieved among the cellular, the tissular, the organ and the whole plant levels (Bull and Cox, 1994). Therefore, a fine regulation between Cu uptake and its metabolic use is required. Rae *et al*. (1999) made the remarkable observation that the upper limit of so-called "free pools" of Cu is less than a single atom per cell. Until recently, it was commonly accepted that metal ions were in equilibrium with metalloproteins. However, their results suggest that there is a significant overcapacity for Cu chelation in the cell. Thus, there must be multiple processes for Cu binding which preventing it from being randomly available. The implications of these findings are profound, especially on the mechanisms of intracellular free radical formation by means of Fenton chemistry (Rae *et al.*, 1999).

3. COPPER CONTENT AND UNADEQUACY SYMPTOMS IN ARABIDOPSIS

The amount of Cu in green plant tissues typically ranges around 2–50 ppm of dry weight, although, is largely dependent on species. The broad range in Cu content suggests variable needs for Cu, which might be related to differences in cell wall structure or other metabolic adaptations. According to the data obtained in the model plant *Arabidopsis thaliana*, the physiological Cu levels in leaves range from 5 to 20 ppm. At these concentrations, neither deficiency nor toxicity symptoms are developed (Cohu and Pilon, 2007).

Most soils have sufficient Cu to sustain plant growth, although scarcity occurs frequently in those with high levels of organic material or excess nitrogen-phosphorus-potassium fertilization (Dobermann and Fairhurst,

2000). When grown in unfertilized soils, *Arabidopsis* suffers often a slight Cu deficiency. This is also true when grown in standard plant growth medium for *in vitro* culture, half-strength Murashige and Skoog medium (½ MS) (Murashige and Skoog, 1962). This medium contains 0.05 µM $CuSO_4$ and needs to be supplemented with 1 µM $CuSO_4$ for maximum *Arabidopsis* seedlings photosynthetic activity (Yamasaki *et al.*, 2007). In addition, because Cu is fairly immobile between cell tissues, deficiency symptoms appear first in the newly formed, younger cells and the reproductive organs (Marschner, 2012). Classic deficiency symptoms include stunted growth due to defects in apical meristems, rolling-up and wilting of leaves, and impaired photosynthetic electron transport and reduced mitochondrial respiration (Marschner, 2012). Even if primary plant productivity is not affected, the Cu feedstock content has a large economic impact because Cu is essential for animal development and affects key animal functions, including lipid metabolism (Davies and Mertz, 1987; Engle, 2011).

On the other hand, widespread inappropriate agricultural practices, such as overusing fungicides with high Cu concentrations, release of industrial wastewater and soil used after mining activities, have increased Cu contamination in irrigation water and in cultivated soils at specific locations (Marschner, 2012). Cu excess symptoms in plants share similarities with those related to Fe-deficiency, such as the presence of chlorosis in the vegetative tissues, decreased root growth and enhanced oxidative stress (Printz *et al.*, 2016). Cu toxicity in plants affects the photosynthetic activity due to the fact that Cu^{2+} can replace Mg^{2+} in the center of the chlorophyll porphyrin ring, producing the inactivation of Phaeophytin a (Phaeo a) in photosystem II (Küpper *et al.*, 2002). Most plants can acclimate to Cu excess by tuning the expression of transporters to limit uptake and by activating the production of sequestering compounds, such as metallothioneins and phytochelatins (Cobbett and Goldsbrough, 2002).

Another factor that should be mentioned is the effect of climate change in plant nutrient content. Growing levels of atmospheric CO_2 are increasing the synthesis of carbohydrates, which affects mineral assimilation in plants, resulting in a general decrease of their nutritional quality. Indeed, recent meta-analyses have indicated that Cu and other metal deficiencies would be exacerbated in forthcoming years due to a rise in CO_2, with increasing obesity and "hidden hunger" problems in the world (Loladze, 2014; Myers *et al.*, 2014). Since plants constitute one of the main entrances of micronutrients into trophic chains, deciphering the regulatory mechanisms underlying dynamical hormonal interactions with Cu uptake and distribution of edible plant parts is relevant for optimal plant development and to avoid plant nutritional deficiencies or excesses from being transferred to consumers.

4. COPPER HOMEOSTASIS

Cu-dependent organisms have developed a conserved and complex network of proteins to handle Cu in order to prevent its deficiency and to avoid its toxic effects when in excess.

4.1. Long distance transport and copper acquisition

During plant growth and development, ions are taken up by epidermal root cells, radially driven towards the root centre, through the parenchyma and the endodermis cell layers, and loaded into the xylem. This unidirectional transport of transition metals towards the xylem is accomplished by different transporters. A coordinated activity among these transporters and the storage and cuproteins acquisition pathways is required for and adequate distribution of the minerals in all cells and tissues at all stages of development (Printz *et al.*, 2016).

The mechanisms of Cu uptake in plants have not been completely elucidated, although a strong overlap between Fe-uptake and Cu-uptake mechanisms have been suggested (Ryan *et al.*, 2013). In dicotyledons, such Arabidopsis, and non graminaceous monocotyledons has been proposed a reductive Cu-uptake mechanisms, based on the idea that Cu^{2+} is reduced to Cu^+ at the root surface (Bernal *et al.*, 2012; Printz *et al.*, 2016; Ryan *et al.*, 2013).

Even when abundant, metals can be inaccessible in the soil due to their tendency to be present predominantly in an insoluble form. Cu^{2+} is the most abundant form in soil solution and, probably, it enters in plant root cells through divalent cation low-affinity transporters, such as some members of the ZIP family (ZIP2 and ZIP4) (Wintz *et al.*, 2003). However, whether this fact is taking place, it still has to be proven *in vivo*. Under metal deficiencies, plants acidify the external medium by using H^+-ATPases (AHA) to extrude protons into the rhizosphere to decrease the pH of the soil under metal limiting conditions making metals soluble (Santi and Schmidt, 2009).

When Cu is scarce, Arabidopsis uses a Cu^+-specific transport system based on Cu^{2+} reduction by plasma membrane ferric reductase oxidases 4 and 5 (FRO4 and FRO5) (Bernal *et al.*, 2012) and on the cytosolic uptake by plasma membrane high affinity Cu transporters (COPT1, COPT2 and COPT6) (Sancenón *et al.*, 2003) (Figure I2).
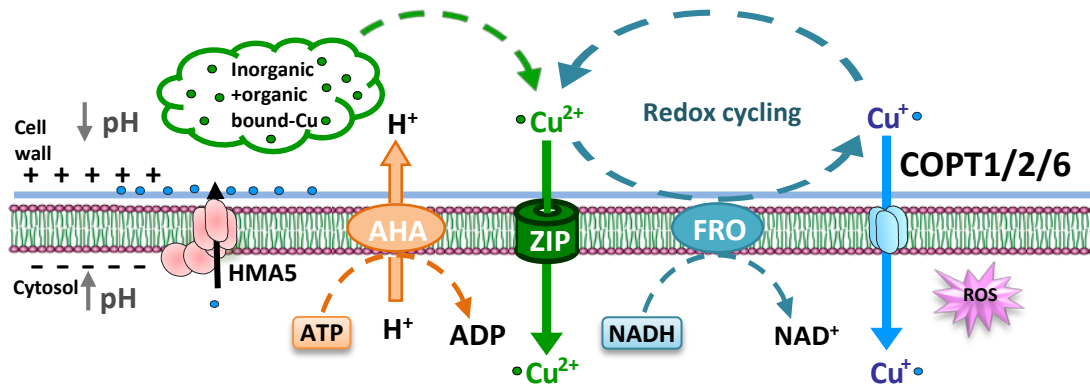
Figure I2. Cu transport into the cytosol through the plasma membrane. The *Arabidopsis* H$^+$A-ATPase (AHA) pumps protons to the extracellular space decreasing the pH to increase Cu^{2+} availability. Cu^{2+}can be uptaken by non-selective ZIP proteins or reduced to Cu$^+$ by FRO4 and FRO5 (FRO) and enters into the cytosol through the COPT1, COPT2 and COPT6 (COPT1/2/6) transporters. Cu^{2+} efflux is mediated Cu transport to extracellular compartments is mediated by heavy metal P-type ATPase (HMA5) proteins.

COPT substrate availability depends on both free external Cu (not bound to inorganic and organic complexes) and the Cu$^+$/Cu^{2+} ratio, according to external redox status conditions and the enzymatic activity of ferric reductase oxidases. This reductive strategy used for Cu$^+$ uptake is energetically expensive, and it has been shown to be the predominant and ubiquitous mechanism for Cu acquisition in dicotyledons (Jouvin *et al.*, 2012; Ryan *et al.*, 2013). This Cu$^+$ uptake strategy could be an adaptation that may be required for high-affinity specific monovalent cation selection or/and for meeting specific Cu$^+$ intracellular needs.

Once in plants, Cu is root-to-shoot translocated as Cu-complexes, where xylem loading is a key controlling factor in the transport of minerals to the aerial parts. However, Cu xylem loading in dicotyledons is poorly understood. The heavy metal P-type ATPase (HMA5) has been postulated as a Cu translocator from the roots to the vascular axes (Andrés-Colás *et al.*, 2006; Kobayashi *et al.*, 2008). Once in the xylem, Cu forms complexes with nicotianamine (NA), which can transport Cu^{2+} in a long distance distribution through the xylem and phloem pathways due to the fact that Cu^{2+}-NA complexes are stable under mild acidic conditions (Curie *et al.*, 2009). Besides, Cu^{2+}-NA complexes, Cu can be also transported by yellow stripe-like (YSL) transporters across plant cell membranes, being this step crucial in a long distance metal distribution through the entire plant (Curie *et al.*, 2009). Once reaching leaves, Cu^{2+} ions need to cross membranes being reduced to Cu$^+$ by the FRO4 activity (Bernal *et al.*, 2012) and uptaken through COPT transporters into the cell (Puig *et al.*, 2007).

4.2. The CTR/COPT transporter family

Numerous studies in yeasts, mammals, insects, algae, and plants have revealed that eukaryotes utilize the conserved family of Cu transporter proteins (CTR/COPT) to facilitate high affinity (K_m = 1–5 µM) cellular Cu acquisition at the plasma membrane, but also to mobilise Cu from intracellular storage compartments, when Cu bioavailability decreases (Puig and Thiele, 2002). CTR/COPT proteins are highly specific for Cu^+ transport (Sancenón *et al.*, 2003). Consequently, they function in coordination with membrane metalloreductases that previously catalyse Cu^{2+} reduction to Cu^+ (Hassett and Kosman, 1995). The conserved features in CTR/COPT proteins include three transmembrane domains (TMDs), an amino-terminal region, rich in methionine and/or histidine residues, and an essential Mx3Mx12Gx3G signature motif, embedded within transmembrane domains TMD2 and TMD3 (Puig, 2014) (Figure I3A).
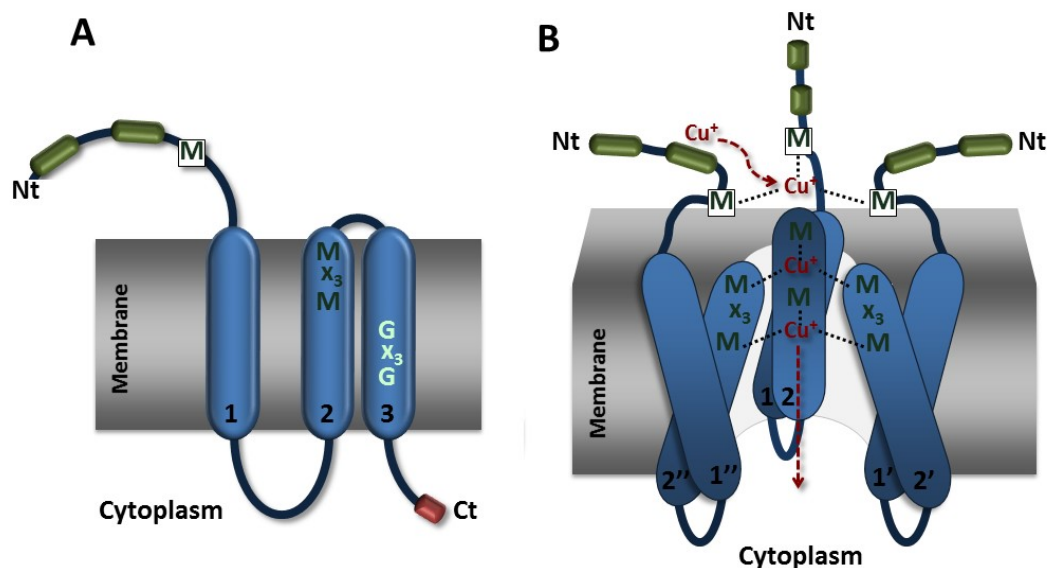
Figure I3: Conserved features in the CTR/COPT transporter family. CTR/COPT topology and conserved domains and motives. The three TMDs are shown in blue. Dark green boxes represent extracellular methionine/histidine-rich motifs and red boxes indicate cytoplasmic cysteine/histidine motifs (A). Representation of the CTR/COPT trimers assembly in the membrane (B). The model highlights the role of methionines (M) in the mechanism of Cu^+ transport. For simplicity, only TMDs 1 and 2 have been represented (Puig, 2014).

Genetic, biochemical, and structural data suggest that, in the first steps of Cu transport, extracellular methionine/histidine-rich motifs recruit Cu^+ to the entrance of the pore and facilitate its subsequent translocation to a set of stacked methionine triads that provide a central Cu^+-driving path from the external

domain of the complex (Figure I3B). After passing through the pore, Cu^+ would bind to the carboxy-terminal cysteine/histidine motifs facing the cytoplasm, which modulate Cu^+-transport activity and delivery to membrane associated metallochaperones for targeted intracellular distribution (Klomp *et al.*, 2003; Puig and Thiele, 2002).

4.2.1. COPT transporters in *Arabidopsis*

The *Arabidopsis* COPT transporters family has 6-members (*COPT1-COPT6*) (Puig, 2014). These transporters have been classified into two subgroups. First is formed by COPT1, COPT2 and COPT6 transporters, located at the plasma membrane (pmCOPT), which fully complement the corresponding yeast mutants, and are implicated in the Cu uptake into the cytoplasm. The second subgroup is composed by COPT3 and COPT5 transporters, that are located in intracellular membranes (imCOPT) and that partially complemented the yeast phenotypes, and their function is the intracellular Cu recycling (Andrés-Colás *et al.*, 2010; García-Molina *et al.*, 2011; Perea-García *et al.*, 2013; Sancenón *et al.*, 2003). Each family member shows a tissue-specific expression pattern and performs specialised functions, as denoted by the phenotypes associated with knockout *copt* mutant plants. Furthermore, the mRNAs encoding *COPT* transporters located at the plasma membrane (*COPT1*, *COPT2* and *COPT6*) are up-regulated by Cu deficiency, whereas the internal *COPTs* (*COPT3* and *COPT5*) are not (García-Molina *et al.*, 2011; Perea-García *et al.*, 2013; Puig, 2014).

COPT2 is the most expressed member of the family. For that reason, its expression can be used as a molecular marker in Cu starved plants (Andrés-Colás *et al.*, 2013). Among the COPT genes, *COPT2* mRNA also displays the most marked increase in response to Cu- deficiency (see section 3.2) (Sancenón *et al.*, 2003; Yamasaki *et al.*, 2009; Garcia-Molina *et al.*, 2011; Perea-García *et al.*, 2013). Under low Cu conditions, *COPT2* is mainly expressed in the vasculature of cotyledons and young leaves, apical meristems, trichomes, and in the root elongation zone (Perea-García *et al.*, 2013) (Figure I4). In reproductive tissues, *COPT2* concentrates mostly in stigma, anthers and pollen (Perea-García *et al.*, 2013) (Figure I4). Transcript expression pattern of *COPT2* in the shoots is similar to *COPT1* but these transporters have different expression patterns in roots where *COPT2* is almost absent from elongation and meristematic zones (Perea-García *et al.*, 2013).
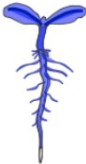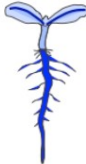
	Subcellular localization	Expression pattern			Response to Cu deficiency
		Seedling	Roots and shoots	Flowers	
COPT2					Yes
COPT5					No

Figure I4. *COPT2* and *COPT5* expression patterns. Subcellular localization and GUS expression pattern in 7 day-old seedlings, roots and shoots and flowers are represented by blue zones.

On the other hand, at the intracellular membranes, the most expressed member is *COPT5* that shares just a 20% of sequence identity with *COPT2* (Sancenón *et al.*, 2003). The *COPT5* transporter is not regulated at the transcriptional level by Cu (see section 4.4) (García-Molina *et al.*, 2011). COPT5 localizes to the tonoplast and the membranes of pre-vacuolar compartments in *Arabidopsis* cells. The *copt5* mutants exhibit chlorosis, impaired photosynthetic electron transfer, root elongation defects and compromised vegetative growth under severe Cu starvation conditions (García-Molina *et al.*, 2011; Klaumann *et al.*, 2011). *COPT5* is expressed mostly in root vascular tissues and siliques (Figure I4). Nonetheless, it has also been detected, but to a lesser extent, in trichomes, meristems, the vascular conduits of cotyledons, leaves and reproductive organs, but not in pollen (García-Molina *et al.*, 2011) (Figure I4). Biochemical studies have demonstrated that *copt5* plants display reduced vacuolar Cu export, which leads to Cu accumulation in roots and low Cu in siliques and seeds, and strongly suggests that COPT5 functions in Cu distribution from roots to reproductive tissues (Klaumann *et al.*, 2011).

Under Cu deficiency conditions, members of the COPT family participate in metal supply to the cytosol in order to reach appropriated Cu levels and allow its redistribution among the different intracellular compartments. As a result, plants selectively incorporate Cu^+ under deficiency by paying both a high energy cost and an increase in oxidative stress with the subsequent damage and alterations in different signalling pathways caused by high Cu^+ reactivity (Rodrigo-Moreno *et al.*, 2013; Ravet and Pilon, 2013).

4.3. Intracellular copper traffic

The strategies that organisms use to maintain Cu homeostasis include the regulation of Cu uptake in cells, Cu trafficking via P-type ATPases and Cu chaperones, and the regulation of the cuproproteins levels in response to changes in metal availability.

As previously reported, *Arabidopsis* uses COPT transporters for Cu uptake to the cytosol when Cu is scarce (Figure I5). Because Cu reactivity, once in the cell, it has to be chelated and acquired by cuproproteins in a controlled way. Cu ions are therefore thought to be bound by low molecular-weight proteins, named metallochaperones, which take the metal probably from transporters and insert Cu into the active site of cuproproteins (O'Halloran and Culotta, 2000). So far, the function of seven Cu chaperones has been investigated in *Arabidopsis*. They have been divided into three classes, according to their interaction partners and function. The cuprochaperone which provides Cu^+ to the Cu/ZnSOD1 is denoted CCS (Abdel-Ghany *et al.*, 2005b). The antioxidant 1 (ATX1) and the Cu chaperone (CCH) interact with Cu-transporting ATPases (Mira *et al.*, 2001). The cytochrome c oxidase 11 (COX11), cytochrome c oxidase 17 (COX17) and two homologs of the yeast Cu chaperone SCO (HCC1 and HCC2) function in the synthesis of cytochrome c oxidase for mitochondrial respiration (Attallah *et al.*, 2011; Burkhead *et al.*, 2009; Cohu and Pilon, 2007).

When Cu^+ enters the cytosol, it could be bound by the different cuprochaperones. One of them is ATX1 which delivers the metal to Cu^+ P-type ATPases, such as response to antagonist 1 (RAN1) located in the endoplasmic reticulum (ER). Subsequently, RAN1 pumps Cu^+ into the ER lumen, where it is acquired by cuproproteins (Hirayama *et al.*, 1999). Most extracellular and endomembrane cuproproteins follow the endocytic pathway to their final destinations and probably incorporate Cu, while transiting through the ER or the trans-Golgi network. Thus, based on the relative abundance of cuproproteins, endocytic compartments are expected to display higher Cu levels than the nucleo-cytoplasmic space and, consequently, the main Cu^+ flux should follow the COPT-ATX1-RAN1 pathway. In line with this, Cu delivery to cytosolic Cu/ZnSOD1 by the CCS cuprochaperone could represent a quantitatively minor Cu route (Robinson and Winge, 2010). Taken together, these facts predictably lead to Cu^+ distribution between the nucleo-cytoplasmic and endocytic compartments with one or the other being favoured, depending on the relative influx-efflux transport activity of COPT and Cu^+-ATPases, respectively.
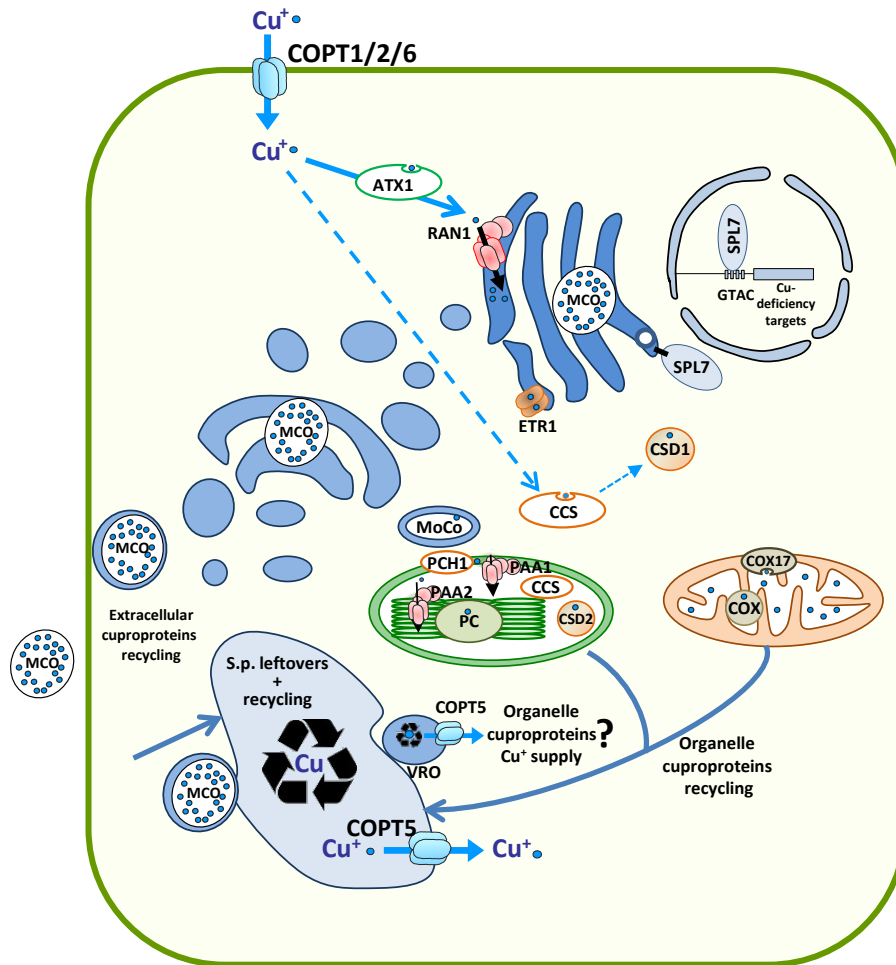
Figure I5. Cu intracellular traffic in *Arabidopsis*. Cu$^+$ uptake through COPT plasma membrane transporters (COPT1/2/6) is coupled to metallochaperones transfer and its delivery to targets. Cuprochaperone CCS provides Cu$^+$ to cytosolic Cu/ZnSOD1. ATX1 transfers Cu$^+$ to P-type ATPase RAN1, located in the ER, where Cu$^+$ is probably acquired by cuproproteins, such as MCOs, ETR1 and MoCo. The Cu resulting from recycling and from the secretory pathway leftovers converges into the vacuole or into vacuolar-related organelles (VRO) being COPT5 efflux function important in this part. The Cu$^+$ supply to chloroplast and mitochondria can take place from the lumen through the COPT5 efflux function. The direction of Cu$^+$ traffic is indicated by arrows and Cu content is indicated in different intensities of blue according to predicted quantity.

Chloroplasts are major Cu consumers in plants, where Cu is incorporated into the PC and Cu/ZnSOD2, among other proteins (Ravet and Pilon, 2013). Once inside the chloroplast intermembrane space, the Cu$^+$-loaded plastid chaperone 1 (PCH1) delivers Cu$^+$ to the internal membrane-located chloroplast P-type ATPase in *Arabidopsis* 1 (PAA1) (Blaby-Haas *et al.*, 2014), which pumps Cu$^+$ into the stroma (Shikanai and Fujii, 2013).

PCH1 evolves by an alternative splicing event of the pre-mRNA encoding PAA1 (Blaby-Haas *et al.*, 2014). Once inside the stroma, the CCS chaperone delivers Cu to chloroplastic Cu/ZnSOD2 and also to PAA2, which is the Cu^+ P-type ATPase that delivers Cu to the thylakoids for PC supply (Abdel-Ghany *et al.*, 2005a; Blaby-Haas *et al.*, 2014). The chloroplast caseinolytic protease (Clp) system is involved in specific PAA2 turnover under Cu excess in the stroma (Tapken *et al.*, 2015). In mitochondria, Cu is required mainly for the assembly and activity of COX in the respiratory chain (Garcia *et al.*, 2014). Cu delivery and insertion into COX is a complex process mediated by different metallochaperones present in the mitochondrial intermembrane space, such as COX17 (Attallah *et al.*, 2007; Balandin and Castresana, 2002) (Figure I5).

How Cu reaches organelles from an endosymbiotic origin, such as mitochondria and chloroplasts, is a poorly understood process. Since free Cu^+ levels are extremely low in the cytosol (Rae *et al.*, 1999), at least under Cu-limiting conditions, there must be other intracellular sources of Cu to ensure its arrival to organelles. Thus, under nutrient deprivation, a putative Cu source could be the vacuole or the VRO. In these compartments, the valued metal arising from recycling metalloproteins and the scarce leftovers from secretory/endocytic pathways would converge (Figure I5). In addition, these compartments have been recently shown to participate in dynamic intracellular metal homeostasis (Blaby-Haas and Merchant, 2014; Hong-Hermesdorf *et al.*, 2014). An increase in interorganellar communications with the membrane contact sites between mitochondria and the vacuole under nutrient deprivation stress has been recently described in yeast, which mainly serve for lipid and ion exchanges (Elbaz-Alon *et al.*, 2014). If this were also the case in plants, organelles would be at "*the end of the line*" of the secretory pathway to acquire Cu which, under Cu deficiency, could lead to a competitive balance between previous Cu incorporation by in transit cuproproteins on the secretory pathway and the Cu leftovers available for the Cu supply to organelles.

4.4. Regulation of gene expression under copper deficiency

Most advances in understanding regulation of Cu homeostasis have been obtained from studies wherein plants were subjected to Cu deficiency. Cu deprivation in plants induces the reprogramming of a number of metabolic processes aimed at a strict economy in Cu-use in order to optimize its delivery to the most essential cellular processes, which represent an adaptive mechanism that has developed to survive under adverse conditions (Printz *et al.*, 2016).

Cu homeostasis is mainly regulated by a central Cu homeostatic machinery which involves a Zn finger transcription factor SQUAMOSA-promoter binding-like protein 7 (SPL7). This transcription factor belongs to the SQUAMOSA-PROMOTER BINDING PROTEINS (SBP) family that display a highly conserved DNA-binding domain. SPL7 is essential for the response to Cu deficiency in *Arabidopsis* through specific binding of its SBP-domain to the GTAC motifs in the promoters of target genes (Bernal *et al.*, 2012; Yamasaki *et al.*, 2009). In

plants, under Cu sufficiency conditions, SPL7 may bind Cu^{2+} displacing Zn^{2+} from the Zn fingers and the subsequent inability to bind the GATC motifs in target promoters (Figure I6) (Sommer *et al.*, 2010). SPL7 was shown to be constitutively expressed in plants independently of soil Cu availability. Consequently, part of its regulation may occur at post-transcriptional level (Yamasaki *et al.*, 2009). SPL7 has been recently shown to interact with DNA/RNA-binding protein Kin17 (KIN17) (Figure I6), a conserved curved DNA-binding domain protein located in the nucleus. This interaction promotes Cu-deficiency responses and alleviates oxidative stress responses, perhaps by preserving cell integrity and plant growth under Cu scarcity (Garcia-Molina *et al.*, 2014a). SPL7 displays an operative transmembrane domain that has been shown to insert the protein into the endomembrane system. Recent studies revealed the possible dual subcellular localization of SPL7 in both the nucleus and the ER (Figure I6) (Garcia-Molina *et al.*, 2014b). It has been hypothesized that Cu-deficiency induces ER stress, thereby promoting activation of SPL7. In addition, SPL7 may homodimerize outside the nucleus, preventing its entry in the nuclear pore due to its size, as a negative feedback mechanism (Garcia-Molina *et al.*, 2014b). These processes render SPL7 a crucial Cu sensor molecule in two topological spaces where Cu is initially distributed, the nucleo-cytoplasmic and the lumen of secretory pathway compartments. Thus, SPL7 could be able to perceive both ER stress, mediated by Cu deficiency through its C-terminal part, and Cu status in the nucleo-cytoplasmic space, through its SBP domain, maybe driving a converging and regulated response under Cu scarcity. This response could be even more complex if other components of the 16 SPL family members participate in some SPL7 regulatory mechanisms (García-Molina *et al.*, 2014b).

Furthermore, SPL7 interacts physically and genetically with ELONGATED HYPOCOTYL5 (HY5) which encodes a bZIP-type transcription factor that functions downstream of multiple photoreceptors to promote photomorphogenesis (Figure I6) (Zhang *et al.*, 2014). This dual interaction allows a feedback mechanism for linking the light- and Cu-responsive gene networks and confirm that the tight spatio-temporal regulation of Cu homeostasis is part of the integral cellular circadian system (Andrés-Colás *et al.*, 2010; Zhang *et al.*, 2014).
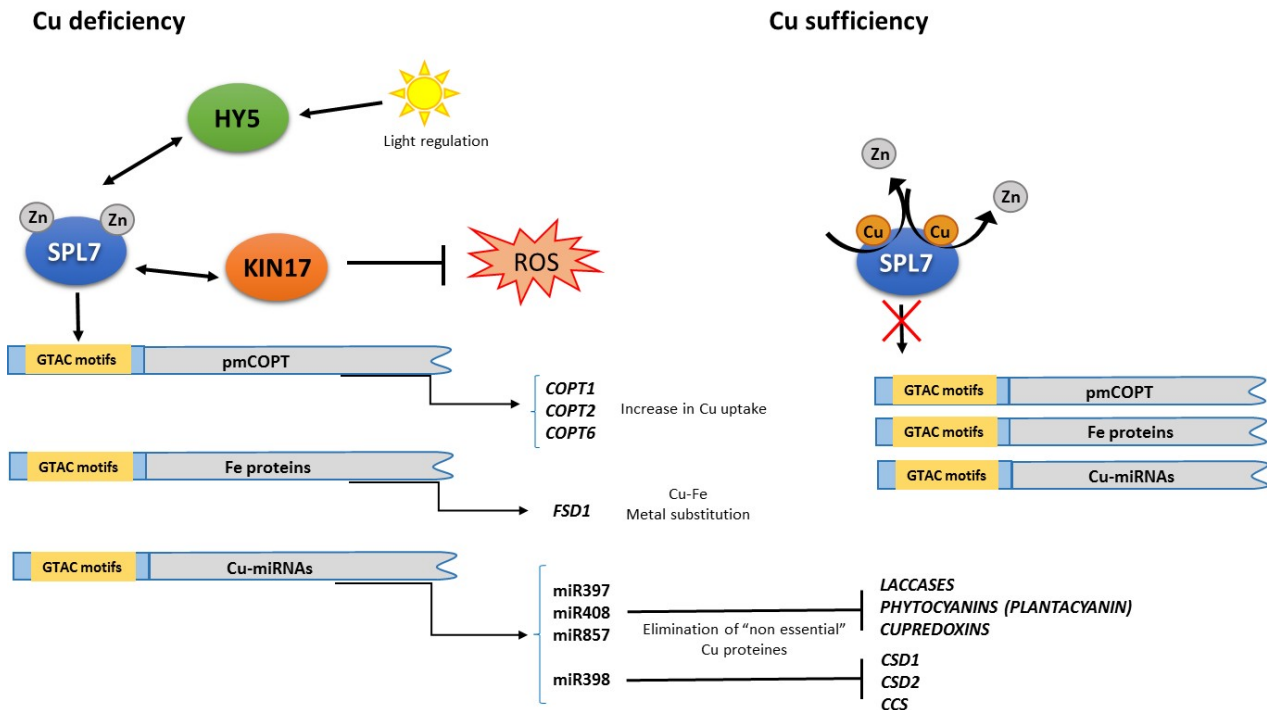
Figure I6. SPL7-dependent regulation of gene expression. Under Cu deficiency conditions SPL7 transcription factor binds GTAC motifs inducing the expression of SPL7-responsive genes, triggering an increase in Cu uptake through COPT transporters, an elimination of "non-essential" cuproteins and the substitution of these Cu proteins by Fe proteins. SPL7 can interact with HY5 linking the photomorphogenic processes to Cu homeostasis. Additionally KIN17 can bind to SPL7 to enhance the Cu-starvation response and reinforcing the cellular antioxidant system. Under Cu sufficiency conditions, Zn ions in the SPL7 Zn fingers, can be replaced by Cu ions and affect the SPL7 capacity to bind GTAC motifs.

It is worth mentioning that the SPL7-mediated Cu-miRNA expression serves Cu redistribution in order to establish a priority ranking for Cu delivery to essential cuproteins by avoiding Cu incorporation in non-essential proteins (Pilon, 2016). In this switch to an "economy" mode, SPL7-mediated strategies, used when Cu is limiting, consists in replacing "non-essential" cuproteins by other metalloproteins, usually Fe proteins, which play a similar role, probably in order to save Cu for essential cuproteins, such as PC (Printz *et al.*, 2016). The SPL7-mediated replacement of the Cu/ZnSOD form for the FeSOD counterpart under Cu-limited conditions is performed by expressing FeSOD mRNA (*FSD1*) and miR398, since miR398 targets Cu/ZnSOD mRNAs (*CSD1* and *CSD2*) for degradation (Abdel-Ghany *et al.*, 2005a; Ravet and Pilon, 2013; Yamasaki *et al.*, 2007). Apart from metalloprotein substitution, SPL7 activates the transcription of COPT family transporters, such as *COPT1*, *COPT2* and *COPT6*, whereas *COPT3* and *COPT5* are not regulated by SPL7 according to the absence of GTAC motifs in their promoters (Puig, 2014).

Another strategy for establishing a priority ranking in Cu delivery under deficiency is the miRNA-mediated elimination of the first located cuproproteins on the pathway of Cu incorporation. In this case, other denoted Cu-miRNAs, such as miR408, target laccases (*LAC3, LAC12* and *LAC13*) (Abdel-Ghany and Pilon, 2008; Yamasaki *et al.*, 2007). These cuproproteins predictably acquire Cu on the secretory pathway when transiting to their final destinations. Strikingly, miR408 accumulation and the subsequent down-regulation of the miR408 target genes in transgenic plants rescue developmental defects of the *spl7* mutant. This indicates that diminished Cu delivery of the endomembrane system to *en route* laccases redounds in increased Cu acquisition by PC at chloroplasts (Zhang *et al.*, 2014). These results further reinforce the suggested hypothesis for chloroplasts' Cu supply dependency on secretory pathway leftovers under Cu deficiency conditions. Accordingly, the miR408 strategy could consist in shortening "*the Cu metallation line*" by eliminating cuproproteins, located upstream on the spatiotemporal Cu delivery pathway, in order to allow further Cu delivery to the cuproproteins situated downstream. Thus, in this way, the scarce Cu atoms would arrive at the essential cuproproteins in the organelles situated at the end of the intracellular Cu delivery pathway.

5. ROLE OF COPPER IN PHYTOHORMONES BIOSYNTHESIS AND PERCEPTION

As already indicated, plants employ complex homeostatic networks to increase uptake and tolerance to cope with non-optimal nutrients supply. Moreover, both local root responses and systemic signalling, have to be integrated in order to drive optimised metal nutrients acquisition for acclimation to changing environmental conditions. In many cases, these processes may alter the whole plant morphology and metabolism (López-Bucio *et al.*, 2003). In order to orchestrate morphological, physiological and molecular adaptive responses to soil mineral bioavailabilities, phytohormones act as major endogenous cues (Rubio *et al.*, 2009).

Nutrients affect multiple levels and components in hormone biosynthesis, perception and signalling pathways. In turn, hormones influence root growth, stomatal movements and stress tolerance, among other processes, and have a huge impact on plant mineral nutrition, which underlies the close interrelation between hormonal stimuli and nutritional homeostasis (Rubio *et al.*, 2009). Consequently, crop yields increase through hormonal supply when optimising mineral nutrition (Zaman *et al.*, 2015).

Plants' nutrient requirements vary along daily cycles, in different plant development stages and during stress responses (Marschner, 2011). The circadian regulation of the ion channels and nutrient transporters involved in the carbohydrates, nitrogen, sulphate, phosphate and micronutrients transport is a pervasive phenomenon (Haydon *et al.*, 2013). These processes have been proposed to regulate downstream targets to further spread circadian signalling which, in turn, provides feedback on the central oscillator (Haydon *et al.*, 2011; Ko *et al.*, 2009). Hormones can also affect time-of-day-dependent changes in metal fluxes, known as metal muffling. This term refers to the non-steady state dynamics in metal ions that involves temporal expression changes in

homeostatic components, such as uptake, efflux and intracellular compartmentalisation transporters (Colvin *et al.*, 2010).

The role of Cu in hormone biosynthesis and perception has long since been known, mainly for its structural role in ethylene receptors (Rodriguez *et al.*, 1999), and for MoCo formation (Kuper *et al.*, 2004), which is required for the biosynthesis of abscisic acid (ABA) and auxin indol-3-acetic (IAA) *via* indol-3-aldehyde, and is involved in the degradation of polyamines (PA). More recent evidence has shown that Cu homeostasis also play a prominent role in the salicylic acid (SA) signalling pathway (Wu *et al.*, 2012; Yan and Dong, 2014).

5.1. Ethylene

The gaseous plant hormone ethylene is an important regulator of plant growth, development, and responses to abiotic/biotic stresses. During various developmental stages and stress events, such as in senescing plants, ripening fruits, stressed or infected plants, ethylene production can be dramatically induced, which can in turn affect local or neighbouring cells (Kende, 1993; Wang *et al.*, 2002; Yang and Hoffman, 1984). Thus, crucial to the ethylene function is the tight regulation of its biosynthesis. Furthermore, unlike auxin or other plant hormones, ethylene does not need to be actively transported or degraded, making ethylene biosynthesis the key regulatory point to control ethylene levels in plant cells (Bürstenbinder and Sauter, 2012).

Ethylene is synthesized from S-adenosylmethionine (SAM), an activated form of methionine and a common precursor to many biosynthetic pathways (Yang and Hoffman, 1984). SAM is converted to 1-aminocyclopropane-1-carboxylic acid (ACC) by ACC synthase (ACS), and ACC is then oxidized by ACC oxidase (ACO) to produce ethylene (Kende, 1993; Yang and Hoffman, 1984).

Different components of both the ethylene biosynthesis and signal transduction pathways have been identified and, some of them are differentially regulated depending on metal, mainly Fe and Cu, homeostasis (Iqbal *et al.*, 2013). The family of ethylene receptors (ETR1 is one of its members) are cuproproteins where the Cu cofactor is necessary for hormone perception (Rodriguez *et al.*, 1999). In fact, Cu and ethylene form a stable coordination complex that is capable of functioning within a protein (Thompson *et al.*, 1983). Rodriguez *et al.* (1999) showed that, of the many transition metals tested, Cu ions acted as a cofactor for ethylene binding to ETR1. In addition to Cu, only the non-physiological silver and gold ions were capable of supporting ethylene-binding activity in exogenously expressed ETR1 (Binder *et al.*, 2007; Rodriguez *et al.*, 1999).

Further evidence for the importance of Cu on the ethylene-signalling pathway emerged with the discovery that ETHYLENE-INSENSITIVE PROTEIN 2 (EIN2), a central signal transducer on the ethylene-signalling pathway, has a significant homology to NATURAL RESISTANCE-ASSOCIATED MACROPHAGE PROTEIN (NRAMP) divalent cation transporters (Alonso *et al.*, 1999). It has been shown that both ETR1 and EIN2 are also involved in some

ABA responses, and serve as integration knots between both hormones signalling pathways (Wilkinson and Davies, 2010).

Several reports have shown that the effects of metal stress on ethylene production in plants are both metal and concentration specific (reviewed in Keunen *et al.*, 2016). Thus, ethylene overproduction has been reported in *Arabidopsis* plants following Cu excess (Mertens *et al.*, 1999). However, this effect has not been observed when studying plants grown hydroponically (Arteca and Arteca, 2007) or in seedlings (Lequeux *et al.*, 2010), suggesting an effect of plant age. The Cu-inducible expression of *ACS* genes has been described in several species, such as potatoes, garden geraniums and different tobacco cultivars (Schlagnhaufer *et al.*, 1997). A range of Cu concentrations have also produced high ethylene levels, accompanied by toxicity symptoms in leaves and adventitious root formation in white poplars (Franchin *et al.*, 2007).

5.2. Abscisic acid

ABA is a phytohormone that regulates diverse physiological processes such as seed maturation, seed dormancy and stress adaptation (Conti *et al.*, 2014). ABA is also synthesized in various organisms other than plants. These physiological responses are triggered by the fluctuation of endogenous ABA levels, in accordance with changing surroundings or developmental stimuli. Endogenous ABA levels are largely controlled by the balance between biosynthesis and catabolism (Endo *et al.*, 2014).

The novo ABA synthesis and all the catalytic steps take place in the plastids (Finkelstein, 2013). However, ABA is converted into its biologically active form in the cytosol by two enzymatic steps (Nambara and Marion-Poll, 2005; Wasilewska *et al.*, 2008). First, the xanthoxin is translocated to the cytoplasm and reduced to abscisic aldehyde by ABA2 and then, the aldehyde is oxidized to convert its functional group in a carboxylic acid (Cheng *et al.*, 2002; González-Guzmán *et al.*, 2002). This second step is the last step in ABA biosynthesis and, is catalysed by ALDEHYDE OXIDASE1 (AAO1), which requires a MoCo sulfurase (ABA3) (Schwarz and Mendel, 2006). The biosynthesis of MoCo, been widely studied and is closely related to the homeostasis of other metallic elements, such as Cu (Tejada-Jiménez *et al.*, 2013). Although the role of Cu has not been fully elucidated, it is required for the activity of Cnx1G, an enzyme that catalyses the insertion of Mo into molybdopterin (Kuper *et al.*, 2004). To date, Cu was identified as an intermediate in the Mo insertion into the pterine through a metal exchange reaction (Mendel and Kruse, 2012). In agreement with the Cu requirement for MoCo biosynthesis, increased Mo uptake has been observed under Cu deficiency in *Brassica napus* (Billard *et al.*, 2014), although Cu treatment has been reported to inhibit *in vitro* MoCo biosynthesis (Kuper *et al.*, 2004).

In addition to biosynthesis, Cu levels can also affect ABA signalling. The central core of the ABA transduction signal consists of a double negative regulatory system by which ABA binding to a soluble receptor (PYR/PYL) acts as a repressor of type 2C protein phosphatases (PP2C), in turn, negative regulators of SNF1-related protein

kinase 2 (SnRK2). Activated SnRK2 phosphorylates transcription factors, such as ABA-responsive element Binding Factors (ABFs) and ABA Insensitive (ABI), thus affecting gene expression during seed germination and postembryonic growth (Cutler *et al.*, 2010; Umezawa *et al.*, 2009). In addition, ABFs and ABIs are themselves subjected to transcriptional regulation, with WRKY domain transcription factors among their regulators. WRK40 binds the *ABI5* promoter and represses its expression (Chen *et al.*, 2010; Shang *et al.*, 2010). ABI5 participates in the integration of light and ABA signalling since the well-known light signalling transcription factor HY5 binds to the *ABI5* promoter, and ABI5 overexpression restores ABA sensitivity in the *hy5* mutant (Chen *et al.*, 2008; Lau and Deng, 2010). Thus, HY5 plays a critical role in ABA signalling by binding to *ABA-RESPONSIVE ELEMENT* (ABRE) regulatory sequences (Hobo *et al.*, 1999; Marcotte *et al.*, 1989). As reported before (see section 4.4), HY5 has been recently shown to interact with SPL7 (Zhang *et al.*, 2014), which indicates that HY5 is a putative integrator between the ABA and Cu deficiency responses. In line with this, the results obtained by Romero *et al.*, (2012) reported that an ABA-deficient citrus mutant, which is prone to fruit dehydration, was unable to induce early molecular responses to moderate water stress observed in wild-type fruit. Among the transcriptomic responses described, citrus *COPT1*, *COPT2* and *COPT5* transporters were induced in parental, but not in ABA-deficient citrus fruit. Other di- and trivalent inorganic cation transporters were also induced only in parental fruit under those conditions, such as citrus Fe transporters *IRT1*, *NRAMP1*, *NRAMP3* and *FERRITIN*. These results further support the idea of ABA/drought-mediated regulation of the genes involved in metal homeostasis.

6. CADMIUM AND IRON IN RELATION TO COPPER HOMEOSTASIS

Although the molecular mechanisms of metal homeostasis details are being deciphered for individual metals, the putative cross-interactions among diverse metal pathways, that might take place at different levels, remain mostly uncovered. These potential interactions range from metals affecting transcription of the components of a different metal homeostasis element to mis-metalation of proteins that greatly affect their activities (Foster *et al.*, 2014).

6.1. Cadmium toxicity in plants

Cd is a transition metal found naturally in the earth's crust at trace levels, but its concentrations in the environment are rising due to human activities. Although Cd is highly toxic for all organisms, plants are more tolerant and constitute the main entry of Cd to trophic chains, which can contaminate human food [Agency for Toxic Substances and Disease Registry (ATSDR)]. The limit set for Cd in agricultural soils is less than 3 µg g^{-1} dry soil (Clemens, 2006). Plant exposure to large amounts of Cd is especially toxic in roots, where it can be sequestered within vacuoles or incorporated into the xylem, along which it is redistributed throughout the

plant (Lux *et al.*, 2011). Cd concentrations are usually higher in roots than in aerial parts (Fargašová, 2001; Rubio *et al.*, 1994), which not only suggests that the transport of this metal via the xylem is restricted in many plants, but explains why it is found in very small quantities in seeds, fruits and tubers (Lux *et al.,* 2011). In roots, Cd acts as a potent rhizotoxin and affects overall plant growth (Rodríguez-Serrano *et al.*, 2009). Photosynthesis is also sensitive to Cd exposure since chlorophyll and the enzymes involved in CO_2 fixation are Cd targets (Herbette *et al.*, 2006), and it also inhibits PSII photoactivation. Cd toxicity is associated with alterations in the entry and distribution of macro- and micronutrients (Rubio *et al.*, 1994; Tsyganov *et al.*, 2007) as it competes with other cations at protein binding sites and transporters (Clemens, 2006). It is, therefore, important to study how plants are able to adapt and survive differences in the supply of different nutrients when the Cd is present.

Considerable natural variation exists in Cd accumulation in plants, which allows to dissect the processes mediating Cd translocation and accumulation in grains, mainly in rice (Clemens *et al.*, 2013). The study of two Zn and Cd-hyperaccumulators, *Arabidopsis halleri* and *Noccaea caerulescens*, has shed light on the genetic basis of Cd hyperaccumulation. Two genes, which are highly expressed in *A. halleri* roots, are responsible for efficient root-to-shoot Cd translocation: *HMA4* and *NAS2* (Deinlein *et al.*, 2012; Hanikenne *et al.*, 2008). Low xylem loading of Cd in roots has been reported to be responsible for the reduced root-to-shoot translocation of Cd and its accumulation in grains (Uraguchi *et al.*, 2009).

NADPH oxidases have been suggested to play a key role in Cd-induced ROS production (Cuypers *et al.*, 2010; Smeets *et al.*, 2009), and one of the first effects observed in plants exposed to Cd is ROS production, mainly H_2O_2 (Martínez-Peñalver *et al.*, 2012). Depending on the levels, H_2O_2 can either serve as a component in signalling processes or induce a response to oxidative stress damage (Rodríguez-Serrano *et al.*, 2009). Cd also regulates the expression of those genes that encode proteins and are involved in defense against oxidative stress (Cuypers *et al.*, 2011; Keunen *et al.*, 2013; Smeets *et al.*, 2013). Cd-induced changes vary according to the concentration of the metal, plant age, exposure time, and the tissue or organ being studied (Llamas *et al.*, 2000; Rodríguez-Serrano *et al.*, 2009; Sanz *et al.*, 2009).

Moreover, Cu can be substituted by Cd affecting ethylene perception since Cd can be chelated by Atx1 and delivered to Etr1 (Heo *et al.*, 2012). It has been suggested that Cd could be the most phytotoxic inorganic ion able to stimulate ethylene production in plants(Arteca and Arteca, 2007). Cd-induced increases in ethylene production were observed in *Hordeum vulgare*, *Lycopersicon esculentum*, *Pisum sativum*, *Brassica juncea*, *Glycine max*, *A. thaliana* and *Triticum aestivum* plants (Keunen *et al.*, 2016). Therefore, ethylene evolution is observed generally in response to Cu and other metals within a wide range of plant species (Maksymiec *et al.*, 2007).

Among molecular responses in low Cd-accumulating plants, *Solanum torvum* induces the *COPT5* homolog expression under Cd stress in roots (Yamaguchi *et al.*, 2010). Cd has been recently shown to modify Cu

deficiency responses in yeast (Heo *et al.*, 2012). In *Arabidopsis thaliana*, Cd also affect SPL7-mediated expression, including the three plasma membrane-localized Cu transporters, COPT1, COPT2 and COPT6, which are required for basal Cd tolerance (Gayomba *et al.*, 2013).

6.2. Iron availability and its effects on copper homeostasis

Insights into Cu metabolism initially came from experiments aimed at understanding how cells take up the Fe (Andrews, 2001). When Dancis and co-workers were trying to identify components of the high-affinity Fe uptake system in yeast cells, one of the first genes they found encoded a putative transmembrane transport protein that, to their surprise, had no affinity for Fe, but rather transported Cu (Dancis *et al.*, 1994b). This protein supplies the metal for an MCO needed for Fe transport and resulted to be the high affinity Cu transporter Ctr1p (Dancis *et al.*, 1994a). Three groups independently confirmed the presence of MCOs required for Cu transport in mammalian cells (Lee *et al.*, 2001). Thus, proper Cu homeostasis is required for the normal metabolism in most organisms, since Fe mobilization requires ferroxidases, which are MCOs (Gulec and Collins, 2014; Kosman, 2010). Despite the large number of proteins annotated as MCOs in higher plants, no direct correlation between MCO-encoded ferroxidases and Fe transport has been established yet (Bernal *et al.*, 2012).

Fe, as well as Cu, is a transition metal, and both are required by organisms to perform a remarkable wide array of functions that are critical for life. These metal ions are cofactors in proteins that mediate diverse biochemical processes, including energy conversion, synthesis and regulation of nucleic acids, ROS detoxification, as well as signalling events that trigger molecular, cellular and systemic responses (Ravet and Pilon, 2013). Thus, Fe deficiency in plants induces impairment of the respiratory chain and the subsequent retrograde signalling pathways aimed to reprogram the metabolism. These responses include a number of changes that likely represent an adaptive mechanism developed to survive under conditions of nutritional deficiency (Vigani and Briat, 2016).

Although plant Fe acquisition of soil has been traditionally divided into two strategies, recent results have blurred the boundaries that separate them (Kobayashi and Nishizawa, 2012; Darbani *et al.*, 2013). Plants with the strategy I, which includes all plants except grasses, acquire Fe after reduction of Fe^{3+} chelates by a reductase of ferric chelates at the plasma membrane. In *Arabidopsis thaliana* this reductase is encoded by FRO2 and the resulting Fe^{2+} is incorporated by a ZIP family transporter denoted IRT1 (Connolly *et al.*, 2003). Our current understanding of the Fe deficiency sensor and signalling mechanisms in plants is rather limited (Darbani *et al.*, 2013; Kobayashi and Nishizawa, 2012). In *Arabidopsis*, the genes involved in the Fe remobilization and incorporation (such as IRT1 and FRO2) are regulated by the helix-turn-helix type transcription factor FIT (bHLH29) (Colangelo and Guerinot, 2004). Other subgroup Ib bHLH factors (bHLH38,

bHLH39, bHLH100 and bHLH101) are regulated by Fe deficiency (Wang *et al.*, 2007) but, while the first two could act in concert with FIT, mediating Fe responses (Yuan *et al.*, 2008), bHLH100 and bHLH101 control Fe homeostasis by a FIT-independent pathway (Sivitz *et al.*, 2012). In strategy II plants, phytosiderophore of the mugineic acid family chelate Fe^{3+}, that is incorporated through the YSLs. bHLH transcription factors have been also involved in the networks that regulate Fe sensing, uptake and intracellular distribution (Kobayashi and Nishizawa, 2012). Post-transcriptional regulation processes are essential in the Fe deficiency responses (Brumbarova *et al.*, 2015) and BRUTUS (BTS), which is a functional RING E3 ubiquitin ligase with a hemerythrin domain, has been proposed to function as a potential Fe sensor (Kobayashi *et al.*, 2013).

At the intracellular level, a parallel COPT5 function, but with Fe instead of Cu as a substrate, is performed by NRAMP3 and NRAMP4, which redundantly function in Fe mobilization from the vacuole, during seed germination and in adult plants (Lanquar *et al.*, 2005; Lanquar *et al.*, 2010). When grown in Fe-deficient media, the double *nramp3nramp4* mutant is chlorotic and its development is arrested (Lanquar *et al.*, 2005). Mutations in the *VACUOLAR IRON TRANSPORTER 1* (*VIT1*), involved in Fe influx into the vacuoles during embryogenesis (Kim *et al.*, 2006), also compromise the growth of seedlings in Fe limiting conditions. Recently, a genetic screen showed that the *vit1* mutation suppresses the *nramp3nramp4* phenotype, illustrating the plasticity of Fe storage in *Arabidopsis* embryos (Mary *et al.*, 2015).

There are several experimental evidences, other than the MCOs, linking the Cu and Fe homeostases. First, it has been shown that ethylene participates in Fe deficiency responses (Iqbal *et al.*, 2013; Lingam *et al.*, 2011; Lucena *et al.*, 2015) and, as already mentioned, the ethylene receptors, require Cu to trigger downstream signalling (Binder *et al.*, 2010; Rodriguez *et al.*, 1999). Second, the growth defect of the *spl7* mutant in Cu deficient media is partially rescued by Fe addition (Bernal *et al.*, 2012). Moreover, Cu deficiency activates the expression of Fe deficiency markers and the translocation of Fe from the roots to the aerial part is defective when Cu is scarce (Bernal *et al.*, 2012; Waters *et al.*, 2012). On the other hand, opposite to the process taking place under Cu deficiency (section 4.4), under Fe deficiency, the FeSOD is replaced by the Cu/ZnSOD, in a process mediated by the Fe-dependent down-regulation of the *miR398* (Waters *et al.*, 2012). Finally, the *copt2* mutant, has been shown to participate in both Cu and Fe homeostasis (Perea-García *et al.*, 2013). *COPT2* transcript levels also respond to Fe deficiency showing a different expression pattern than the pattern observed under Cu deficiency (Perea-García *et al.*, 2013). Although the role of COPT2 in the intersection between Fe metabolism and in transporting Cu is still poorly understood, a new and uncharacterized Cu-Fe crosstalk process has been suggested, where phosphate metabolism is also involved (Perea-García *et al.*, 2013).

OBJECTIVES

The general purpose of this thesis is the study of the influence of Cu homeostasis on the stress-related hormone biosynthesis and the interaction with other metals in *Arabidopsis thaliana*. To that aim, we have used different mutants affected in high affinity Cu transport, being focussed in the *copt2* and *copt5* loss of function mutants since corresponding to the main plasma membrane and tonoplast COPT transporters, respectively. More specifically, the principal objectives of this work are:

I)   Characterization of the interaction between Cu transport and ABA hormone metabolism.

I.1. Study of Cu transport deregulation effects on ABA metabolism through the phenotypic and molecular characterization plasma membrane COPT transporters, focussing in the *copt2* loss-of-function mutant.

I.2. Biochemical and molecular analysis effects on Cu homeostasis caused by ABA treatments in plants subjected to different Cu availabilities.

I.3. Determination of the influence of Cu scarcity on ABA metabolism by using ABA biosynthesis or signalling mutants and performing their physiological and molecular characterization under Cu deficiency.

II)   Study of the influence of altered intracellular Cu trafficking on other metal homeostasis processes.

II.1. Analysis of the physiological and molecular effects of Cd toxicity in the *copt5* loss-of-function mutant, focusing on the ROS responses under Cu deficiency conditions and the participation of the ethylene hormone in the process, as a stress marker.

II.2. Physiological, molecular and biochemical characterization of the *copt5* mutant under Fe deficiency conditions to analyse a putative interaction between Cu and Fe homeostases.

MATERIALS AND METHODS

1. PLANT MATERIAL

In the present work, *Arabidopsis thaliana* plants ecotype *Columbia* (Col-0) were used as the wild-type (WT) control genotype and transgenic lines indicated in Table M.1 were compared to control when grown on diverse media to determine their phenotypic differences.

Table M.1. Transgenic lines used in the present work.

Name	Type	Origin
copt2		Perea-García *et al.* (2013)
copt1copt2copt6		Gayomba *et al.* (2013)
copt5-2	Loss-of-function by	Garcia-Molina *et al.* (2011)
copt5-3	T-DNA insertion	Garcia-Molina *et al.* (2011)
spl7		Yamasaki *et al.* (2009)
aba2		Saez *et al.* (2006)
hab1-1abi1-2		Saez *et al.* (2006)
nramp3nramp4		Lanquar *et al.* (2005)
COPT1^{OE}	Constitutive overexpression	Andrés-Colás *et al.* (2010)
COPT5^{OE}	driven by the CaMV35S promoter	Garcia-Molina *et al.* (2011)
pCOPT2::GUS	β-glucuronidase activity driven	Perea-García *et al.* (2013)
pCOPT5::GUS	by the endogenous promoter	Garcia-Molina *et al.* (2011)
pCOPT2::LUC	Luciferase activity driven by the endogenous promoter	Perea-García *et al.* (2016)
pCOPT5::COPT5::GFP	*complemented COPT5*	Garcia-Molina *et al.* (2011)

1.1. Growth conditions of the *Arabidopsis thaliana* plants

Along this work, three different systems were used to grow *A. thaliana* seedlings and plants:

1.1.1. Soil

The soil composition used to grow *Arabidopsis* seeds was peat moss, sand and vermiculite in these proportions 2:1:1. The plants were grown in greenhouse conditions (SCSIE, Universitat de València). Plants were watered with 0,5X Hoagland's solution (*Sigma*) twice a week. This system was used to obtain the seeds for the rest of experiments performed in the laboratory.

To quantify metal content in seeds, the plants were watered with tap water until 20 day-old and, at that point, Cu treatments were initiated, using Hoagland's solution with 0.1 µM $CuSO_4$ (+Cu) or not (-Cu). The Hoagland's solutions composition used was:

Hoagland 0.5X: [K_2SO_4 0.44 mM, KH_2PO_4 0.125 mM, NaCl 10 µM, $Ca(NO_3) \cdot 4H_2O$ 1 mM, $Mg(SO_4) \cdot 7H_2O$ 1 mM, $Na_2SO_4 \cdot 10H_2O$ 1 mM, Fe-EDTA 20 µM, H_3BO_3 10 µM, $ZnSO_4 \cdot 7H_2O$ 1 µM, $MnSO_4 \cdot H_2O$ 1 µM, MoO_3 0.1 µM, $CuSO_4 \cdot 7H_2O$ 0.1 µM], buffer MES 0.05 % (p/v) and pH 5.7-5.8 with KOH (Hoagland and Arnon, 1950).

1.1.2. Petri dish culture

This system was used for short-term experiments with *Arabidopsis* seedlings, usually 7 days after germination, to test their sensibility to the nutritional treatment. Before sown, seeds were stratified for 2 days at 4°C and surface-sterilized with sequential washes in 70% ethanol (5 min), bleach (5 minuts) and water (2 x 2 minuts), resuspended in agar 0.1% (w/v). The *A. thaliana* seedlings were grown in chambers (*Sanyo MLR-350*) with 50-60% of relative humidity. The light intensity, generated by fluorescent tubes of white light, was approximately 65 µmol/m^2/s. The photoperiod and the temperature used were intermedium or neutral day, 12 hours of light at 23°C and 12 hours of darkness at 16°C (LDHC). Seeds were sown on Petri dishes containing:

a) Standard growing medium ½ MS (Murashige and Skoog, 1962) [Murashige and Skoog (MS) basal salt mixture *Sigma*] supplemented with sucrose 1% (w/v), MES 0.5% (w/v), KOH pH 5.7 and 0.8% agar (w/v).

b) Standard medium ½ MS supplemented with 1 µM $CuSO_4$ to generate Cu sufficiency.

c) Standard medium ½ MS supplemented with 100 µM bathocuproinedisulfonic acid disodium (BCS) *(Sigma)* to generate Cu severe deficiency.

d) Standard medium ½ MS supplemented with 30 µM $CdCl_2$ to test Cd toxicity.

e) Standard medium ½ MS supplemented with ABA (2-cis, 4-trans-Abscisic acid, *Sigma*) hormone at different concentrations to study exogenous treatment.

f) Standard medium ½ MS supplemented with 200 mM NaCl for salt stress treatment.

g) Growing medium ½ MS prepared with Murashige and Skoog basal salt macronutrient solution (*Sigma*) and micronutrient solution containing: H_3BO_3 50 μM, $MnSO_4 \cdot H_2O$ 36.6 μM, $ZnSO_4 \cdot 7H_2O$ 15 μM, $NaMoO_4 \cdot 2H_2O$ 0.57 μM y $CoCl_2 \cdot 6H_2O$ 0.05 μM, Fe-citrate 50 μM, KI 0.25 mM, $CuSO_4$ 1 μM, MES 0.05%, sucrose 1 % (w/v), MES 0.5% (w/v), KOH pH 5.7 and 0.8% agar (w/v).

h) ½ MS medium with 1 μM $CuSO_4$ and 50 μM Fe-citrate to generate both Cu and Fe sufficiency.

i) ½ MS medium supplemented with metal chelators, 50-100 μM BCS (*Sigma*) and/or 100 μM Ferrozine [3-(2-Pyridyl)-5,6-diphenyl-1,2,4-triazine-p,p'-disulfonic acid monosodium salt hydrate *Sigma*], to obtain both Cu and Fe deficiency.

j) Liquid medium: the same as the ½ MS medium without agar.

1.1.3. Hydroponic system

Hydroponic cultures were performed from seedlings germinated in eppendorf tubes filled with standard ½ MS medium without sucrose, to avoid contaminations, for 2 weeks. Then, they were transferred to black boxes (*Araponics* systems) containing Hoagland (0.5X) nutrient solution, as described in (Hermans and Verbruggen, 2005), during 1 week. After that, different treatments were performed. This system was used for long-term treatments during 16-day period. Plants were grown in this system for 31 days and the solution was changed every 3 days to avoid changes in pH, nutrient consumption, contaminations and anaerobic conditions. The different treatment solution used were:

a) Hoagland 0.5X from stock solutions [K_2SO_4 0.44 mM, KH_2PO_4 0.125 mM, NaCl 10 μM, $Ca(NO_3) \cdot 4H_2O$ 1 mM, $Mg(SO_4) \cdot 7H_2O$ 1 mM, $Na_2SO_4 \cdot 10H_2O$ 1 mM, Fe-EDTA 20 μM, H_3BO_3 10 μM, $ZnSO_4 \cdot 7H_2O$ 1 μM, $MnSO_4 \cdot H_2O$ 1 μM, MoO_3 0.1 μM, $CuSO_4 \cdot 7H_2O$ 0.1 μM], MES 0.05 % (w/v) buffer and pH 5.7-5.8 with KOH (Arnon and Hoagland, 1938).

b) For Cu-deficiency treatment, $CuSO_4 \cdot 7H_2O$ was removed from the Hoagland solution.

c) To test Cd toxicity, $CdCl_2$ (2.5-10 μM) was added to the original solution.

In all cases, intermediate photoperiodic conditions (12 hours light, 20-23°C/12 hours darkness, 16°C) were used in the growing chambers.

2. TECHNIQUES FOR PLANT STUDIES

2.1. Physiological parameters

For primary root length determinations, plates were placed vertically in a growth chamber and roots were measured with the *Image J 1.42 q software* (https://imagej.nih.gov/ij/). The green cotyledon rate (GCR) was calculated as percentage of green cotyledons over total germinated seeds. Leaf chlorophyll was measured as the chlorophyll content index (CCI) by a portable chlorophyll meter (CCM-200, *Opti Sciences*, USA). Average values per plant were obtained from three different leaves. Five plants were analyzed for each sampling condition.

Absolute growth rates (AGR) represent the mean daily length (roots) or fresh weight (aerial part) increase during this period, and are expressed as percentages of the WT control plants.

2.2. Determination of ethylene production and Abscisic Acid (ABA), Indol-Acetic Acid (IAA) and Jasmonic Acid (JA) content

Plants were introduced into glass flasks containing 3 ml of nutrient solution, sealed with a rubber septum and kept for 24 hours in the darkness. The ethylene released to the head space was analyzed in a gas chromatograph (*Shimadzu* GC-14B) equipped with a packed alumina column and a Flame Ionization Detector (FID). One ml of gas from the head atmosphere of the flasks was extracted with a syringe, injected at 120°C and run isothermally at the same temperature. Detection was performed at 150°C. An external standards quantitation method was followed with the *Shimadzu* CLASS-VP™ program.

Fresh *Arabidopsis* material was washed once with 20 μM EDTA and 3 times with MilliQ water. For ABA, IAA and JA determinations, plant material was lyophilized and then analyzed by HPLC at the phytohormones quantification service at IBMCP (CSIC, Valencia, Spain).

2.3. Determination of metal content

The fresh *Arabidopsis* material was washed once with 20 μM EDTA and 3 times with MilliQ H_2O, dried at 65°C for 2 days and digested with 65% (v/v) HNO_3 at 80-90°C. Digested samples were then diluted with Millipore H_2O (*Purelab Ultra*), and the Cu, Mo and Fe contents were determined by ICP-MS at the "Servicios Centrales de Soporte a la Investigación" (Universidad de Almeria, Spain).

For the results obtained in chapter 3, Cu and Fe contents were determined by Microwave Plasma- Atomic Emission Spectroscopy (MP-AES *Agilent technologies*) at the INRA institute (Montpellier, France) using manufacturer's standard solutions for the calibration curves. The plant material was digested using the same method as mentioned before in this section.

3. HISTOLOGICAL PROCEDURES

3.1. Fixation, dehydration and resin inclusion

Plant material was fixed for 24 hours in 90 ml of 70% ethanol, plus 5 ml of 40% formaldehyde and 5 ml of glacial acetic acid. Next, plant material was dehydrated in consecutive baths at increasing ethanol concentrations: 70%, 96% and 100% (2 x 30 minutes each). Finally, plant material was incubated at 4°C for 3 hours in *LR-White* resin (*Sigma*) in 100% ethanol (1:3, v/v) and the sections obtained were stained with toluidine blue. The roots and 3 day-old seedlings were previously rinsed with EDTA and distilled water. The fixed samples were washed with 0.1 M Na-phosphate buffer (pH 7.4) three times, and dehydrated in successive baths of 50, 70, 90, 95, and 100% Ethanol, butanol/ethanol 1:1 (v/v) and 100% butanol. Then, the tissues were embedded in the *Technovit 7100* resin (*Kulzer*) according to the manufacturer's instructions and thin sections (3 µm) were sliced.

3.2. Oxidative stress staining

In order to detect the *in situ* production of H_2O_2, 3, 3'-diaminobenzidine tetrahydrochloride (DAB) (*Sigma*) staining was carried out according to (Thordal-Christensen *et al.*, 1997) with minor modifications. Seven-day-old plants were grown as described above, incubated in 1 mg/ml DAB solution (pH 3.5) for 4 hours in the dark at room temperature and then transferred to 90% (v/v) ethanol at 90°C to completely remove chlorophylls from green tissues. Prior to imaging, samples were suspended in 10% lactic acid.

3.3. Perls staining coupled to diaminobenzidine intensification

For organ staining, the seedlings were vacuum infiltrated with equal volumes of 4% (v/v) HCl and 4% (w/v) K-ferrocyanide (Perls stain solution) for 15 minutes and incubated for 30 minutes at room temperature (Stacey

et al., 2008). The DAB intensification was performed according to Roschzttardtz *et al.*, 2009. After washing with distillated water, the seedlings were incubated in a methanol solution containing 0.01 M NaN_3 and 0.3% (v/v) H_2O_2 for 1 hour, and then washed with 0.1 M phosphate buffer (pH 7.4). For the intensification reaction, the seedlings were incubated between 10 and 30 minutes in a 0.1 M phosphate buffer (pH 7.4) solution containing 0.025% (w/v) DAB, 0.005% (v/v) H_2O_2, and 0.005% (w/v) $CoCl_2$ (intensification solution). Rinsing with distilled water stopped the reaction. For the *in situ* Perls/DAB/H_2O_2 intensification, different organs were vacuum infiltrated with the fixation solution containing 2% (w/v) paraformaldehyde, 1% (v/v) glutaraldehyde, 1% (w/v) caffeine in 100 mM phosphate buffer (pH 7) for 30 minutes and incubated for 15 hours in the same solution. The roots were previously rinsed with EDTA and distilled water. The fixed samples were washed with 0.1 M Na-phosphate buffer (pH 7.4) three times, and dehydrated in successive baths of 50, 70, 90, 95, and 100% ethanol, butanol/ethanol 1:1 (v/v) and 100% butanol. Then, the tissues were embedded in the *Technovit 7100* resin (*Kulzer*) according to manufacturer's instructions and thin sections (3 μm) were cut. The sections were deposited on glass slides that were incubated for 45 minutes in Perls stain solution. The intensification procedure was then applied as described above. The pictures of the cross sections were obtained using the microscope *Olympus* BX61 and the software was Cell-A. For the pictures of whole seedlings, a stereoscopic microscope *Olympus* SZX16 was used.

3.4. Beta-glucuronidase assay

Assays were performed as described (Jefferson *et al.*, 1987). Briefly, the seedlings and organs from the adult *pCOPT5::GUS* and *pCOPT2::GUS* plants were embedded with the substrate solution [100 mM $NaPO_4$, pH 7.2, 0.5 mM $K_3Fe(CN)_6$, 0.5 mM $K_4Fe(CN)_6$, 0.1% (v/v) Triton X-100, 0.5 mM 5-bromo-4-chloro-3-indolyl-β-D-glucuronide (*AppliChem*) and 10 mM EDTA, pH 7.2]. Reactions took place at 37°C and were stopped with ethanol (70%). The material was fixed, dehydrated and imbibed in resin to obtain cross sections (see section 3.1). The pictures of the cross sections were obtained using the microscope *Olympus* AT70F and the Infinity software.

4. ISOLATION AND ANALYSIS OF NUCLEIC ACIDS

4.1. Total RNA extraction

The plant material was collected and washed with EDTA 20 µM and H_2O Milli-QPLUS (*Millipore*) and then was frozen with liquid N_2 and kept in -80°C until its utilization. Total *Arabidopsis* RNA was extracted with *Trizol Reagent (Ambion)* using the instructions of the manufacturer. Briefly, 100 mg of tissue was used for 1 ml of Trizol reagent previously grinded with micropistil. Then, it was centrifuged at 4°C during 10 minutes at full speed. After that, the supernatant was mixed with 200 µM chloroform and it was centrifuged again, with that was obtained an aqueous phase containing the nucleic acids. This phase was mixed with isopropanol (1:1) during 20 minutes at -20°C to precipitate the RNA. The mix was centrifuged during 10 minutes at 4°C to collect the precipitate, and then was washed with ethanol 70%. The sediment was resuspended in 100 µM of H_2O and was incubated during 10 minutes at 65°C. Finally, the samples were centrifuged during 5 minutes at 8000 rpm and the supernatant was recovered. The extract (1 µl) was quantified using a spectrophotometer *NanoDrop 2000* (*Thermo Scientific*). The RNA extraction for the hybridization of the microarray was performed using *RNeasy Plant Mini* (*Qiagen*).

Thereafter, the quality of the RNA was checked by gel electrophoresis (see section 4.2.1). The next step after RNA extraction was to remove the DNA in the samples. For that, the samples were treated with *Dnase I Amp Grade (Invitrogen)*, RNAse free, at 25°C during 15 minutes. To stop the treatment, 1 µl of EDTA 25 mM was added to each sample and were incubated at 65°C during 10 minutes.

4.2. Analysis of nucleic acids

4.2.1. RNA electrophoresis

The RNA electrophoresis gels were prepared using agarose 1% (w/v) in MOPS buffer [MOPS 40 mM, sodium acetate 10 mM, EDTA 1 mM pH 8.0] and formaldehide 2.2 M. The samples were solubilized with sample buffer [deionized formamide 65% (v/v) in MOPS 1X, formaldehide 7% (v/v) and etidium bromide 20 µg/ml], were denaturated at 65°C during 10 minutes and were separated at 70-100 V in an electrophoretic systems (*Biorad*). Finally, the gel was visualized using an ultraviolet transilluminator (*Uvitec*).

4.2.2. cDNA synthesis

Firstly, the cDNA was synthesized from RNA (1.5 µg/µl) by reverse transcription reaction (RT-PCR). The RT-PCR was performed by adding reverse oligonucleotides [oligo (dT)15] 50 µg/µl (*Roche*). Thereafter, the RNA was denaturated at 70°C during 10 minutes, and then, was cooled on ice. Secondly, 4 µl of RT 5 X buffer and 2 µl of 0.1 M of DTT (both from Invitrogen), 0.5 µl of *RNase OUT* (*Invitrogen*), 1µl of dNTPs 10 mM (Promega) and 1 µl of *SuperScript II reverse transcriptase* 200 U/µl *(Invitrogen)* were added. The reaction took place during 1 hour and 30 minutes at 42°C. Finally, the enzyme was inactivated at 70°C during 10 minutes.

4.2.3. Semiquantitative PCR

The cDNA obtained was used as a template for the amplification of a housekeeping gene as a control of the quality of cDNA synthesis. A PCR was performed with a reaction mix that contained template, forward and reverse oligonucleotides (0.5 µM) of the Actine (housekeeping gene) (Table M.2), 0.5 µl of dNTPs 10 mM, 2.5 µl of buffer 10 X (*Bioline*) and 0.75 µl of $MgCl_2$ (*Bioline*) 1.5 mM with 0.2 µl BioTaq polymerase 0.5 U (*Bioline*), in a final volume of 25 µl. The PCR conditions were denaturation at 94°C, hybridization at 55°C and elongation at 72°C. The PCR products were analyzed by electrophoresis.

4.2.4. Real-time quantitative PCR

qRT-PCR was carried out with SYBR-Green qPCR Super-Mix-UDG with ROX (*Invitrogen*). Gene-specific primers were designed with the Primer3 software (http://bioinfo.ut.ee/primer3-0.4.0) and are detailed in Table M.2. The mix containing cDNA and SYBR-Green was used in a CFX96 Touch™ Real-Time PCR Detection System (*BioRad*) with 1 cycle of 50°C for 2 minutes, an initial denaturation cycle at 95°C for 2 minutes, and a series of 40 cycles of denaturation and amplification at 60°C for 30 seconds, and 72°C for 10 seconds. To transform fluorescent intensity measurements into relative mRNA levels, the analysis method of $2^{-\Delta\Delta Ct}$ (Livak and Schmittgen, 2001) was used. The *UBIQUITIN10* reference gene was used for data normalization. Each sample was analyzed in triplicate and mean ratios ± SE were calculated.

Table M.2. Selected genes and primers used for PCR and qRT-PCR analyses.

GENE	FORWARD (5'→3')	REVERSE (5'→3')
ACTIN	GGCGATGAAGCTCAATCCAAACG	GGTCACGACCAGCAAGATCAAGACG
ABI5	ACTTCCAGCTCCGCTTTGTA	GGTTGTCTAGCCGCAGTCTC
BCB	CGGAGGACTACGATGTTGGT	TAATTTTGACCGGAGGAACG
BHLH38	AGAGCTGCAACAGCAAGTGA	ACCAAGCCTAGTGGCAGAAA
BHLH39	CAGAGCTGCAAGAGCAAGTG	ACCAAGCCTAGTCGCAGAAA
BHLH100	AAACCGACGACGTATCCAAC	GATTGGTGGGAGGAGACAA
BHLH101	TTGCTGTCCAGTTGCTACG	GGCGTAATCCCAAGAGACATA
BRUTUS	GCTCTGGCACAAGTCAATCA	CGTTCATCAAATGCCGATAA
COPT1	TTGCAATTTTCCTCTCCTCCCAA	ATGATGGTCGAGGCATT
COPT2	CCTTTCGTATTTGGTGATGCT	AAACACCTGCGTTAAAGGAC
COPT5	TTGCAGCTATGTCTTTCAA	CGGCGGTTAATCCGACGACA
COPT6	GCAGTCTACACACTCAAGACA	AAAGGACATAACGGCGAGCA
CSD1	CATCATTGGTCTCCAGGGCT	GACCTCCTTATTACATCAAT
CSD2	GTCCTACAACTGTGAAT	TCCATGAGGCCCTGGAGT
FIT	TTTTCGCGGTATCAATCCTC	GGTATGTGTCCGGAGAAGGA
FRO2	GTTGGTTTATAGCCCGACGA	GGGCCGTAAGGACCTTCTAC
FSD1	ACCGAAGACCAGATTACATA	TGGCACTTACAGCTTCCCAA
HY5	GTTTGGAGGAGAAGCTGTCG	TCTTGCTTGCTGAGCTGAAA
IRT1	CCCCGCAAATGATGTTACCTT	GGTATCGCAAGAGCTGTGCAT
NRAMP4	TTGGAGCATTGGTCCCTAAG	GAAAGAAACCGCAAGAGCAC
NCED3	ATTGGCTATGTCGGAGGATG	CGACGTCCGGTGATTTAGTT
RBOHD	CGAGGAGCTAACTCGGACAC	GCGTGATCTCCACGTACTCA
SPL7	AGTTTGACGGGACCTGAATG	AGTTTGACGGGACCTGAATG
UBQ10	TAATCCCTGATGAATAAGTGTTCTAC	AAAACGAAGCGATGATAAAGAAG
WRKY18	ACAGCTCCAGCAACGAAGAT	GGTGACGGGTTGTCTCTTGT
WRKY40	GTGGAGGATCAGTCCGTGTT	TCTGAACTTGGGGAAAATCG
ZIP2	CGCTTGGAGAAACCTATGGA	CGACACCTATGGGACTCGAT

4.2.5. Microarray analysis

Three biological replicates (7 day-old seedlings of WT and *copt5-2* plants grown in a 12 h light/12 h dark photoperiod) were obtained for each treatment. Cu-deficient medium was supplemented with 100 µM BCS, whereas Cu sufficiency was 1 µM $CuSO_4$. Total RNA was isolated using the RNeasy Plant Mini Kit (*Qiagen*) as mentioned in section 4.1, and antisense RNA was amplified using the *MessageAmp II aRNA Amplification kit* (*Ambion*). The slide *Arabidopsis* (V4) Gene Expression Microarray, 4 x 44K (*Agilent technologies*) was provided and hybridized by the technical services of IBMCP (Valencia, Spain). The expression values (log_2), data normalization and statistical analyses were obtained using the Genespring GX microarray analysis software (*Agilent technologies*). Differential expressed genes (DEG) were identified applying a false discovery rate (FDR) lower than 1% and 1.5-fold change ($log_2 |1.5|$). Gene expression values there were scaled as Z core (Zhang *et al.*, 2014) and then plotted in a heatmap. FatiGO[+] (Babelomics, http://bioinfo.cipf.es/), developed by Al-Shahrour *et al.*(2004), was used to identify biological processes significantly under- or overrepresented in a set of DEG belonging to one heatmap pattern. The microarray raw data were deposited in the National Center for Biotechnology Information Gene Expression Omnibus (Edgar *et al.*, 2002) and are accessible through accession number GSE91044.

5. ISOLATION AND ANALYSIS OF PROTEINS AND LIPIDS

5.1. Protein extraction

The total soluble protein extraction was performed using 7 day-old seedlings material frozen and grinded with liquid N_2. Next, cold grinding buffer [1 M K_2HPO_4 (2 ml), 1 M KH_2PO_4 (495 µl), Ascorbate (50 mg), beta-mercaptoethanol (25 µl), Triton X-100 (100 µl), H_2O d (until 50 ml)] (Abdel-Ghany *et al.*, 2005b) was added to all samples and vortex for 2 minutes. Samples were centrifuged for 10 minutes at 14000 rpm at 4°C. After, the supernatant was removed, transferred in a new tube and centrifuge for another 10 minutes. The remaining supernatant contained native soluble protein extraction. Total protein was quantified according to Bradford (1976) method using bovine serum albumin as a standard.

5.2. Immuno-detection of proteins

The soluble proteins were denaturated by adding sample buffer with SDS and incubating the samples for 5 minutes at 98°C. 35 μg of protein extract were loaded into 15% electrophoresis gel SDS-PAGE. The proteins were electrotransferred into a nitrocellulose membrane and stained with Ponceau staining as a loading control. Membranes were incubated with blocking solution (milk 5%) during 20 minutes. First antibody anti-FeSOD (1:2000) and anti-CSD2 (1:2000) rabbit polyclonal (*Agrisera*) was added and incubated o/n at 4°C with shaking. Next, after several washes with Tween-TBS, membranes were incubated with secondary antibody (goat anti-rabbit) conjugated with peroxidase (*Sigma*) enzyme during 1 hour. Protein detection was revealed using chemiluminescent *ECL* kit (*Amersham*).

5.3. Superoxide dismutase activity

For SOD isoenzyme separation and activity, 100 μg of protein extract were loaded into 15% non-denaturating polyacrylamide gels. Then, the gels were stained with NBT (*Sigma*) (1 mg/1 ml) during 30 minutes in darkness. The excess of NBT was removed with H_2O d and gels were incubated with untreated strain [1 M K_2HPO_4 (1.47 ml), 1 M KH_2PO_4 (148 μl), Riboflavine (450 μl), TEMED (145 μl), H_2O d (until 45 ml)] during 25 minutes shaking in darkness. The gels were washed with H_2O d to remove the excess of the untreated strain and were exposed to intense light until bands appeared (Abdel-Ghany *et al.*, 2005b; Beauchamp and Fridovich, 1971). Each experiment was replicated five times with identical results, and representative gels are shown.

5.4. Bioluminiscense luciferase assays

To perform the bioluminescence assays, the *pCOPT2::LUC* plants were grown for 6 days in an intermediate photoperiod (LDHC) in ½ MS dishes, as described above. Afterward, seedlings were transferred to a 96-well white plate (*Thermo-fisher*) with ½ MS medium containing 3% sucrose, and were supplemented with increasing concentrations of ABA. Assays were performed as described by Jefferson *et al.* (1987). Briefly, for the enzymatic reaction, substrate D-luciferine (*Sigma*) (0.42 mg/ml), resuspended in 0.01% Triton X-100, and Tris-acetate 1 M pH 7.75 buffer were added to each individual well. The plate was closed with optic film cover Microseal B# Film (*Biorad*). After one more cycle under the LDHC conditions (acclimation), the plate was transferred to continuous light and constant temperature conditions (LLHH). Bioluminescence intensity was measured in a Luminoskan Ascent luminometer. Data were processed with the Ascent 2.6 software (*Thermo Scientific*) and expressed in 'relative light units'.

5.5. Determination of lipid peroxidation

To measure lipid peroxidation, frozen rosette leaves and roots were ground in malondialdehyde (MDA) extraction buffer [15% (v/v) trichloracetic acid, 0.37% (w/v) 2-thiobarbituric acid, 0.24N HCl, 0.0001% (w/v) butilatedhydroxytoluene] to be then boiled at 80°C for 1 hour to generate MDA-derivatives, which were determined by subtracting A_{535}-A_{600} (ε = 1.56 x 10^5 $M^{-1}cm^{-1}$). Values were normalized to nmol g^{-1} FW.

6. DATA PROCESSING

6.1. Statistical analyses

The statistical analysis of the relative expression was performed by comparing the relative expression of the genes (RT-PCR) based on the pair-wise fixed reallocation randomization test (P <0.05) (Pfaffl *et al.,* 2002). Chi-squared tests, followed by two-tailed z-tests, were run for the analysis of rates (P ≤ 0.05). For the other parameters, one-way ANOVAs were performed. Significant differences between means were established after *post hoc* tests (Tukey or Games-Howell, according to data homoscedasticity, P ≤ 0.05) using the *IBM* SPSS Statistics software, version 19.0.0. Data are provided as the mean values ± SD of at least three independent experiments, as indicated in the figure legends.

6.2. *in silico* analyses

The genomic sequences from *Arabidopsis thaliana* were obtained from the Phytozome Database (www.phytozome.net). The promoter sequences were defined as the 2000 bp upstream of the five prime untranslated region (5'-UTR) from the corresponding genes. Then, they were analyzed in the PLACE database (www.dna.affrc.go.jp/PLACE). The Cu-responsive elements (CuRE, GTAC) and the commonest and most abundant ABA responsive elements, including ABRE (ACGTGG/TC), MYB (CNGTTR) and MYC (CANNTG), were identified and an approximate scale drawing was shown.

RESULTS AND DISCUSSION

CHAPTER 1:

INTERACTION BETWEEN ABA SIGNALLING AND COPPER HOMEOSTASIS IN *ARABIDOPSIS THALIANA*

1. COPT transporters and hormonal effects

Little is known about how hormones influence Cu homeostasis to adapt nutrient availability to the growth requirements while avoiding its toxic effects. As a first approach to address hormone influence on Cu homeostasis, an *in silico* search for the putative hormone-responsive elements present in the promoters of the high affinity COPT transporters from *Arabidopsis thaliana* was undertaken (Table P.1).

The most abundant putative hormone-responsive *cis*-elements present in the promoters from *Arabidopsis COPT* family members are those involved in gibberellic acid (GA) and ABA signalling. It should be noted that the number of GA-related elements is larger in the *imCOPTs* than *pmCOPTs*. In addition, the *pmCOPTs* show more ABA-related elements than *imCOPTs* (Table P.1). Otherwise, ethylene and auxin presented a similar number of *cis*-elements. For ethylene, all *COPTs* members' show a similar number of regulatory elements while for auxin, *COPT1* has no elements and *COPT5* has the largest number of them. JA-related elements are less abundant in *Arabidopsis COPT* family members being present just in *COPT1* (Table P.1).

The *cis*-acting elements and *trans*-acting factors involved in ABA-induced gene expression have been extensively analysed. The main ABA responsive *cis*-elements are ABRE (ABA-responsive element), MYB/MYC and DPBF (Dc3–Promoter Binding Factor; Nakashima *et al.*, 2014). The ABRE motifs have been identified in the promoter region of ABA-inducible genes and several basic leucine zipper proteins (bZIP) have been shown to bind these motifs (Fujita *et al.*, 2011). The presence of ABRE motifs in the *Arabidopsis COPTs* promoters of the members located at the plasma membrane (Table P.1) could be related to an early response to dehydration in vegetative parts with dark-induced senescence, as suggested by Simpson *et al.*(2003). The presence of drought- and ABA-related MYB and MYC motifs, mostly in the *COPTs* promoter members of the *Arabidopsis* plasma membrane-located transporters (Table P.1), also suggests that these transporters could be regulated under developmental or stressful conditions by increasing ABA content. DPBF and DREB (dehydration responsive element binding) motifs, which have been described to play an important role in the ABA response, in seeds and during early seedling establishment stages (López-Molina and Chua, 2000), though scarce, are present in internal membrane-located *Arabidopsis COPTs* members (Table P.1).

Table P.1. Analysis of the putative hormone-responsive cis-elements in the COPTs promoters. The *Arabidopsis thaliana* COPTs genomic sequences were obtained from the phytozome database (www.phytozome.net). The COPT promoter sequences were defined as the 1000 bp upstream of the five prime untranslated region (5'-UTR) from the corresponding genes. The *in silico* analysis of the *cis*-elements present in the promoter regions was performed in the PLACE database (www.dna.affrc.go.jp/PLACE). The commonest and most abundant *cis*-elements are shown for each hormone, including ABRE (ACGTGG/TC), DPBF (ACACNNG), DREB (A/GCCGACNT), MYB (CNGTTR), MYC (CANNTG), CARE (CAACTC), GARE (TAACAAA), WRKY (C/T)TGAC(T/C), ERE (AWTTCAAA), WBOX ERF3 (TGACY), ASF1 (TGACG), the SAUR motif (CATATG), SURE (GAGAC), the GCC core (GCCGCC) and T/G BOX (AACGTG). The rest of the putative *cis*-elements are included in the "Others" group.

Hormones	Motifs	*Arabidopsis thaliana*					Total
		COPT1	*COPT2*	*COPT3*	*COPT5*	*COPT6*	
ABA	ABRE	4	3	-	3	8	18
	DPBF	1	-	1	2	2	6
	DREB	-	-	-	1	-	1
	MYB-MYC BOX	6	6	2	1	4	19
	Others	-	-	-	-	1	1
	TOTAL	**11**	**9**	**3**	**7**	**15**	**45**
GA	CARE	-	1	-	1	1	3
	GARE	1	5	8	2	2	18
	WRKY	3	4	9	9	9	34
	Others	3	1	3	3	2	12
	TOTAL	**7**	**11**	**20**	**15**	**14**	**67**
ETHYLENE	ERE	-	1	-	-	-	1
	WBOX ERF3	2	4	4	4	7	21
	Others	1	-	-	1	-	2
	TOTAL	**3**	**5**	**4**	**5**	**7**	**24**
AUXIN	ASF1	-	3	3	3	1	10
	SAUR	-	-	-	-	-	-
	SURE	-	-	1	6	1	8
	Others	-	-	-	4	-	4
	TOTAL	**-**	**3**	**4**	**13**	**1**	**22**
JA	GCC CORE	-	-	-	-	-	-
	T/G BOX	1	-	-	-	-	1
	TOTAL	**1**	**-**	**-**	**-**	**-**	**1**

GA is an essential phytohormone that controls many aspects of plant development and its antagonist role with ABA is well-known (Weiss and Ori, 2007). The WRKY family is one of the largest transcription factor families involved in GA and ABA responses, and in defence against pathogens and senescence in *Arabidopsis* (Eulgem *et al.*, 2000). Accordingly, many WRKY putative *cis*-elements are present in *COPTs* promoters in *Arabidopsis* (Table P.1). Most published

WRKY proteins bind to the cognate *cis*-acting element containing the W-box in the promoter (Xie *et al.*, 2005). The GA response GARE *cis*-element and the pyrimidine box (included in *"Others"*; Table P.1) are required in *Arabidopsis* to modulate endogenous GA concentrations during seed germination (Ogawa and Hanada, 2003).

ETHYLENE INSENSITIVE3 (EIN3) is a transcription factor that binds to the promoters of the target genes denoted *ETHYLENE RESPONSIVE FACTORS* (*ERFs*). ERFs might also play a role in ABA signalling, and they encode transcription factors that bind to the promoters containing a GCC motif by either activating or repressing target genes (Nakano *et al.*, 2006). Ethylene WBOX ERF3 is the prevalent *cis*-element in *COPTs* promoters (Table P.1). ERFs are often involved in the transcription of the defence genes that encode antifungal proteins, including chitinases and glucanases, in response to ethylene and fungal elicitors (Nishiuchi *et al.*, 2004).

Available data indicate that auxins seem to be the main hormonal mediators of root responses at soil nutrient levels. According to Lequeux *et al.* (2010), Cu excess remodelates root auxin distribution, and thus affects the mitotic activity of the meristem. Yuan *et al.*, 2013 reported that this Cu-induced auxin redistribution involves efflux carrier PIN1, which is responsible for root acropetal auxin transport. Among auxin *cis*-elements, SURE and ASF1 are the prevalent elements (Table P.1) and are related to sulfur transport in the root epidermis and cortex cells (Maruyama-Nakashita *et al.*, 2005).

Taken into account that one of the most abundant elements in this *in silico* study is the putative ABA-responsive *cis*-regulatory boxes, we tested the responses of the knockout *COPT* mutants available in the lab for ABA exogenous treatment (Figure P.1.1 and P.1.2). These mutants include the *pmCOPTs*: *copt1*, *copt2*, *copt6* and the triple *copt1copt2copt6* and the *imCOPTs*: *copt3* and *copt5*. To that end, the mutants were grown in ½ MS standard medium and different ABA concentrations were added to the medium. The sensitivity of the mutants to the exogenous application of ABA in the medium was analysed by measuring two physiological parameters, the root length (Figure P.1.1) and the green cotyledon rate (GCR) (Figure P.1.2).
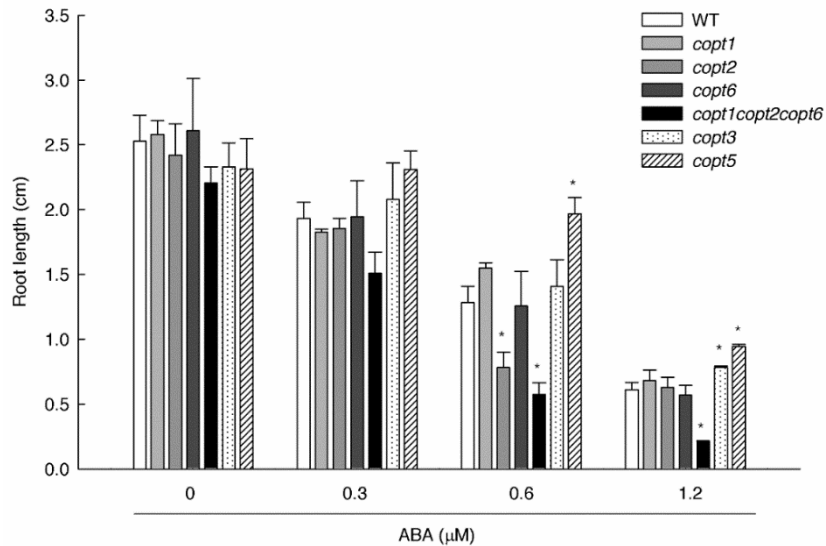
Figure P.1.1. Root length sensitivity to ABA treatments of the *copts* mutants. Root length of 7 day-old WT, *copt1*, *copt2*, *copt6*, *copt1copt2copt6*, *copt3* and *copt5* mutant seedlings grown in ½ MS standard medium in the presence of different ABA concentrations (0, 0.3, 0.6, 1.2 μM). Asterisks indicate statistical differences (P<0.05) according to Tukey's test with respect to the WT under the same condition.

The WT and *pmCOPTs* and *imCOPTs* mutant seedlings were grown for 7 days in ½ MS standard medium, which was slightly Cu deficient (see materials and methods). There were no differences in root length between WT and *copt* mutants in ½ MS with 0 μM of ABA (Figure P.1.1). However, when the ABA was added to the growing medium, as the concentration of ABA increased, the root length decreased (Figure P.1.1). In the presence of ABA 0.3 μM, a general shortening in the root length was observed with respect to the control condition (0 μM ABA), but there were no significant differences between WT and the *copt* mutants. However, under 0.6 μM ABA the differences between the WT and some *copt* mutants were significant, being *copt2* and *copt1copt2copt6* the most sensitive mutants to this treatment. In contrast, the *copt5* mutant was more resistant than WT to 0.6 μM ABA (Figure P.1.1). The highest ABA concentration checked was 1.2 μM and roots were extremely short compared to the other treatments, especially in the sensitive *copt1copt2copt6* mutant (Figure P.1.1). Otherwise, *copt3* and *copt5* mutants were less sensitive to this treatment than the WT (Figure P.1.1). In addition to the root length, we also analyse the effect of the ABA treatment on the plant establishment by using the GCR as an indicative parameter (see materials and methods) (Figure P.1.2).
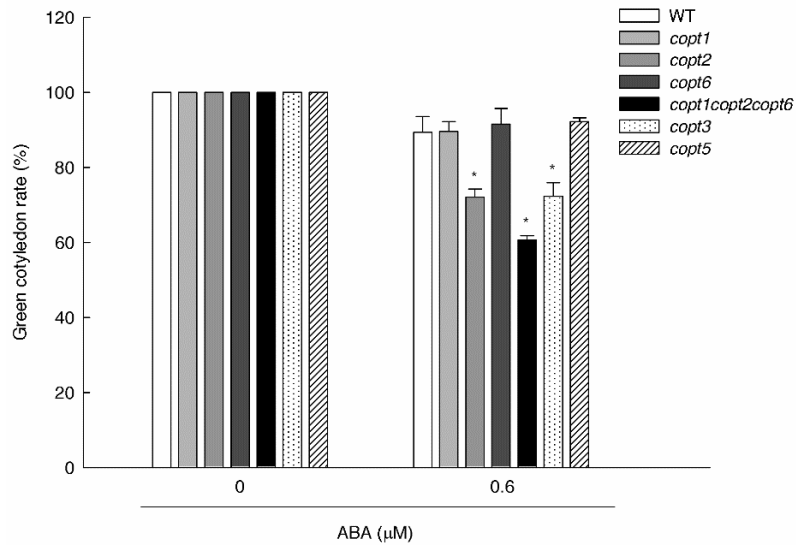
Figure P.1.2. Green cotyledon rate of the *copts* mutants under ABA treatments. WT, *copt1*, *copt2*, *copt6*, *copt1copt2copt6*, *copt3* and *copt5* 7 day-old seedlings were grown in ½ MS standard medium in the presence of 0.6 µM ABA. The percentage of the green cotyledon rate was determined in both conditions, 0 and 0.6 µM ABA. Asterisks indicate statistical differences (P<0.05) according to Z test with respect to the WT under the same condition.

Following the results obtained in the Figure P.1.1, we used 0.6 µM ABA treatment to analyse the GCR (Figure P.1.2) in the WT and the same COPT genotypes used before. The seedlings establishment under control conditions was not affected (Figure P.1.2). However, when ABA treatment was applied, *copt2*, *copt1copt2copt6* and *copt3* showed a decreased GCR with respect to the WT (Figure P.1.2). According to these results, the *copt2* and *copt1copt2copt6* mutants were the most sensitive to ABA when grow under ½ MS standard Cu conditions. In addition, these results match with the number of ABA-related elements found in the *pmCOPTs* members in the *in silico* analysis (Table P.1).

RESULTS

1.1. Sensitivity to exogenous ABA is enhanced in knockout, but reduced in overexpressing, *pmCOPT* mutants

To check the possible influence of Cu homeostasis on ABA responses in Arabidopsis seedlings, the sensitivity to the hormone of different mutants with an altered expression of *pmCOPT* transporters was analysed by treatments in which different ABA and Cu concentrations were employed. Addition of the specific Cu chelator 100 µM BCS was required to obtain severe Cu deficiency conditions since standard commercial ½ MS medium just falls within the mild Cu deficiency range (Andrés-Colás *et al.*, 2013). To generate Cu sufficiency, 1 µM Cu was added to the ½ MS medium, and 25 µM was added for Cu excess. As the ABA concentration increased, root length decreased for all the genotypes and Cu conditions (Figure R.1.1A). Globally, ABA sensitivity reduced as Cu decreased in the medium. Thus, under Cu excess (25 µM), root growth was almost completely hindered by 0.6 µM ABA (Figure R.1.1A), and the effect diminished with lower Cu concentrations, as indicated by the slopes of the regression lines obtained for each genotype (inset in Figure R.1.1A). With sufficient and excess Cu, the *copt2* and the triple *copt1copt2copt6* knockout mutants showed greater sensitivity to ABA (higher slope values) than the WT seedlings which, in turn, were more sensitive than the *COPT1^{OE}* mutant. Under Cu deficiency, however, the slope values lowered and differences among genotypes became less marked, both of which indicate a stronger effect of ABA in the presence of Cu, particularly on knockout mutants (Figure R.1.1A). Since differences between genotypes were significant at 0.6 µM ABA, this ABA concentration was used in the following experiments. The observed pattern of sensitivity to ABA in terms of root length was further confirmed by the GCR (Figure R.1.2A). The ABA-treated *copt2* and triple knockout mutant seedlings showed a lower GCR than the WT, while the overexpressing *COPT1^{OE}* mutant was less sensitive to ABA than the control seedlings under Cu sufficiency conditions. These differences were lost under Cu deficiency (Figure R.1.2A).
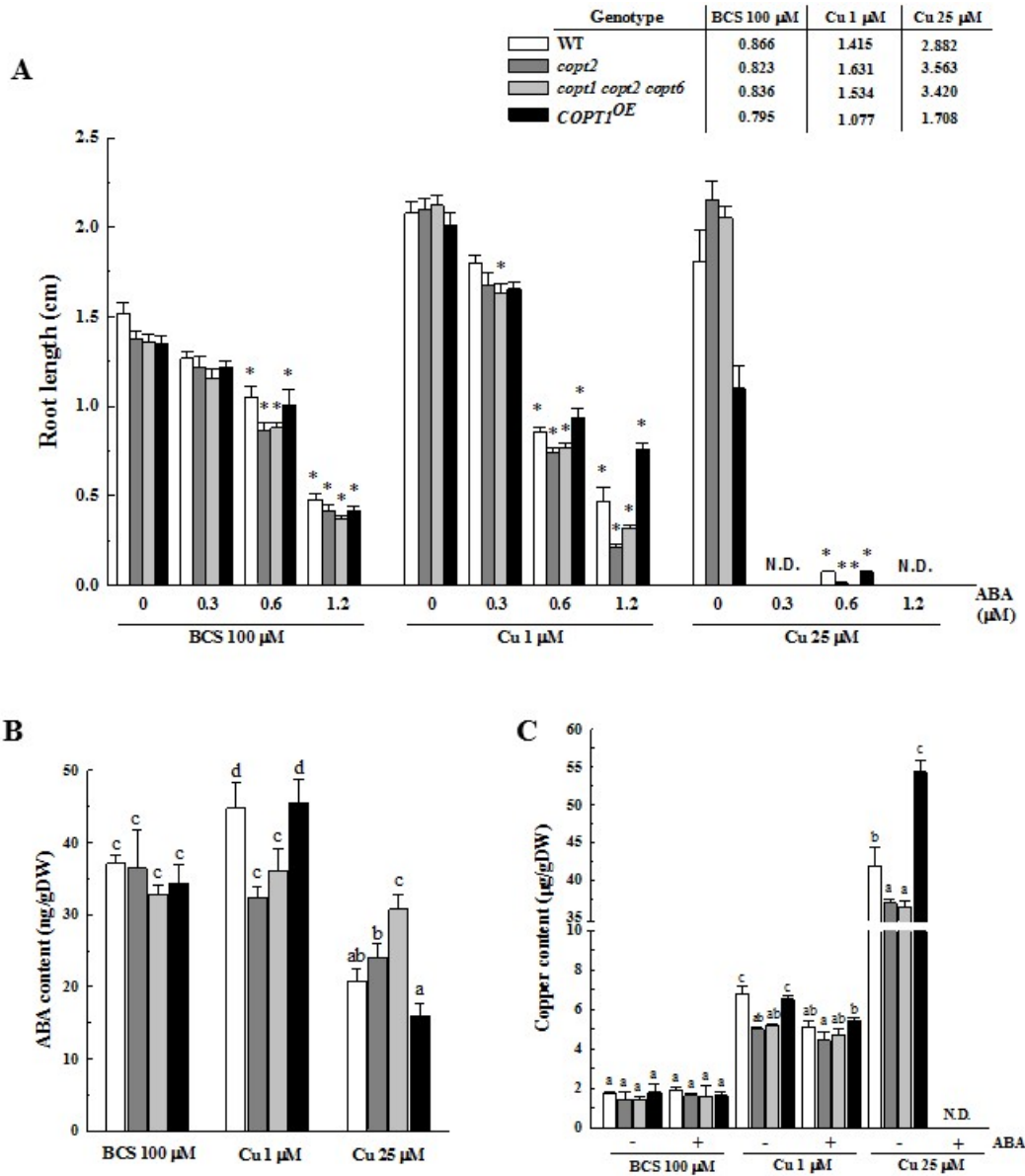
Figure R.1.1. Sensitivity to ABA treatment in the *pmCOPT* mutants. In these experiments, the WT, *copt2*, *copt1copt2copt6* and *COPT1OE* seedlings grown under Cu-deficiency (BCS 100 μM), Cu-sufficiency (Cu 1 μM) and Cu-excess (25 μM) conditions were used. (A) Root length of the 7-day-old plants grown in the presence of increasing ABA concentrations (0, 0.3, 0.6, 1.2 μM). Asterisks indicate statistical differences (P<0.05) according to Tukey's test with respect to the non ABA-treated (control) plants of each genotype under the same Cu condition. The slope values obtained by linear regression are shown in the legend. (B) ABA content in non ABA-treated WT, *copt2*, *copt1copt2copt6* and *COPT1OE*. (C) Cu content in control and ABA-treated (0.6 μM) WT, *copt2*, *copt1copt2copt6* and *COPT1OE*. Bars are means ± SD of 3 replicates of at least 10 plants (A) or of 200 mg FW (B and C) each. In C, each Cu condition was analyzed separately. In A and C, N.D. indicates no data. Different letters indicate statistical differences (P<0.05) according to Tukey's test.

The relationship between Cu availability and ABA metabolism was studied by measuring the endogenous hormone levels in the control and ABA-treated WT seedlings grown under different Cu conditions. The seedlings grown under Cu sufficiency had a significantly higher ABA content compared with the severe Cu deficiency conditions (Figure R.1.2B). In both cases, exogenous ABA treatment triggered an approximately 12-fold increase in hormone accumulation. Consequently, the ABA levels under Cu deficiency were lower than for Cu sufficiency after hormone treatment (Figure R.1.2B).
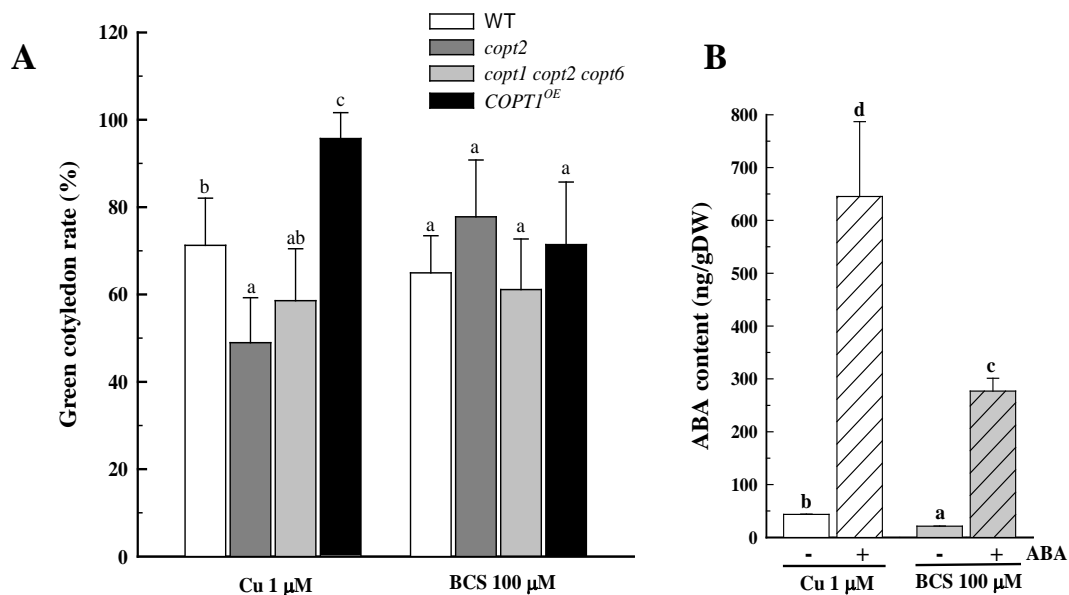
Figure R.1.2. Sensitivity to exogenous ABA. (A) Green cotyledon rate (GCR) measured in the presence of 0.6 μM ABA. Values for the control plants were 100% in all genotypes. Different letters indicate statistical differences (P<0.05) according to two-tailed z-tests for each Cu condition. (B) ABA content after 7 days of 0.6 μM ABA treatment applied to WT seedlings. Different letters indicate statistical differences (P<0.05) according to Tukey's test.

It was also interesting to note in the non-ABA-treated plants that the endogenous ABA content in the WT and *COPT1*^{OE} seedlings was higher than in the *copt2* and the triple *copt1copt2copt6* knockout mutants under Cu sufficiency, but these differences were lost under Cu deficiency, or were even reversed with excess Cu (Figure R.1.1B). As with the WT, the ABA levels in the *COPT1*^{OE} seedlings were significantly lower under Cu deficiency than under optimal Cu conditions, and no variation in ABA content was noted between these growth conditions in the *copt2* mutant (Figure R.1.1B). ABA content diminished with excess Cu compared with Cu sufficiency and deficiency in all genotypes, except in the triple *copt1copt2copt6* knockout mutant (Figure

R.1.1B). The effect of exogenous ABA on Cu content was also analysed for all three Cu conditions. No significant differences in Cu content were found among genotypes for Cu deficiency, regardless of the exogenous ABA treatment (Figure R.1.1C). Yet when ABA was absent, the *copt2* and triple knockout mutants displayed significantly lower Cu levels for sufficient and excess Cu than the WT and *COPT1*^{OE} seedlings, which had similar or increased Cu contents for sufficient and excess Cu, respectively. Finally, the exogenous ABA treatment significantly reduced the Cu content of the WT and *COPT1*^{OE} seedlings, but not that of the knockout mutants (Figure R.1.1C).

1.2. Exogenous ABA inhibits the expression of *pmCOPT* and other Cu homeostasis-related genes

The presence of putative ABA-responsive *cis*-regulatory elements (ABREs) in the promoter region of *pmCOPT* transporters (table P.1), suggests that the expression of these transporters could be influenced by ABA. To better address the effects that ABA can have on Cu homeostasis, we have extended this *in silico* analysis to other Cu deficiency-induced genes (Yamasaki *et al.*, 2009), such as *pmCOPTs* transporters *COPT1*, *COPT2* and *COPT6*, divalent metal transporter *ZIP2* and *YSL2*, and *SPL7,* the main transcription factor that regulates Cu deficiency responses. Other genes related to ABA homeostasis, such as *NCD3*, *HY5*, *WRKY40* and *ABI5* were also included*.* They were all found to contain a large number of ABREs elements in their promoters and at least one CuRE box, except for *SPL7* (Figure R.1.3).
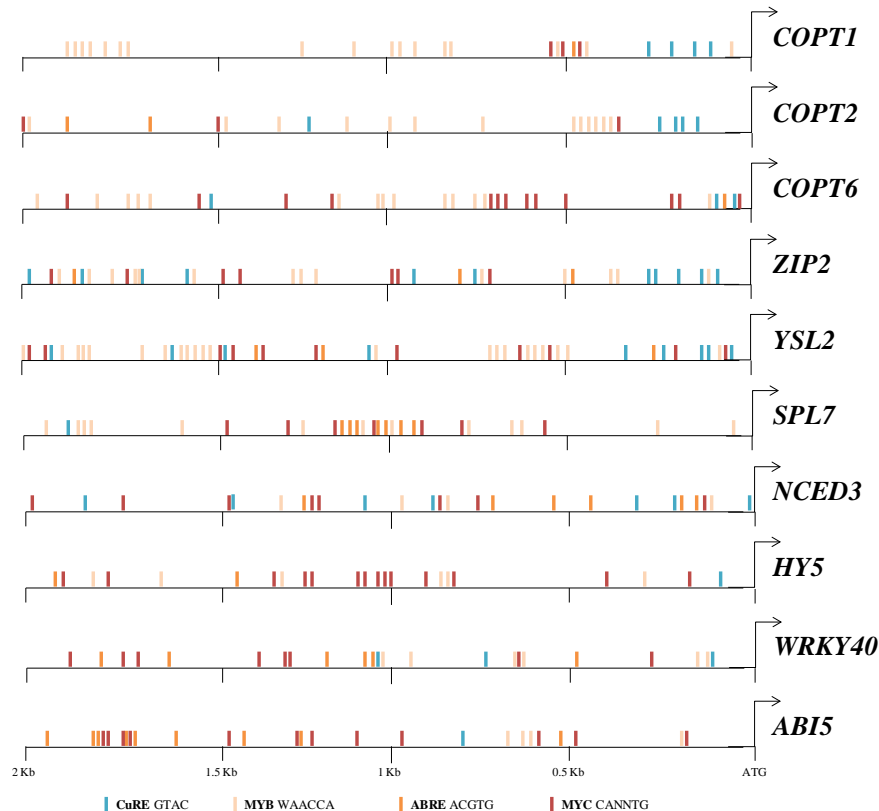
Figure R.1.3. Analysis of putative ABF and SPL7 recognized sites in the promoter sequences of ABA- and Cu deficiency-related genes. Positions of the *cis*-regulatory elements are marked in different colors as indicated in the figure legend. Promoter regions were defined as the 2000 bp upstream of the five prime untranslated region (5'-UTR) from the corresponding genes. The *in silico* analysis of the *cis*-elements present in the promoter regions was performed in the PLACE database.

The effect of ABA on the molecular mechanisms that modulate Cu homeostasis has been analysed by the transcriptional analysis of those genes in the ABA-treated plants grown according to Cu deficiency and sufficiency statuses. The *spl7* mutant was included in these analyses to decipher whether the regulation carried out by ABA is dependent on SPL7 (Figure R.1.4). Exogenous ABA treatment consistently lowered the expression levels of the *pmCOPT* genes in the WT when grown under Cu sufficiency conditions (Figure R1.4; Figure R.1.5A). Yet when Cu availability decreased, even though *pmCOPT* genes were up-regulated, the exogenous ABA treatment did not seem to affect their expression (Figure R.1.4; Figure R1.5B).
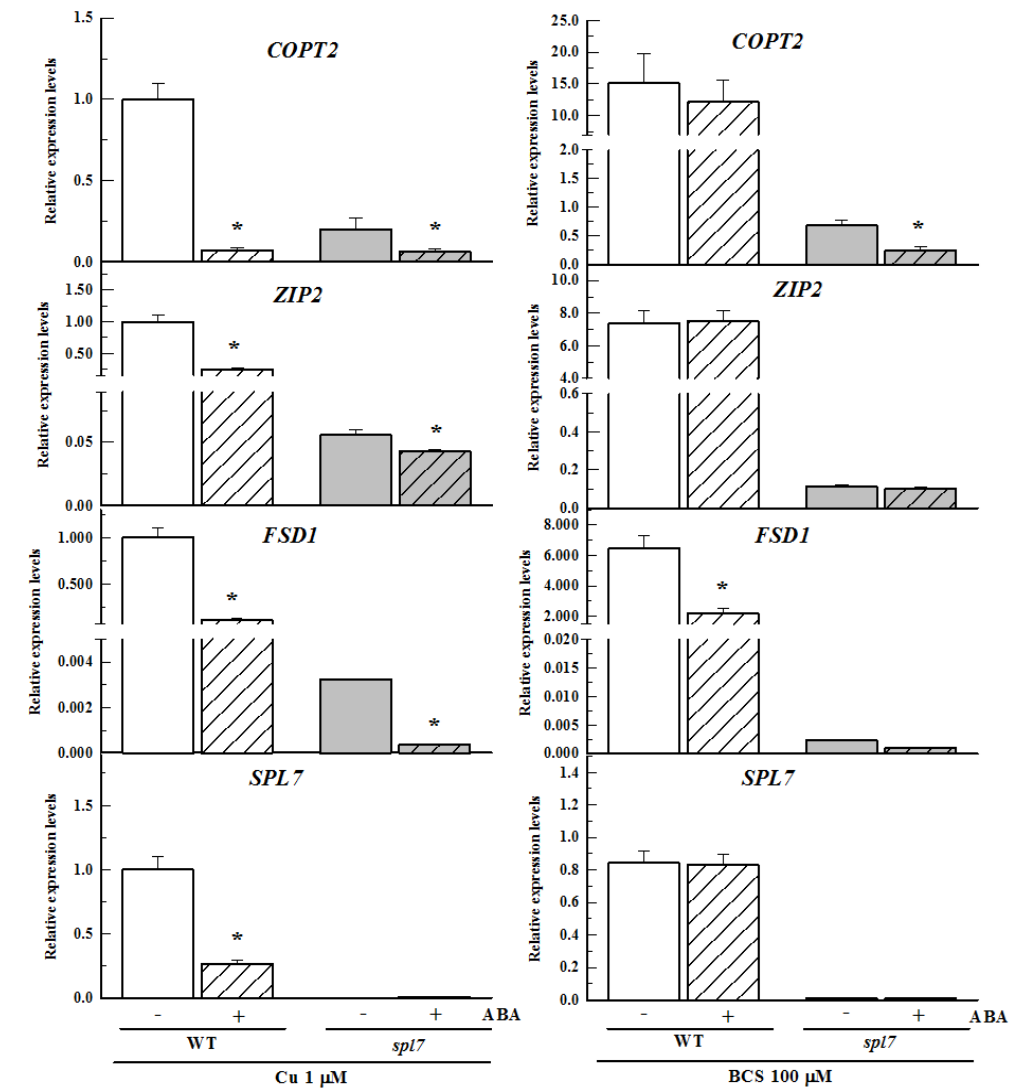
Figure R.1.4. Effect of ABA treatment on the transcriptional regulation of Cu homeostasis-related genes. Transcript levels of genes *COPT2*, *ZIP2*, *FSD1* and *SPL7* in the WT and *spl7* seedlings, treated or not with ABA (0.6 μM), and grown under Cu-sufficiency and Cu-deficiency conditions. Expression values are relative to those reported in the non ABA-treated (control) WT seedlings grown under the Cu-sufficiency conditions per gene. Bars correspond to arithmetic means ($2^{-\Delta\Delta Ct}$) ± standard deviation (SD) (n=3). For each particular gene, asterisks indicate statistical differences (P<0.05) with values of the control plants of each genotype.

When considering the different scales in Figure R.1.4, the transcript levels of *COPT2* increased more drastically (15-fold) than the other *pmCOPT* transporters (Figure R1.5). These inductions were almost undetectable in the *spl7* mutant, which confirms that *COPT2* is the best SPL7-

dependent COPT marker for Cu deficiency. Unlike that found for *pmCOPT*, the *SPL7* expression levels were not regulated by Cu availability and did not vary significantly when Cu was present in the growing medium (Figure R.1.4).
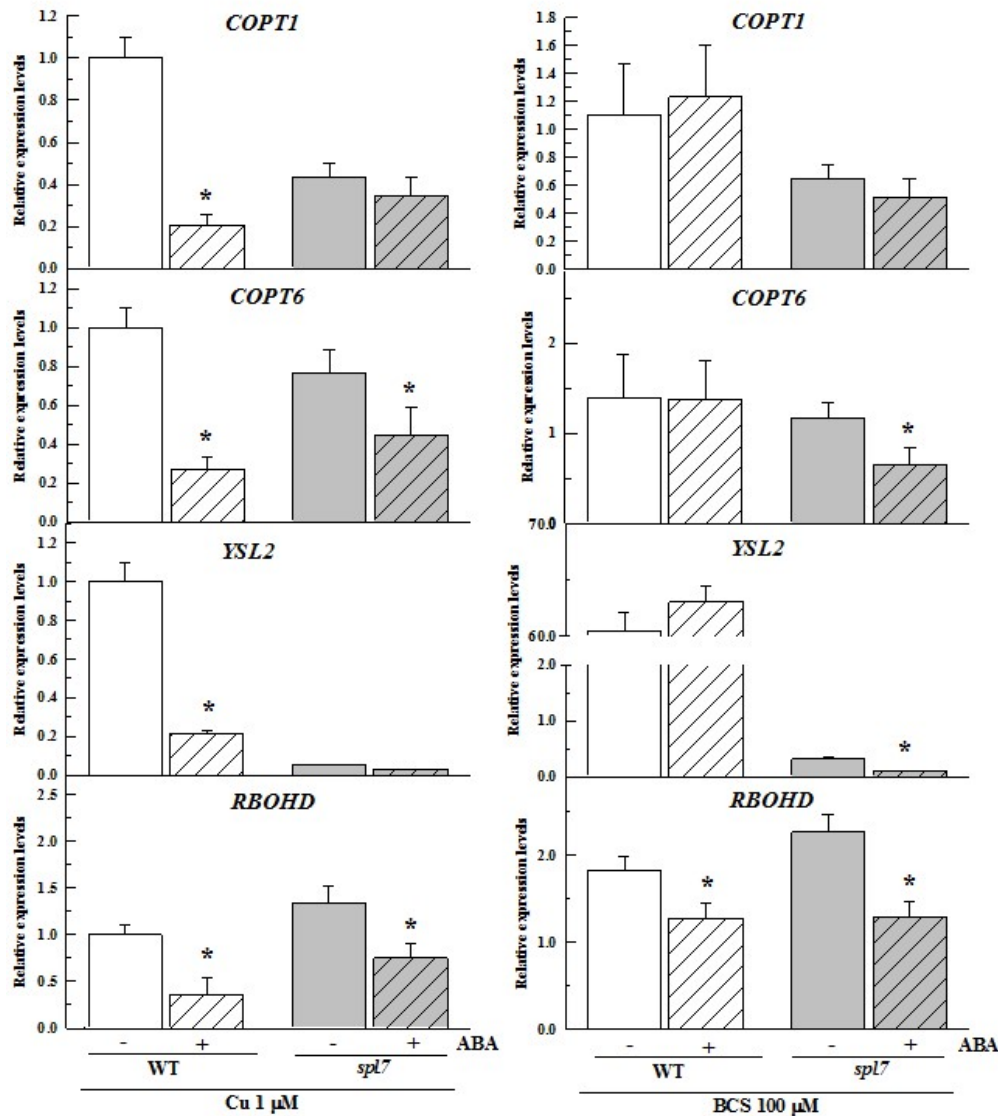
Figure R.1.5. The transcriptional response to ABA treatment of Cu homeostasis-related genes. Transcript levels of genes *COPT1*, *COPT6, YSL2* and *RBOHD* in the WT and *spl7* seedlings, treated or not with ABA (0.6 µM), and grown under Cu-sufficiency and Cu-deficiency conditions. Expression values are relative to those reported in the non ABA-treated (control) WT seedlings grown under the Cu-sufficiency conditions per gene. Bars are the means ± SD of 3 replicates of at least 10 plants each. For each particular gene, asterisks indicate statistical differences (P<0.05) with the control plants of each genotype.

Surprisingly, *SPL7* was repressed by ABA under Cu sufficiency conditions, but not under Cu deficiency, which might account for the reduction noted in expression of its targets, at least in part. A further reduction in *COPT2* expression took place in the *spl7* mutant, which suggests that ABA also plays a role independently of the SPL7 function (Figure R.1.4). Expression patterns of *ZIP2*, *YSL2* and *FSD1* were most consistent with those of *pmCOPT* in the WT plants (Figure R1.4; Figure R.1.5). Hence the expression of these genes was induced by Cu deficiency in an SPL7-dependent manner, and ABA treatment significantly lowered the transcript levels in the WT seedlings under Cu sufficiency (Figure R.1.4; Figure R.1.5).

1.3. The root growth phenotype of ABA mutants depends on Cu status

To uncover the putative role of Cu in ABA-dependent root length, two ABA mutants with different Cu statuses were used in a root growth assay (Figure R.1.6): the *aba2* mutant, which presents a block of the ABA biosynthetic pathway upstream of the NCED-catalysed step (Schwartz *et al.*, 1997) and, hence, lowered ABA levels; and the double *hab1-1abi1-2* mutant, which exhibits hypersensitivity to the hormone (Saez *et al.*, 2006).

Under all the tested Cu conditions, the *aba2* mutant plants were more resistant to root growth inhibition by exogenous ABA than the WT plants, whereas the *hab1-1abi1-2* mutants were more sensitive (Figure R.1.6A) in accordance with their ABA- dependent phenotype. As previously indicated, Cu is required for reducing root growth in all the tested genotypes as this reduction is impaired by severe Cu deficiency (Figure R.1.6A). So whereas WT root reduction was around 50% when Cu was present, it was not significant when it was severely lacking. The *aba2* mutant was resistant mostly to root growth inhibition under any Cu condition, while *hab1-1abi1-2* mutant hypersensitivity to ABA required Cu (Figure R.1.6A).
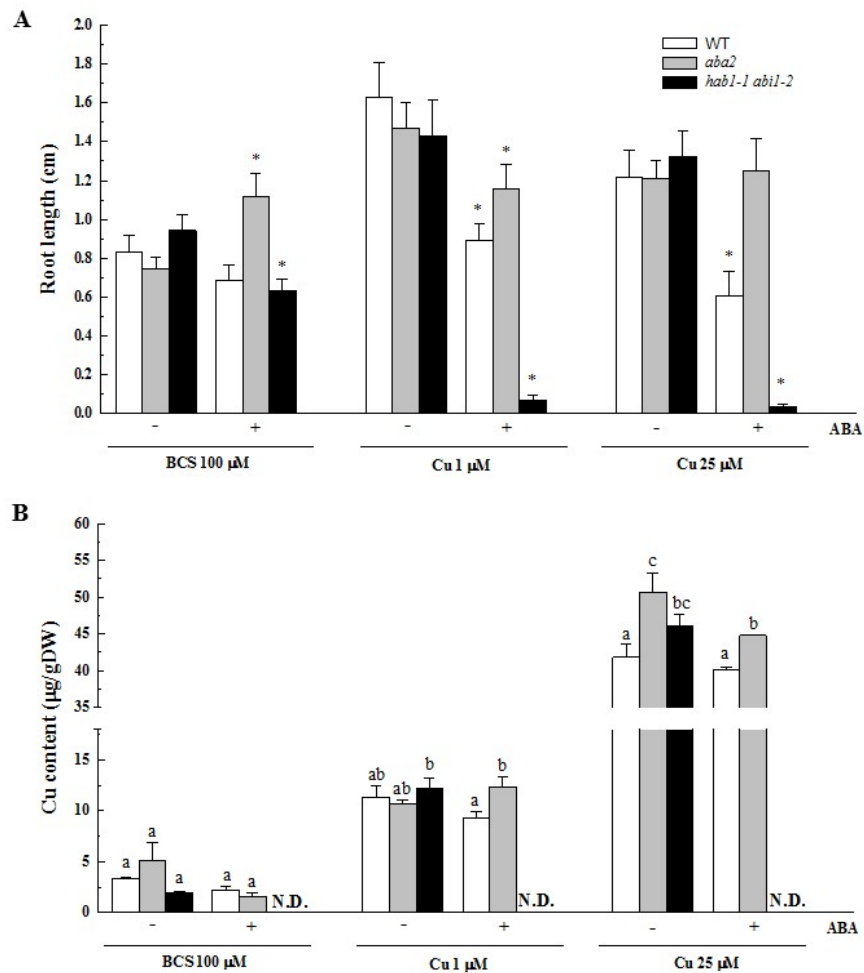
Figure R.1.6. Sensitivity to Cu treatment in the ABA mutants. In these experiments, the WT, *aba2* and *hab1-1 abi1-2* seedlings grown under Cu-deficiency (BCS 100 μM), Cu-sufficiency (Cu 1 μM) and Cu- excess (25 μM) conditions were used. (A) Root length of the 7-day-old plants grown in the presence of 0.6 μM ABA. Asterisks indicate statistical differences (P<0.05) according to Tukey's test with respect to the non ABA-treated (control) plants of each genotype under the same Cu condition. (B) Cu content in both ABA-treated (0.6 μM) and non ABA-treated WT, *aba2* and *hab1-1abi1-2*. N.D. indicates no data. Bars are means ± SD of 3 replicates of at least 15 plants (A) or of 200 mg FW (B) each. In B, each Cu condition was analysed separately.

Due to this hypersensitivity, it was not possible to determine the Cu content in these plants (Figure R.1.6B). Although the Cu content was still not affected by severe Cu deficiency, with Cu excess it increased in the ABA mutants in both the presence and the absence of ABA (Figure R.1.6B). Taken together, these results indicate that Cu status affects ABA responses and is, in turn, influenced by ABA.

1.4. The expression of Cu homeostasis-related genes is altered in ABA mutants

To unravel further how ABA affects Cu homeostasis, the expression of the Cu deficiency markers was studied in the ABA biosynthesis and signalling mutants with different Cu statuses (Figure R.1.7). With low Cu, the expression of the Cu deficiency markers generally increased in the *aba2* mutant and reverted to the WT levels after treatment with exogenous ABA, as expected for an ABA-deficient mutant (Figure R.1.7A).
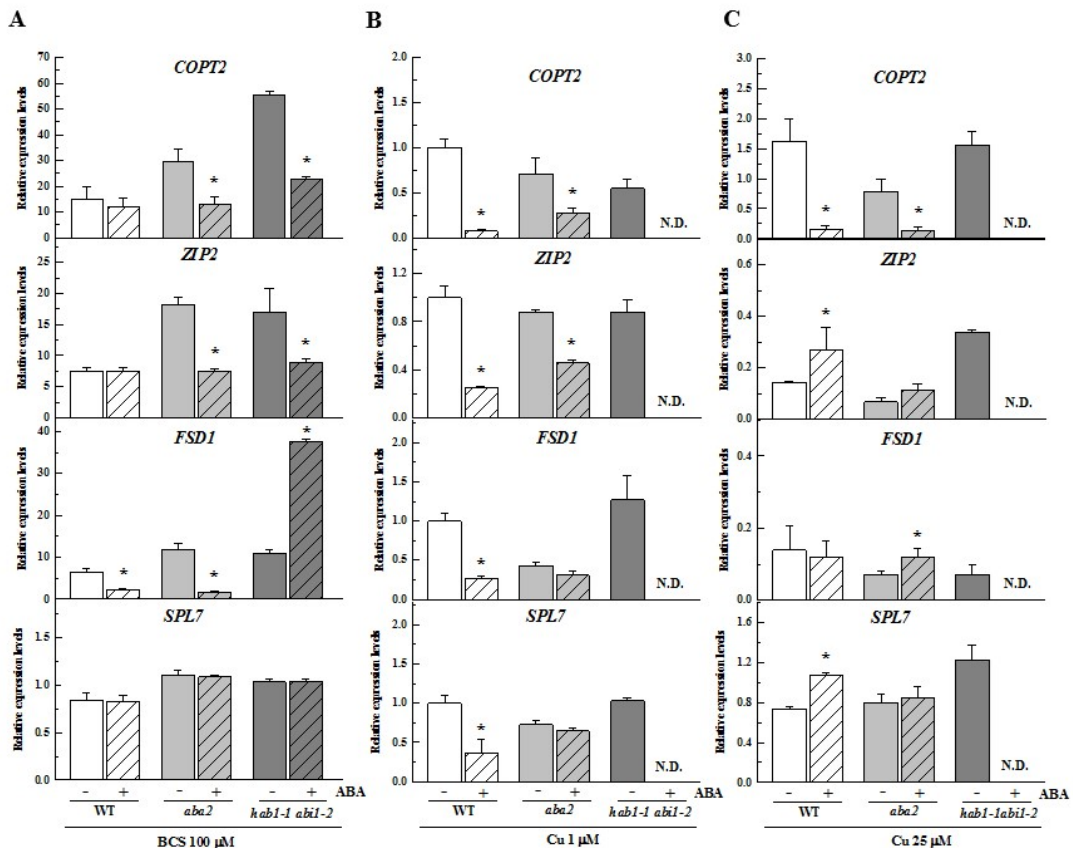
Figure R.1.7. Effect of Cu treatment in ABA mutants on the transcriptional regulation of Cu homeostasis-related genes. Transcript levels of genes *COPT2*, *ZIP2*, *FSD1* and *SPL7* in the WT, *aba2* and *hab1-1abi1-2* seedlings, treated or not with ABA (0.6 μM) and grown under Cu-deficiency (A), Cu-sufficiency (B) and (C) Cu-excess conditions. Expression values are relative to those reported in the non ABA-treated (control) WT seedlings grown under the Cu-sufficiency conditions per gene. N.D. indicates no data. Bars correspond to arithmetic means ($2^{-\Delta\Delta Ct}$) ± standard deviation (SD) (n=3). For each particular gene, asterisks indicate statistical differences (P<0.05) with values of the control plants of each genotype.

SPL7 expression slightly increased in the *aba2* mutant, but was not modulated by exogenous ABA for any Cu status (Figure R.1.7), which allowed endogenous/exogenous ABA effects to be differentiated. So whereas regulation by endogenous ABA could be, at least in part, mediated by the increase in the transcriptional activator, the effects of exogenous ABA were not dependent on *SPL7* expression levels. When Cu was sufficient and excessive, the expected increase in the responses of the Cu deficiency markers in the *aba2* mutant, and the reversion by exogenous ABA, were both lost (Figure R.1.7B, C). Instead, a more or less marked decrease took place, which also occurred for SPL7 under Cu sufficiency.

The expression of the Cu deficiency markers mostly increased in the *hab1-1 abi1-2* mutant, and the effects after ABA treatment varied depending on the gene and Cu conditions (Figure R.1.7). Once again, *hab1-1abi1-2* mutant hypersensitivity to ABA in the presence of Cu prevented these samples from being analysed. With Cu deficiency, the effect of exogenous ABA was SPL7 independent because, as indicated before, *SPL7* expression was not affected by ABA treatment, whereas distinct and significant effects were observed for the analysed Cu deficiency markers (Figure R.1.7A). With both Cu sufficiency and excess, the similar expression levels of the Cu deficiency markers in the *hab1-1abi1-2* mutant and WT plants (Figure R.1.7B, C) indicate that endogenous ABA signalling slightly modulates Cu responses. Taken together, these data indicate a complex scenario in which Cu status could affect ABA homeostasis in multiple steps, such as biosynthesis and signalling, and, vice versa, ABA alterations could drive changes in Cu homeostasis.

1.5. ABA and Cu status both influence oxidative stress levels

To unravel whether ABA treatment influences oxidative stress status according to Cu availability, the plasma membrane-associated NADPH oxidase RBOHD (respiratory burst oxidase homolog D) was studied as it has been reported to be involved in ABA-promoted reactive oxygen species (ROS) production (Kwak *et al.*, 2003). *RBOHD* gene expression was not dependent on SPL7, but was induced by Cu deficiency in all the studied genotypes. In contrast to what was found for the SPL7-dependent genes, ABA treatment generally lowered *RBOHD* gene expression under both Cu sufficiency and Cu deficiency conditions (Figure R.1.5).

H_2O_2 was detected in the WT, *pmCOPT*, *spl7* and *aba2* mutants subjected to ABA treatment and grown under Cu sufficiency and Cu deficiency conditions (Figure R.1.8).
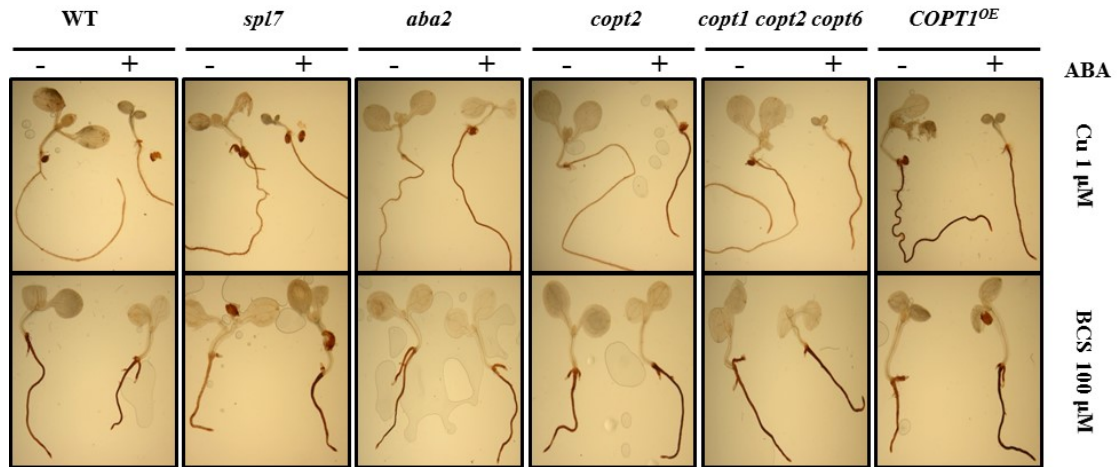
Figure R.1.8. Effect of ABA and Cu availability on oxidative stress status. Hydrogen peroxide detection in WT, *spl7*, *aba2, copt2, copt1copt2copt6* and *COPT1OE* 7 day-old *Arabidopsis* seedlings grown under Cu sufficiency and deficiency conditions treated (+) or not (-) with ABA (0.6 μM, 7 days). Shown is DAB staining in a representative 7 day-old seedling for each genotype and condition.

For Cu sufficiency, H_2O_2 production in the WT was poor and ABA treatment had no significant influence. In contrast, oxidative stress was evident in the roots of the WT seedlings grown under Cu deficiency, regardless of ABA treatment (Figure R.1.8). Under Cu sufficiency conditions, however, the *copt2* seedlings drastically increased oxidative stress after ABA treatment, whereas ROS accumulation became evident in *COPT1OE*, even with no hormonal treatment (Figure R.1.8). The *aba2* mutant behaved similarly to the *copt2* seedlings, and the *spl7* and *copt1copt2copt6* mutants also showed increased ROS content after ABA treatment when grown under optimal Cu availability conditions (Figure R.1.8).

1.6. ABA modifies the spatial COPT2 gene expression pattern

The effect of ABA on the spatiotemporal *COPT2*-driven expression pattern was analysed using *pCOPT2::GUS* (Perea-García *et al.*, 2013) and *pCOPT2::LUC* (Perea-García *et al.*, 2016) transgenic plants. Since this gene is expressed mainly under Cu deficiency conditions, we selected a mild metal deficiency (½ MS) to allow gene induction. In the 7-day-old seedlings, GUS expression was located mainly at the cotyledon apex, on the base of true leaves and along root tissues (Figure R.1.9A–D).
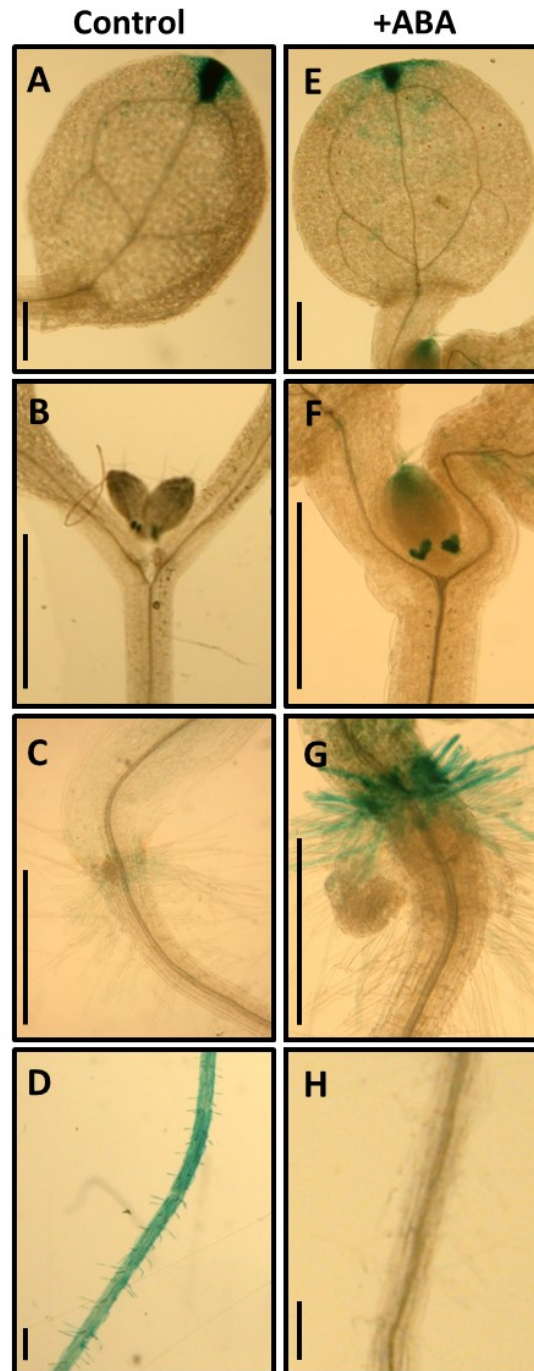
Figure R.1.9. Effect of ABA treatment on the spatial *COPT2* gene expression pattern. *COPT2* expression pattern in the Arabidopsis *pCOPT2::GUS* transgenic seedlings treated (+ABA) or not (control) with ABA (0.6 µM), and grown under mild Cu deficiency (½ MS). GUS staining is shown in a representative 7-day-old seedling cotyledon (A, E), detail of shoot meristem and trichomes (B, F), root crown (C, G) and a portion of root tissues (D, H). GUS reaction was performed at 6 h from the onset of the light period. Bars indicate 1 cm in each particular photograph.

The exogenous ABA treatment did not modify the distribution of *COPT2*-driven *GUS* expression in aerial parts, but *GUS* expression was almost abolished from tissues along the root, and concentrated in the root crown and root hairs after hormone treatment (Figure R1.9E–H). Increasing ABA concentrations did not modify the parameters related to the daily *COPT2*-driven oscillation pattern, such as amplitude, phase and period (Figure R.1.10).
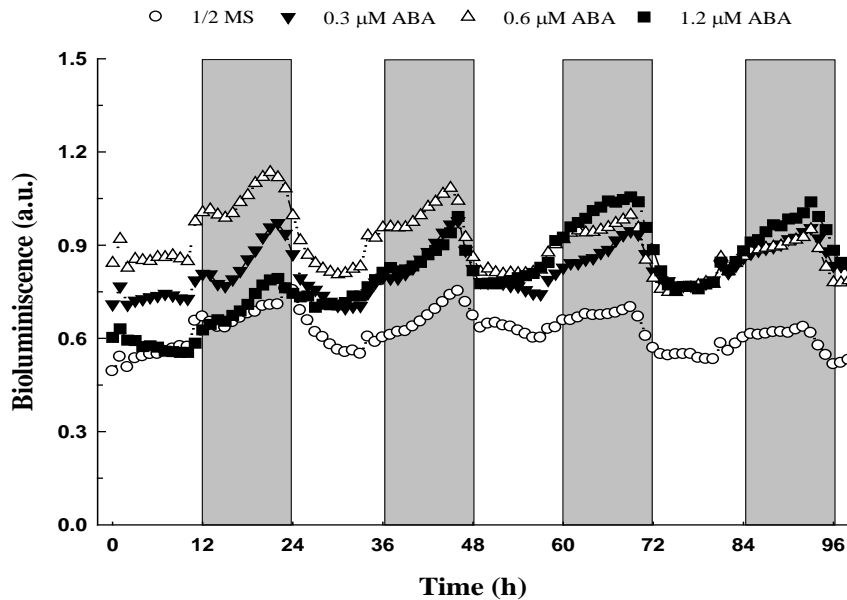
Figure R.1.10. Effect of ABA on the oscillatory *COPT2* gene expression pattern. *COPT2* expression pattern in *Arabidopsis pCOPT2::LUC* transgenic seedlings treated with different ABA concentrations and grown under mild Cu deficiency (½ MS). Shown is luciferase activity measured as bioluminescence emission.

Whether or not lack of ABA affects temporal regulation was assessed in the *pCOPT2::GUS* plants subjected to ABA treatments at different times (Figure R.1.11).
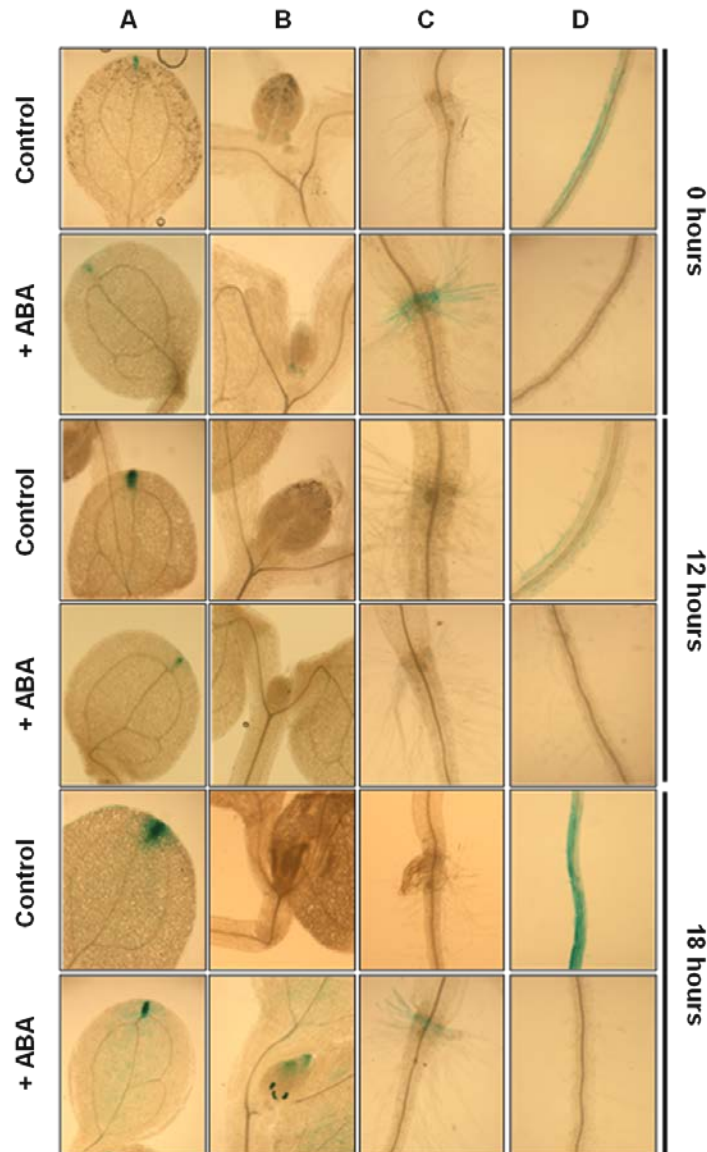
Figure R.1.11. Effect of ABA on the spatial *COPT2* gene expression pattern. *COPT2* promoter-driven expression pattern in *Arabidopsis pCOPT2::GUS* transgenic seedlings treated (+ABA) or not (Control) with ABA (0.6 μM) and grown under mild Cu deficiency (½ MS) conditions. A representative 7 day-old seedling cotyledon (A), detail of shoot meristem and trichomes (B), root crown (C) and a portion of root tissue (D) is shown for GUS staining. GUS reaction was performed at 0, 12 and 18 h from the onset of the light period.

The results demonstrate that *COPT2*-driven gene expression consistently focused on the root crown and root hair zones in the ABA-treated seedlings at the same times as the control samples, and induction occurred at the transcript level along root tissues (Figure R.1.11).

1.7. ABA biosynthesis and signal transduction vary with Cu availability

To study the effects of Cu availability on hormonal content, WT seedlings were grown in a wide range of Cu concentrations. Compared with Cu sufficiency, both severe Cu deficiency and moderate metal excess displayed lower ABA levels (Figure R.1.12A). Therefore, optimal Cu availability was necessary for normal endogenous ABA content in Arabidopsis seedlings.
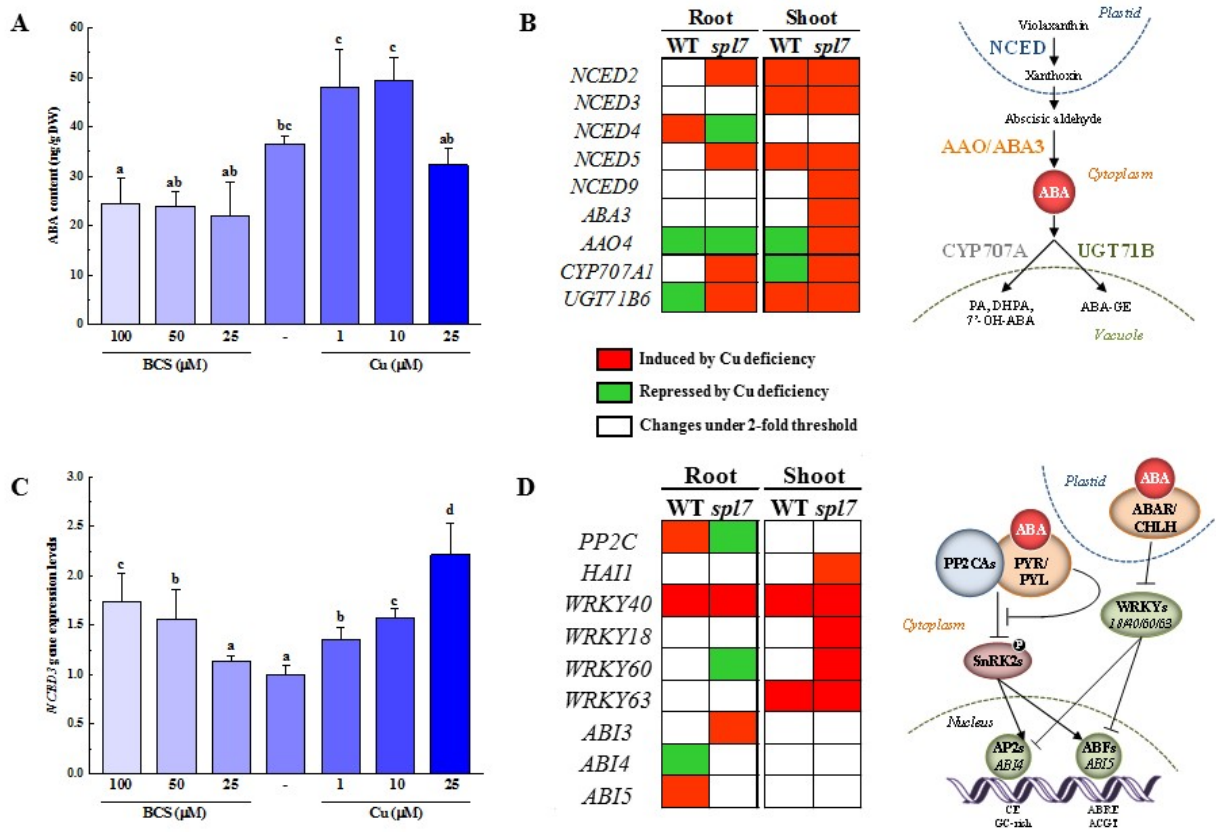
Figure R.1.12. Effect of Cu availability on ABA accumulation. (A) ABA content in the 7-day-old WT seedlings grown on a Cu gradient scale, which ranged from severe deficiency (100 µM BCS) to moderate excess (25 µM $CuSO_4$). Bars are means ± SD of 3 independent replicates of 200 mg FW each. Different letters indicate statistical differences (P<0.05) according to Tukey's test. (B) ABA biosynthetic genes differentially expressed under Cu deficiency, as reported by Bernal *et al.*, 2012. Colors indicate at least a 2-fold induction (red), repression (green) or less than 2-fold change (white) in the plants grown under the Cu deficiency vs. optimal Cu conditions. Analyses were performed on root and shoot tissues from the WT and spl7 mutant plants. *NCED*: nine-cis-epoxycarotenoid dioxygenase; *ABA3*: ABA deficient 3; *AAO*: ABA aldehyde oxidase; *CYP707A*: ABA 8'-hydroxylases; *UGT71B6*: UDP-glucosyltransferase. Diagram of the main steps in ABA biosynthesis and catabolism (right). (C) *NCED3* gene expression levels in the WT seedlings grown as indicated in panel A. Transcript levels are relative to those reported in the ½ MS samples. Bars are means±SD

of 3 replicates of 200 mg FW each. Different letters indicate statistical differences (P<0.05) according to Tukey's test. (D) ABA signalling genes differentially expressed under Cu deficiency, as reported by Bernal et al. 2012. Key of colors as described in (B). *PP2CAs*: clade A protein phosphatases 2C; *WRKY*: transcription factors that contain the WRKY DNA-binding domain; *ABI*: Abscisic acid insensitive. Diagram of the main steps in ABA perception and downstream signaling (right). PYR/PYL: Pyrabactin resistant; PP2CAs: clade A protein phosphatases 2C; SnRK2s: subclass III Sucrose non fermenting-related protein kinases. ABAR/CHLH: Magnesium chelatase H subunit. AP2: Apetala 2-related transcription factors; ABF: ABRE binding factors.

Significant differences were not detected in the auxin (IAA) and jasmonic acid (JA) contents for the assayed experimental conditions (Figure R.1.13A), or in the IAA and JA contents for Cu availability and ABA treatment (Figure R.1.13B).

The influence that Cu homeostasis alteration may have on the expression of ABA metabolic and signalling genes was studied in the RNA sequencing (RNA-Seq) analysis performed by (Bernal *et al.*, 2012), in which responses to Cu deficiency conditions were compared in root and shoot tissues from WT and *spl7* knockout mutant plants. After analysing the transcriptional response of about 60 of the genes involved in ABA biosynthesis and ABA signalling, the genes which displayed a value that changed at least 2-fold compared with the Cu sufficiency conditions are shown (Figure R.1.12B and D, respectively). Induction by Cu deficiency prevailed among the genes related to ABA metabolism in the shoots of WT plants, and in the shoots and roots of *spl7* mutants (Figure R.1.12B, D). This analysis allowed us to address the influence of the SPL7 transcription factor on the regulation of these ABA-related genes.
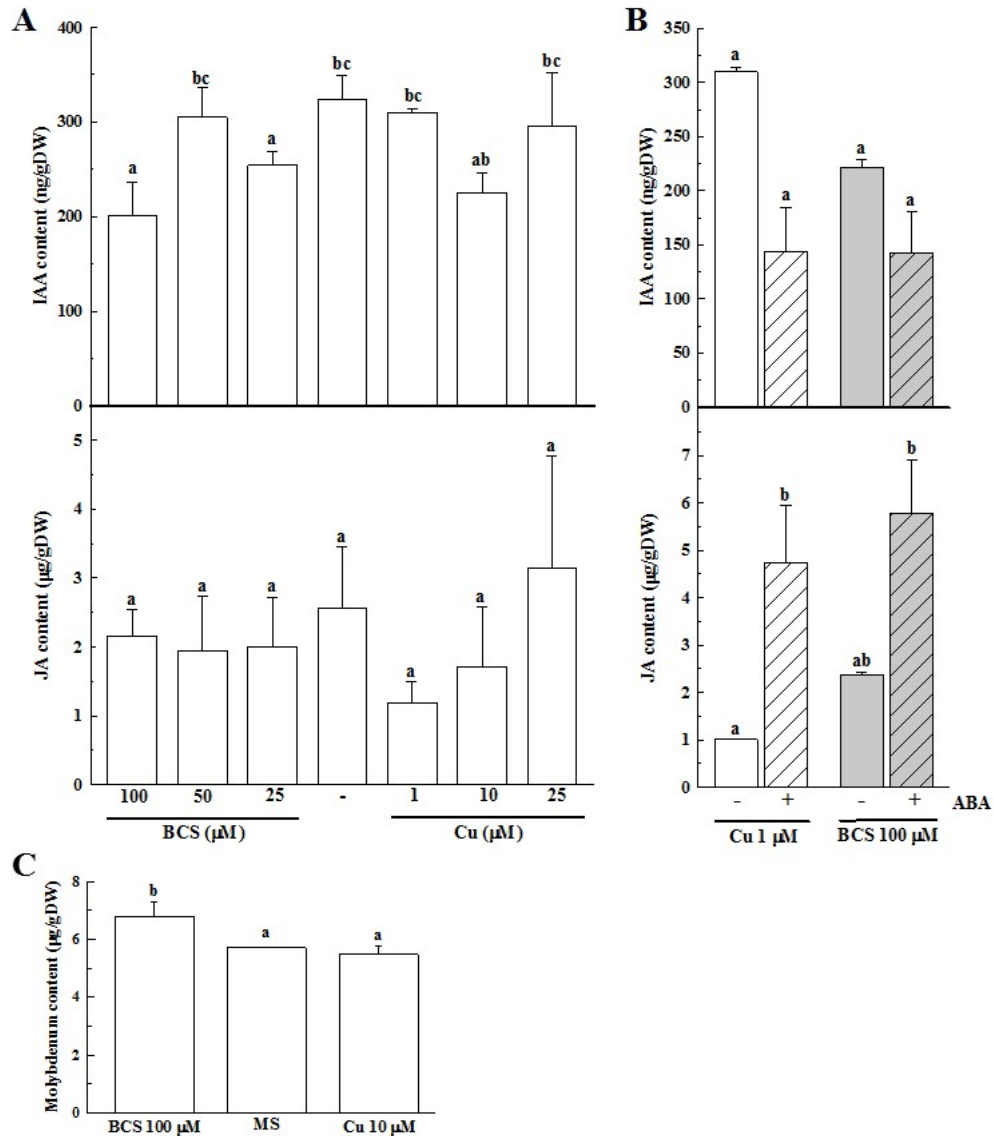
Figure R.1.13. Effect of Cu availability and ABA on hormone accumulation. (A) IAA and JA content were measured in 7 day-old WT seedlings grown under a Cu range from severe deficiency (BCS 100 µM) to Cu excess (25 µM). (B) IAA and JA levels measured in control and ABA-treated (0.6 µM) 7 day-old WT seedlings grown under Cu sufficiency (Cu 1 µM) and severe Cu deficiency (BCS 100 µM). (C) Molybdenum content in WT seedlings grown under different Cu availability conditions. Bars are means ± SD of 3 biological replicates of 200 mg FW. Different letters indicate statistical differences ($P<0.05$) according to a Tukey's test.

Complex differential *SPL7* responsiveness of ABA biosynthetic genes was envisaged, and these responses were also organ dependent (Figure R.1.12B). Several genes showed the same

expression pattern in the WT and *spl7* mutants, which indicates SPL7-independent Cu regulation, and this was the case for *NCED2*, *NCED3*, *NCED5* and *UGT71B6* in shoots. An SPL7-dependent gene expression pattern was obtained for *NCED2*, *NCED4*, *NCED5*, *CYP707A1* and *UGT71B6* in roots (Figure R.1.9B). In this context, it is important to note that *NCED3* has been shown to be the most expressed gene that codes for the limiting step in ABA biosynthesis positive feedback regulation (Barrero *et al.*, 2006), which was why the expression pattern of *NCED3* was checked herein at different Cu concentrations (Figure R.1.12C). The *NCED3* transcript levels described an opposite pattern to that of ABA content under the same experimental conditions (Figure R.1.12A, B), and with higher expression levels for both severe Cu deficiency and excess Cu compared with the Cu sufficiency growing conditions. These results demonstrate that Cu availability affects ABA biosynthesis. The in silico analysis revealed that ABA signalling genes were also affected by Cu availability (Figure R.1.12D). Of the >30 ABA signalling- related genes evaluated, only a couple of *PP2CAs* and seven transcription factors were differentially affected by Cu status and attained the 2-fold threshold (Figure R.1.12D). Most of these signalling genes were differently regulated in the WT and *spl7* mutant seedlings in root and shoot tissues, which suggests SPL7-dependent regulation (Figure R.1.12D). In line with this, we found that the promoter regions of some of these ABA-related genes contained putative CuREs (Figure R.1.3), which indicates reciprocal regulation between Cu homeostasis and ABA metabolism and signalling.

To gain a better insight into this mutual regulation, the effect of ABA and Cu availability on the transcriptional regulation of *NCED3*, *HY5*, *WRKY40* and *ABI5* was studied. Based on the differential sensitivity to ABA observed in the *copt2* knockout and *COPT1^{OE}* overexpressing mutants (Figure R.1.1), these genotypes were included in our assays (Figure R.1.14).

Figure R.1.14. Effect of Cu availability on the transcriptional regulation of the ABA-related genes. Transcript levels of genes *NCED3*, *HY5*, *WRKY40* and *ABI5* in WT, *spl7*, *copt2* and *COPT1^{OE}* in the 7-day-old seedlings treated or not with ABA (0.6 μM), grown under Cu-sufficiency and Cu-deficiency conditions. Expression values ($2^{-\Delta\Delta Ct}$) are relative to those reported in the control WT seedlings. Bars are means ± SD of 3 replicates of at least 10 plants each. Numbers indicate the fold changes in the transcript levels of the ABA-treated with respect to control samples per genotype. Asterisks indicate statistical differences (P<0.05).

The expression of the *NCED3* gene was induced by ABA treatment under Cu sufficiency in all the tested genotypes (Figure R.1.14). Although the basal expression level of *NCED3* under the Cu-deficient conditions was higher than that for the Cu sufficiency conditions in the WT seedlings, the fold changes in the transcript levels of this gene after ABA treatment were significantly lower in Cu deficiency vs. Cu sufficiency (4.5- vs. 1.9-fold; Figure R.1.14). The expression levels of the ABA biosynthetic gene *NCED3* were higher in the *pmCOPT* mutants than in the WT if ABA was present. Despite *NCED3* induction by Cu deficiency in the WT seedlings (Figures R.1.12B, C, R.1.14), *NCED3* expression drastically decreased (Figure R.1.14) in the genotypes that showed altered Cu homeostasis (*spl7*, *copt2* and *COPT1^{OE}*). Under optimal Cu conditions, ABA lowered the *HY5* and *WRKY40* expression levels, although *WRKY40* expression was also induced by Cu deficiency, and the *HY5* transcript levels increased in response to ABA treatment with severe Cu deficiency (Figure R.1.14). The expression levels of the ABA signalling gene *WRKY40* did not significantly change in the *pmCOPT* mutants in the absence and presence of ABA. Certain genes showed an increased expression in specific genotypes, such as *HY5* in *copt2* and *WRKY40* in the *spl7* seedlings grown under Cu sufficiency (Figure R.1.14). A clear trend was observed for the *HY5*, *WRKY40* and *ABI5* transcripts in the non-ABA-treated seedlings for Cu deficiency. Whereas the transcript levels in the *COPT1^{OE}* seedlings were consistently higher than in the WT, their expression levels were lower in the *copt2* mutant (Figure R.1.14). These expression patterns of the ABA signalling genes in *pmCOPT* mutants matched their observed ABA responses shown in Figure R.1.1.

The same set of genes in the *aba2* and *hab1-1abi1-2* mutants was also analysed (Figure R.1.15). Their expression generally increased as Cu decreased in the medium. As regards *NCED3*, the expression in the *hab1-1abi1-2* mutant was higher than in the WT, irrespective of Cu levels (Figure R.1.15).
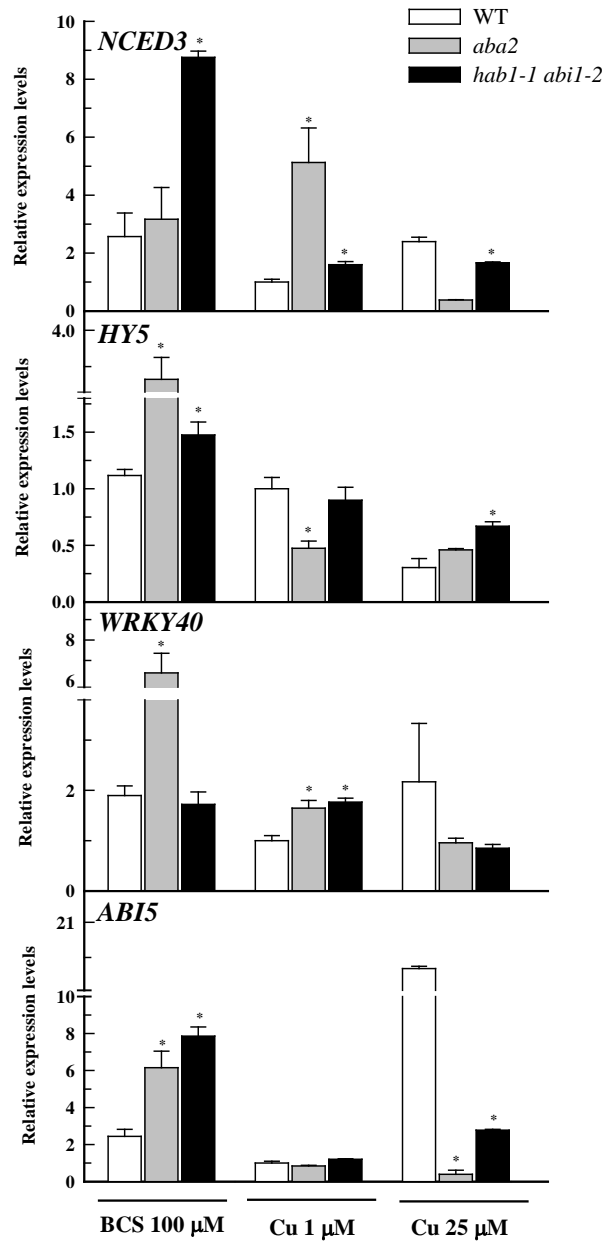
Figure R.1.15. Effect of Cu availability on the transcriptional regulation of ABA-related genes in ABA mutants. Transcript levels of genes *NCED3*, *HY5*, *WRKY40* and *ABI5* in WT, aba*2* and *hab1-1abi1-2* in the 7-day-old seedlings grown under Cu-deficiency (BCS 100 μM), Cu-sufficiency (Cu 1 μM) and Cu-excess (Cu 25 μM) conditions. Expression values are relative to those reported in the control WT seedlings. Values correspond to arithmetic means (2$^{-\Delta\Delta Ct}$) ± standard deviation (SD) (*n*=3). Asterisks indicate statistical differences (P<0.05).

However, the *aba2* mutant showed identical levels to the WT for deficient and excess Cu, but higher levels for Cu sufficiency (Figure R.1.15), which indicates the influence of Cu in the feedback regulatory loop of ABA on its own synthesis. Once again, the *HY5* levels were more affected in the mutants with Cu deficiency, and the same occurred with *WRKY40* in the *aba2* mutant. The signalling transcription factor ABI5 was not affected by Cu sufficiency compared with the WT, and its levels were regulated in the ABA mutants under Cu deficiency and excess conditions. Once again this suggests a complex interaction of Cu and ABA biosynthesis and signalling (Figure R.1.15).

1.8. Sensitivity to salt stress is enhanced in *copt2*, but reduced in *COPT1*^{OE} mutants

To study whether ABA sensitivity is similarly regulated by Cu availability independently of the ABA signal source (exogenous application/stress-induced endogenous biosynthesis), the WT, *copt2*, *copt1copt2copt6* and *COPT1*^{OE} seedlings were subjected to salt stress under both optimal Cu and severe Cu deficiency conditions.

Salt stress increased ABA content in all the tested genotypes and under both the Cu sufficiency and Cu severe deficiency conditions (Figure R.1.16A and Figure R.1.17A, respectively). This increment was more marked in the WT than in the *copt2* mutant seedlings under Cu sufficiency conditions (Figure R.1.16A).
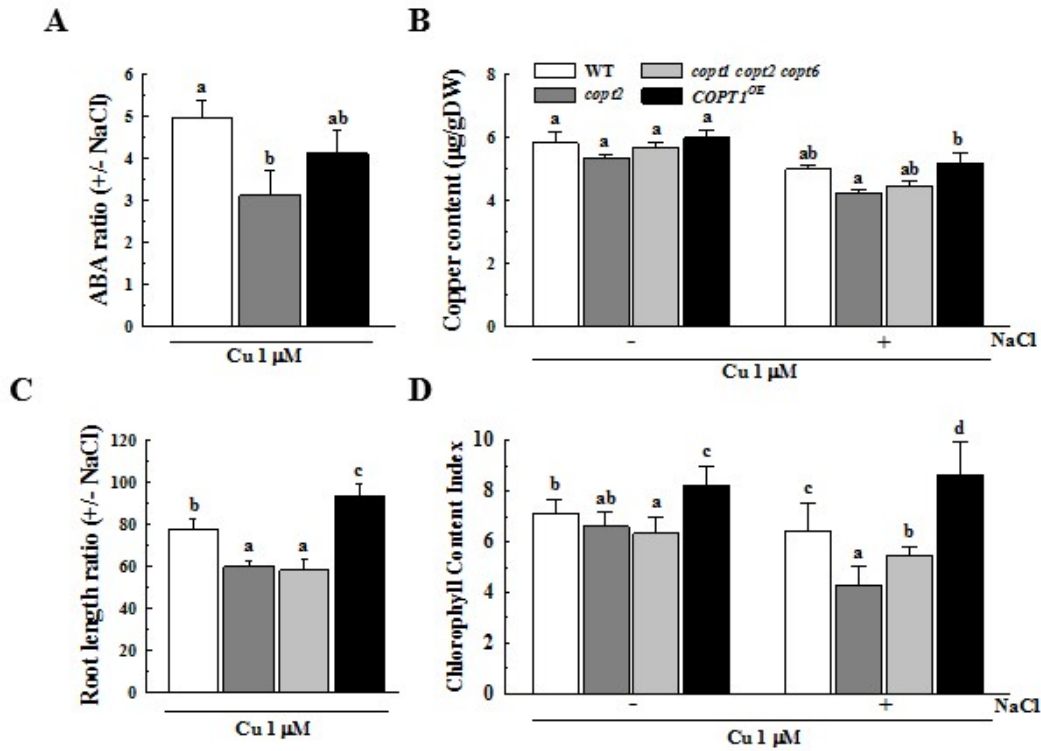
Figure R.1.16. Sensitivity to salt stress in the knockout and overexpressing *pmCOPTs* mutants under Cu-sufficiency conditions. The control and salt-stressed (200 mM NaCl) WT, *copt2*, *copt1copt2copt6* and *COPT1*[OE] 14-day-old seedlings, grown under Cu-sufficiency conditions, were used to determine the ABA content ratio (A), Cu content (B), root length ratio (C) and chlorophyll content index (D). Bars are means ± SD of 3 replicates of at least 200 mg FW. Different letters indicate statistical differences (P<0.05) according to Tukey's test for each particular condition.

NaCl treatment barely reduced the Cu content in the genotypes. However, the *copt2* knockout mutant seemed more affected by salt stress, and had a significantly lower metal content than the *COPT1*[OE] seedlings (Figure R.1.16B). With Cu deficiency, no differences in either Cu content or ABA levels were found among genotypes, regardless of them being subjected to the control conditions or salt stress (Figure R.1.17A, B).
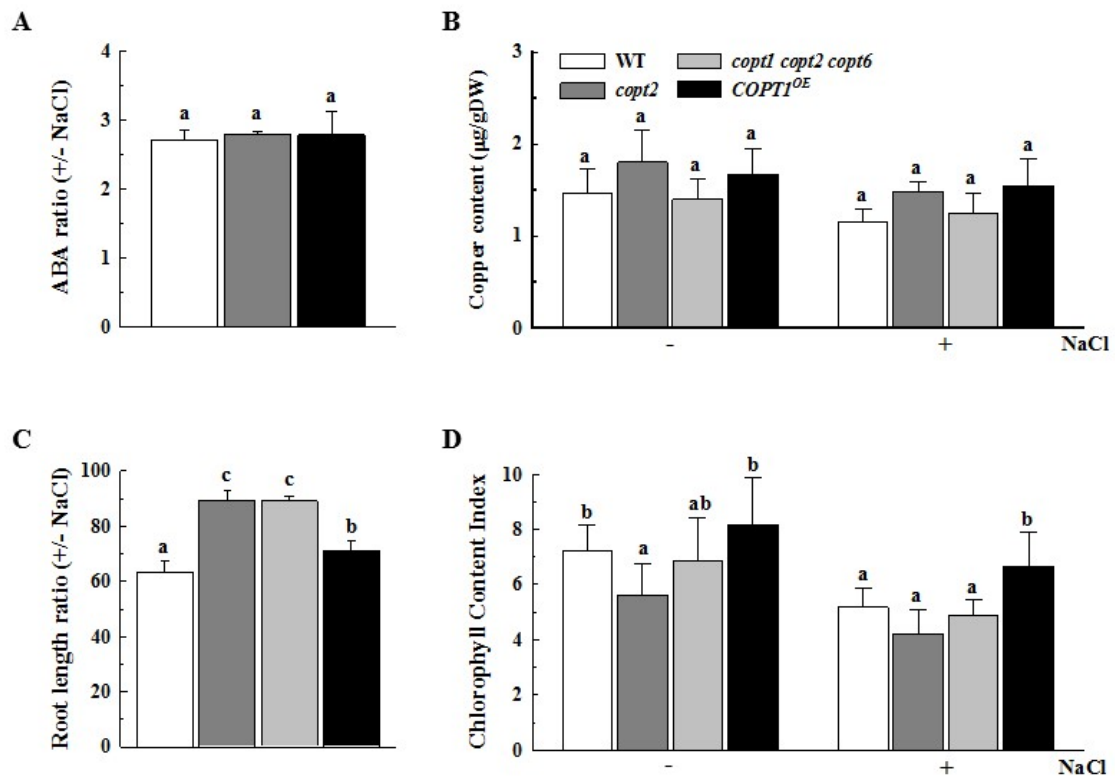
Figure R.1.17. Sensitivity to salt stress in knockout and overexpressing *pmCOPT*s mutants under Cu deficiency conditions. Measurements were performed in 14 day-old WT, *copt2* and *COPT1^{OE}* seedlings grown under Cu deficiency which were salt stressed (200 mM NaCl) during the last 7 days. In (B) and (D) the triple mutant *copt1copt2copt6* was also studied. (A) ABA content ratio between salt-stressed and control seedlings. (B) Cu content in control and salt-stressed seedlings. (C) Root length ratio between salt-stressed and control seedlings. (D) Chlorophyll content index in control and salt-stressed seedlings. Bars are means of 3 replicates of at least 200 mg FW. Different letters indicate statistical differences (P<0.05) according to Tukey's tests for each particular condition.

The response to stress-induced endogenous ABA variations was studied by determining root length and changes in the Chlorophyll content index (CCI) after salt stress as both are classical parameters used to describe the effect of ABA and the severity of the salt stress applied. As with the exogenous ABA treatment (Figure R. 1.1A), the root lengths of the *copt2* and *copt1copt2copt6* knockout mutants were more affected by stress than those of the WT which, in turn, had a lower root length ratio than the *COPT1^{OE}* seedlings under Cu sufficiency (Figure R.1.16C). This pattern was confirmed by studying the changes in CCI. The *copt2* and triple knockout seedlings were more sensitive to stress than the WT (Figure R.1.16D), while the overexpressing *COPT1^{OE}* mutant showed a higher CCI. The differences among the genotypes in

CCI were lost under the Cu deficiency conditions, but the root length ratio indicated that the *copt2* and the triple knockout mutants were more resistant to salt stress when Cu was scarce (Figure R.1.17C, D). These results indicate that knockout mutants are more sensitive to ABA variations since stress-induced endogenous ABA was lower (Figure R.1.16A), while reductions in Cu content, root length ratio and CCI were more marked than in the WT and the overexpressing mutant (Figure R.1.16B–D).

In line with this idea, the transcriptional regulation of Cu related homeostasis genes by salt stress-mediated ABA increments under Cu optimal conditions mostly paralleled that obtained with the exogenous ABA treatment, except for *COPT1* in the WT seedlings. NaCl treatment significantly lowered the *pmCOPT* and *SPL7* gene expression levels in the 14- day-old WT, *copt2* and *COPT1^{OE}* seedlings (Figure R.1.18).
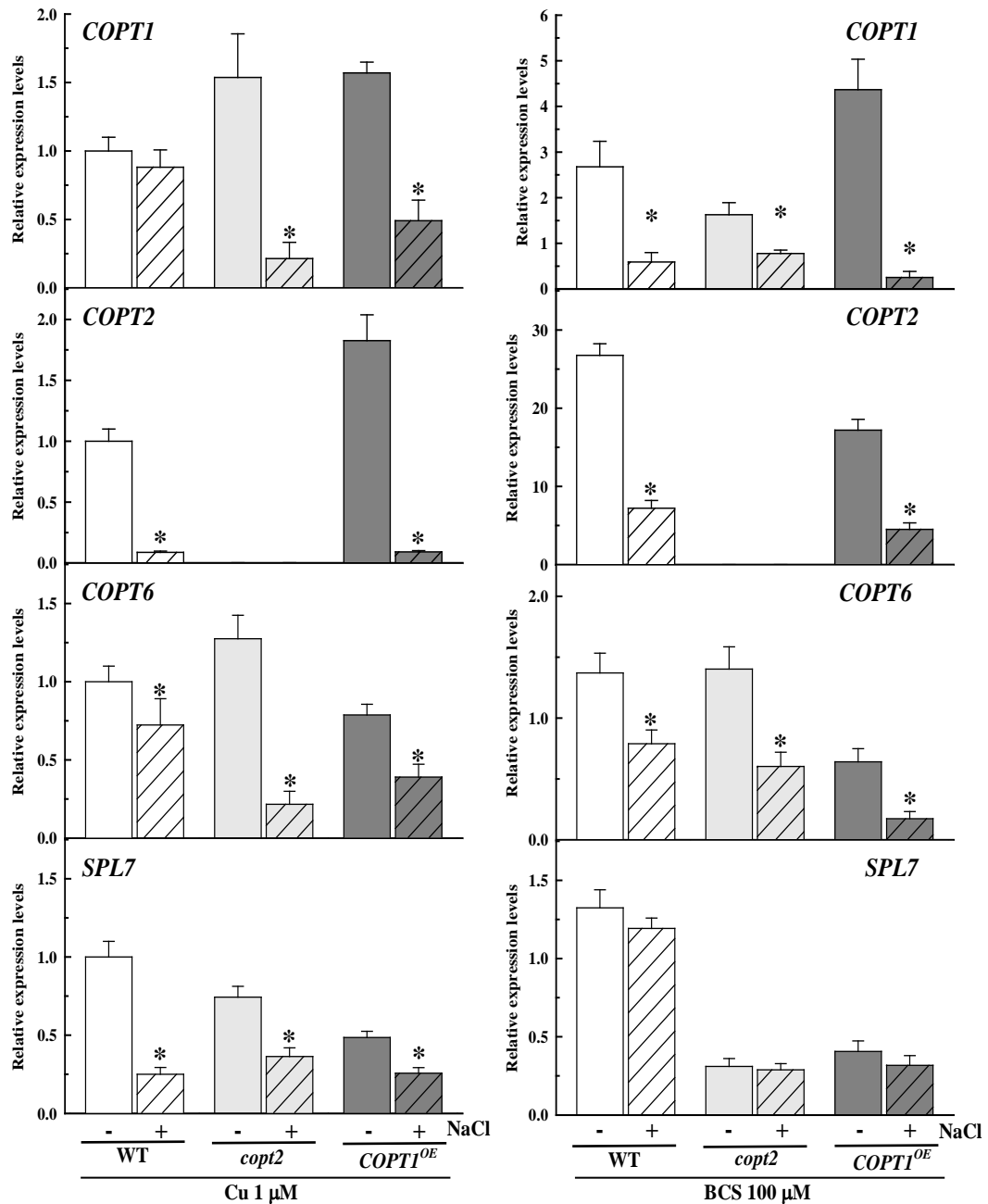
Figure R.1.18. Effect of salt stress on *COPT*s and *SPL7* transcriptional regulation. Transcript levels of *COPT1*, *COPT2*, *COPT6* and *SPL7* genes in WT, *copt2*, and *COPT1^OE* 14 day-old seedlings treated or not with NaCl (200 mM, 7 days) and grown under Cu sufficiency and deficiency conditions. Expression values are relative to those reported in non NaCl-treated (control) WT seedlings grown under Cu sufficiency conditions for each gene. Bars are means ± SD of 3 replicates of at least 10 plants each. Asterisks indicate statistical differences (P<0.05) according to Tukey's test respect to values of control plants of each genotype.

Under these experimental conditions, the effect of Cu availability on the transcriptional regulation of the ABA biosynthetic (*NCED3*) and signalling (*HY5*, *WRKY40* and *ABI5*) genes was also studied. *NCED3* was induced by Cu deficiency and salt stress, but only under optimal Cu conditions, and not in the *pmCOPT* mutants (Figure R.1.19).

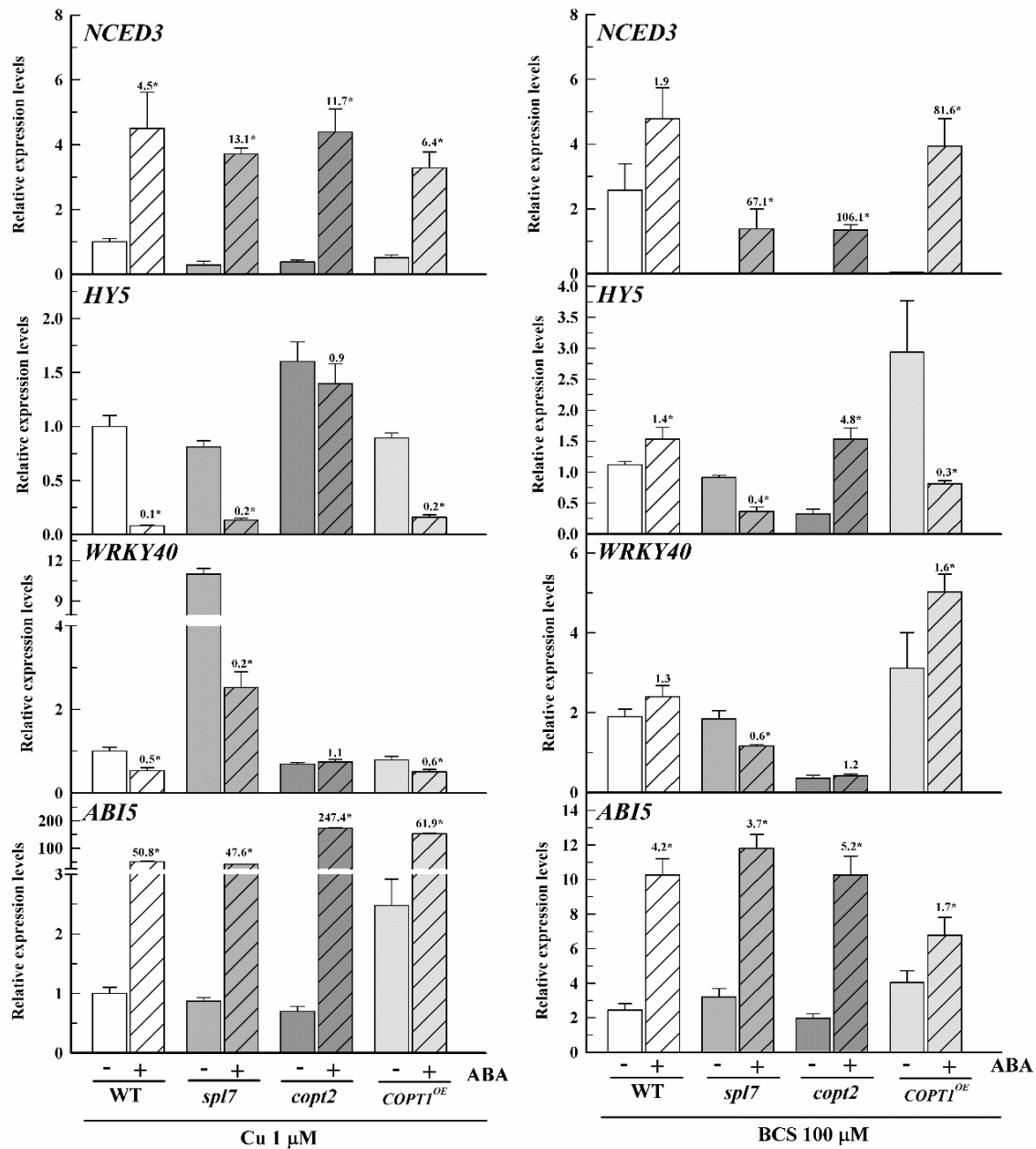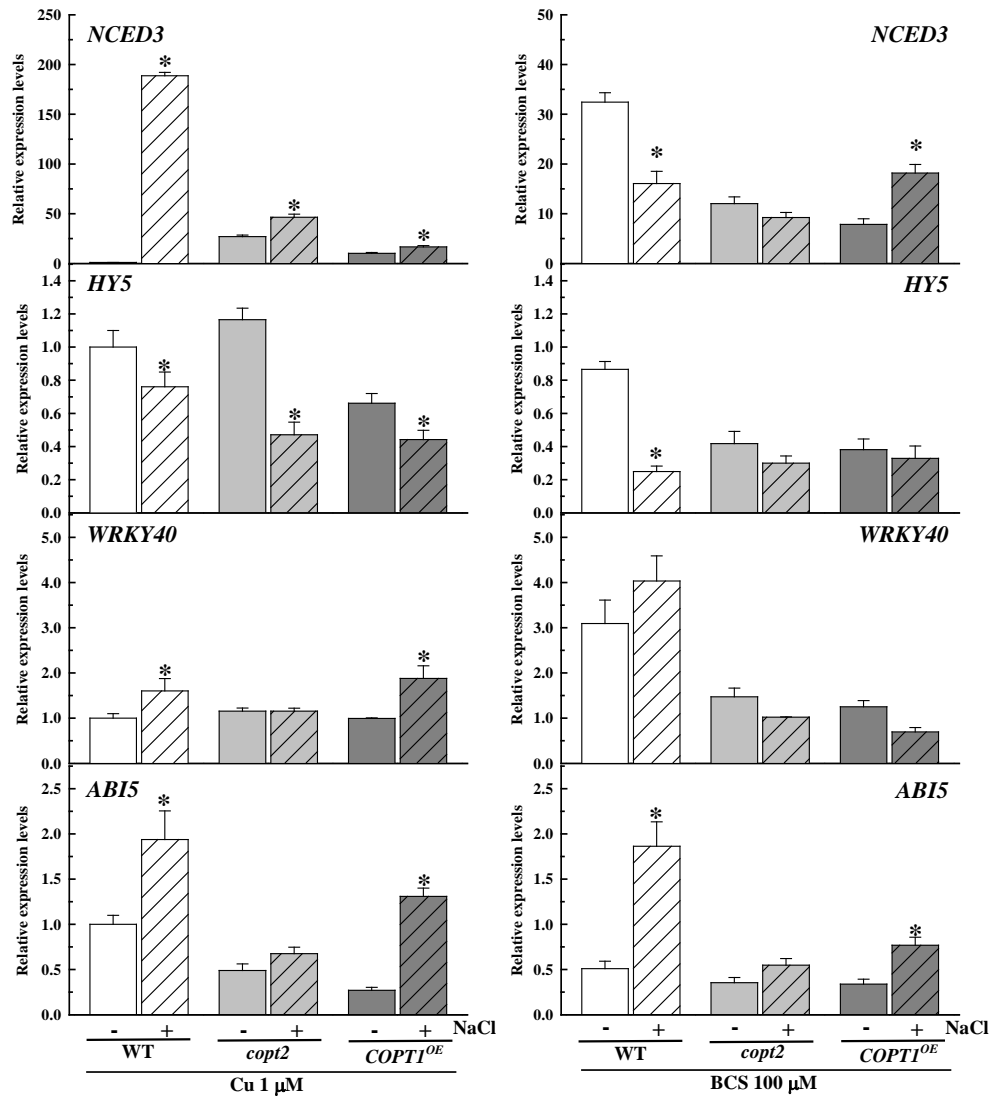**Figure R.1.19. Effect of salt stress on the transcriptional regulation of ABA-related genes.** Transcript levels of *NCED3*, *HY5*, *WRKY40* and *ABI5* genes in WT, *copt2*, and *COPT1^{OE}* 14 day-old seedlings treated or not with NaCl (200 mM, 7 days) and grown under Cu sufficiency and deficiency conditions. Expression values are relative to those reported in non NaCl-treated (control) WT seedlings grown under Cu sufficiency conditions for each gene. Bars are means ± SD of 3 replicates of at least 10 plants each. Asterisks indicate statistical differences (P<0.05) according to Tukey's test respect to values of control plants of each genotype.

Similarly, the *pmCOPT* mutants did not achieve the *ABI5* expression levels observed in the WT, irrespective of the growing media or stress applied. *HY5* and *WRKY40* responses were also affected by Cu status and in the *pmCOPT* mutants. Whereas Cu deficiency slightly lowered and salt stress repressed the *HY5* transcript levels, the *WRKY40* gene expression was induced by both Cu deficiency and endogenous increases in ABA levels caused by abiotic stress under the optimal Cu growing conditions (Figure R.1.19). Taken together, these results indicate that both ABA biosynthesis and signalling produced by environmental stress conditions, such as high salt, are affected by Cu status.

DISCUSSION

Understanding molecular responses of crop plants to the abiotic stresses in which ABA is involved is critical for facing environmental challenges in which the cross-talk between ABA and nutrient homeostasis plays a central role (Boursiac *et al.*, 2013). The cross-talk between Cu homeostasis and ABA responses is explored herein. Attenuated ABA responses were observed under Cu deficiency (Figures R.1.1A, B, R.1.5 and R.1.2). This indicates that ABA effects depend on plant Cu status, which could be evidenced by modifying the Cu content in the medium or studying transgenic plants affected in Cu transport. ABA affects expression of Cu deficiency markers in a complex process that depends on Cu status (Figures R.1.4, R.1.6, R.1.9).

Although increased stress ABA levels have been described for higher (100 µM) Cu concentrations (Kim *et al.*, 2014; Ye *et al.*, 2014), no increases in stress ABA content were detected (Figure R.1.12A) within the mild Cu concentration range used herein (0– 25 µM). Instead a slight decrease in ABA content was observed with both Cu deficiency and excess compared with Cu sufficiency (Figure R.1.12A). The Cu requirement for normal ABA content can be explained by the role that Cu plays in the MoCo biosynthesis pathway (Schwarz and Mendel, 2006). The effect of Cu excess can be due to the fact that Cu may compete with Mo during MoCo biosynthesis (Kuper *et al.*, 2004). Mo content increased under Cu deficiency conditions (Figure R.1.13C), as reported in *Brassica napus* for Cu deficiency (Billard *et al.*, 2014). Although Cu effects have been proposed for other hormones (Arteca and Arteca, 2007; Kazan, 2013; Lequeux *et al.*, 2010; Maksymiec *et al.*, 2007; Wu *et al.*, 2012; Yan and Dong, 2014), no significant changes were observed for auxins and JA at the mild Cu levels used herein (Figure R.1.13).

Exogenous ABA increased the expression of ABA biosynthesis genes, e.g. *NCED3* (Figure R.1.14). The fact that this induction was repressed in BCS and in Cu⁺ transport-altered mutants *slp7* and *copt2* (Figure R.1.14) suggests a key effect of spatiotemporal-regulated Cu homeostasis on ABA biosynthesis. This regulation is at least partially dependent on SPL7, and the fact that the NCED3 promoter displays seven putative GTAC boxes (Figure R.1.3) agrees with this. Taken together, these results indicate a delicate balance in the negative feedback loop established between the Cu requirement for ABA biosynthesis and the regulatory role of this hormone in Cu uptake. Apart from affecting ABA biosynthesis, Cu deficiency drastically modified ABA signaling (Figure R.1.12D, R.1.14). The induction of *ABI5* expression by exogenous ABA was greatly compromised under Cu deficiency given the poor ABA sensitivity exhibited in BCS (Figure R.1.1A). In agreement with their putative roles as *ABI5* repressors, the expression of two transcription factors that bind the *ABI5* promoter, *WRKY40* and *HY5* (Chen *et al.*, 2014, 2010), was down-regulated by ABA in

the WT plants under Cu sufficiency (Figure R.1.14A). HY5 was highly expressed in the *aba2* mutant (Figure R.1.15) and the *COPT1^{OE}* line under the Cu deficiency conditions, and also in the *copt2* mutant with Cu sufficiency (Figure R.1.14). These results indicate that both Cu and ABA might be needed to repress *HY5* synergistically, which would be a plausible explanation for the ABA-related phenotypes shown by the *copt2* and *COPT1^{OE}* lines (Figure R.1.1A, B). Since *hy5* mutants are less sensitive to ABA (Chen *et al.*, 2014), the *copt2* mutant, which expressed higher *HY5* levels, consequently gave an enhanced response to ABA under Cu sufficiency (Figure R.1.1A, B). Since HY5 interacts with SPL7 (Zhang *et al.*, 2014), these results show HY5 to be a putative integrator between the ABA and Cu deficiency responses.

The attenuation of Cu deficiency responses by exogenous ABA, including *pmCOPT* genes and their transcriptional regulator SPL7 (Figure R.1.4), could explain how ABA affects the endogenous Cu content (Figure R.1.1E). The promoters of SPL7 and its *pmCOPT* targets display putative ABRE cis-elements (Nakashima *et al.*, 2006; Figure R.1.3), which could account for their ABA mediated negative regulation with Cu sufficiency (Figure R.1.4A). ABA acts on the target expression both dependent on and independently of the SPL7 transcription factor. Other metal transport systems, such as Fe and Zn, have been reported to be affected by exogenous ABA (Lei *et al.*, 2014; Shi *et al.*, 2015), which indicates a widespread effect of ABA on metal transport.

Cu deficiency-related regulation could be explained by interference in *pmCOPT* promoters of different transcription factors. As the promoters of *pmCOPT* genes present both ABRE and CuRE elements (Figure R.1.3), this could account for ABA and Cu deficiency regulation, respectively(Nakashima *et al.*, 2006; Yamasaki *et al.*, 2009). In the presence of Cu, SPL7 binding to its target promoters is considerably reduced (Yamasaki *et al.*, 2009). In these circumstances, other ABA repression factors could bind Cu deficiency targets with ABA-related cis-regulatory elements in their promoters, such as *pmCOPT* genes. Accordingly, a slight regulation in pmCOPT expression by ABA was observed in the spl7 mutant in both Cu regimes (Figure R.1.4; Figure R.1.7). Exogenous ABA drastically modified the *COPT2*-driven localization pattern from tissues along the root towards the crown (Figure R.1.9; Figure R.1.11). ABA levels in root vascular bundles have been reported to increase with nutrient shortage (Vysotskaya *et al.*, 2008) and different abiotic stresses, such as drought and salinity (Nambara and Marion-Poll, 2005; Waadt *et al.*, 2014). The results obtained here indicate that Cu uptake under stress conditions would be inhibited in the locations where increased ABA caused by stress was present, and could be restricted to the locations where ABA remained unchanged. One relevant issue is to determine the importance of *pmCOPT* expression in the relative resistance of plants subjected to environmental stress such as salinity by inducing increases in ABA. With our experimental conditions, the absence of *pmCOPT* expression under Cu sufficiency led to increased sensitivity

(Figure R.1.16), which mostly reproduced the changes observed after exogenous ABA application (Figure R.1.1).

Hormones probably play a fundamental role in the spatial arrangement and temporal schedule of metal transport processes by affecting plant development. Metal availabilities could interfere with hormone biosynthesis transport and signaling processes at many levels. These interactions could co-ordinate and integrate spatiotemporal information to optimize plant metabolism and physiology (Haydon *et al.*, 2013; Sanchez *et al.*, 2011), and the understanding of these complex mechanisms is a pressing challenge to face foreseen unfavorable climate change effects on agriculture.

CHAPTER 2:

DEFECTIVE COPPER TRANSPORT IN THE *copt5* MUTANT AFFECTS CADMIUM TOLERANCE

RESULTS

2.1. Effect of cadmium on the root growth of the *copt5* mutant seedlings and its interaction with copper

The *copt5* mutant exhibit altered metal sensitivity under severe Cu deficiency conditions (García-Molina *et al.*, 2011). The ½ MS medium has been shown to be slightly Cu-deficient (Abdel-Ghany *et al.*, 2005a; Andrés-Colás *et al.*, 2013; Yamasaki *et al.*, 2009). In order to further characterize the *copt5* phenotype in the commonly used ½ MS medium, we checked the root length of 7-day-old WT and *copt5-2* mutant seedlings supplemented with various Zn and Cd concentrations (Figure R.2.1A and B).
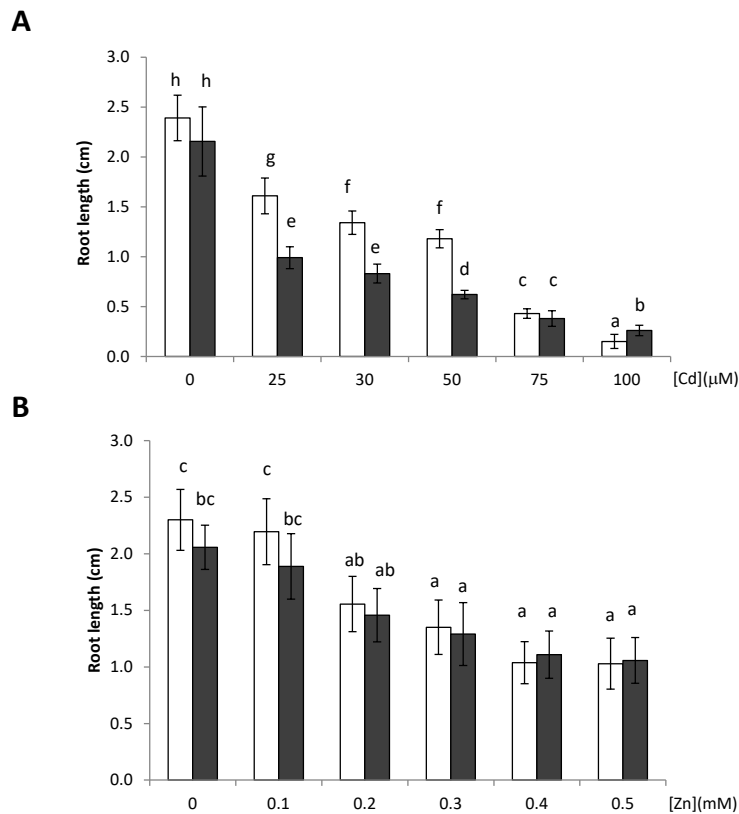
Figure R.2.1. Effect of Cd and Zn toxicity on root length in the *copt5* mutant. Root length from 7 day-old WT (white bars) and *copt5-2* (black bars) seedlings. Seedlings were grown in ½ MS medium supplemented with different Cd concentrations (0-100 μM CdCl$_2$) (A) or with Zn concentrations (0-0.5 mM ZnSO$_4$) (B). Different letters indicate significant differences (*P* < 0.05) (n=30).

Under low Cu (½ MS medium), the *copt5-2* mutant showed a significant differential effect on root length by Cd, but not by Zn treatments (Figure R2.1A and B). In order to exacerbate the Cu-deficiency conditions, and to further confirm the metal sensitivity displayed by the *copt5* mutant (García-Molina *et al.*, 2011), the experiment was performed in the presence of Cu chelator BCS at 50 µM at different Zn concentrations (Figure R.2.2). Indeed, under severe Cu-deficient conditions (50 µM BCS), the *copt5* mutant was sensitive to the presence of metals, as previously reported (García-Molina *et al.*, 2011). In order to understand the role of COPT5 on metal toxicity under mild conditions, we selected the low Cu ½ MS medium for further experiments, as well as a Cd concentration which, without being excessively toxic, had a differential effect on the WT and *copt5* plants. Thus unless otherwise stated, the chosen Cd concentration hereinafter was 30 µM.
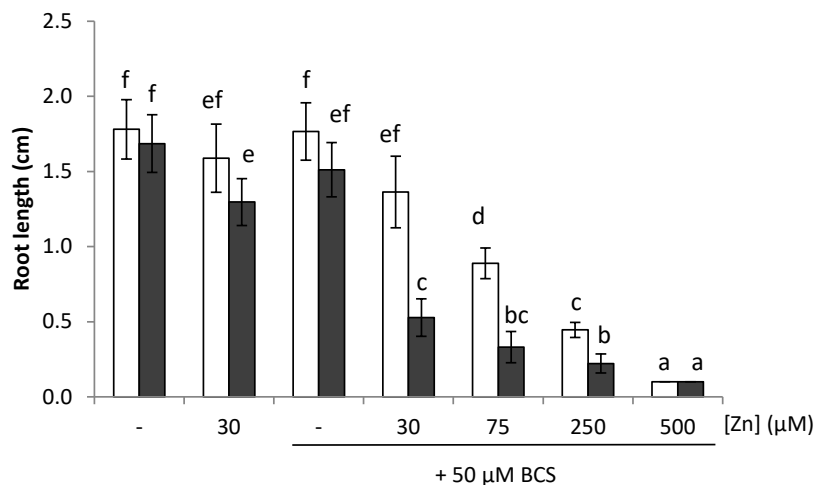
Figure R.2.2. Effect of Zn toxicity on root length in the *copt5* mutant under severe Cu deficiency. Root length from 7 day-old WT (white bars) and *copt5-2* (black bars) seedlings. Seedlings were grown in ½ MS medium supplemented with Zn (0-500 µM Zn) and with or without 50 µM BCS. Different letters indicate significant differences ($P < 0.05$) (n=30).

Under the slightly Cu-deficiency conditions of the ½ MS medium, the knock-out mutant lines (*copt5-2* and *copt5-3*) did not show significant differences in root growth if compared to WT, while the *COPT5^{OE}* line was higher (Figure R.2.3A). In order to ensure Cu-sufficient conditions, 1 µM Cu was added to the ½ MS medium, which had no influence on root growth (Figure R.2.3A). Cd toxicity was also tested under these two Cu conditions (½ MS medium and the same medium with 1 µM Cu) (Figure R.2.3A). Whereas both *copt5* mutant lines show increased sensitivity to

30 µM Cd under low Cu (½ MS), when compared to the WT, the *COPT5^{OE}* line maintained the opposite phenotype with roots, which grew slightly longer than the controls (Figure R.2.3A).
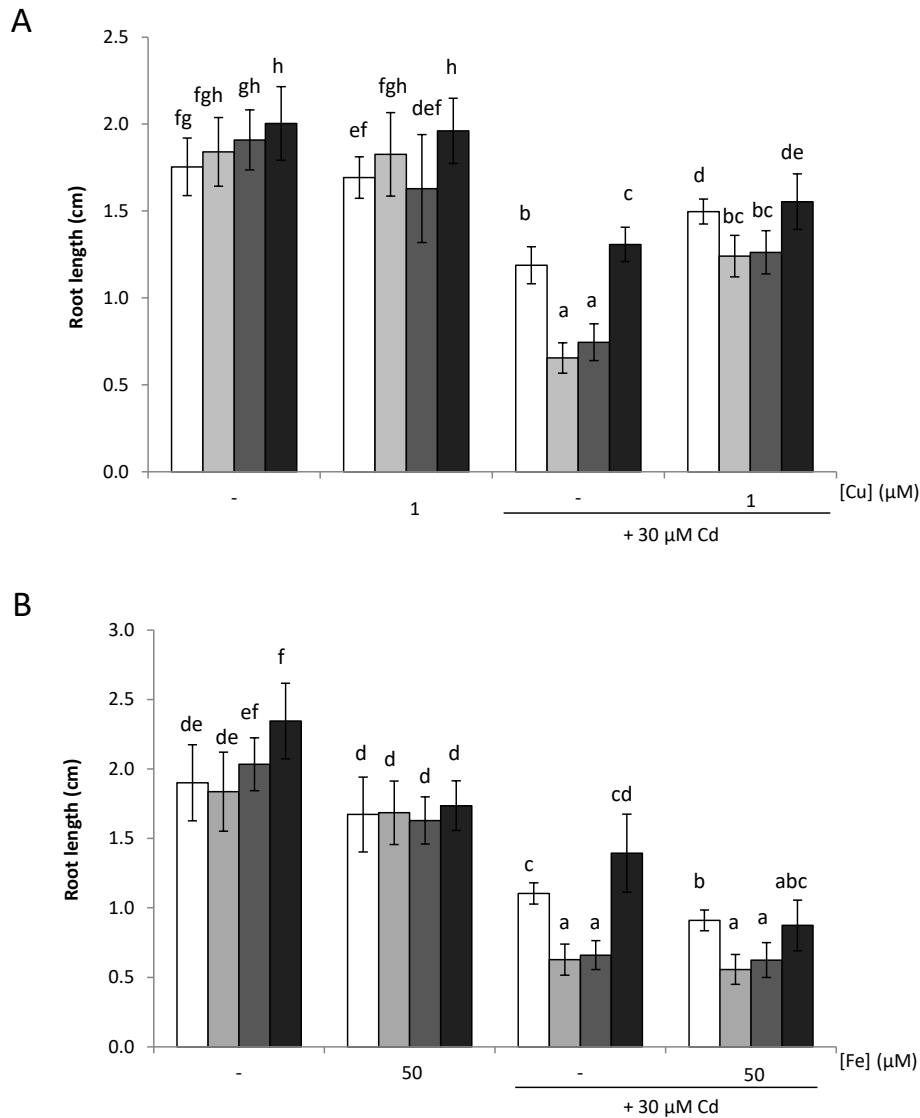
Figure R.2.3. Interaction of Cu and Fe with Cd toxicity. Root length of 7 day-old wild-type (white bars), *copt5-2* (gray bars), *copt5-3* (dark grey bars) and *COPT5^{OE}* (black bars) seedlings grown in the ½ MS medium (-) and the same medium supplemented with 1 µM Cu, containing or not Cd (30 µM) (A), or in the ½ MS medium (-) and the same medium supplemented with 50 µM Fe, containing or not Cd (30 µM) (B). Different letters indicate significant differences (P< 0.05, n=21-30).

Strikingly, by adding only 1 µM Cu to the growth medium, root growth notably increased in all four lines and Cd sensitivity was almost reversed, which indicates the strong Cu effect on Cd sensitivity (Figure R.2.3A). The 15 µM Cu concentration, which fell within the upper sufficiency range, fully reverted the root growth defects of the *copt5-2* mutant at two Cd concentrations (10 and 30 µM) (Figure R.2.4A). The *copt5* line complemented with *COPT5* under its own promoter (García-Molina *et al.*, 2011) also significantly reverted root growth inhibition, indicating partial phenotype restoration (Figure R.2.4B).
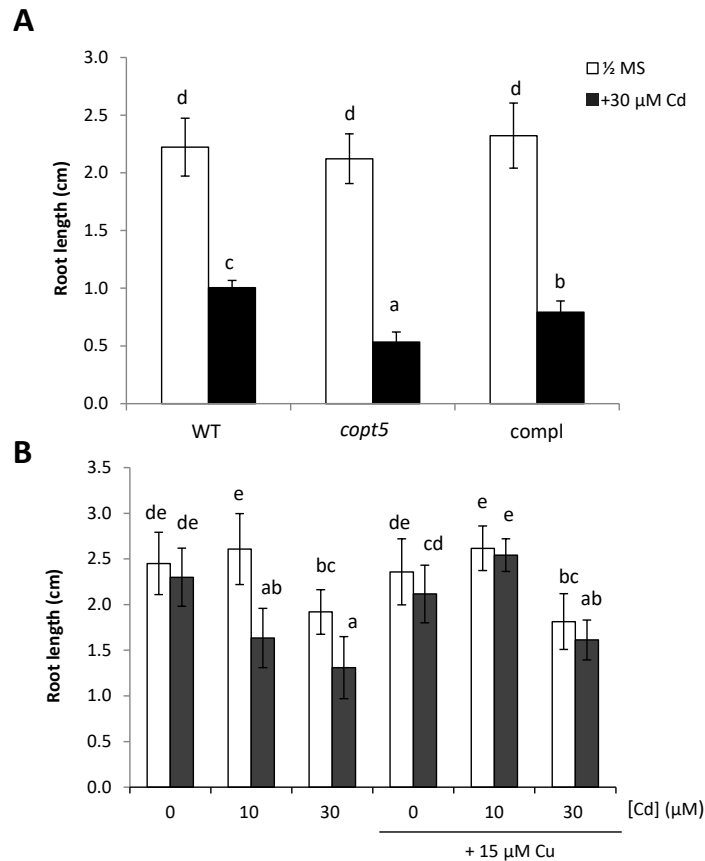
Figure R.2.4. Recovery of Cd sensitivity by Cu addition and in the complemented *COPT5* line. Root length of 7 day-old WT (white bars) and *copt5* (black bars) seedlings grown in the ½ MS medium containing different Cd concentrations (0, 10 and 30 µM) and supplemented (A), or not, with 15 µM Cu or 15 µM Fe (B). Root length of the 7-day-old WT, *copt5* and *pCOPT5::COPT5::GFP* (compl) seedlings grown in the ½ MS medium supplemented, or not, with 30 µM $CdCl_2$. Different letters indicate significant differences ($P \leq 0.05$) (n=25).

We also checked the Cd sensitivity of the plasma membrane COPT transporters under our experimental conditions by analyzing the root length of the corresponding single mutants (*copt1*, *copt2* and *copt6*). None showed significant differences with the WT controls (Figure R.2.5). To check if this effect was Cu-specific, the same experiment shown in Figure R.2.3A was carried out in the presence of 50 µM Fe instead of Cu.
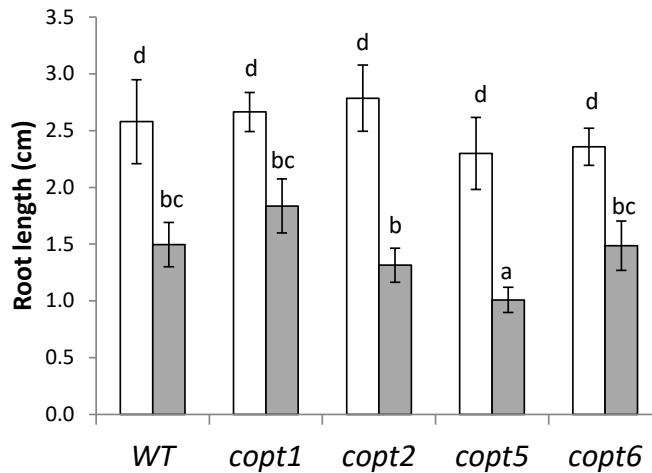
Figure R.2.5. Effect of Cd stress in *copts* mutants. Root length of 7 day-old WT and *copt1*, *copt2*, *copt5* and *copt6* seedlings grown in the ½ MS medium (white bars) or supplemented with 30 µM Cd (grey bars). Different letters indicate significant differences ($P \leq 0.05$) (n=15).

The results obtained revealed that Fe was unable to reverse Cd-induced root length inhibition or the increased Cd toxicity in the knock-out mutant (Figure R.2.3B), which implies that the Cd sensitivity exhibited by the *copt5* mutants is Cu-specific. Taken together, these results indicate that the Cd sensitivity phenotype is indeed *COPT5*-dependent and is due to the COPT5 function in Cu homeostasis.

2.2. Ethylene perception in the *copt5* mutant seedlings

Since ethylene has been implicated in plant responses to stress by heavy metals (Arteca and Arteca, 2007), and as Cu is involved in ethylene perception (Hirayama *et al.*, 1999), the possibility of the observed responses to Cd treatments in the *copt5* mutant being mediated by changes in

ethylene perception was studied in etiolated seedlings, where ethylene promotes well-known hypocotyl shortening (Guzmán and Ecker, 1990). The hypocotyls and root length in the WT, the two *copt5* mutants and the *COPT5^{OE}* lines were measured in etiolated seedlings under these four conditions: 1) ½ MS; 2) ½ MS with 1 µM Cu; 3) ½ MS with 30 µM Cd; and 4) ½ MS with 1 µM Cu and 30 µM Cd. The results obtained from these experiments are presented in Figure R. 2.6 As observed, hypocotyls length became significantly shorter under Cd treatment, irrespectively of the presence of Cu in the medium, and no consistent differences were observed in the *copt5* mutants (Figure R.2.6A).
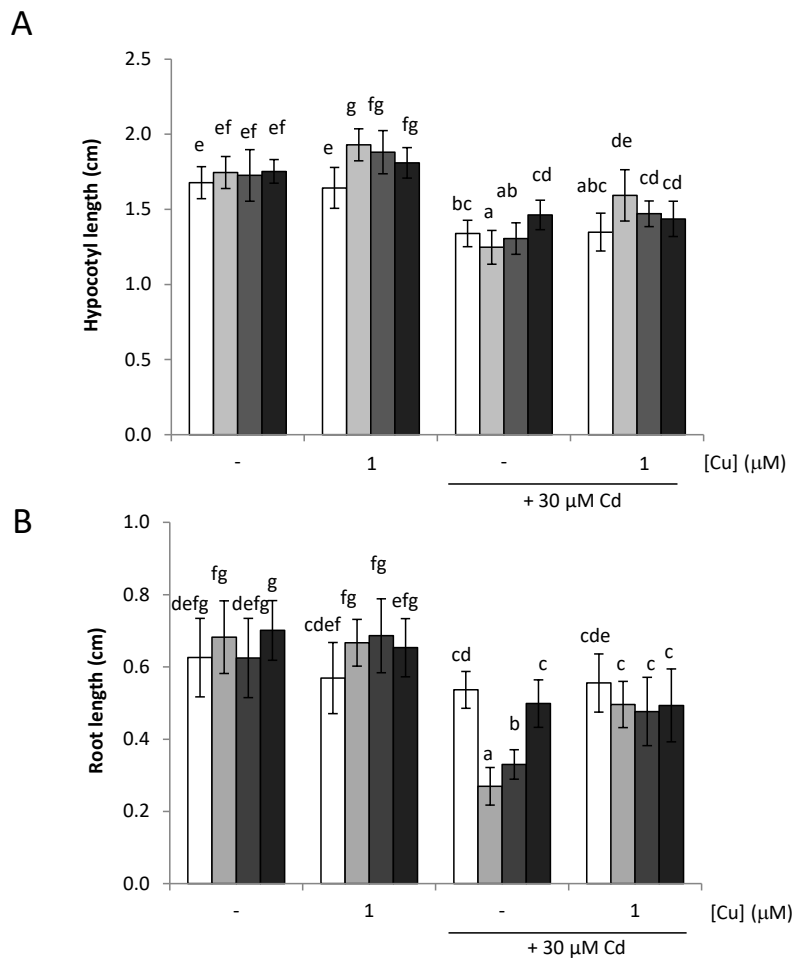
Figure R.2.6. Effect of Cd on etiolated seedlings. Hypocotyl (A) and root (B) length of the WT (white bars), *copt5-2* (grey bars), *copt5-3* (dark grey bars) and *COPT5^{OE}* (black bars) seedlings grown for 7 days in the absence of light in ½ MS medium (-), and in the same medium supplemented with 1 µM Cu, containing or not Cd (30 µM). Mean values ± standard deviation (SD) are shown (n=18). Different letters indicate significant differences ($P< 0.05$).

The greater sensitivity of the *copt5* mutants to Cd in ½ MS was particularly evident in roots given the reduction in length under these conditions (Figure R.2.6B), and was even greater than in the plants grown in the light/dark cycles at the same Cd concentration (Figure R.2.3). *COPT5^{OE}* plants behaved as the controls under all the tested conditions (Figure R.2.6).

Root length in the presence of ethylene is greatly reduced, which precluded to us measuring them. However, Cd-induced hypocotyl growth inhibition in the etiolated plants, a well-known parameter affected by ethylene (Guzmán and Ecker, 1990), was drastically reduced by around half, as measured in its absence of both the *copt5* lines and the WT plants (Figure R.2.7).
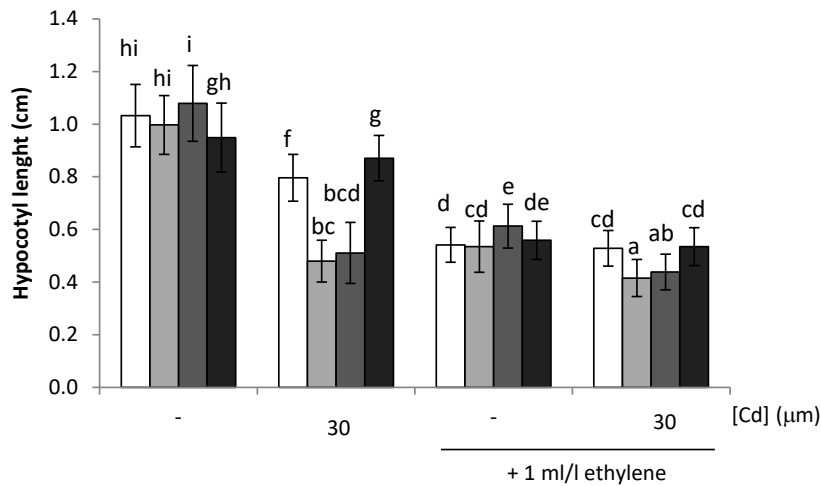
Figure R.2.7 Effect of ethylene on hypocotyl elongation of etiolated seedlings under Cd stress. Hypocotyl length of etiolated 7-day-old WT (white bars)*, copt5-2* (light grey bars), *copt5-3* (grey bars) and *COPT5^{OE}* (black bars) seedlings grown in sealed pots containing ½ MS medium either without or with 30 μM Cd, and in the absence or presence of 1mL L^{-1} of ethylene (+ ethylene). Mean values ± standard deviation (SD) are shown (*n*=40). Different letters indicate significant differences (*P*< 0.05).

Mutants showed greater sensitivity to Cd than the WT, even in the presence of ethylene. Moreover, the WT plants were not significantly affected by Cd when the hormone was present, while a further reduction in hypocotyls length was measured in the *copt5* seedlings (Figure R.2.7).

2.3. Effect of cadmium on gene expression in the wild type and *copt5* mutant seedlings

The effect of Cd on COPT gene expression was checked in the WT seedlings germinated on plates under the four above-defined different Cu and Cd conditions. The obtained results indicate that, unlike *COPT1* and *COPT2*, *COPT5* was not regulated by Cu, which agrees with previously reported data (Sancenón *et al.*, 2003). Thus, the relative expression of *COPT1* and *COPT2* lowered significantly in the 1 µM Cu medium, while the *COPT5* expression remained constant. At the concentrations used, its expression remained unaltered in the presence of Cd, while the regulation of *COPT1* and *COPT2* by Cu was still observed, or even further reduced, in this medium (Figure R.2.8).
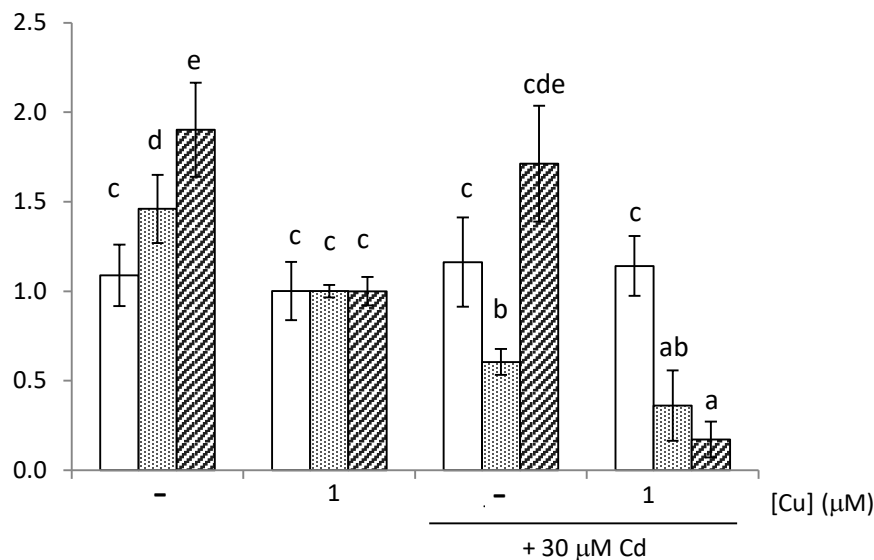
Figure R.2.8. Expression of COPTs under Cd stress. Relative mRNA levels of *COPT5* (white bars), *COPT1* (dot bars) and *COPT2* (grated bars) in the 7-day-old WT seedlings grown in the ½ MS (-), supplemented with 1 µM Cu, 30 µM Cd or 1 µM Cu plus 30 µM Cd. Total RNA was extracted and analyzed by qRT-PCR. Values correspond to arithmetic means ($2^{-\Delta\Delta Ct}$) ± standard deviation (SD) (*n*=3). Different letters indicate significant differences ($P \leq 0.05$).

The expression of *FSD1*, a Cu-deficiency target regulated by the SPL7 transcription factor (Andrés-Colás *et al.*, 2013; Yamasaki *et al.*, 2009), was also determined. The analysis of the *FSD1* expression in the 7-day-old WT, *copt5-2, copt5-3* and *COPT5^{OE}* seedlings, grown under the four experimental conditions, revealed that this expression in the WT seedlings in ½ MS lowered by more than 75% when Cu was added to the ½ MS medium (Figure R.2.9A), as also occurred in the

copt5-2 and copt5-3 seedlings. However under low Cu conditions, it was significantly lower in the mutants than in the WT (Figure R.2.9A). In addition to being regulated by Cu, the *FSD1* expression also lowered under Cd treatment, and a further reduction was noted in the presence of both metals (Figure R.2.9A), similarly to the effect observed on the *COPT1* and *COPT2* expressions (Figure R.2.8).
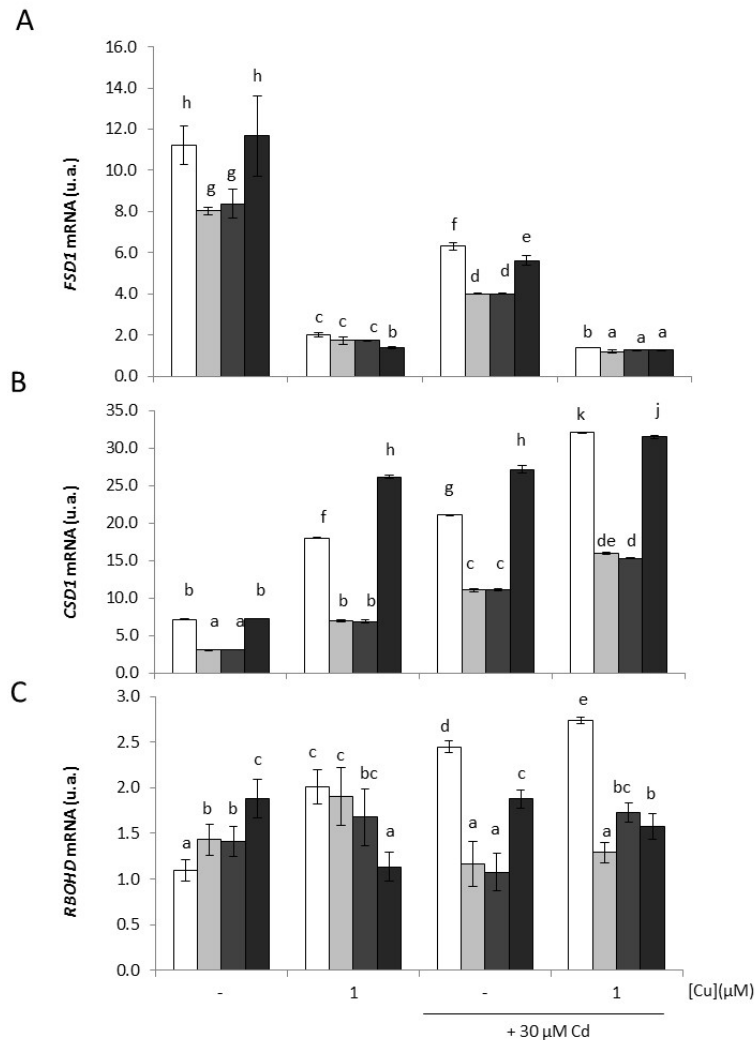
Figure R.2.9. Expression of oxidative stress markers. Relative expression of *FSD1* (A), *CSD1* (B) and *RbohD* (C) mRNA in the WT (white bars), *copt5-2* (grey bars), *copt5-3* (dark grey bars) and *COPT5^OE* (black bars) seedlings grown for 7 days in the ½ MS medium (-), supplemented with 1 µM of Cu, containing or not Cd (30 µM). Total RNA was extracted and analyzed by qRT-PCR. Values correspond to arithmetic means ($2^{-\Delta\Delta Ct}$) ± standard deviation (SD) (*n*=3). Different letters indicate significant differences (*P* ≤ 0.05).

As the SPL7 transcription factor also regulates *MIR398b/c* under Cu deficiency which, in turn, regulates the *CSD1* expression at the post-transcriptional level (Yamasaki *et al.,* 2007), the *CSD1* expression in the same samples was also checked (Figure R.2.9B). Unlike *FSD1*, the *CSD1* expression in the WT more than doubled when Cu was added to the medium, and it became exacerbated in the presence of Cd (Figure R.2.9B). These findings further indicate that Cd attenuates Cu deficiency responses, which agrees with the results obtained for plasma membrane-regulated transporters *COPT1* and *COPT2* (Figure R.2.8) and *FSD1* (Figure R.2.9A). The *CSD1* expression values ½ MS in the *copt5-2* and *copt5-3* seedlings were also significantly lower than in the WT under all the studied conditions, whereas *COPT5^{OE}* seedlings behaved mostly like the WT (Figure R.2.9B).

The expression of a ROS-generating enzyme encoded by *RBOHD,* which has been used as a control for gene expression under Cd toxicity (Keunen *et al.*, 2013), was employed to study the effect of both metals on gene expression under the above-described four conditions. As shown in Figure R.2.9C, the WT seedlings grown in ½ MS showed a 50% lower *RBOHD* expression than when grown under Cu sufficiency conditions. The same effect was observed when Cd was present in the medium as the *RBOHD* expression levels increased significantly in the 1 µM Cu medium, in addition to the effect caused by Cd alone. Conversely in the *copt5-2* and *copt5-3* mutant plants, the relative *RBOHD* expression remained almost constant under the 4 different conditions (Figure R.2.9C). *COPT5^{OE}* showed the opposite *RBOHD* pattern of expression since the presence of Cu reduced it and it remained unaffected by Cd under low Cu conditions, but slightly increased when Cu was present (Figure R.2.9C).

The expression pattern of these three genes in the *spl7* mutant under the same four experimental conditions (Figure R.2.10) allowed us to identify the Cd effects deriving from the altered Cu-deficiency responses in the *copt5* mutants.
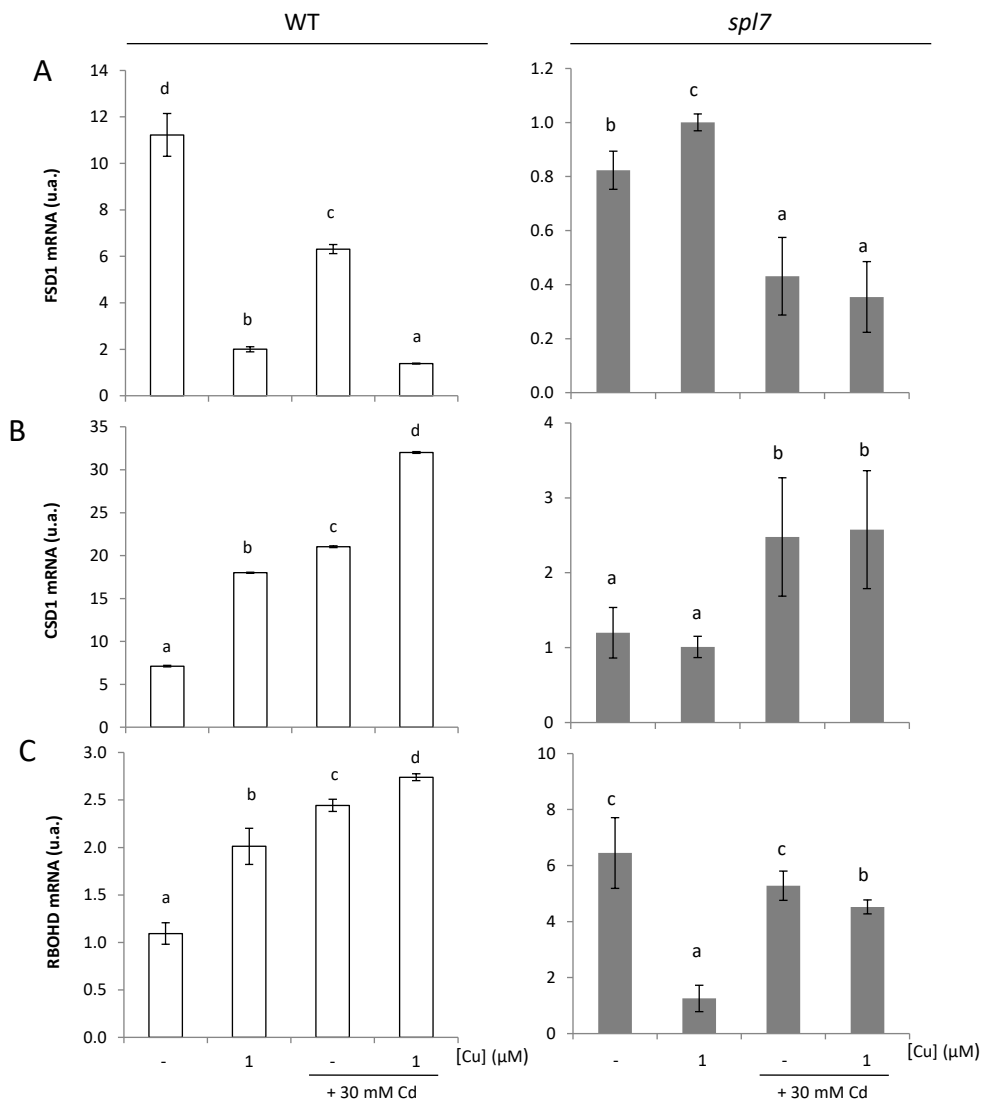
Figure R.2.10. The oxidative stress marker expression. Relative expression of *FSD1* (A), *CSD1* (B) and *RbohD* (C) mRNA in the 7 day-old WT (left) and *spl7* (right) seedlings grown in the ½ MS (-), supplemented with 1 µM Cu, 30 µM Cd or 1 µM Cu and 30 µM Cd. Total RNA was extracted and analyzed by qRT-PCR. Values correspond to arithmetic means ($2^{-\Delta\Delta Ct}$) ± SD (*n*=3). Different letters indicate significant differences ($P \leq 0.05$).

As expected, the characteristic Cu regulation of *FSD1* and *CSD1* (Figure R.2.9A and B) was not observed in the *spl7* seedlings (Figure R.2.10A and B). However, *FSD1* attenuation and *CSD1* induction observed in the presence of Cd were maintained in the *spl7* mutant, which indicates that the Cd effects on Cu-deficiency markers are at least partially independent of master

regulator SPL7. In contrast, the responses of the *RBOHD* expression pattern to Cu altered in the *spl7* mutant, where no activation was observed by either Cu or Cd. This indicates that oxidative stress is a putative mediator of Cd effects and alters SPL7-dependent responses (Figure R.2.10C).

2.4. Longer term effects of cadmium on plant growth and oxidative stress

In order to study the possible distinctive effects of Cd on roots and shoots, the WT and *copt5* plants were grown for 31 days in hydroponic culture in modified Hoagland without Cu. Afterward, both the WT and *copt5-2* mutants were subjected to 16-day Cd treatments by adding different concentrations to the nutrient solution (2.5-10 µM, Figure R.2.11). Root growth was very sensitive to the presence of Cd in the medium. Thus at the end of the 16-day treatment, both plant types showed a progressively lower absolute growth rate (AGR) with an increased Cd concentration. The largest root length difference between the WT and *copt5-2* mutant plants was measured at 2.5 µM (16% lower in the mutant). Both plant types revealed an almost total cessation of root growth at 10 µM Cd (Figure R.2.11A). Growth of aerial parts (Figure R.2.11B), measured as increased fresh weight, was impaired by the longer-term Cd treatments and, as indicated for seedlings (Figure R.2.1), the *copt5-2* plants showed greater sensitivity than the WT at the 5 µM Cd concentration. At this concentration, the AGR was 18% lower in the mutant than in the WT, which is a similar difference to that found for root growth at a lower concentration (2.5 µM Cd).
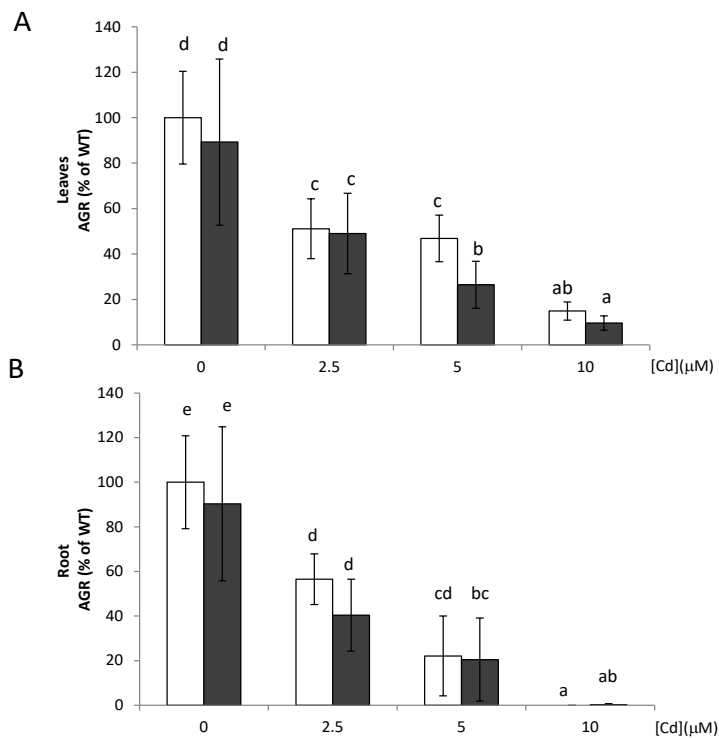
Figure R.2.11. Effects of Cd exposure on plant growth in the hydroponic medium. Absolute growth rates (AGR), calculated from changes in root length (A) and in the fresh weight of aerial parts (B) during the 16-day treatment of the 47 day-old WT and *copt5* plants grown in the Hoagland's hydroponic medium supplemented with different Cd concentrations. Values are expressed as a percentage of the WT control plants. Different letters indicate significant differences ($P \leq 0.05$) (n≤8).

To investigate the functional role of COPT5 in Cd translocation to shoots, lipid peroxidation (measured as MDA content) was quantified in leaves and roots (Figure R.2.12A and B) under 0, 5 and 10 µM Cd to check whether putative changes in Cd transport can be revealed by differences in oxidative stress levels. Despite MDA contents being similar in the absence of Cd in the WT and *copt5-2* mutant plants in leaves and roots, lipid peroxidation increased in the WT leaves when Cd was added to the media, but remained mostly unaffected in *copt5-2,* or with even lower, but non-significant, values than in WT leaves (5 µM Cd, Figure R.2.12A).
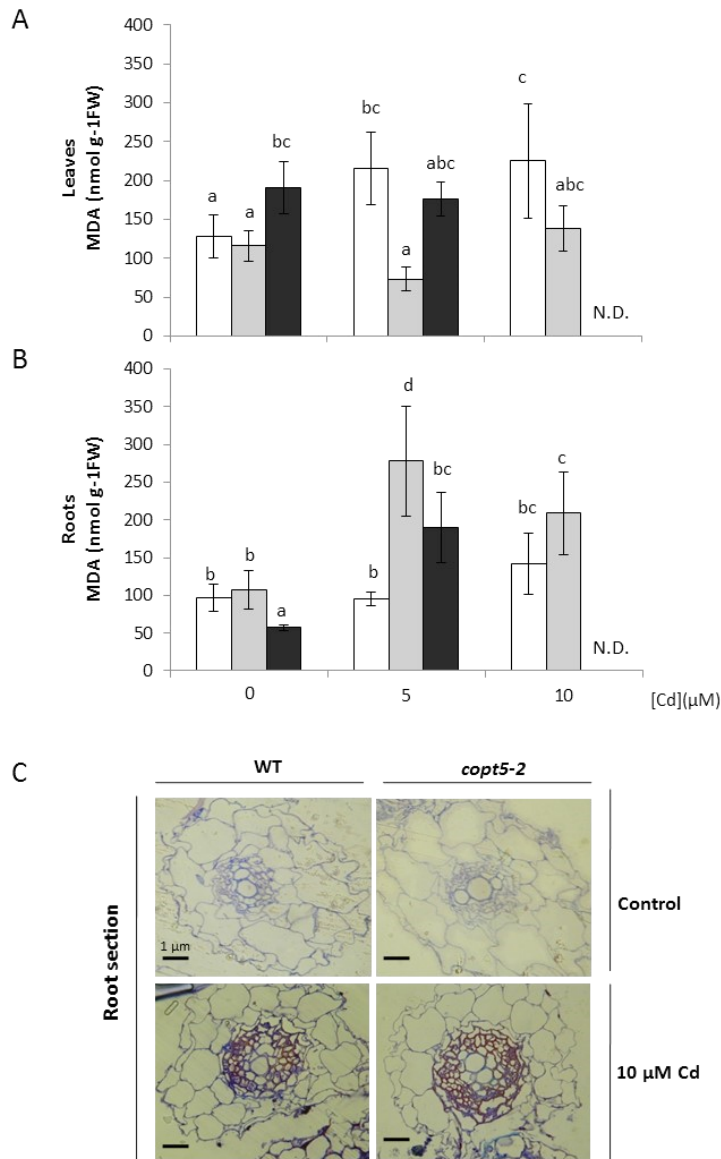
Figure R.2.12. Lipid peroxidation in Cd-stressed adult plants. MDA contents in the leaves (A) and roots (B) of the 47-day-old WT (white bars), *copt5-2* (grey bars) and *COPT5^OE* (black bars) plants grown during the last 16 days of culture in Hoagland's hydroponic medium containing different Cd concentrations. Mean values ± standard deviation (SD) are shown (*n*=3-6). Different letters indicate significant differences ($P \leq 0.05$). FW, fresh weight. Cross-sections of the WT and *copt5* root tissue from the Cd-stressed and control plants stained with toluidine blue (C). Photographs were taken with an optical microscope (the black bar represents 1 μm). The sites of plasma membrane damage are stained in red.

Remarkably, the lipid peroxidation levels showed a completely reversed pattern of change in roots as MDA content considerably increased in the *copt5-2* mutant at the lower Cd concentration tested (5 μM), and remained higher than in the WT roots at higher Cd levels

(Figure R.2.12B). Accordingly, the *COPT5*^{OE} line showed the opposite effect with increased MDA content in leaves and decreased in roots when compared to the *copt5-2* mutant (Figure R.2.12A and B). The location of the oxidative damage caused by Cd in roots was studied. For this purpose, histologic sections were performed from the roots of those plants grown in hydroponic Hoagland (0.1X) solution with or without 10 µM Cd (Figure R.2.12C), and they were stained with toluidine blue dye. Lipid peroxidation in the tissues surrounding the vascular bundles, detected by the appearance of a reddish-blue color (black arrows in Figure R.2.12C), was higher and more widely extended in the vascular bundles of the *copt5-2* roots at 10 µM Cd. Thus, Cd differentially affects *copt5-2* roots.

2.5. Effect of cadmium on ethylene release according to copper levels

The possibility of the observed responses to Cd treatments being mediated by changes in ethylene biosynthesis in Cd-treated plants was studied in hydroponically grown WT and *copt5-2* adult plants subjected to four test conditions: modified Hoagland 0.1X without Cu; the same medium with Cu (0.1 µM), or Cd (5 µM); and both Cu (0.1 µM) and Cd (5 µM). The most remarkable result obtained from these experiments was under the 0.1 µM Cu conditions, where ethylene release was significantly stronger than in the absence of Cu because when Cu was added, the values almost doubled in the WT, and they quadrupled in the mutant, if compared to those in the modified Hoagland 0.1X without Cu medium (Figure R.2.13).
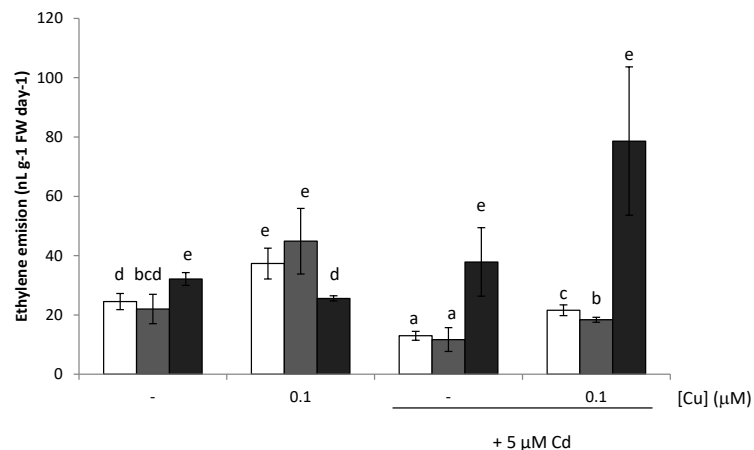
Figure R.2.13. Effect of Cd stress on ethylene biosynthesis according to Cu status. Ethylene emission in the 47-day-old WT (white bars), *copt5-3* (dark grey bars) and *COPT5*^{OE} (black bars) plants grown in modified Hoagland's hydroponic medium without Cu and treated during the last 16 days of culture with 0.1 µM Cu, 5 µM Cd or 0.1 µM Cu plus 5 µM Cd. Different letters indicate significant differences ($P \leq 0.05$) (n≤5). FW, fresh weight.

Thus, surprisingly, a deficit in Cu content seemed to limit ethylene biosynthesis. The presence of Cd further reduced the biosynthesis of the hormone in both the WT and *copt5-2* plants under both Cu conditions (Figure R.2.13).
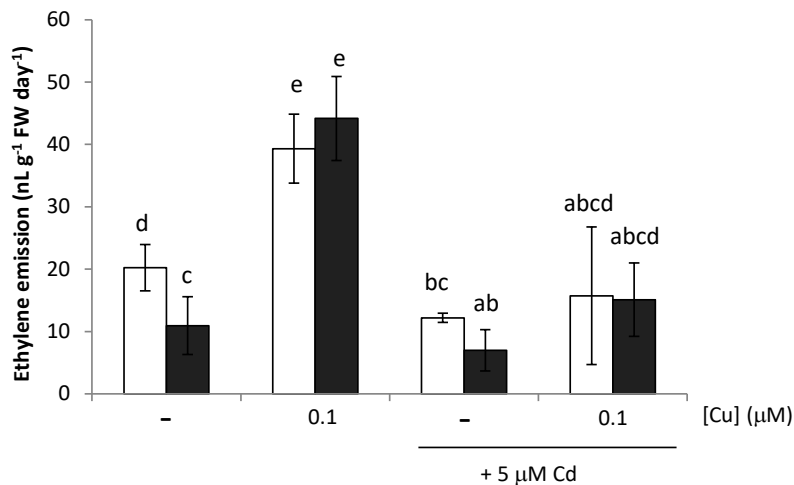
Figure R.2.14. Effect of Cd stress on ethylene biosynthesis at different Cu status. Ethylene emission in the 47 day-old WT (white bars), *copt5-3* (black bars) plants grown in modified Hoagland's hydroponic medium without Cu (-) and treated during the last 16 days of culture with 0.1 µM Cu, containing or not Cd (5 µM). Mean values ± standard deviation (SD) are shown (*n*=7-9). Different letters indicate significant differences (*P* ≤ 0.05). FW, fresh weight.

In an independent experiment, the WT and *copt5-3* lines exhibited the same trends (Figure R.2.14), which further indicates decreased ethylene production under Cu deficiency, which became more exacerbated under Cd stress.

2.6. Cadmium content in the WT and *copt5* plants with different copper statuses

The Cd concentration was separately measured in the roots and leaves of the WT, *copt5-2*, *copt5-3* and *COPT5^{OE}* hydroponically grown plants in Hoagland without Cu, but with 0.1 µM Cu, to ascertain whether Cd content or distribution alters in the *copt5* mutants (Figure R.2.15). Cu content was also determined in the Cd-treated plants, and was significantly higher in the *copt5-2 and copt5-3* leaves and roots than in the WT (Figure R.2.16).

A

B
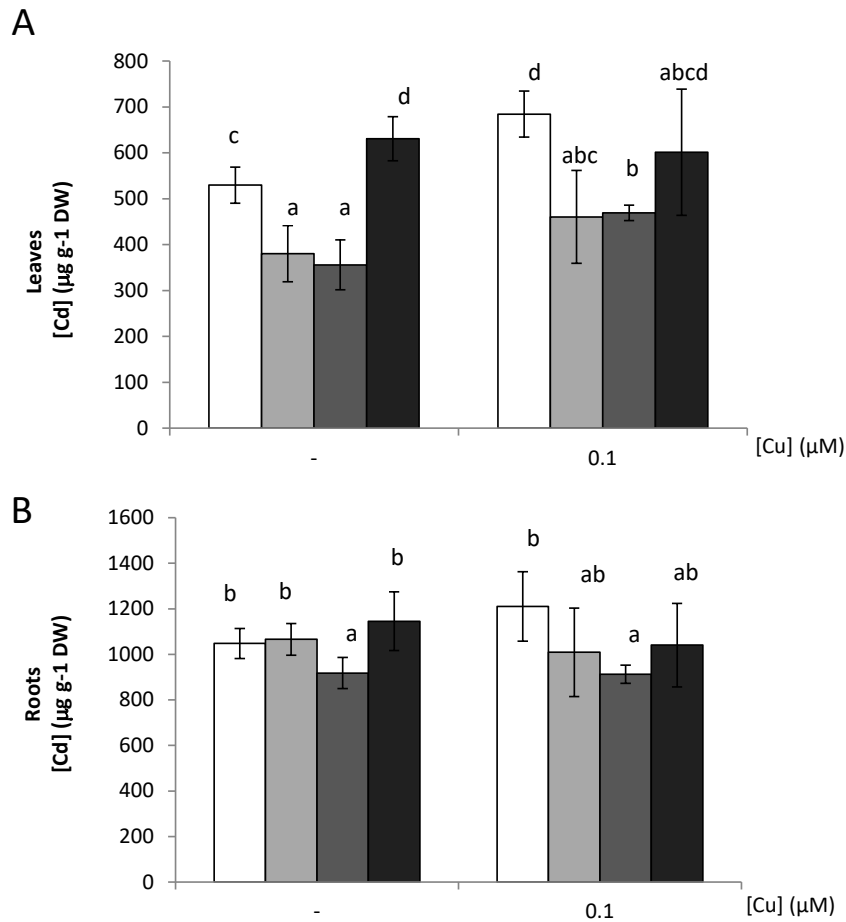
Figure R.2.15. Cd accumulation in different plant organs. Cd content in the leaves (A) and roots (B) of the 47-day-old WT (white bars), *copt5-2* (grey bars), *copt5-3* (dark grey bars) and *COPT5^{OE}* (black bars) plants exposed to 5 µM Cd added to the Hoagland's hydroponic medium supplemented, or not, with 0.1 µM Cu during the last 16 days of culture. Mean values ± standard deviation (SD) are shown (*n*=5-9). Different letters indicate significant differences ($P \leq 0.05$). DW, dry weight.

It is noteworthy that the Cd content in WT shoots increased significantly when grown in the medium supplemented with 0.1 µM Cu (Figure R.2.15A), which indicates that the Cu status in the plant influences Cd translocation.
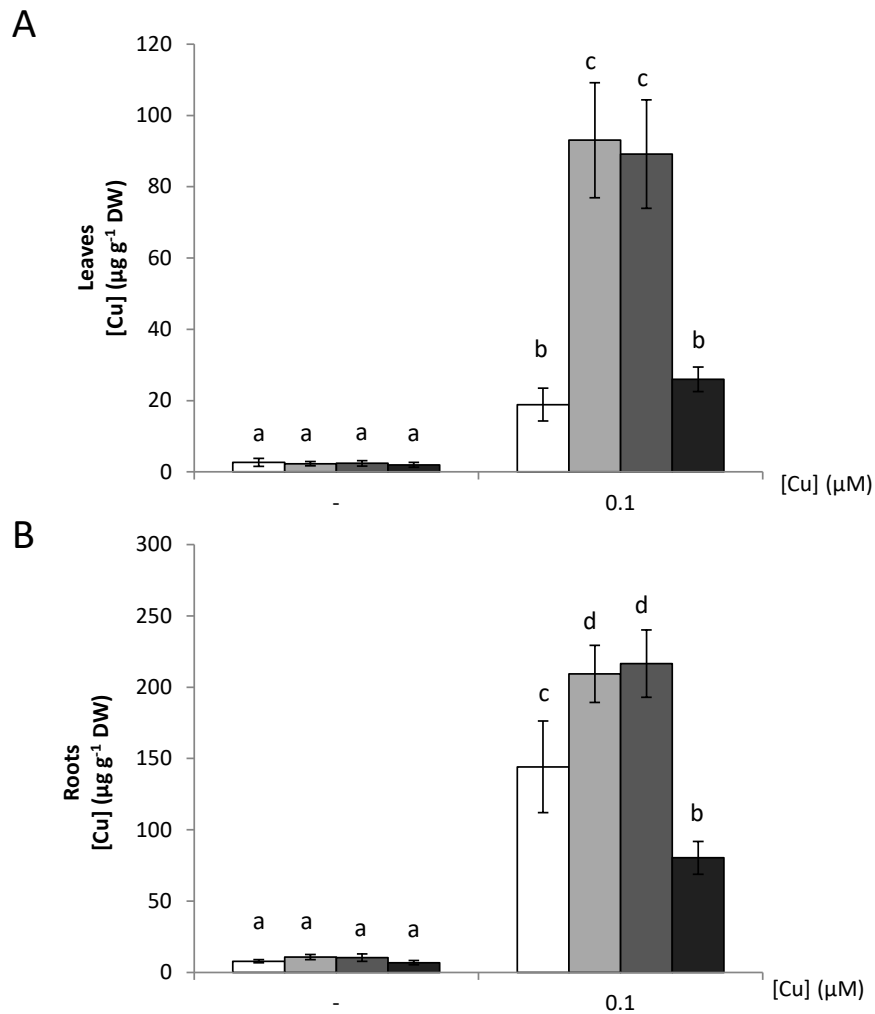
Figure R.2.16. Cu content in the Cd-treated plants. Cu content in the leaves (A) and roots (B) of the 47-day-old WT and *copt5* plants exposed to 0.1 µM Cu plus 5 µM Cd in Hoagland's hydroponic medium during the last 16 days of culture. In each organ, different letters indicate significant differences ($P \leq 0.05$) (n≤ 9). DW, dry weight.

This effect did not reach levels of statistical significance in roots (Figure R.2.15B). It is remarkable that Cd translocation to upper plant parts was significantly impaired in the *copt5-2 and copt5-3* mutants (Figure R.2.15A) since Cd content was around 15% lower in the *copt5-2 and copt5-3* leaves than in the WT despite being similar in roots, at least in *copt5-2* (Figure R.2.15). This suggests that the COPT5 function participates in Cd translocation to plant shoots.

DISCUSSION

Extensive studies on the underlying mechanisms of Cd toxicity in plants under metal stress or in plant hyperaccumulators have been reported (Clemens *et al.*, 2013; Cuypers *et al.*, 2010; Krämer, 2010), but the understanding of how plants acclimate to high Cd levels under metal deficiencies is poor. In this work, we explored the role of the Cu transporter COPT5 in Cd tolerance by using the *copt5-2* and *copt5-3* mutants, which displayed increased sensitivity to Cd toxicity, to better understand the interaction between Cu homeostasis and Cd root-to-shoot translocation in higher plants.

A role of COPT5 in Cd sensitivity has been previously suggested as the expression of the *COPT5* homolog gene in the low Cd-accumulating plant *Solanum torvum,* which was induced with mild Cd exposure (Yamaguchi *et al.*, 2010). However, under the experimental conditions used herein (30 µM Cd), *Arabidopsis COPT5* expression remained unaffected (Figure R.2.8). Nevertheless, the obtained data indicate that *Arabidopsis* COPT5 plays a role in root-to-shoot Cd translocation and in Cd tolerance. These data are based on the characterization of the phenotypes shown by transgenic plants with altered levels in COPT5 grown in the presence of 30 µM Cd under mild Cu deficiency (½ MS) conditions if compared to Cu-sufficient media (½ MS plus 1 µM Cu). COPT5 has been previously shown to be expressed mostly in vascular bundles in roots and to localize at the prevacuolar/vacuolar compartment where it functions transporting Cu^+ towards the cytosol from the lumen of these storage or recycling compartments (García-Molina *et al.*, 2011; Klaumann *et al.*, 2011). Mutants lacking COPT5 display impaired Cu distribution at the cellular level, where Cu accumulates at the vacuoles, and at different organs, where Cu increases in lower parts (roots and rosette leaves), whereas reproductive organs (siliques and seeds) show a decreased Cu content if compared to controls (Klaumann *et al.*, 2011). Cu^+ efflux from root cells is mediated by heavy metal P-type ATPase HMA5 (Andrés-Colás *et al.*, 2006) (Figure D.2.1). A putative direct effect of COPT5 on the compartmentalization of Cd has been ruled out since COPT transporters have been shown to be Cu^+-specific (Sancenón *et al.*, 2003), and Cd^{2+} is probably not a substrate for Cu^+ HMA5 ATPase. Instead Cd^{2+} is transported through divalent cation transporters, such as HMA4 (Lin and Aarts, 2012).
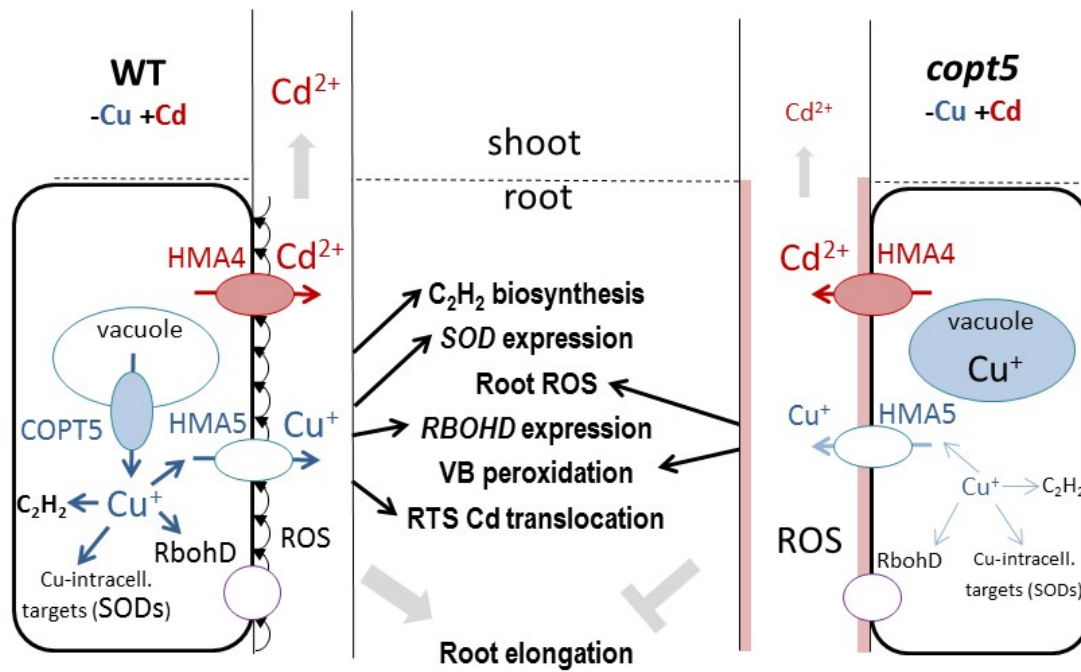
Figure D.2.1. Model of the COPT5 function in Cd root shoot translocation and tolerance. The phenotypic characteristics of the WT (left panel) and *copt5* mutants (right panel) described in the text are shown under Cu deficiency and in the presence of Cd. Intracellular Cu deficiency was exacerbated in the *copt5* mutants, which led to Cu accumulation in roots, reduced ethylene emissions and defective *copt5* SOD antioxidative defenses and *RbohD* expression. As a result of the defects in both the intercellular and interorgan Cu distribution in the copt5 mutants, Cd transport to the aerial plant parts and root elongation was impaired. RTS, root to shoot; VB, vascular bundle cells. Arrows indicate the processes that were favored in the WT or the *copt5* mutants.

Our data indicate that Cd effects are indeed due to the COPT5 function on Cu transport since addition of Cu, but not other metals, reverts the growth inhibition of the *copt5* mutants caused by Cd (Figure R.2.3). Based on the presented results, an indirect effect should be considered to explain the enhanced Cd-sensitivity of the *copt5* mutant. To further pursue the COPT5 function in Cd tolerance, we followed three processes where evidence for a putative interaction between Cu deficiency and Cd toxicity has already been suggested; first, the influence of ethylene biosynthesis and/or signaling on plant growth (Schellingen *et al.*, 2014); second, the effect of Cd on Cu-deficiency responses that affect Cd tolerance (Gayomba *et al.*, 2013); finally, oxidative stress generated by both the scarcity of Cu and the presence of Cd, which could also affect root elongation (Smeets *et al.*, 2013).

Regarding the putative role of ethylene, it has been reported that ethylene seems to play a crucial role in the Cd-induced inhibition of root growth in both barley and *Arabidopsis* (Schellingen *et al.*, 2014; Valentovičová *et al.*, 2012). Since Cd binding to the Atx1 metallochaperone provokes defects in Cu delivery to cuproproteins in yeast (Heo *et al.*, 2012), and as ethylene receptors are cuproproteins (Rodriguez *et al.*, 1999), a similar effect in *Arabidopsis* would negatively affect ethylene perception. Although according to the obtained results, the exacerbated sensitivity of the *copt5* mutants to Cd is not dependent on a poorer perception of ethylene (Figure R.2.7), since both Cd and ethylene reduce hypocotyl growth, further experiments will be needed to asses a role for ethylene perception in the *copt5* phenotype. In addition, ethylene biosynthesis can be affected by Cd. Opposite effects of Cd on ethylene biosynthesis have been reported depending on the Cd levels and the experimental system used (Arteca and Arteca, 2007; Rodríguez-Serrano *et al.*, 2009; Schellingen *et al.*, 2014). Under the experimental conditions presented herein, long-term (16-days) Cd (5 µM) treatments inhibited ethylene biosynthesis in the WT and *copt5* plants, but not in the *COPT5*^{OE} line, under low Cu (Hoagland 0.1X in Figures R.2.13 and R.2.14). Increased ethylene levels have been shown to alleviate the Cd-induced inhibition of photosynthetic capacity in mustard (Masood *et al.*, 2012). Along the same lines, Lu and Kirkham (1991) indicated that a correlation might exist between the genotypes that emit more ethylene and heavy metals resistance. Accordingly, the reduced ethylene production measured in low Cu plants could explain, at least partially, the increased Cd sensitivity observed in the *copt5* mutants since exacerbated Cu deficiency effects have been described in these mutants (García-Molina *et al.*, 2011). Despite the role that Cu plays in ethylene perception being well-established, this work uncovers a new role in ethylene production. However, the specific effects of Cu status on ethylene biosynthesis merit further studies.

Recent data on the *copt2* mutant indicate that Cd stimulates the SPL7-dependent expression (Gayomba *et al.*, 2013). Under the experimental conditions reported herein, the expression of plasma membrane-located COPT family members, such as *COPT1* and *COPT2,* was down-regulated by both metals, while the *COPT5* expression was regulated by neither Cu nor Cd (Figure R.2.8). Moreover, we were unable to detect significant differences in Cd sensitivity in root growth of the single *copt1*, *copt2* and *copt6* mutants if compared to the controls (Figure R.2.5). These apparent discrepancies can be attributed to the genotypic differences and diverse Cd exposure conditions. Thus Gayomba *et al.* (2013) used 10-day-old seedlings, which had been subjected to 50 µM Cd treatment, while in this work, 7-day-old seedlings were used which had been grown in 30 µM Cd. According to the presented results, Cd interacts with SPL7-mediated responses (Figures R.2.8 and R.2.9), which agrees with a putative role of Cd that affects SPL7 transcriptional activation by replacing the Zn ions at the Zn fingers in the SBP DNA-binding

domain (Hartwig, 2001). Among the Cu-deficiency SPL7 targets we find SODs, encoded by *FSD1* and *CSD1,* whose expressions were respectively reduced and increased by Cd (Figure R.2.9A and B). Accordingly, *FSD1* and *MIR398* are direct SPL7 targets, and *CSD1* expression was regulated post-transcriptionally by *MIR398*, whose decreased expression led to increased *CSD1* levels (Yamasaki, *et al.*, 2007). However, both *FSD1* and *CSD1* expressions notably reduced in the *copt5* mutants, independently of Cd treatment (Figure R.2.9A and B). Since it has been recently suggested that Cu-deficiency perception can take part in the lumen of the endoplasmic reticulum through SPL7 (García-Molina *et al.*, 2014b), a complex scenario is envisaged for the Cu-deficiency responses in the *copt5* mutants. Whereas Cu delivery to the target intracellular cuproproteins was impaired under Cu deficiency, surplus Cu accumulated in the lumen of another secretory pathway compartment, the vacuole, to provoke a stressful imbalance in cellular Cu redistribution in *copt5* mutants. Our results agree with the reported hypersensitivity to Cd in the *nramp3nramp4* mutant impaired in vacuolar metals (mainly Fe and Mn) mobilization that identified chloroplasts as a target probably related to a Cd-mediated decreased availability of essential metals in these organelles (Molins *et al.*, 2013).

Since SODs are among the main antioxidative defense enzymes, ROS can be involved in the deficient SOD response in the *copt5* mutants. In fact, two separate types of oxidative stress effects can be considered through the COPT5 function. First, a malfunctioning chloroplast photosynthetic electronic transfer chain has been previously described in the *copt5* mutants, when plants were subjected to severe Cu scarcity conditions, likely due to a defect in the Cu recycling from the vacuole (García-Molina *et al.*, 2011). These defects in chloroplast function are a well-known source of ROS production (Yruela, 2013). Second, the function of COPT proteins has been recently linked to Cu^+-mediated production of hydroxyl radicals, which leads to the activation of cation channels (Rodrigo-Moreno *et al.*, 2013). As a result of both the disturbed Cu localization, that exacerbates at least part of Cu-deficiency in roots, and reduced antioxidative defenses, *copt5* root cell membranes were especially sensitive to oxidative stress, and those in the vascular bundles cells became differentially peroxidated when Cd was present (Figure R.2.12C). Xylem loading of ions is dependent on normal functioning of membrane-bound transport systems located in the parenchima cells around the vascular bundles. Disruption of membrane integrity caused by lipid peroxidation is among the factors involved in the reduction of metals and macronutrient contents observed in leaves of Cd-treated plants (Rubio *et al.*, 1994; Sandalio *et al.*, 2009). Xylem loading could also be impaired by cell wall lignification. A ROS-increased lignification has been hypothesized to prevent xylem Cd entry (Sandalio *et al.*, 2009).

The role of ROS in plant signaling and defense against biotic and abiotic stresses has begun to be deciphered reviewed in Gilroy *et al.*, 2014. It has also been suggested that Cd produces both oxidative damage and increased antioxidant defense (Cuypers *et al.*, 2010). In line with this, lack of induction by Cd of the NADPH oxidase (*RBOHD*), described as a major player in Cd-induced ROS production (Cuypers *et al.*, 2010; Smeets *et al.*, 2009), was observed in the *copt5* mutants (Figure R.2.9C). However, *RBOHD* was not induced in a *spl7* mutant in the presence of Cu (Figure R.2.10C), which indicates that COPT5-mediated *RBOHD* expression is dependent of SPL7. Based on the recently published data about the ROS-mediated vascular homeostatic control of root-to-shoot element translocation and the role of NADPH oxidases in this process (Jiang *et al.*, 2013), a model is proposed in which lack of the COPT5 function prevents *RBOHD* induction, probably in the root stele, which leads to lower Cd concentrations in root vasculature cells and in xylem sap to reduce the delivery of damaging amounts of Cd to shoots (Figure D.2.1). Accordingly, MDA content in leaves followed the Cd content in the WT and *copt5* mutant plants (Figures R.2.11A and R.2.16A), which suggests that oxidative stress damage is caused by Cd. These results agree with the recently published work on OXI1 (oxidative signal-inducible kinase 1), where *FSD1* and *MIR398* expressions were regulated by the OXI1 pathway by acting downstream of NADPH oxidase activity (Smeets *et al.*, 2013). These results demonstrate that, in addition to and independently of the SPL7-mediated responses, Cu transport plays a key role in Cd resistance, and suggest that by producing damage to membranes, oxidative stress triggers an NADPH oxidase/ROS signaling pathway, which contributes to Cd translocation and basal plant resistance (Figure D.2.1).

Taken together, the results presented herein match a model where the COPT5 function is an important component of basal Cd resistance in *Arabidopsis*. The inability to retrieve Cu from the vacuole in the *copt5* mutants under Cd treatment affects root growth in a complex manner, driving to defective antioxidative defenses. Under Cu deficiency and in the presence of Cd, all these defects are further aggravated, and lead to a higher and broader peroxidation of the membranes at the vascular bundles in the *copt5* mutants, impairing normal functioning of membrane-bound transport systems which would result in inhibition of root-to-shoot Cd translocation and of root elongation. The slightly impaired Cd distribution in *copt5* plants suggests a biotechnological approach to minimize entry of Cd into edible parts of crop plants to avoid Cd reaching animals and humans.

CHAPTER 3:

THE HIGH AFFINITY INTERNAL COPPER TRANSPORTER COPT5 PARTICIPATES IN IRON MOBILIZATION IN *ARABIDOPSIS THALIANA*

RESULTS

3.1. Knockout COPT mutants display different sensitivity to Fe deficiency

It has been previously shown that *COPT2* mRNA levels increase under both Cu and Fe deficiency and that the *Arabidopsis copt2* seedlings are more resistant to the ferric chlorosis than WT when Fe is scarce (Perea-García *et al.*, 2013). These results supported the idea of a tight relationship between Cu and Fe signaling and also pointed out the key role of the COPTs transporters in that crosstalk. In order to have a deeper insight about the role of COPTs transporters under Cu and Fe deficiencies, we determined the root lengths of the WT and the *copts* mutants (*copt1*, *copt2*, *copt6*, *copt1copt2copt6*, *copt3* and *copt5*) grown under control (+Cu+Fe), Cu deficiency (-Cu+Fe), Fe deficiency (+Cu-Fe) and both Cu and Fe deficiency (-Cu-Fe) conditions (see materials and methods) (Figure R.3.1).
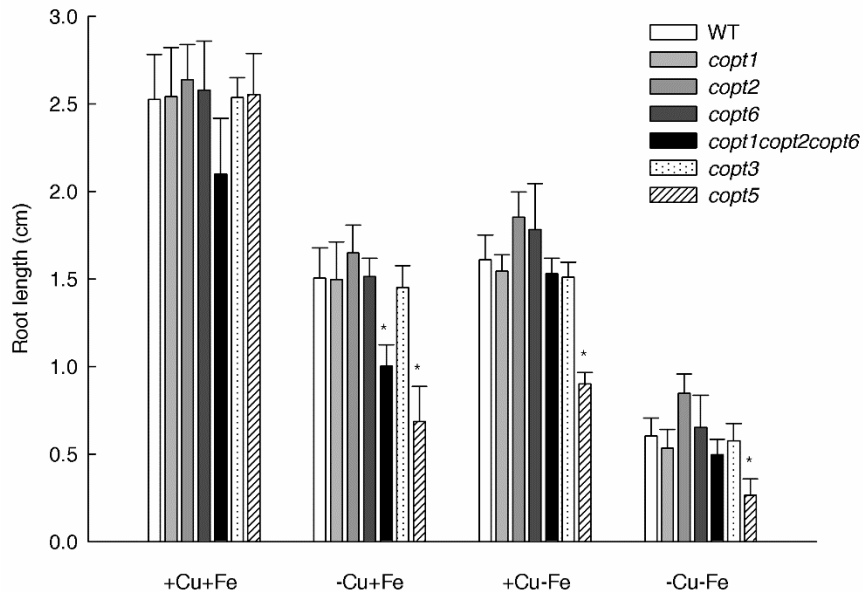
Figure R.3.1. Root length of the *copts* mutants grown under different metal availability conditions. Root length of 7 day-old WT, *copt1*, *copt2*, *copt6*, *copt1copt2copt6*, *copt3* and *copt5* grown in ½ MS medium supplemented with 1 µM CuSO$_4$ and 50 µM Fe-citrate (+Cu+Fe), 100 µM BCS and 50 µM Fe-citrate (-Cu+Fe), 1 µM CuSO$_4$ and 100 µM Ferrozine (+Cu-Fe) and, 100 µM BCS and 100 µM Ferrozine (-Cu-Fe). Asterisks indicate statistical differences ($P<0.05$) according to Tukey's test with respect to the WT under the same condition.

The root length of seedlings grown under Cu and Fe sufficiency did not show differences among genotypes (Figure R.3.1). Cu deficiency conditions diminished root length in all genotypes, being this reduction significantly higher in the *copt1copt2copt6* and *copt5* mutants compared to WT (Figure R.3.1). Under Fe deficiency, the WT root length is similar to that observed under Cu deficiency, which indicates a similar effect of Cu and Fe deficiencies under our experimental conditions. In agreement with previous results (Perea-García *et al.*, 2013), the *copt2* mutant is slightly less sensitive to Fe deficiency, although differences with WT were not statistically significant in these conditions. On the contrary, *copt5* was more sensitive than WT to Fe deficiency (Figure R.3.1) and showed a reduced root length by about 50%. In addition, *copt5* was also significantly more sensitive to both Cu and Fe deficiencies (Figure R.3.1). The *copt5* mutant is as sensitive to Cu scarcity as the triple mutant in plasma membrane transporters (*copt1cop2copt6*), but it is the only mutant in COPT transporters showing a significantly exacerbated sensitivity response to Fe deficiency. These results suggest that COPT5 might play a pivotal role in both Cu and Fe deficiencies, and bring to question the common or specific COPT5-dependent molecular mechanisms regulating each response.

3.2. Biological processes affected in the *copt5* mutant under different Cu status

To further identify COPT5-dependent functions in *Arabidopsis*, we performed a microarray analysis of 7 day-old Arabidopsis WT and *copt5* mutant. Seedlings were grown under severe Cu deficiency conditions (½ MS with 100 μM BCS; -Cu) and Cu sufficiency considered as the control (½ MS with 1 μM $CuSO_4$; C). Venn diagrams (Figure R.3.2A and 2B) summarize the number of differentially expressed genes (DEG) (ANOVA, FDR ≤ 0.01) in WT and *copt5* seedlings in response to changes in Cu regime. The highest number of DEG was found in the *copt5* mutant, when grown under Cu deficiency conditions (Figure R.3.2A and 2B). Results showed that the number of genes induced in *copt5* compared to WT was lower than that of repressed genes independently of the Cu availability. In addition, the number of DEG between both genotypes was almost 3-fold higher when Cu was scarce. It is also interesting to note that the number of DEG between both genotypes regardless of the Cu condition (intersection in the Venn diagram, Figure R.3.2A) was lower than that of the genes specifically regulated under Cu deficiency. Therefore, it appears that the lack of function of COPT5 provokes the deregulation of a high number of genes, mainly under severe Cu deficiency conditions. Complementary, we carried out a comparison of Cu deficiency with respect to control conditions in both genotypes (Figure R.3.2B). Repression prevailed in both genotypes, being the number of repressed genes higher in the *copt5* mutant. Likewise, the number of induced genes by Cu deficiency was also higher in

the mutant genotype. It should be mentioned that the high number of DEG regulated by Cu availability is independent of the genotype (intersection in the Venn diagram, Figure R.3.2B). Nevertheless, the number of DEG of each genotype (294 for WT and 728 for *copt5*) still suggests a wide divergence between WT and *copt5* seedlings in the molecular mechanisms underlying the response to Cu availability.
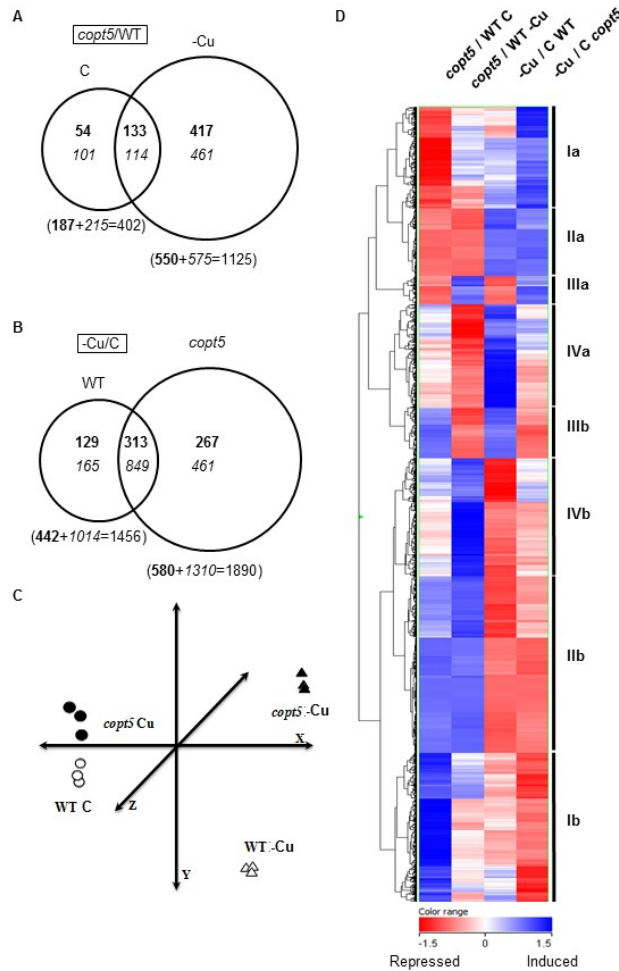
Figure R.3.2. **Transcriptomic analyses on WT and *copt5* seedlings grown under different Cu availability conditions.** Venn diagrams of the distribution of differentially expressed genes (ANOVA, FDR ≤ 0.01) when compared *copt5* respect to WT samples grown under control (C) and BCS (-Cu) media (A) and when compared -Cu respect to C samples in both *copt5* and WT genotypes (B). Up-regulated (**bold**) and down-regulated (*italics*) genes included in these diagrams satisfied a fold change ≥ 1.5 cut-off. Numbers in brackets are the sum of all induced (**bold**) or repressed (*italics*) genes under each particular condition. The sizes of the circles are shown relative to the total number of differentially expressed genes for each condition. Principal component analysis, PCA, based on the transcriptional profile of those genes that satisfied an ANOVA analysis (*P-value* ≤ 0.01) from WT and *copt5* knockout mutant seedlings

grown under Cu sufficiency (C) and Cu deficiency (BCS; -Cu) conditions. The three axes on PCA account for 91.37 % of the total variance among genotypes and Cu availability conditions. Hierarchical clustering analysis, HCA, of *COPT5-related* genes (D). The heat map was generated with differentially expressed genes from four pairwise comparisons distributed in four columns: 1) *copt5* versus WT under control conditions, 2) *copt5* versus WT under Cu deficiency, 3) Cu deficiency versus control conditions in the WT, and 4) Cu deficiency versus control conditions in the *copt5* mutant. Each row represents a gene whose scaled expression value, denoted as Z score, is plotted in a color scale with blue indicating higher expression and red indicating lower expression. Grouping of the eight major clusters is indicated in the right. Three biological replicates from each condition were used for all the analyses.

A principal component analysis (PCA) was performed to validate the repeatability of the microarray data across replications and to cluster samples according to their global gene expression profiles (Figure R.3.2C). Under all conditions, the transcriptional profiles of the three RNA samples were tightly clustered (Figure R.3.2C). PCA revealed marked differences in gene expression patterns depending on Cu availability and genotypes. In agreement with the number of DEG shown in the Venn diagrams (Figure R.3.2A and 2B), *copt5* and WT seedlings grown under optimal control conditions were distributed far to those grown under severe Cu deficiency. In turn, seedlings from both genotypes grown under severe deficiency were more separated than those grown under control conditions (Figure R.3.2C).

To further validate the transcriptomic analysis, we compared the fold change expression values obtained by qRT-PCR and those from the 44 K Agilent microarray (Figure R.3.3) for 5 genes highly induced or repressed (Figure R.3.3) in the studied conditions. Multiple linear regression analysis (r^2= 0.84) indicated that the results of the microarray analysis were robust.
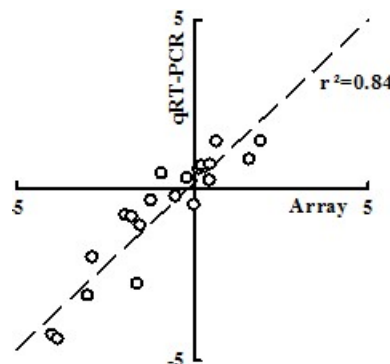
Figure R.3.3. Validation of microarray data. Multiple linear regression analysis (r^2=0.84) for selected genes was performed by comparing qRT-PCR values and the *Affimetrix* 44 K microarray gene expression data for all the studied genotypes and growing conditions. Individual regression analyses for each gene (*WRKY40*, *WRKY18*, *NRAMP4*, *ETR2* and *BCB*) revealed r^2 values ranging from 0.69 to 0.99 (data not shown).

To identify the molecular processes involved in the Cu availability response in which COPT5 plays a role, transcriptomic data was plotted in a Heatmap. Eight differential patterns (Ia, IIa, IIIa, IVa, Ib, IIb, IIIb, IVb) were observed when comparing the two genotypes under both conditions as indicated in Figure R.3.2D, being complementary two by two. The Gene Ontology (GO) analysis identified biological processes significantly under- or over-represented in the sets of genes belonging to each pattern (Table R.3.1), including Fe ion binding, ethylene-activated signalling pathway, oxidative stress, SOD activity, and response to carbohydrate stimulus.

Table R.3.1. Biological processes overrepresented (FatiGo, P<0.05) in the DEG included in the Heatmap and Hierarchical Cluster Analysis. DEG were filtered by a false discovery rate (FDR) lower than 1% and a cut-off of 1.5-fold change (log$_2$ |1.5|).

Pattern	GO level	GO code	Description	Classification
Ia	2	GO:0009636	response to toxin	biological process
	3	GO:0006857	oligopeptid transport	biological process
	4	GO:0015198	oligopeptid transporter activity	molecular function
	4	GO:0010114	response to red light	biological process
	5	GO:0000041	transition metal ion transport	biological process
	7	GO:0009620	response to fungus	biological process
Ib	1	GO:0016757	transferase activity, trasferring glycosyl groups	molecular function
	1	GO:0016758	transferase activity, trasferring hexosyl groups	molecular function
	2	GO:0009733	response to auxine	biological process
IIa	1	GO:0005506	iron ion binding	molecular function
	1	GO:0019825	oxygen binding	molecular function
	1	GO:0046906	tetrapyrrole binding	molecular function
	1	GO:0016705	oxidoreductase activity with incorporation or reduction of molecular oxygen	molecular function
	1	GO:0004497	monooxygenase activity	molecular function
	1	GO:0008168	methyltransferase activity	molecular function
	2	GO:0020037	heme binding	molecular function
IIb	1	GO:0006800	oxygen and ractive oxygen species metabolic process	biological process
	1	GO:0009743	response to carbohydrate stimulus	biological process
	1	GO:0007047	cell wall organization	biological process
	1	GO:0016758	transferase activity, transferring hexosyl groups	molecular function
	2	GO:0004784	superoxide dismutase activity	molecular function
	2	GO:0008794	arsenate reductase (glutaredoxin)activity	molecular function
	2	GO:0009733	response to auxin	biological process
	2	GO:0006952	defense response	biological process
	2	GO:0009620	response to fungus	biological process
	3	GO:0004888	transmembrane receptor activity	molecular function
	4	GO:0009873	ethylene-activated signaling pathway	biological process
	4	GO:0012501	programmed cell death	biological process
IIIa	1	GO:0009725	response to hormone stimulus	biological process
IIIb	1	GO:0051260	protein homooligomerization	biological process
	2	GO:0051301	cell division	biological process
	2	GO:0051726	regulation of cell cycle	biological process
	5	GO:0007018	microtubule-based movement	biological process
	5	GO:0003777	microtubule motor activity	molecular function
IVa	1	GO:0048827	phyllome development	biological process
	1	GO:0007267	cell-cell signaling	biological process
	1	GO:0016042	lipid catabolic process	biological process
	1	GO:0004091	carboxylesterase activity	molecular function
	1	GO:0006790	sulfur metabolic process	biological process
	1	GO:0019760	glucosinolate metabolic process	biological process
	1	GO:0005506	iron ion binding	molecular function
	1	GO:0004497	monooxygenase activity	molecular function
	2	GO:0016538	cyclin-dependent protein kinase regulator activity	molecular function
	2	GO:0007018	microtubule-based movement	biological process
	2	GO:0020037	heme binding	molecular function
	3	GO:0003777	microtubule motor activity	molecular function
IVb	1	GO:0009611	response to wounding	biological process
	1	GO:0009743	response to carbohydrate stimulus	biological process
	2	GO:0006952	defense response	biological process
	2	GO:0042744	hydrogen peroxide catabolic process	biological process
	2	GO:0009733	response to auxine	biological process
	2	GO:0006863	purine transport (related to citokinin transport)	biological process
	2	GO:0009739	response to gibberellin	biological process
	2	GO:0009753	response to jasmonic acid	biological process
	2	GO:0004871	signal transducer activity	molecular function
	3	GO:0050688	regulation of defense response to virus	biological process
	3	GO:0051740	ethylene binding	molecular function
	3	GO:0009968	negative regulation of signal transduction	biological process
	4	GO:0010200	response to chitin	biological process
	4	GO:0004888	transmembrane receptor activity	molecular function
	5	GO:0006915	apoptosis	biological process
	5	GO:0010104	regulation of ethylene-activated signaling pathway	biological process
	6	GO:0034050	host programmed cell death induced by symbiont	biological process
	6	GO:0009626	plant-type hypersensitive response	biological process

3.3. Iron homeostasis is altered in the *copt5* mutant depending on copper status

COPT5 was previously shown to participate in Cu release from vacuoles and Cu redistribution to chloroplasts under Cu deficiency (García-Molina *et al.*, 2011; Klaumann *et al.*, 2011). The microarray analysis revealed Fe-related processes that were identified in patterns I, II and IV (Table R.3.2.), envisaging a complex Cu-Fe interaction in the *copt5* mutant.

Table R.3.2. Genes belonging to the Fe-related biological processes overrepresented (FatiGO, P<0.05) in the expression patterns described in the Hierarchical Cluster Analysis. DEG were filtered by a false discovery rate (FDR) lower than 1% and 1.5-fold change (log$_2$ |1.5|).

Locus	Short name	Description	FC value *copt5* C/ WT C	FC value *copt5* -Cu/ WT -Cu	Pattern	Biological process
AT5G67330	NRAMP4	metal transporter Nramp4	-1.14	1.86		
AT1G55910	ZIP11	putative zinc transporter ZIP2 - like protein	-1.14	1.14	Ia	Transition metal ion transport
AT3G56240	CCH	copper chaperone	-1.08	1.25		
AT3G46900	COPT2	copper transporter 2	-1.05	1.1		
AT2G30750	CYP71A12	cytochrome P450 71A12	-2.04	-2.01		
AT1G01600	CYP86A4	cytochrome P450 86A4	-1.62	-1.7		
AT3G10150	PAP16	purple acid phosphatase 16	-1.41	-1.54		
AT5G36110	CYP716A1	cytochrome P450 716A1	-1.23	-1.57		
AT2G23180	CYP96A1	cytochrome P450 96A1	-1.22	-1.03		
AT2G46660	CYP78A6	cytochrome P450 78A6	-1.16	-1.08	IIa	Iron ion binding
AT4G25100	FSD1	superoxide dismutase [Fe]	-1.15	-1.4		
AT4G36430	PER49	peroxidase 49	-1.14	-1.91		
AT5G06720	PER53	peroxidase 53	-1.12	-1.25		
AT3G26830	PAD3	protein PHYTOALEXIN DEFICIENT 3	-1.09	-1.96		
AT2G34490	CYP710A2	cytochrome P450 710A2	-1.02	-1.2		
AT1G06100	T21E18.15	delta-9 desaturase-like 2 protein	-2.32	-15.41		
AT3G10570	CYP77A6	cytochrome P450 77A6	-1.85	-2.92		
AT5G04660	CYP77A4	cytochrome P450 77A4	-1.8	-5.23		
AT1G02205	CER1	protein ECERIFERUM 1	-1.78	-4.6		
AT1G65670	CYP702A1	cytochrome P450 702A1	-1.67	-3.13		
AT5G52320	CYP96A4	cytochrome P450 96A4	-1.65	-3.51		
AT1G06360	T2D23.6	delta-9 desaturase-like 5 protein	-1.46	-2.95		
AT4G39950	CYP79B2	tryptophan N-monooxygenase 1	-1.42	-1.91		
AT2G46650	CB5-C	cytochrome B5 isoform C	-1.42	-2.77	IVa	Iron ion binding
AT5G42650	AOS	allene oxide synthase	-1.39	-2.2		
AT4G15393	CYP702A5	cytochrome P450 702A5	-1.25	-3.9		
AT1G16410	CYP79F1	dihomomethionine N-hydroxylase	-1.18	-3.4		
AT1G11600	CYP77B1	cytochrome P450 77B1	-1.13	-2.04		
AT5G06730	PER54	peroxidase 54	1.03	-1.39		
AT5G59920	ULI3	UV-B light insensitive 3	1.06	-1.21		
AT2G45560	CYP76C1	cytochrome P450 76C1	1.07	-1.09		
AT5G05340	PER52	peroxidase 52	1.97	-2.21		

Following the data obtained in Table R.3.2, among the regulated Fe-related genes, *COPT2* and *NRAMP4,* caught our attention. Whereas the induction of the high affinity Cu transporter *COPT2* was previously shown as a good marker for Cu and Fe deficiency responses (Perea-García *et al.*, 2013), NRAMP4 is a protein involved in Fe remobilization from the vacuole (Lanquar *et al.*, 2005). The expression of these genes were validated by qRT-PCR showing that both *COPT2* and *NRAMP4* were up-regulated in the *copt5* mutant compared to WT under Cu deficiency

conditions (Figure R.3.4). These results reinforced the alteration of Cu and Fe homeostasis in the mutant.
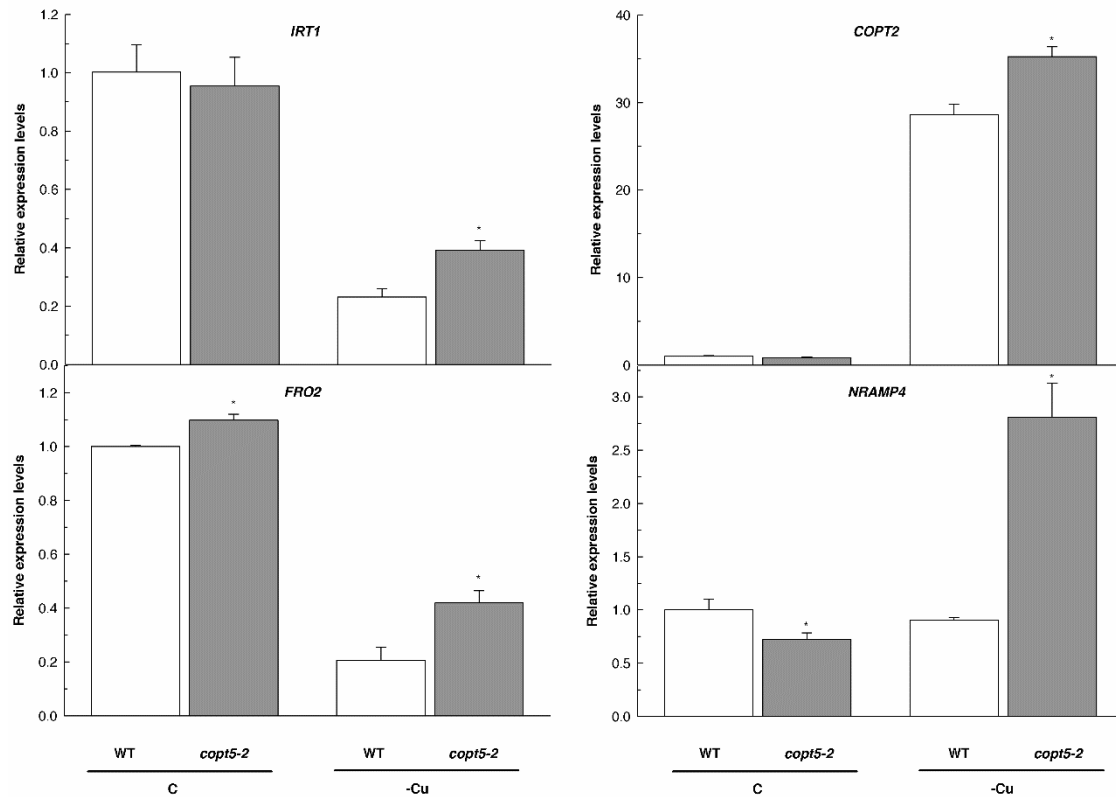
Figure R.3.4. Cu-dependent transcription regulation of metal-related genes in the *copt5* mutant. The relative expression of the *IRT1, FRO2, COPT2 and NRAMP4* genes was determined by qRT-PCR in WT (white bars) and *copt5-2* (grey bars) from mRNA extracted of 7 day-old seedlings grown under Cu sufficiency (½ MS with 1 μM CuSO₄; C) and Cu deficiency (½ MS with 100 μM BCS; -Cu). Expression levels are relative to those obtained in WT seedlings grown under Cu sufficiency conditions. Bars correspond to arithmetic means ($2^{-\Delta\Delta Ct}$) ± standard deviation (SD) (n=3). Asterisks indicate statistical differences (P < 0.05) between WT and *copt5-2* for each growing condition.

In order to further asses the Fe status in *copt5* mutant, two well-known molecular markers of Fe deficiency, such as *IRT1* and *FRO2,* that are not present in the *Agilent* microarrays, were analised by qRT-PCR under Cu deficiency conditions. These two genes are involved in Fe adquisition by strategy I plants and their expressions are up-regulated under Fe deficiency (Vert *et al.*, 2003). *IRT1* and *FRO2* expressions were down-regulated by Cu deficiency in both WT and *copt5*

seedlings. However, despite the fact that the *copt5* mutant is suffering from exacerbated Cu deficiency, the expression levels of both genes were higher in the *copt5* mutant than in WT under Cu scarcity (Figure R.3.4).

Taken together, these results reinforced the idea that the *copt5* mutant, in addition to showing exacerbated Cu deficiency conditions (García-Molina *et al.*, 2011), also displays increased Fe deficiency responses compared to the WT under Cu deficiency. They also point to an altered Fe homeostasis in the *copt5* mutant that cannot be simply explained by the Cu deficiency phenotype since some of the Fe-related genes are differentially affected in the mutant depending on the Cu status.

3.4. The *nramp3nramp4* mutant is highly sensitive to Cu deficiency

Indeed, *NRAMP4* expression is highly affected under Cu deficiency and differentially regulated in the *copt5* mutant depending on the Cu status (Figure R.3.4). NRAMP4 is involved in vacuolar Fe release (Lanquar *et al.*, 2005), a parallel function to the COPT5 role in Cu traffic (García-Molina *et al.*, 2011). Based on these facts and since the *copt5* mutant is sensitive to Fe deficiency (Figure R.3.1), we wondered if the *nramp3nramp4* double mutant, which relies on external Fe supply to sustain its growth (Lanquar *et al.*, 2005) was sensitive to the Cu availability in the growth media (Figure R.3.5). Thus, the double *nramp3nramp4* mutant was grown in different Cu conditions. Under control conditions (Fe and Cu sufficiency), there were no phenotypical differences between WT and *nramp3nramp4* mutant (Figure R.3.5A and R.3.5B). However, the *nramp3nramp4* double mutant was highly sensitive to severe Cu deficiency conditions (½ MS with 50 µM BCS; -Cu) (Figure R.3.5A), showing a drastic decrease in root length (83% reduction with respect to the WT) (Figure R.3.5B). The sensitivity of the *nramp3nramp4* mutant to low Cu suggest that the mutant could be explained if experiencing exacerbated Cu deficiency. To check this possibility, we tested Cu deficiency responses in the *nramp3nramp4* mutant by analyzing the expression of the *SPL7* transcription factor and some of their best targets, such as *COPT2* and *ZIP2,* when grown under Cu scarcity (½ MS with 0 µM Cu; 0 Cu) (Figure R.3.5C). In this assay, the Cu deficiency conditions have been alleviated (0 Cu) compared to previous experiments (-Cu), since the drastic phenotype showed by the *nramp3nramp4* mutant under severe Cu deficiency could further preclude the analysis of the mutant transcriptional responses. Both *COPT2* and *ZIP2* markers are as well induced under this new 0 Cu condition in the WT seedlings (Figure R.3.5C).
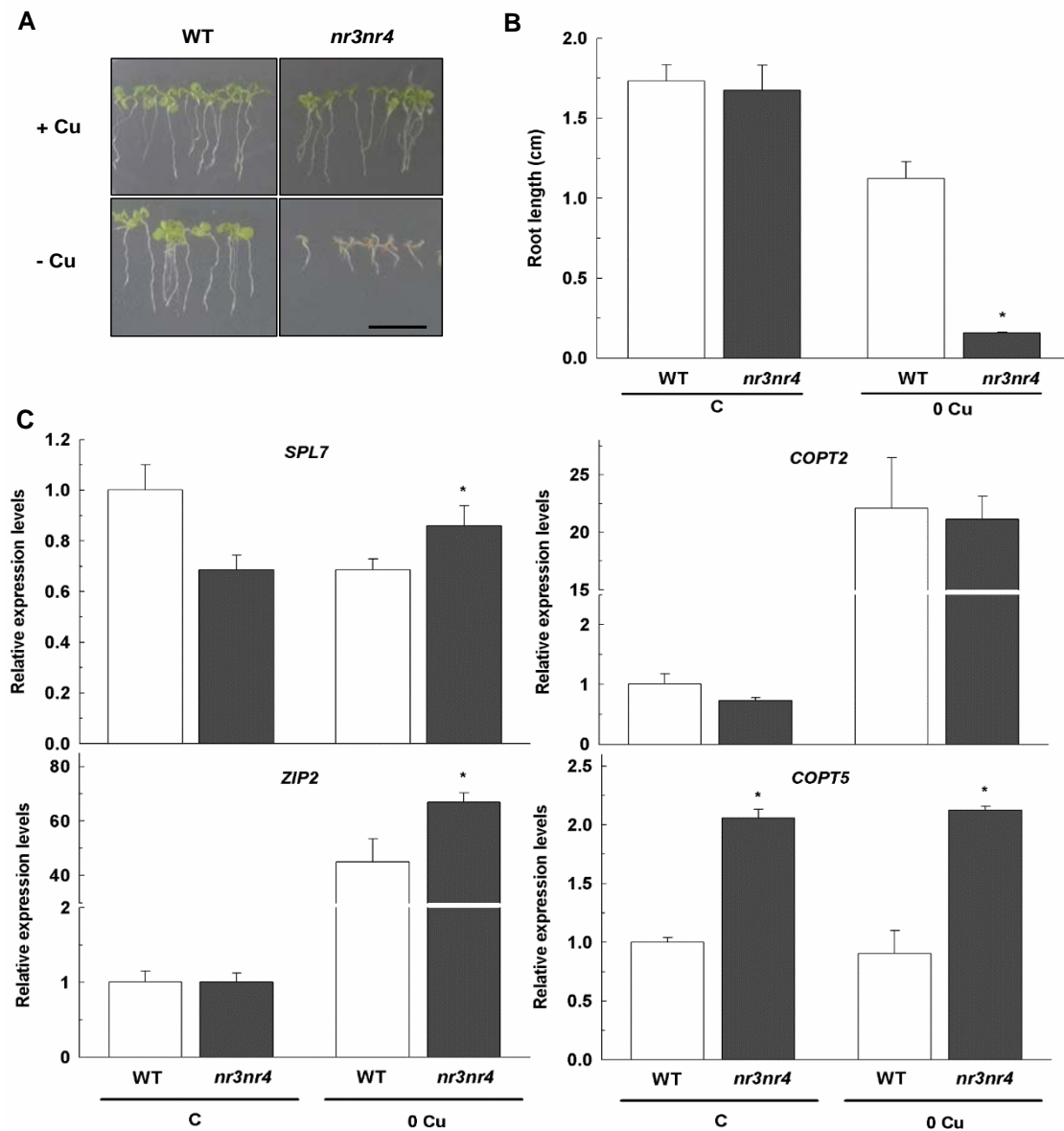
Figure R.3.5. Characterization of the *nramp3nramp4* seedlings under Cu deficiency. Photographs of the 7 day-old WT and *nramp3nramp4* (*nr3nr4*) seedlings grown under Cu sufficiency control conditions (½ MS with 1 µM CuSO₄; C) and Cu deficiency (½ MS with 50 µM BCS; -Cu) conditions (A). Bar scale corresponds to 1 cm. Root length of the plants shown in A (B). Asterisks indicate statistical differences (P < 0.05) according to Tukey test. Bars are means ± SD of 3 replicates of at least 15 plants. Analysis of the relative expression of the genes *SPL7*, *ZIP*, *COPT2* and *COPT5* involved in Cu deficiency responses in WT and *nr3nr4* 7 day-old seedlings grown under Cu sufficiency control conditions (½ MS with 1 µM CuSO₄; C) and Cu scarcity (½ MS with no added CuSO₄; 0 Cu) conditions (C). Expression levels are relative to those obtained in WT seedlings grown under Cu sufficiency conditions. Bars correspond to arithmetic means (2$^{-\Delta\Delta Ct}$) ± SD (n=3). Asterisks indicate statistical differences (P < 0.05) respect to WT values in each condition.

Although *SPL7* and *ZIP2* levels were slightly higher in the *nramp3nramp4* mutant compared to the WT under Cu scarcity conditions (0 Cu), *COPT2* expression remained mostly unchanged, pointing to a slight effect, if any, on SPL7-mediated Cu deficiency responses. On the other hand, the increased *NRAMP4* expression observed in the *copt5* mutant (Figure R.3.4 and Table R.3.2), brings to question whether *COPT5* expression is affected in the *nramp3nramp4* mutant. *COPT5* expression was indeed increased in the *nramp3nramp4* mutant regardless of the Cu availability in the medium (Figure R.3.5C), suggesting that Cu intracellular trafficking is affected in the double mutant. Taken together these data indicate an unanticipated connection between the roles of NRAMP3/NRAMP4 and COPT5 and suggests that when Fe remobilization from internal storage compartments is compromised, the Cu redistribution is also affected.

3.5. *COPT5* expression and phenotype under different metal availabilities

To further address a putative role of COPT5 in Fe homeostasis, *COPT5* expression was checked under different metal conditions (Figure R.3.6). To that end, 7 day-old WT seedlings were grown under control (½ MS with 1 µM $CuSO_4$ and 50 µM Fe citrate; C), Cu deficiency (½ MS with 100 µM BCS; -Cu) and Fe deficiency (½ MS+ 100 µM Ferrozine; -Fe) conditions (Figure R.3.6A). Whereas, as already reported (García-Molina *et al.*, 2011), *COPT5* mRNA is not regulated by the Cu status, a repression was observed under Fe deficiency (Figure R.3.6A). In addition, *pCOPT5::GUS* transgenic plants (García-Molina *et al.*, 2011) were grown under the same metal conditions to follow *COPT5* promoter activity as a readout for *COPT5* expression (Figure R.3.6B and 6C). *COPT5* was widely expressed in roots and especially at the root central cylinder under control conditions (Figure R.3.6B and 6C). On the contrary, under Cu deficiency, the *COPT5* promoter was mainly active in vascular bundles of the cotyledons. Moreover, the GUS staining pattern changes in Cu deficiency treatment respect to the control in root tissues. *COPT5* promoter apparently have no activity in vascular bundles, whereas expression is concentrated in cortex and endodermis layers (Figure R.3.6C). Besides, *COPT5* expression almost disappears from root and concentrates in the crown from seedlings grown under Fe deficiency (Figure R.3.6B and 6C). These results indicate that Fe deficiency greatly affects the *COPT5* root spatial expression pattern.
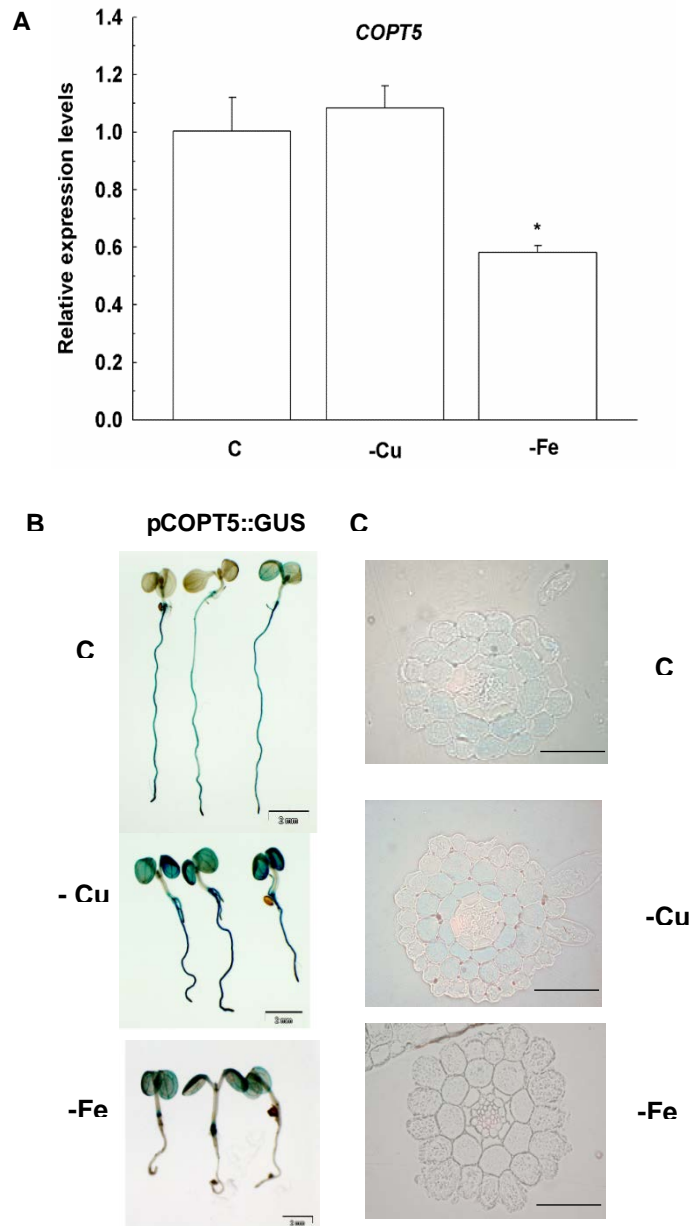
Figure R.3.6. *COPT5* regulation by Fe and Cu availabilities. The relative expression of the *COPT5* gene was determined by qRT-PCR in 7 day-old WT seedlings grown under Cu and Fe sufficiency control conditions (½ MS with 1 µM CuSO$_4$ and 50 µM Fe citrate; C), Cu deficiency (½ MS with 100 µM BCS; -Cu) and Fe deficiency (½ MS with 100 µM Ferrozine; -Fe) (A). Bars correspond to arithmetic means (2$^{-\Delta\Delta Ct}$) ± SD (n=3). Asterisks indicate statistical differences (P < 0.05) between values of the control condition of each treatment. *COPT5* expression pattern in the Arabidopsis *pCOPT5::GUS* transgenic plants. GUS staining in 3 representative 7 day-old seedlings grown as in A (B). Cross sections of the GUS-stained roots shown in B (C)**.**

To further pursuit the COPT5-mediated Cu-Fe crosstalk, we examined the development of WT and *copt5* seedlings under variable Cu and Fe conditions (Figure R.3.7).
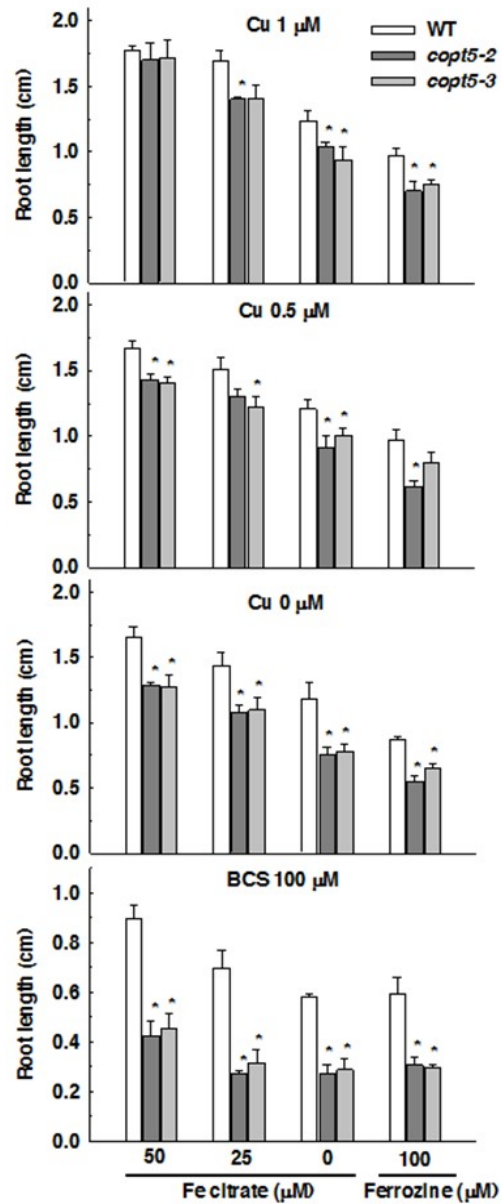
Figure R.3.7 Root length of *copt5* seedlings grown under different Cu and Fe availabilities. Root length of the 7 day-old plants WT and *copt5* seedlings grown under Fe deficiency (Fe-citrate 0 µM), Fe mild deficiency (Fe-citrate 25 µM) and Fe sufficiency (Fe-citrate 50 µM) conditions and in the presence of Cu sufficiency (1 µM Cu), mild Cu deficiency (0,5 and 0 µM Cu) and severe Cu deficiency (100 µM BCS) conditions. Asterisks indicate statistical differences (P<0.05) according to Tukey test. Bars are means ± SD of 3 replicates of at least 15 plants.

Under control conditions (Cu 1 µM and Fe 50 µM), the root length of WT and *copt5* plants was indistinguishable. As already reported (García-Molina *et al.*, 2011), the *copt5* mutant is more sensitive to Cu deficiency (BCS 100 µM and Fe 50 µM) than WT seedlings, showing a 50% reduction of root length compared to the WT. In addition, *copt5* is significantly sensitive to Fe deficiency conditions (Cu 1 µM and Ferrozine 100 µM), displaying a 20% reduction of root length compared to the WT (Figure R.3.7). Besides, under severe Cu deficiency conditions (BCS 100 µM), the WT root length responds to Fe increase, whereas the *copt5* mutants are unable to respond to Fe supply in the medium when Cu becomes unavailable.

It is also noticing that, under Fe sufficiency conditions (Fe 50 µM), the WT root length decreases concomitantly with Cu concentration being more exacerbated with BCS (Figure R.3.7). Following this result, a Perls staining in WT roots under Fe sufficiency but with different Cu concentrations was performed. As shown in Figure R.3.8, the Fe staining (blue color) decreases with Cu availability being undetectable under severe Cu deficiency. This result suggested a possible cooperative process between Cu availability and Fe uptake.
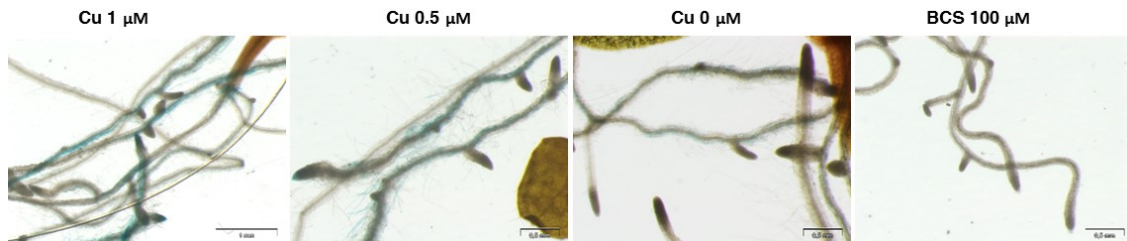
Figure R.3.8. Fe staining depending on Cu availability. Photographs of Perls staining in roots of 7 day-old WT seedling under Fe sufficiency (Fe citrate 50 µM) and different Cu concentrations (from left to right: sufficiency to severe deficiency).

To better understand the effects on Fe homeostasis experienced by the *copt5* mutant, we analyzed both Cu and Fe content in cotyledons from WT and *copt5* seedlings grown under different Cu and Fe conditions (Figure R.3.9A). As expected, the *copt5* cotyledons showed a decrease in Cu content under Cu deficiency. However, despite the exacerbated sensitivity to Fe deficiency observed in this mutant, *copt5* cotyledons contained more Fe than the WT (Figure R.3.9A).
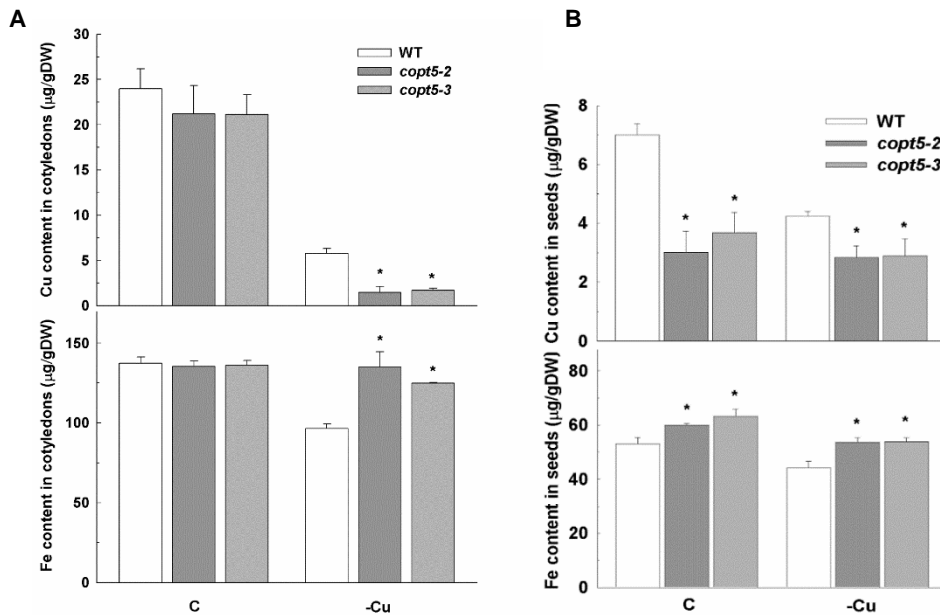
Figure R.3.9. Cu and Fe deficiency responses in the *copt5* mutant. Cu and Fe content in cotyledons from 7 day-old seedlings grown under Cu sufficiency control (C) and Cu deficiency (-Cu) conditions (A). Asterisks indicate statistical differences (P < 0.05) according to T test. Bars are means ± SD of 3 replicates of 20 mg of DW from seedlings. Cu and Fe content in seeds from adult plants grown in the greenhouse conditions (see material and methods) (B). Asterisks indicate statistical differences (P < 0.05) according to T test. Bars are means ± SD of 3 replicates of 15 mg of DW from seed.

Increased Fe content in sink organs, such as seeds, is an interesting biotechnological application that could be addressed with the aim of producing Fe biofortified food (Vasconcelos *et al.,* 2017). To determine if metal content was altered in seeds, WT and *copt5* mutant plants were grown in the greenhouse under different Cu supply (see materials and methods section) and metal content was determined in seeds (Figure R.3.9B). In the WT seeds, the content of both Cu and Fe was reduced under Cu deficient conditions. However, despite *copt5* seeds contained less Cu than the WT, significantly increased Fe content were determined regardless of the Cu availability in the medium (Figure R.3.9B). This result agrees with the higher Fe content detected in the *copt5* mutant cotyledons when compared to the WT (Figure R.3.9A).

Overall, these results further indicate that the putative difficulty to either acquire, signal or perceive Fe from the medium under Cu scarcity is exacerbated in the *copt5* mutant, which has impaired Cu retrieval from internal storages (García-Molina *et al.*, 2011; Klaumann *et al.*, 2011).

3.6. Superoxide dismutase expression in the *copt5* mutants

As already described, an explanation for the Cu-Fe interaction is metalloprotein substitution, where SODs are the best-known example (Yamasaki *et al.*, 2007). Whereas *FSD1*, encoding the FeSOD, is expressed under Cu deficiency, *CSD2* and *CSD1*, encoding the chloroplastic and cytosolic Cu/Zn SODs, respectively, are mostly expressed under Cu sufficiency (Yamasaki *et al.*, 2007). SOD expression in the WT and the *copt5* mutant under different Cu and Fe availabilities in the media has been analyzed (Figure R.3.10). In agreement with exacerbated Fe deficiency experienced in the *copt5* mutant, *FSD1* expression is lower in the mutant compared to the WT under Cu deficiency (-Cu +Fe) (Figure R.3.10A), maybe aimed to minimize Fe delivery to FeSOD. With regard to the *CSDs*, a slight decrease in *CSD2* mRNA was measured in the *copt5* mutants with respect to the WT under metal sufficiency (Figure R.3.11B), whereas *CSD1* expression was markedly reduced in the *copt5* mutants in the presence of Cu (Figure R.3.10C).
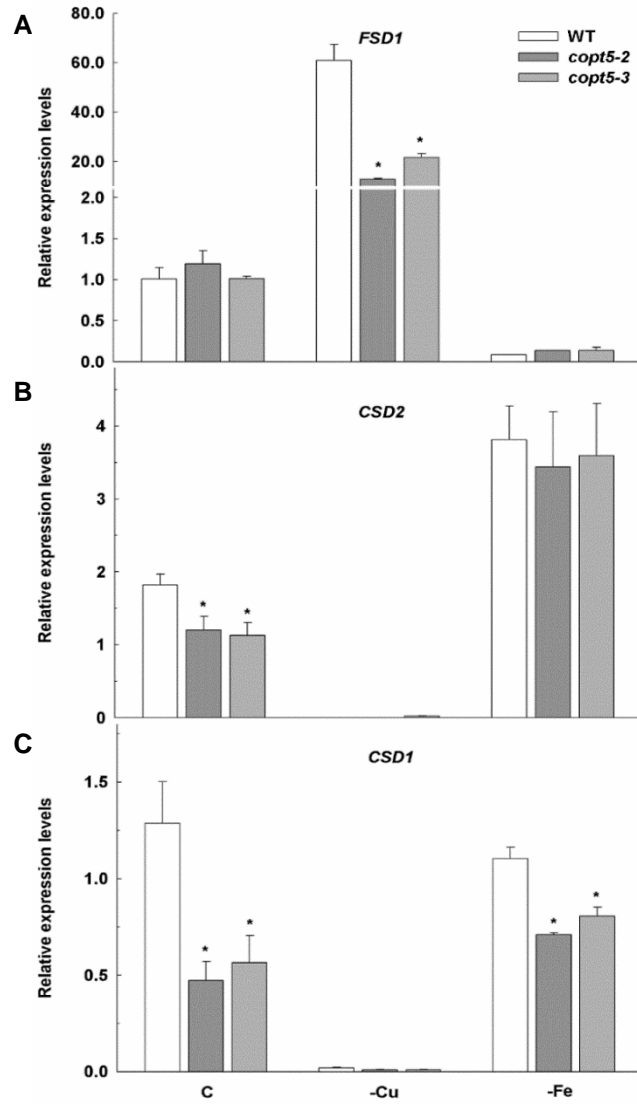
Figure R.3.10. SOD expression in *copt5* seedlings. *FSD1* relative expression. qRT-PCR analysis in 7 day-old WT, *copt5-2* and *copt5-3* seedlings grown under the same conditions used in Figure R.3.5 (A). *CSD2* relative expression (B) and *CSD1* relative expression (C). Bars correspond to arithmetic means ($2^{-\Delta\Delta Ct}$) ± SD (n=3). Asterisk indicates statistical differences (P < 0.05) respect to the control in each condition.

Then, SOD protein accumulation by immunoblot assays was assessed and their enzymatic activity tested through in-gel assays (Figure R.3.11) For the FeSOD protein content (Figure R.3.11A) and in FeSOD activity in gels (Figure R.3.11B) followed the mRNA pattern with a reduced content in the *copt5* mutants under Cu deficiency. With regard to the Cu/ZnSOD a reduced level of protein and activity was also observed in the *copt5* mutants with respect to the WT under Cu sufficiency (Figure R.3.11).
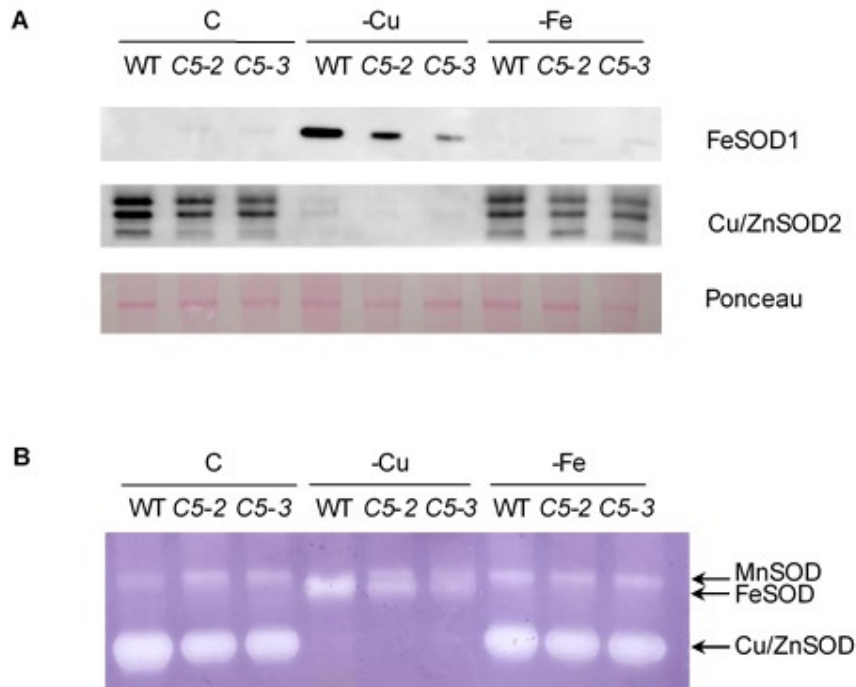
Figure R.3.11. SOD enzymatic activities and immune-detection. Soluble protein extraction was performed from WT, *copt5-2* (C5-2) and *copt5-3* (C5-3) 7 day-old seedlings grown under the same conditions used in Figure R.3.5. Immuno-detection of FSD1 and CSD2 using 35 µg of protein extract (A). Ponceau staining is shown as a loading control. SOD enzyme activities analysed in native gels loaded with 100 µg of protein extract (B). The gel was stained for total SOD activity.

Whereas *CSD2* mRNA was increased about twofold under Fe deficiency compared to the control conditions, both in the WT and the mutant (Figure R.3.10B), the protein levels were slightly reduced (Figure R.3.11A). These data suggest that Cu/ZnSODs proteins are post-transcriptionally modulated under Fe deficiency and this effect could be more relevant in the *copt5* mutant, most likely due to its exacerbated Fe deficiency responses.

Next, SOD expression was also examined in the *nramp3nramp4* mutant (Figure R.3.12). The SOD expression patterns under control conditions revealed a general decrease in the *nramp3nramp4* mutant (Figure R.3.12A). However, the protein level and SOD activity showed an unexpected result under control conditions, being Cu/ZnSOD protein content and activity absent in the *nramp3nramp4* mutant, which instead showed FeSOD activity (Figure R.3.12B and C). Since the absence of other Cu-deficiency effects (Figure R.3.5C), this result rather point to a specific effect of the lack of NRAMP4 function on Cu/Zn SOD.
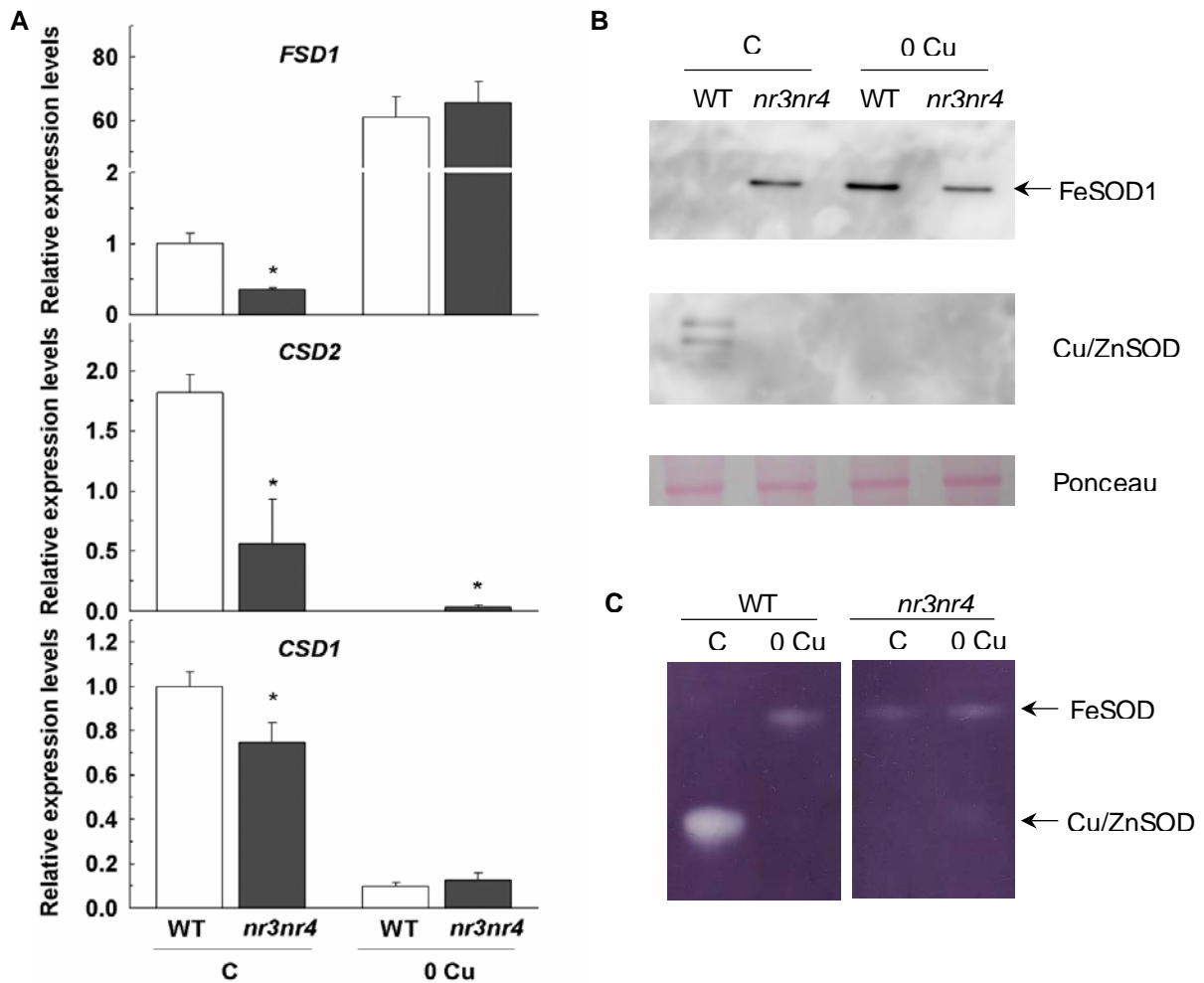
Figure R.3.12. SOD analysis in the *nramp3nramp4* mutant under Cu deficiency conditions. *FSD1*, *CSD2* and *CSD1* relative expression genes (A). qRT-PCR analysis in 7 day-old WT and *nramp3nramp4* (*nr3nr4*) seedlings grown under the same conditions used in Figure R.3.4C. Bars correspond to arithmetic means ($2^{-\Delta\Delta Ct}$) ± SD (n=3). The asterisk indicates statistical differences (P < 0.05) respect to the control in each condition. Immuno-detection of FSD1 and CSD2 using 35 µg of protein extract. Ponceau staining is showed as a loading control (B). SOD enzyme activities analyzed in native gels loaded with 100 µg of protein extract (C). The gel was stained for total SOD activity.

Overall, under the experimental conditions used here, the described decrease in SOD activities in both *copt5* and *nramp3nramp4* mutants is far from accounting for the increases in metal consumption due to SODs substitution that could justify the observed Cu-Fe interaction. Instead, these results rather point to a putative increase in ROS production in the mutants, which may be caused by a decrease in SOD activities upon metal deficiencies.

3.7. Fe localization and consumption in the *copts* mutants

To analyse possible changes in Fe localization in the *copt5* mutant compared to the WT and to other *copts* mutants, a commonly used method for Fe detection, such as the Perls/DAB staining (Roschzttardtz *et al.*, 2009) was carried out (Figure R.3.13). To that end, the WT, *copt2*, *copt1copt2copt6*, *copt3* and *copt5* seeds were germinated in ½ MS standard liquid medium and collected after 2 days. Next, these seedlings were subjected to Perls/DAB staining (see materials and methods).

Figure R.3.13. Iron localization in WT and *copts* seedlings. Perls/DAB staining 2 day-old WT, *copt2*, *copt1copt2copt6, copt3* and *copt5* seedlings grown in ½ MS liquid medium. The mark of Fe staining appears in black.

Whereas the other mutants apparently did not show differences, the *copt5* mutant clearly displayed a strong decrease in the Perls/DAB staining compared to the WT (Figure R.3.13). This result suggests that the subcellular membrane localization of the COPT transporters is a relevant fact on the Fe and Cu interaction in *Arabidopsis*. Since the *copt5* seedlings displayed an increased Fe content (Figure R.3.9), we further address the study of the crosstalk between Cu and Fe homeostases by analyzing the Fe distribution in 7 day-old seedlings of WT and *copt5* mutant

grown under either Cu sufficiency or deficiency (Figure R.3.14). No differences were observed in Perls/DAB staining under Cu sufficiency between the WT and the *copt5* mutant (Figure R.3.14A). However, under Cu deficiency, the *copt5* mutant displayed higher Fe staining in the root, specialy around the crown (Figure R.3.14A).

The roots cross sections of seedlings grown under the same previous conditions indicate that Fe distribution was modified under Cu deficiency (Figure R.3.14B). In the WT, while Fe reached the vascular cylinder under Cu sufficiency, most of the Fe remained at the epidermal cells under Cu deficiency (Figure R.3.14B). On the other hand, the *copt5* mutant showed a clear Fe staining pattern at the root endodermis under Cu sufficiency when compared to the WT. Moreover, when Cu was scarce, staining of the epidermal cells of the *copt5* mutant appeared to be reduced compared to the WT (Figure R.3.14B).
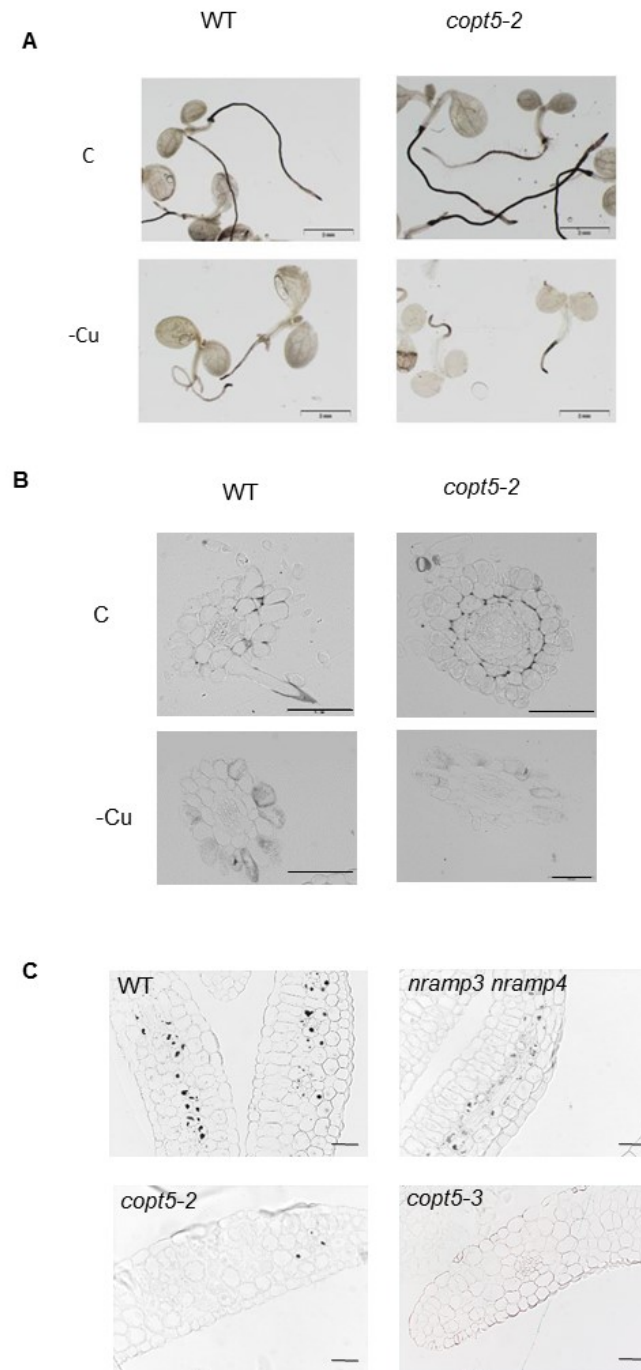
Figure R.3.14. Perls /DAB staining of WT and *copt5* seedlings. Perls /DAB staining of 7 day-old seedlings from WT and *copt5* seedlings grown under Cu sufficiency control (½ MS with 1 µM CuSO₄; C) and Cu deficiency (½ MS with 100 µM BCS; -Cu) (A). Perls /DAB staining of root sections from the plants shown in A (B). Perls /DAB staining of cotyledon sections from 3 day-old seedlings from WT, *nramp3nramp4, copt5-2* and *copt5-3* grown under control conditions (C).

Furthermore, we analysed the Fe stored in cotyledons tissues in WT, *copt5* and *nramp3nramp4* seedlings 3 days after germination (Figure R.3.14C). As already reported, the Fe vacuolar pool in WT seedlings starts to disappear 3 to 4 days after germination (Lanquar *et al.*, 2005), but at an earlier stage the *nramp3nramp4* and WT storage Fe pools, supposed to be in vacuole, were undistinguishable (Figure R.3.14C). However, at this early stage, the *copt5* mutant almost lack vacuolar stored Fe (Figure R.3.14C), indicating either that Fe was not initially present in the *copt5* mutant vacuole or that Fe mobilization was faster in the *copt5* mutant than in both WT and *nramp3nramp4* seedlings. In any case, the reduced Fe content in the *copt5* vacuoles is likely to be the consequence of the observed up-regulated *NRAMP4* expression and the subsequent increase in Fe transport from stores in the *copt5* mutant (Figure R.3.4). Overall, these results indicate that the phenotype of exacerbated Fe deficiency responses observed in the *copt5* mutant under Cu deficiency could be due to a differential Fe localization and point to a key role of Cu coming from the vacuole in this phenotype.

3.8. Expression of Fe-related transcription factors in the *copt5* mutant

To test for a putative role of *COPT5* in Fe deficiency signalling, the expression of the bHLH transcription factors *FIT*, *bHLH38*, *bHLH39*, *bHLH100* and *bHLH101* and the RING E3 ubiquitin ligase *BRUTUS* was monitored in the *copt5* mutant (Figure R.3.15). Except for FIT, all of these regulatory genes were oppositely affected by Cu and Fe deficiencies in the WT plants, being up-regulated by Fe deficiency and down-regulated by Cu deficiency (Figure R.3.15).
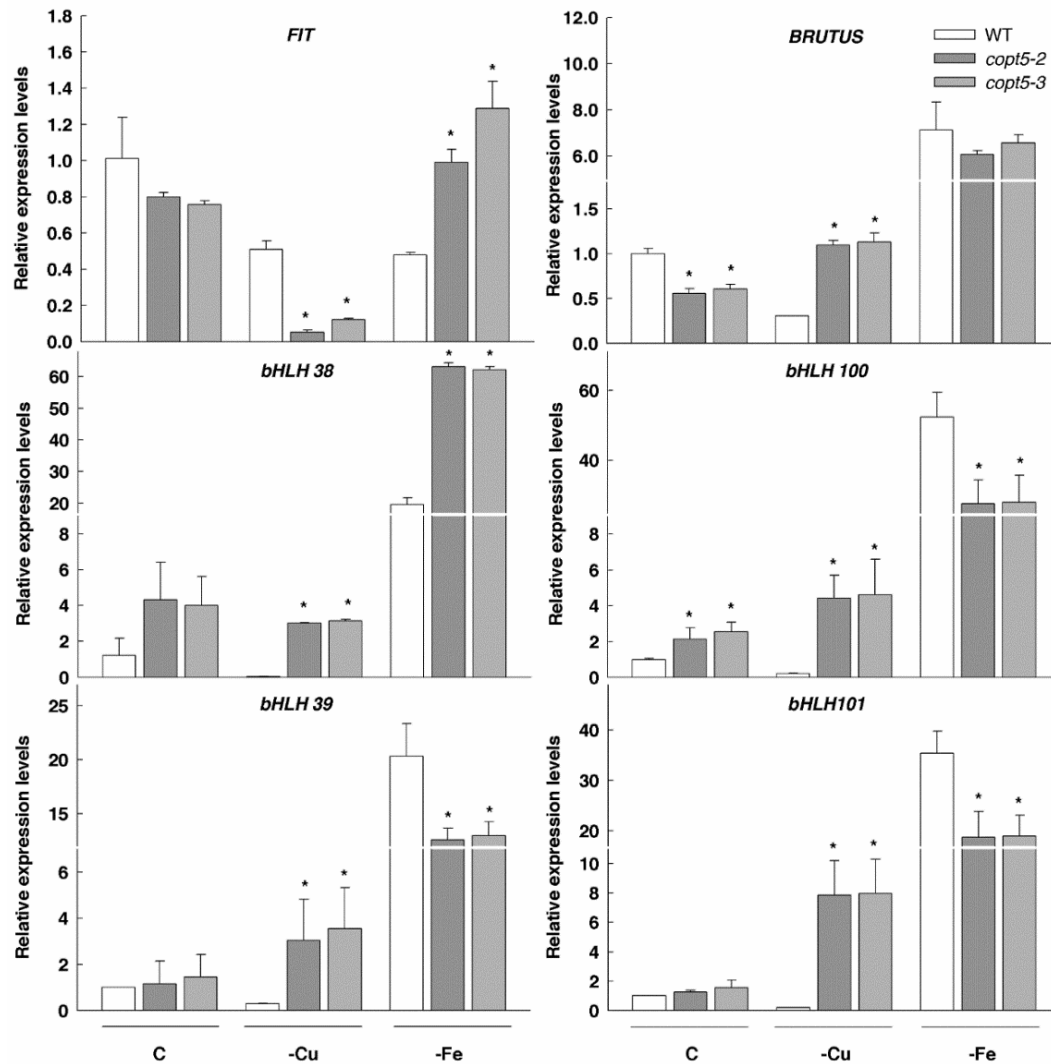
Figure R.3.15. Expression of bHLH subgroup Ib transcription factors and *BRUTUS* genes by Cu in the *copt5* mutant. The relative expression of the genes *FIT*, *bHLH38*, *bHLH39*, *bHLH100* and *bHLH101 and BRUTUS* was determined by qRT-PCR in 7 day-old WT seedlings grown under Cu sufficiency (½ MS with 1 µM CuSO₄; +Cu), Cu deficiency (½ MS with 100 µM BCS; -Cu) and Fe deficiency (½ MS with 100 µM Ferrozine; -Fe). The *UBQ10* gene was used as reference. *mRNA* levels are expressed as relative expression levels. Bars correspond to arithmetic means ($2^{-\Delta\Delta Ct}$) ± standard deviation (SD) (n=3). For each particular gene, asterisks indicate statistical differences (P < 0.05) between values of the control plants of each genotype.

Moreover, *FIT* and the rest of the genes oppositely behaved in the *copt5* mutant under Cu deficiency. Indeed, in the *copt5* mutants the abundance of the transcripts was greatly reduced for FIT (sevenfold) and highly (from four to eighty-five fold) increased for the rest of the

regulatory genes under Cu deficiency. This result indicates that the COPT5 function participates in the decreased expression of these regulatory factors (except for FIT) under Cu deficiency, since no decrease or even increased expression is observed in the *copt5* mutants. On the other hand, under Fe deficiency, all but one gene (*BRUTUS*) were deregulated in the *copt5* mutants. Among these, two opposite behaviour were observed again: *FIT* and *bHLH38* were up-regulated, whereas *bHLH39, bHLH100* and *bHLH101* were down-regulated (Figure R.3.15). Once again, this fact suggests that COPT5 function could interfere in Fe deficiency signalling. Collectively, these results envisage a complex and specific modification of Fe signalling in the *copt5* mutant when subjected to metal deficiencies.

DISCUSSION

Extensive studies on the Fe deficiency responses in plants have been reported (Bashir *et al.*, 2016; Bisson and Groth, 2014; Brumbarova *et al.*, 2015; Darbani *et al.*, 2013), but the understanding of how plants acclimate to low levels of Fe under other metal deficiencies remains obscure. Although the Fe-Cu interplay has been recognized for more than a century, the mechanistic insight into how Fe and Cu homeostasis are intertwined at the subcellular and whole plant levels, the variety of processes affected and the physiological significance of their interactions have just begun to be explored (Bernal *et al.*, 2012; Perea-García *et al.*, 2013; Waters *et al.*, 2012).

In addition to the previously reported exacerbated Cu deficiency responses in the *copt5* mutants under low Cu supply, which are probably due to the lack of Cu remobilization from vacuoles (García-Molina *et al.*, 2011; Klaumann *et al.*, 2011), Fe homeostasis is also affected in the *copt5* mutant (Table R.3.2, Figures R.3.4 and R.3.7). *NRAMP4* is among the genes overexpressed in *copt5* under Cu deficiency (Figure R.3.4). With this, we have characterized the double mutant *nramp3nramp4* under Cu deficiency, being this double mutant even more sensitive than the *copt5* mutant. Indeed, whereas the root length of the *copt5* mutant is reduced by approximately 50% under severe Cu deficiency (Figure R.3.7), the decrease in the *nramp3nramp4* mutant is more than 80% under Cu scarcity (Figure R.3.4B).

The hipersensitivity of *nramp3nramp4* to Cu deficiency is an unexpected result not easy to explain. According to our data, we propose that Cu homeostasis in the double mutant is affected at subcellular trafficking level. Since the *nramp3nramp4* mutant showed a slight increase in *ZIP2* and no differences in *COPT2* expression compared to the WT, it can be concluded that SPL7-dependent Cu deficiency responses remained mostly unaffected. However, *COPT5* expression levels are up-regulated in the double mutant, independently of Cu status, indicating that the Cu vacuolar storage pools can be affected. As previously stated, COPT5 supplies Cu to the aerial plant parts being involved in Cu redistribution in the whole plant (Klaumann *et al.*, 2011). If this is the case, the increased localization Cu in the aerial parts and the concomitant decrease in roots could account for the exacerbated sensitivity to Cu deficiency in the media. Moreover, Cu deficiency in roots drives Fe uptake difficulties (Figure R.3.8), further making the *nramp3nramp4* mutant highly Fe deficient since Fe uptake from both external and internal pools is impaired (Lanquar *et al.*, 2010).

A more complex picture arises from the Fe deficiency phenotype shown by the *copt5* mutant (Figure R.3.7A) since probably affecting multiple steps in Fe uptake, perception and signaling

involving long distance processes (Curie and Briat, 2003). As we can see in Figure R.3.12, only *copt5* mutant, among the other *copts*, showed differences in Fe localization respect to the WT. The Fe-deficiency impact on root growth shows a clear dependency on Cu in the WT (Figure R.3.11), possibly caused by the altered Fe long-distance transport under Cu deficiency (Figure R.3.13). In agreement with these results, Fe deficiency responses are exacerbated in the *copt5* mutant (Table R.3.2 and Figure R.3.4), since altered Cu distribution has been observed in this mutant compared to the WT plants, being Cu higher in roots and lower in aerial tissues (Klaumann *et al.*, 2011). A possible explanation is that Cu could be necessary for the Fe mobilization through MCO or other Cu-dependent ferroxidases, as reported in other organisms and suggested in plants (Bernal *et al.*, 2012; Kosman, 2010; Waters *et al.*, 2012). Thus, under Cu deficiency, a down-regulation of MCO activities in roots would redound in a lower Fe mobility. If this is the case, COPT5 could play a role in Cu delivering to specific ferroxidases during Fe scarcity. Thus, the lack of COPT5 function at the tonoplast of root tissues, such as the cortex and endodermis, may further affect Fe mobility. However, the fact that higher Fe levels have been detected under Cu deficiency in *copt5* mutant cothyledons and seeds (Figure R.3.8B) is hard to conciliate with this COPT5-MCO connection. On the other hand, a more plausible explanation to the exacerbated Fe deficiency responses in the *copt5* mutant is a putative increased Fe long-distance transport. Under Cu deficiency, enhanced *NRAMP4* expression in the *copt5* mutant could account for the increased Fe mobilization. In addition, decreased Cu long distance transport in the *copt5* mutant could drive to a lower Cu competition for metal-NA complexes in the vascular bundles further redunding in increased Fe transport to the shoots. This would explain the higher Fe levels found in *copt5* mutants seeds (Figure R.3.8B) and the lack of Perls/DAB staining in 3-days-old seedlings (Figure R.3.14). Moreover, Fe localization visualized by Perls/DAB staining at the root endodermis in the *copt5* mutant (Figure R.3.13B) surrounds the *COPT5* tissue expression pattern (Figure R.3.6C) suggesting a link between COPT5 function in Fe mobilization from roots-to-shoots. This process may affect Fe sensor cells in aerial tissues, driving to enhanced Fe deficiency signalling and further increasing Fe uptake.

In addition, "response to ethylene" is a GO category overrepresented in the *copt5* mutant, including several ethylene responsive factors (ERF) (Table R.3.1). We have previously shown that ethylene production is higher under Cu sufficiency than under deficiency and that *copt5* mutant produces less ethylene than WT (see chapter2). Specifically, the expression of the ethylene receptor, ERS2, is higher in the *copt5* mutant (Table A1 Pattern IVb). Whether the ethylene plays or not a role in the observed *copt5* phenotype is a possibility that deserves further research.

Another well-established interconnection between both metals is metalloprotein substitution, such as the antioxidant enzymes SODs (Waters *et al.*, 2012; Yamasaki *et al.*, 2007). The observed

increase in *CSD2* expression under Cu deficiency is in agreement with previous data where down-regulation of *miR398* by Fe deficiency justified its target increase (Waters *et al.*, 2012). Both Cu/ZnSOD and FeSOD protein and activity levels are lower in the *copt5* mutant (Figure R.3.10). Moreover, the *nramp3nramp4* mutant showed a decrease Cu/ZnSOD protein and activity levels and an increase in FeSOD (Figure R.3.11B) under Cu and Fe sufficiency levels that are not correlated with the level of transcripts (Figure R.3.11A). Post-transcriptional and post-translational mechanisms are commonly used when cells are subjected to Fe deficiency and are aimed to adapt their Fe metabolism under scarcity (Brumbarova *et al.*, 2015; Martínez-Pastor *et al.*, 2013). In this sense, the SUMO E3 ligase SIZ1 is involved in Cu tolerance and in the activity of the Cu/ZnSOD1 (Chen *et al.*, 2011a, 2011b) whereas the chloroplastic CLP protease system controls the turnover of PAA2 Cu transporter protein (Tapken *et al.*, 2015). It would be interesting to identify the molecular cause of the observed metal scarcity effects on SODs to further understand the Cu-Fe crosstalk in plants. As a consequence of this effect and in agreement with exacerbated Fe deficiency responses, the *copt5* mutants present a decrease in both Fe and Cu/Zn SOD under Cu and Fe deficiencies, respectively, even if their corresponding metals are present in the media (Figures R.3.9 and R.3.13). This may account for the presence of the oxidative stress as a GO category overrepresented in the *copt5* mutant (Table R.3.1) and the reported malfunctioning of chloroplast transport chain (García-Molina *et al.*, 2011).

The different localization of COPT2 and COPT5 at the plasma membrane and vacuolar compartments, respectively (García-Molina *et al.*, 2011; Klaumann *et al.*, 2011; Perea-García *et al.*, 2013), could explain the opposite phenotypes observed in the *copt5* and *copt2* mutants in relation to Fe deficiency responses. Effectively, whereas a *copt2* mutant is resistant to the simultaneous Fe and Cu deficiencies (Perea-García *et al.*, 2013), the *copt5* mutants display the opposite phenotype, being sensitive to Cu and Fe deficiencies (Figure R.3.7). This fact illustrates the differential role of internal Cu pools, versus the external Cu content in the media, with regard to the Cu crosstalk with Fe homeostasis. In addition to the membrane localization and the consequent foresee differences in ferroxidase Cu loading, roots at the *copt2* mutant are Cu starved under Cu deficiency and the Fe deficiency resistant phenotype has been postulated to be, at least partially, due to the increased low-phosphate responses in the mutant (Perea-García *et al.*, 2013). However, the *copt5* mutant show no generalized phosphate starvation responses in the microarray analysis (Table R.3.2). Furthermore, whereas the *COPT2* expression is up-regulated by Fe deficiency (Perea-García *et al.*, 2013), *COPT5* is down-regulated (Figure R.3.6A). These results indicate a completely different role of these Cu transporters, and their corresponding mobilization of internal and external Cu cellular pools under Fe deficiency.

The subcellular metal pools and their regulated interconnections play a key role in crop production (Bashir *et al.*, 2016). Our results constitute a strong indication of the interaction between vacuolar Fe and Cu under metal deficiencies. In particular, this fact becomes more evident in the *copt5* and *nramp3nramp4* mutant backgrounds, unable to retrieve Cu and Fe, respectively, from vacuoles (García-Molina *et al.*, 2011; Klaumann *et al.*, 2011; Lanquar *et al.*, 2005). The Cu and Fe vacuolar pools interconnection is underscored by the induction of *NRAMP4* expression in the *copt5* mutant (Figure R.3.4) and *COPT5* in the *nramp3nramp4* mutant (Figure R.3.5C) and may explain, at least in part, the sensitivity of *copt5* to Fe deficiency (Figure R.3.7), as well as *nramp3nramp4* sensitivity to Cu deficiency (Figure R.3.5). Moreover, these internal pools could be also relevant in metal supply to organelles, such as mitochondria and chloroplasts, at least under deficiency conditions (see introduction section 4.3) and, subsequently, in the control of their ROS status and retrograde signalling from the organelles to the nucleus. Curiously, by a split-ubiquitin screen for membrane proteins, the tonoplast located COPT5 has been shown to interact with MRS3 (Jones *et al.*, 2014), the *Arabidopsis* homologue of a mitochondrial yeast Fe transporter (Froschauer *et al.*, 2009). MRS3 participates in the mitochondrial-vacuolar signalling pathway that involves oxidative stress and Cu and Fe metabolism in yeast (Li *et al.*, 2010; Li and Kaplan, 2004; Vest *et al.*, 2016). In agreement with this suggestion, the expression of the WRKY40 transcription factor that modulates mitochondrial and chloroplast stress genes (Van Aken *et al.*, 2013) is up-regulated by Cu and the Cu provided by COPT5 may be involved in this regulation (Table A1 Pattern IVb). Furthermore, the differential and specific regulation of Fe-related factors, such as *FIT*, *bHLH38*, *bHLH39*, *bHLH100*, *bHLH101* and *BRUTUS* in the *copt5* mutants (Figure R.3.15) indicates that Cu transport from the vacuole is modulating the effects of metal deficiencies. Considering a determined FIT to other Ib bHLH factors ratio under control conditions, this ratio would be greatly reduced under Cu deficiency in the *copt5* mutant. Conversely, this ratio would be highly increased under Fe deficiency in the mutant. The transcriptional regulation of subgroup Ib bHLH factors have been shown to participate in the coordination between leaf cell differentiation and chloroplast development (Andriankaja *et al.,* 2014).

Taken together, these results underline the complexity of the interaction between Cu and Fe deficiency responses, where subcellular trafficking, ROS signalling and hormone responses could be also playing a role. In addition, results presented herein envisages the potential of the *copt5* mutant as a tool to further dissect Fe and Cu deficiency signalling and its crosstalk.

CONCLUSIONS

Chapter 1: INTERACTION BETWEEN ABA SIGNALING AND COPPER HOMEOSTASIS IN *ARABIDOPSIS THALIANA*.

1. A putative cross-talk between hormones and Cu homeostasis has been stablished based on an *in silico* analysis, being ABA and GA the hormones with highest number of responsive cis-elements in the *COPTs* promoters.

2. The *copt2* and the triple *copt1copt2copt6* mutants are more sensitive to exogenous ABA treatment than the other *copt* mutants.

3. The *copt2* mutant showed a lower sensitivity to ABA treatment under Cu deficiency conditions, indicating that ABA responses are attenuated under Cu scarcity. Exogenous ABA treatment modifies the *COPT2* localization pattern in roots modifying Cu uptake.

4. ABA treatment affects the Cu deficiency-related regulation, while Cu availability disrupts ABA biosynthesis and signalling in *Arabidopsis*.

Chapter 2: DEFECTIVE COPPER TRANSPORT IN THE *copt5* MUTANT AFFECTS CADMIUM TOLERANCE.

1. *COPT5* expression is neither regulated by Cu nor Cd, even though the *copt*5 mutant display increased sensitivity to Cd toxicity.

2. The expression of the Cu-deficiency SPL7-targets such as SODs are altered by Cd, being the expression of *FSD1* and *CSD1* genes reduced and increased, respectively.

3. COPT5 plays a role in root-to-shoot Cd translocation and in Cd tolerance. Cd disrupts ROS signalling in *copt5* under Cu deficiency conditions, increasing its oxidative stress effects. *RBOHD* expression and malondialdehyde content are reduced in *copt5* leaves by Cd. In addition, malondialdehyde content is higher in *copt5* than in wild-type roots, being specifically affected the vascular bundles cells.

4. Long-term Cd treatments affects ethylene biosynthesis in *copt5* that displays a decrease in ethylene production. However, ethylene perception is exacerbated in *copt5* mutants treated with Cd during 7 days.

Chapter 3: THE HIGH AFFINITY INTERNAL COPPER TRANSPORTER COPT5 PARTICIPATES IN IRON MOBILIZATION IN *ARABIDOPSIS THALIANA*.

1. Among all *copt* mutants tested under Fe deficiency conditions, *copt5* is the most sensitive, emphasising the importance of the transporter localization in Cu-Fe interplay at the subcellular level.

2. Despite *COPT5* expression is not regulated by Cu availability, it is down-regulated under Fe deficiency conditions which supress expression in roots.

3. Fe homeostasis is affected in *copt5,* especially under Cu deficiency conditions, since Fe deficiency targets are induced in the mutant and the localization of Fe is also altered.

4. A transcriptomic analysis performed under Cu deficiency conditions revealed that different biological processes are induced in the *copt5* mutant, among others ethylene binding, ROS metabolic processes and Fe ion binding.

5. Under Cu impaired remobilization, Fe homeostasis is altered, indicating a Cu and Fe vacuolar pools crosstalk which is necessary for metal-recycling dependent processes.

ANNEX

Table A.1. Overrepresented biological processes in the *copt5* microarray. Genes belonging to the biological processes overrepresented (FatiGO, P<0.05) in the expression patterns described in the Hierarchical Cluster Analysis (Figure R.3.2). The expression value of the genes was scaled by Z score. DEG were filtered by a false discovery rate (FDR) lower than 1% and 1.5-fold change ($\log_2 |1.5|$).

					FC	
Locus	Short Name	Description	*copt5* +Cu /WT +Cu	*copt5* -Cu /WT -Cu	WT -Cu /WT +Cu	*copt5* -Cu /*copt5* +Cu
Pattern Ia						
Biological process: Defense response						
AT2G26010	PDF1.3	plant defensin 1.3	-4.73	-1.04	-4.50	1.01
AT2G02120	PDF2.1	defensin-like protein 4	-1.89	-1.08	2.67	4.66
AT2G14560	LURP1	protein LURP1	-1.45	3.50	1.76	8.94
AT1G02930	GSTF6	glutathione S-transferase F6	-1.32	1.37	2.72	4.95
AT2G33050	RLP26	receptor like protein 26	-1.31	1.21	1.61	2.55
AT4G11650	OSM34	osmotin-like protein OSM34	-1.27	1.20	2.57	3.90
AT4G37150	MES9	methyl esterase 9	-1.24	1.16	1.31	1.89
AT3G45290	MLO3	MLO-like protein 3	-1.22	1.20	1.23	1.81
AT2G25000	WRKY60	putative WRKY transcription factor 60	-1.21	1.02	1.37	1.69
AT4G23680	MLP	dehydrase and lipid transport superfamily protein	-1.19	1.21	1.54	2.20
AT5G67330	NRAMP4	metal transporter Nramp4	-1.14	1.86	1.27	2.69
AT2G31230	ERF15	ethylene-responsive transcription factor 15	-1.02	1.07	1.90	2.07
Biological process: Oligopeptide transport						
AT5G67330	NRAMP4	metal transporter Nramp4	-1.14	1.86	1.27	2.69
AT1G55910	ZIP11	putative zinc transporter ZIP2 - like protein	-1.14	1.14	1.45	1.88
AT3G56240	CCH	copper chaperone	-1.08	1.25	2.84	3.84
AT3G46900	COPT2	copper transporter 2	-1.05	1.10	5.47	6.31
Biological process: Response to light stimulus						
AT5G24120	SIG5	RNA polymerase sigma factor 5	-1.15	1.05	1.28	1.55
AT1G06040	STO	salt tolerance protein	-1.10	1.13	1.44	1.79
AT1G09530	PIF3	transcription factor PIF3	-1.06	1.75	1.06	1.95
AT2G32390	GLR3.5	glutamate receptor 3.5	-1.04	1.28	1.44	1.94
AT5G67030	ABA1	zeaxanthin epoxidase	-1.01	1.07	1.94	2.09
Biological process: Response to toxin						

163

			FC			
Locus	Short Name	Description	*copt5* +Cu /WT +Cu	*copt5* -Cu /WT -Cu	WT -Cu /WT +Cu	*copt5* -Cu /*copt5* +Cu
AT4G23600	CORI3	cystine lyase CORI3	-2.82	-2.38	1.36	1.62
AT1G02930	GSTF6	glutathione S-transferase F6	-1.32	1.37	2.72	4.95
AT5G62480	GSTU9	glutathione S-transferase tau 9	-1.23	1.38	1.46	2.48
AT3G56240	CCH	copper chaperone	-1.08	1.25	2.84	3.84
Biological process: Transition metal ion transport						
AT5G67330	NRAMP4	metal transporter Nramp4	-1.14	1.86	1.27	2.69
AT1G55910	ZIP11	putative zinc transporter ZIP2 - like protein	-1.14	1.14	1.45	1.88
AT3G56240	CCH	copper chaperone	-1.08	1.25	2.84	3.84
AT3G46900	COPT2	copper transporter 2	-1.05	1.10	5.47	6.31
Pattern Ib						
Biological process: Response to auxin						
AT3G03850	F20H23.11	SAUR-like auxin-responsive protein	1.72	1.10	-2.42	-3.79
AT5G18020	MCM23.12	SAUR-like auxin-responsive protein	1.51	-1.17	-1.31	-2.33
AT5G18010	SAUR19	small auxin up RNA 19	1.47	-1.71	-2.19	-5.49
AT5G18050	MCM23.15	SAUR-like auxin-responsive protein	1.46	-1.42	-2.06	-4.29
AT5G18060	MCM23.16	SAUR-like auxin-responsive protein	1.46	-1.48	-1.81	-3.92
AT3G03820	F20H23.16	SAUR-like auxin-responsive protein	1.39	-1.19	-2.19	-3.63
AT5G47370	HAT2	homeobox-leucine zipper protein HAT2	1.30	-1.12	-1.48	-2.17
AT5G63160	BT1	BTB and TAZ domain protein 1	1.28	-1.02	-4.50	-5.88
AT1G29500	SAUR66	protein SMALL AUXIN UPREGULATED 66	1.27	-1.22	-1.86	-2.89
AT1G29450	SAUR64	protein SMALL AUXIN UPREGULATED 64	1.25	-1.08	-1.46	-1.98
AT5G18080	SAUR24	small auxin up RNA 24	1.24	-1.47	-2.21	-4.05
AT5G59780	MYB59	transcription factor MYB59	1.15	-1.03	-1.70	-2.01
AT4G14560	IAA1	auxin-responsive protein IAA1	1.12	-1.04	-2.24	-2.62
AT4G16780	HB-2	homeobox protein 2	1.08	-1.14	-1.90	-2.33
AT2G42580	TTL3	tetratricopetide-repeat thioredoxin-like 3	1.06	-1.02	-1.47	-1.59
AT4G37260	MYB73	myb domain protein 73	1.04	-1.03	-4.84	-5.19

Locus	Short Name	Description	FC			
			copt5 +Cu /WT +Cu	*copt5* -Cu /WT -Cu	WT -Cu /WT +Cu	*copt5* -Cu /*copt5* +Cu
		Pattern IIa				
		Biological process: Circadian rhythm				
AT5G60100	PRR3	pseudo-response regulator 3	-1.06	-1.24	1.58	1.36
AT1G22770	GI	protein GIGANTEA	1.03	1.03	1.94	1.94
AT5G24470	PRR5	pseudo-response regulator 5	1.15	1.16	1.52	1.53
		Biological process: Heme binding				
AT2G30750	CYP71A12	cytochrome P450 71A12	-2.04	-2.01	5.35	5.42
AT1G01600	CYP86A4	cytochrome P450 86A4	-1.62	-1.70	1.05	1.00
AT5G36110	CYP716A1	cytochrome P450 716A1	-1.23	-1.57	1.29	1.01
AT2G23180	CYP96A1	cytochrome P450 96A1	-1.22	-1.03	1.60	1.90
AT2G46660	CYP78A6	cytochrome P450 78A6	-1.16	-1.08	1.92	2.06
AT4G36430	PER49	peroxidase 49	-1.14	-1.91	6.64	3.96
AT5G06720	PER53	peroxidase 53	-1.12	-1.25	1.80	1.61
AT3G26830	PAD3	protein PHYTOALEXIN DEFICIENT 3	-1.09	-1.96	3.40	1.90
AT2G34490	CYP710A2	cytochrome P450 710A2	-1.02	-1.20	1.98	1.69
		Biological process: iron ion binding				
AT2G30750	CYP71A12	cytochrome P450 71A12	-2.04	-2.01	5.35	5.42
AT1G01600	CYP86A4	cytochrome P450 86A4	-1.62	-1.70	1.05	1.00
AT3G10150	PAP16	purple acid phosphatase 16	-1.41	-1.54	1.84	1.68
AT5G36110	CYP716A1	cytochrome P450 716A1	-1.23	-1.57	1.29	1.01
AT2G23180	CYP96A1	cytochrome P450 96A1	-1.22	-1.03	1.60	1.90
AT2G46660	CYP78A6	cytochrome P450 78A6	-1.16	-1.08	1.92	2.06
AT4G25100	FSD1	superoxide dismutase [Fe]	-1.15	-1.40	17.42	14.21
AT4G36430	PER49	peroxidase 49	-1.14	-1.91	6.64	3.96
AT5G06720	PER53	peroxidase 53	-1.12	-1.25	1.80	1.61
AT3G26830	PAD3	protein PHYTOALEXIN DEFICIENT 3	-1.09	-1.96	3.40	1.90
AT2G34490	CYP710A2	cytochrome P450 710A2	-1.02	-1.20	1.98	1.69
		Biological process: oxygen binding				
AT2G30750	CYP71A12	cytochrome P450 71A12	-2.04	-2.01	5.35	5.42
AT1G01600	CYP86A4	cytochrome P450 86A4	-1.62	-1.70	1.05	1.00

			FC			
Locus	Short Name	Description	*copt5* +Cu /WT +Cu	*copt5* -Cu /WT -Cu	WT -Cu /WT +Cu	*copt5* -Cu /*copt5* +Cu
AT5G36110	CYP716A1	cytochrome P450 716A1	-1.23	-1.57	1.29	1.01
AT2G23180	CYP96A1	cytochrome P450 96A1	-1.22	-1.03	1.60	1.90
AT2G46660	CYP78A6	cytochrome P450 78A6	-1.16	-1.08	1.92	2.06
AT3G26830	PAD3	protein PHYTOALEXIN DEFICIENT 3	-1.09	-1.96	3.40	1.90
AT2G34490	CYP710A2	cytochrome P450 710A2	-1.02	-1.20	1.98	1.69

Pattern IIb						
Biological process: Cell wall modification						
AT2G41850	PGAZAT	polygalacturonase ADPG2	3.18	3.39	-1.39	-1.30
AT1G10550	XTH33	probable xyloglucan hydrolase protein 33	1.96	1.61	-3.27	-3.99
AT5G51490	PME59	putative pectinesterase/pectinesterase inhibitor 59	1.28	1.30	-2.37	-2.34
AT3G10710	RHS12	root hair specific 12	1.24	2.18	-7.39	-4.20
AT1G62980	EXPA18	expansin A18	1.08	1.87	-5.97	-3.44

Biological process: Cell wall organisation						
AT2G41850	PGAZAT	polygalacturonase ADPG2	3.18	3.39	-1.39	-1.30
AT1G10550	XTH33	probable xyloglucan hydrolase protein 33	1.96	1.61	-3.27	-3.99
AT5G51490	PME59	putative pectinesterase 59	1.28	1.30	-2.37	-2.34
AT4G07960	CSLC12	Cellulose-synthase-like C12	1.24	1.04	-2.25	-2.70
AT3G10710	RHS12	root hair specific 12	1.24	2.18	-7.39	-4.20
AT1G32170	XTH30	probable xyloglucan hydrolase 30	1.21	1.15	-1.82	-1.91
AT5G15650	RGP2	reversibly glycosylated polypeptide 2	1.14	1.02	-1.37	-1.53
AT1G62980	EXPA18	expansin A18	1.08	1.87	-5.97	-3.44
AT1G48930	GH9C1	glycosyl hydrolase 9C1	1.07	2.51	-5.20	-2.22

Biological process: Immune response						
AT5G45220	TIR10	TIR-NBS-LRR class disease resistance protein	2.61	3.05	-1.50	-1.28
AT5G40100	TIR12	TIR-NBS-LRR class disease resistance protein	1.70	2.18	-1.83	-1.42
AT5G40090	TIR7	TIR-NBS-LRR class disease resistance protein	1.57	1.25	-1.48	-1.86
AT5G45110	NPR3	NPR1-like protein 3	1.02	1.00	-1.85	-1.88

Biological process: Response to auxin						

Locus	Short Name	Description	*copt5* +Cu /WT +Cu	*copt5* -Cu /WT -Cu	WT -Cu /WT +Cu	*copt5* -Cu /*copt5* +Cu
					FC	
AT4G36110	SAURL	SAUR-like auxin-responsive protein	1.81	1.62	-1.94	-2.17
AT4G34770	F11I11.10	SAUR-like auxin-responsive protein	1.36	2.43	-2.28	-1.28
AT4G31320	F8F16.140	SAUR-like auxin-responsive protein	1.35	1.20	-1.87	-2.11
AT5G10990	T30N20.260	SAUR-like auxin-responsive protein	1.32	1.36	-1.84	-1.78
AT1G29440	SAUR63	protein SMALL AUXIN UPREGULATED 63	1.31	1.03	-1.46	-1.87
AT1G29510	SAUR67	protein SMALL AUXIN UPREGULATED 67	1.18	1.08	-2.55	-2.80
AT3G23030	IAA2	auxin-responsive protein IAA2	1.13	1.53	-2.69	-1.79
AT3G48360	BT2	TAC1-mediated telomerase activation protein BT2	1.10	1.12	-1.87	-1.84
AT1G48690	F11I4.13	auxin-responsive GH3 family protein	1.06	1.32	-2.06	-1.65

Biological process: Response to ethylene						
AT5G64750	ERF111	ethylene-responsive transcription factor ABR1	1.62	1.82	-3.13	-2.78
AT1G36060	ERF55	ethylene-responsive transcription factor ERF055	1.38	2.38	-2.29	-1.32
AT1G71520	ERF20	ERF/AP2 transcription factor family protein DREB A-5	1.34	1.25	-2.11	-2.25
AT5G25190	ERF3	ethylene-responsive transcription factor ERF003	1.23	2.50	-4.01	-1.97
AT1G68840	ERF20	AP2-EREBP family, RAVE subfamily protein RAV2	1.19	1.96	-4.41	-2.43
AT5G61600	ERF104	ethylene-responsive transcription factor ERF104	1.19	1.08	-6.34	-6.95
AT1G13260	ERF4	AP2/ERF and B3 domain-containing transcription factor	1.13	1.17	-4.67	-4.53
AT1G79700	ERF17	AP2-like ethylene-responsive transcription factor WRI4	1.13	1.75	-2.75	-1.78
AT5G67190	ERF10	ethylene-responsive transcription factor ERF010	1.11	1.03	-1.85	-1.99
AT1G22190	ERF58	ethylene-responsive transcription factor RAP2.4	1.10	1.05	-2.09	-2.20
AT5G61590	ERF107	ethylene-responsive transcription factor ERF107	1.08	1.50	-2.94	-2.12
AT1G43160	ERF108	ethylene-responsive transcription factor RAP2-6	1.08	3.04	-5.00	-1.77
AT1G25560	ERF1	AP2/ERF and B3 domain-containing transcription	1.07	2.06	-4.00	-2.06
AT1G21910	ERF12	ethylene-responsive transcription factor ERF012	1.05	1.81	-8.60	-4.97
AT3G23240	ERF1	ethylene-responsive transcription factor 1B	1.01	2.06	-3.10	-1.53

Pattern IIIa						
Biological process: Response to hormone stimulus						
AT3G14050	RSH2	RelA-SpoT like protein RSH2	-1.23	1.84	-1.89	1.20
AT2G44080	ARL	ARGOS-like protein	-1.16	3.20	-2.14	1.74

167

Locus	Short Name	Description	*FC*			
			copt5 +Cu /WT +Cu	*copt5* -Cu /WT -Cu	WT -Cu /WT +Cu	*copt5* -Cu /*copt5* +Cu
AT3G21780	UGT71B6	UDP-glucosyl transferase 71B6	-1.09	1.94	-1.64	1.28
AT3G59900	ARGOS	protein AUXIN-REGULATED GENE INVOLVED IN ORGAN SIZE	-1.02	3.82	-1.89	2.06

Pattern IIIb						
Biological process: Cell cycle						
AT1G76310	CYCB2.4	cyclin-B2-4	1.04	-1.88	1.08	-1.81
AT3G05330	ATN	TANGLED1-like protein	1.00	-1.85	1.14	-1.61
Biological process: Microtubule-based process						
AT2G47500	F3G5.14	ATP binding / microtubule motor	1.16	-1.69	1.03	-1.90
AT3G44050	F3G5.21	kinesin motor protein-like protein	1.02	-1.67	1.04	-1.63
AT2G37420	F3G5.19	ATP binding microtubule motor family protein	1.02	-1.79	1.03	-1.76
AT3G20150	F3G5.75	Kinesin motor family protein	1.00	-1.96	1.10	-1.78

Pattern IVa						
Biological process: Cell cycle						
AT1G02065	SPL8	squamosa promoter binding protein-like 8	-1.15	-2.33	1.04	-1.94
AT5G06150	CYC1BAT	cyclin-B1-2	-1.09	-2.11	1.07	-1.81
AT4G05190	ATK5	kinesin 5	-1.03	-1.97	1.01	-1.89
AT3G23670	KINESIN-12B	kinesin-like protein KIN12B	-1.00	-1.95	1.10	-1.77
AT4G35620	CYCB2;2	cyclin-B2-2	-1.08	-1.89	1.03	-1.70
AT1G03780	TPX2	protein TPX2	-1.05	-1.86	1.05	-1.70
AT3G05330	ATN	TANGLED1-like prtoein	-0.02	-1.85	1.14	-1.61
AT1G44110	CYCA1;1	cyclin-A1-1	-1.12	-1.84	1.08	-1.52
AT5G48820	ICK6	cyclin-dependent kinase inhibitor 3	-1.03	-1.84	1.08	-1.65
Biological process: Cell-cell signalling						
AT3G27920	MYB0	trichome differentiation protein GL1	-1.35	-3.46	1.35	-1.91
AT5G40330	MYB23	transcription factor MYB23	-1.42	-2.18	1.19	-1.29
AT1G72970	HTH	embryo sac development arrest 17	-1.13	-1.95	1.20	-1.44
AT3G29780	RALFL27	protein ralf-like 27	1.22	-1.22	1.50	1.00

			FC			
Locus	Short Name	Description	*copt5* +Cu /WT +Cu	*copt5* -Cu /WT -Cu	WT -Cu /WT +Cu	*copt5* -Cu /*copt5* +Cu
		Biological process: Heme binding				
AT5G04660	CYP77A4	cytochrome P450 77A4	-1.80	-5.23	1.24	-2.33
AT4G15393	CYP702A5	cytochrome P450 702A5	-1.25	-3.90	2.02	-1.54
AT5G52320	CYP96A4	cytochrome P450 96A4	-1.65	-3.51	1.07	-1.98
AT1G16410	CYP79F1	cytochrome P450 79F1	-1.18	-3.40	1.23	-2.34
AT1G65670	CYP702A1	cytochrome P450 702A1	-1.67	-3.13	1.10	-1.70
AT3G10570	CYP77A6	cytochrome P450 77A6	-1.85	-2.92	1.21	-1.32
AT2G46650	CB5-C	cytochrome B5 isoform C	-1.42	-2.77	1.05	-1.86
AT5G05340	PER52	peroxidase 52	1.97	-2.21	10.14	2.33
AT5G42650	AOS	allene oxide synthase	-1.39	-2.20	1.12	-1.40
AT1G11600	CYP77B1	cytochrome P450 77B1	-1.13	-2.04	1.14	-1.59
AT4G39950	CYP79B2	cytochrome P450 79B2	-1.42	-1.91	1.19	-1.13
AT5G06730	PER54	peroxidase 54	1.03	-1.39	2.74	1.93
AT5G59920	ULI3	UV-B light insensitive 3	1.06	-1.21	1.58	1.23
AT2G45560	CYP76C1	cytochrome P450 76C1	1.07	-1.09	1.73	1.48
		Biological process: Iron ion binding				
AT1G06100	T21E18.15	delta-9 desaturase-like 2 protein	-2.32	-15.41	1.12	-5.95
AT3G10570	CYP77A6	cytochrome P450 77A6	-1.85	-2.92	1.21	-1.32
AT5G04660	CYP77A4	cytochrome P450 77A4	-1.80	-5.23	1.24	-2.33
AT1G02205	CER1	protein ECERIFERUM 1	-1.78	-4.60	1.22	-2.12
AT1G65670	CYP702A1	cytochrome P450 702A1	-1.67	-3.13	1.10	-1.70
AT5G52320	CYP96A4	cytochrome P450 96A4	-1.65	-3.51	1.07	-1.98
AT1G06360	T2D23.6	delta-9 desaturase-like 5 protein	-1.46	-2.95	1.10	-1.84
AT4G39950	CYP79B2	tryptophan N-monooxygenase 1	-1.42	-1.91	1.19	-1.13
AT2G46650	CB5-C	cytochrome B5 isoform C	-1.42	-2.77	1.05	-1.86
AT5G42650	AOS	allene oxide synthase	-1.39	-2.20	1.12	-1.40
AT4G15393	CYP702A5	cytochrome P450 702A5	-1.25	-3.90	2.02	-1.54
AT1G16410	CYP79F1	dihomomethionine N-hydroxylase	-1.18	-3.40	1.23	-2.34
AT1G11600	CYP77B1	cytochrome P450 77B1	-1.13	-2.04	1.14	-1.59
AT5G06730	PER54	peroxidase 54	1.03	-1.39	2.74	1.93
AT5G59920	ULI3	UV-B light insensitive 3	1.06	-1.21	1.58	1.23
AT2G45560	CYP76C1	cytochrome P450 76C1	1.07	-1.09	1.73	1.48

Locus	Short Name	Description	FC			
			copt5 +Cu /WT +Cu	*copt5* -Cu /WT -Cu	WT -Cu /WT +Cu	*copt5* -Cu /*copt5* +Cu
AT5G05340	PER52	peroxidase 52	1.97	-2.21	10.14	2.33
Biological process: Lipid catabolic process						
AT5G33370	F19N2.90	GDSL esterase/lipase	-2.96	-10.75	1.10	-3.32
AT5G45960	K15I22.16	GDSL esterase/lipase	-1.40	-2.13	1.01	-1.50
AT4G26790	F10M23.130	GDSL esterase/lipase	-1.30	-3.07	1.19	-1.98
AT3G04290	LTL1	Li-tolerant lipase 1	-1.24	-1.55	1.02	-1.22
AT5G45670	MRA19.6	GDSL esterase/lipase	-1.18	-1.57	1.17	-1.14
AT4G28780	F16A16.110	GDSL esterase/lipase	-1.18	-2.38	1.19	-1.69
AT4G30140	F6G3.170	GDSL esterase/lipase	-1.02	-2.95	1.26	-2.30
AT2G42990	F23E6.2	GDSL esterase/lipase	1.03	-1.68	1.97	1.14
Biological process: Microtubule-based process						
AT1G18370	HIK	kinesin HINKEL	-1.15	-2.02	1.07	-1.65
AT2G28620	T8O18.9	kinesin motor protein-related protein	-1.14	-2.09	1.01	-1.81
AT5G23910	MRO11.5	ATP binding microtubule motor family protein	-1.11	-2.09	1.07	-1.76
AT2G22610	T9I22.5	kinesin motor protein-related protein	-1.08	-1.72	1.01	-1.58
AT1G72250	T9N14.6	kinesin motor protein-related protein	-1.07	-1.95	1.08	-1.69
AT1G03780	TPX2	protein TPX2	-1.05	-1.86	1.05	-1.70
AT4G05190	ATK5	kinesin 5	-1.03	-1.97	1.01	-1.89
AT3G23670	KIN12B	kinesin-like protein KIN12B	-1.00	-1.95	1.10	-1.77
Biological process: Phyllome development						
AT3G01140	MYB106	myb domain protein 106	-1.54	-4.06	1.48	-1.78
AT5G40330	MYB23	transcription factor MYB23	-1.42	-2.18	1.19	-1.29
AT3G27920	MYB0	trichome differentiation protein GL1	-1.35	-3.46	1.35	-1.91
AT5G08370	AGAL2	alpha-galactosidase 2	-1.24	-1.58	1.03	-1.23
AT3G61970	NGA2	B3 domain-containing transcription factor	-1.13	-1.66	1.19	-1.23
AT2G45480	GRF9	growth-regulating factor 9	-1.05	-1.85	1.05	-1.67
AT2G41940	ZFP8	zinc finger protein 8	1.01	-1.16	1.88	1.60
Biological process: Shoot system development						
AT3G01140	MYB106	myb domain protein 106	-1.54	-4.06	1.48	-1.78

			FC			
Locus	Short Name	Description	*copt5* +Cu /WT +Cu	*copt5* -Cu /WT -Cu	WT -Cu /WT +Cu	*copt5* -Cu /*copt5* +Cu
AT5G40330	MYB23	transcription factor MYB23	-1.42	-2.18	1.19	-1.29
AT3G27920	MYB0	trichome differentiation protein GL1	-1.35	-3.46	1.35	-1.91
AT5G08370	AGAL2	alpha-galactosidase 2	-1.24	-1.58	1.03	-1.23
AT1G14350	FLP	MYB transcription factor FLP	-1.15	-1.80	1.09	-1.43
AT3G61970	NGA2	B3 domain-containing transcription factor	-1.13	-1.66	1.19	-1.23
AT1G02730	CSLD5	cellulose synthase-like protein D5	-1.12	-2.09	1.03	-1.80
AT2G45480	GRF9	growth-regulating factor 9	-1.05	-1.85	1.05	-1.67
AT2G41940	ZFP8	zinc finger protein 8	1.01	-1.16	1.88	1.60

Biological process: Sulfur metabolic process						
AT1G54040	ESP	epithiospecifier protein	-2.40	-20.94	-1.03	-8.98
AT1G65860	FMO GS-OX1	flavin-containing monooxygenase	-1.43	-3.88	1.07	-2.53
AT4G39950	CYP79B2	tryptophan N-monooxygenase 1	-1.42	-1.91	1.19	-1.13
AT1G62560	FMO GS-OX3	flavin-containing monooxygenase	-1.22	-3.48	1.26	-2.27
AT5G07690	MYB29	myb domain protein 29	-1.18	-2.84	1.31	-1.83
AT1G16410	CYP79F1	dihomomethionine N-hydroxylase	-1.18	-3.40	1.23	-2.34
AT1G24100	UGT74B1	UDP-glucosyl transferase 74B1	-1.12	-1.60	1.08	-1.32

Pattern IVb						
Biological process: Hydrogen peroxide						
AT5G67400	PER73	peroxidase 73	1.24	3.47	-12.62	-4.52
AT5G22410	PER60	peroxidase 60	1.18	3.21	-10.92	-4.02
AT5G19890	PER59	peroxidase 59	1.16	4.84	-23.67	-5.69
AT3G49960	PER35	peroxidase 35	1.12	4.55	-13.05	-3.20
AT1G49570	PER10	peroxidase 10	1.05	10.26	-13.97	-1.43

Biological process: Immune response						
AT1G65390	PP2-A5	protein PHLOEM protein 2-LIKE A5	-1.89	2.06	-7.00	-1.80
AT1G80840	WRKY40	putative WRKY transcription factor 40	-1.73	1.39	-20.76	-8.61
AT3G04210	T6K12.17	TIR-NBS class disease resistance protein	-1.52	1.24	-3.58	-1.90
AT5G58120	K21L19.1	TIR-NBS-LRR class disease resistance protein	-1.46	1.05	-4.46	-2.90
AT4G23190	CRK11	cysteine-rich receptor-like protein kinase 11	-1.38	1.15	-2.50	-1.59
AT1G56510	WRR4	TIR-NB-LRR disease resistance protein	-1.37	1.12	-2.60	-1.69
AT2G01180	PAP1	lipid phosphate phosphatase 1	-1.35	1.05	-2.91	-2.06

Locus	Short Name	Description	*FC*			
			copt5 +Cu /WT +Cu	*copt5* -Cu /WT -Cu	WT -Cu /WT +Cu	*copt5* -Cu /*copt5* +Cu
AT5G22690	MDJ22.11	TIR-NBS-LRR class disease resistance protein	-1.30	1.11	-3.08	-2.13
AT4G12720	NUDT7	nudix hydrolase 7	-1.29	1.03	-2.57	-1.95
AT1G72930	TIR	toll/interleukin-1 receptor-like protein	-1.29	1.11	-1.63	-1.15
AT1G63750	F24D7.6	TIR-NBS-LRR class disease resistance protein	-1.27	1.34	-3.57	-2.13
AT4G31800	WRKY18	WRKY DNA-binding protein 18	-1.25	1.54	-4.21	-2.27
AT3G45640	MPK3	mitogen-activated protein kinase 3	-1.20	1.21	-2.50	-1.73
AT1G31540	T8E3.20	TIR-NBS-LRR class disease resistance protein	-1.18	1.20	-2.96	-2.09
AT1G28380	NSL1	protein necrotic spotted lesions 1	-1.16	1.01	-1.60	-1.36
AT1G72940	F3N23.14	TIR domain-containing protein	-1.16	1.00	-2.65	-2.27
AT1G29690	CAD1	protein constitutively activated cell death 1	-1.10	1.30	-3.33	-2.31
AT1G63860	K11I1.8	TIR-NBS-LRR class disease resistance protein	-1.07	1.29	-4.39	-3.18

		Biological process: Regulation of signal transduction pathway				
AT3G45640	MPK3	mitogen-activated protein kinase 3	-1.20	1.21	-2.50	-1.73
AT4G09570	CPK4	calcium-dependent protein kinase 4	-1.15	1.09	-1.67	-1.33
AT3G02140	TMAC2	Ninja-family protein AFP4	-1.03	1.46	-2.69	-1.79
AT3G23150	ETR2	ethylene receptor 2	1.21	2.67	-1.35	1.63
AT2G40940	ERS1	ethylene response sensor 1	1.21	1.61	-1.22	1.09
AT5G25350	EBF2	EIN3-binding F-box protein 2	1.32	1.86	-1.17	1.21
AT1G04310	ERS2	ethylene response sensor 2	1.55	1.98	-1.16	1.10

		Biological process: Response to auxin				
AT1G18570	MYB51	myb domain protein 51	-1.34	1.26	-3.34	-1.98
AT1G56150	YUP8H12R.25	SAUR-like auxin-responsive protein	-1.21	1.78	-4.09	-1.91
AT5G54490	PBP1	pinoid-binding protein 1	-1.17	1.22	-3.89	-2.74
AT5G67480	BT4	BTB and TAZ domain protein 4	-1.04	1.03	-3.25	-3.03
AT5G45710	RHA1	heat stress transcription factor A-4c	-1.03	1.11	-1.69	-1.48
AT3G23030	IAA2	auxin-responsive protein IAA2	1.13	1.53	-2.69	-1.79
AT4G34810	AT4G34810	SAUR-like auxin-responsive protein	1.24	1.72	-1.26	1.10
AT5G66700	HB53	homeobox-leucine zipper protein ATHB-53	1.30	2.34	-1.16	1.55
AT5G20820	T1M15.220	SAUR-like auxin-responsive family protein	1.37	6.10	-4.25	1.05

		Biological process: Response to carbohydrate				
AT1G80840	WRKY40	putative WRKY transcription factor 40	-1.73	1.39	-20.76	-8.61

Locus	Short Name	Description	FC			
			copt5 +Cu /WT +Cu	*copt5* -Cu /WT -Cu	WT -Cu /WT +Cu	*copt5* -Cu /*copt5* +Cu
AT2G17040	NAC036	NAC transcription factor family protein NAC036	-1.63	1.33	-3.97	-1.83
AT2G13790	SERK4	somatic embryogenesis receptor kinase 4	-1.34	1.06	-2.03	-1.43
AT4G33050	EDA39	calmodulin-binding protein	-1.33	1.28	-2.94	-1.72
AT2G23320	WRKY15	WRKY DNA-binding protein 15	-1.28	1.16	-2.02	-1.36
AT4G31800	WRKY18	WRKY DNA-binding protein 18	-1.25	1.54	-4.21	-2.27
AT3G45640	MPK3	mitogen-activated protein kinase 3	-1.20	1.21	-2.50	-1.73
AT3G05200	ATL6	E3 ubiquitin-protein ligase ATL6	-1.18	1.10	-2.21	-1.70
AT3G16720	ATL2	RING-H2 finger protein ATL2	-1.13	1.09	-2.75	-2.23
AT1G08930	ERD6	sugar transporter ERD6	-1.11	1.42	-2.75	-1.76
AT4G17230	SCL13	protein scarecrow-like 13	-1.10	1.26	-2.63	-1.90
AT3G46080	ZAT8	zinc finger protein	-1.08	1.48	-3.80	-2.37
AT1G42990	BZIP60	bZIP transcription factor 60	-1.06	1.13	-1.79	-1.49
AT4G26400	M3E9.170	RING/U-box domain-containing protein	-1.04	1.14	-1.71	-1.44
AT3G19380	PUB25	U-box domain-containing protein 25	-1.02	1.29	-2.40	-1.81
AT1G07520	F22G5.41	GRAS family transcription factor	-1.02	1.23	-2.40	-1.91
AT4G17500	ERF1A	ethylene-responsive transcription factor 1A	-1.01	1.29	-3.29	-2.53
AT3G46090	ZAT7	zinc finger protein ZAT7	-1.00	2.97	-13.51	-4.54
AT3G47340	ASN1	asparagine synthetase [glutamine-hydrolyzing]	1.53	4.06	-12.25	-4.42

		Biological process: Response to ethylene				
AT1G18570	MYB51	myb domain protein 51	-1.34	1.26	-3.34	-1.98
AT1G71030	MYBL2	putative myb family transcription factor	-1.04	1.34	-3.14	-2.25
AT4G17500	ERF1A	ethylene-responsive transcription factor 1A	-1.01	1.29	-3.29	-2.53
AT4G06746	ERF7	ethylene-responsive transcription factor RAP2-9	1.08	2.11	-1.38	1.41
AT3G25730	ERF3	ethylene response DNA binding factor 3	1.15	2.06	-1.73	1.04
AT5G13330	ERF113	ethylene-responsive transcription factor ERF113	1.18	2.54	-1.31	1.64
AT1G68840	ERF2	AP2-EREBP family, RAVE subfamily protein RAV2	1.19	1.96	-4.41	-2.43
AT3G23150	ETR2	ethylene receptor 2	1.21	2.67	-1.35	1.63
AT2G40940	ERS1	ethylene response sensor 1	1.21	1.61	-1.22	1.09
AT5G25350	EBF2	EIN3-binding F-box protein 2	1.32	1.86	-1.17	1.21
AT1G04310	ERS2	ethylene response sensor 2	1.55	1.98	-1.16	1.10

		Biological process: Response to gibberellin				
AT1G18570	MYB51	myb domain protein 51	-1.34	1.26	-3.34	-1.98

173

			FC			
Locus	**Short Name**	**Description**	***copt5* +Cu /WT +Cu**	*copt5* -Cu /WT -Cu	WT -Cu /WT +Cu	***copt5* -Cu /*copt5* +Cu**
AT5G51810	GA20OX2	gibberellin 20 oxidase 2	-1.13	1.19	-1.76	-1.31
AT5G50915	bHLH137	transcription factor bHLH137	-1.06	1.40	-2.63	-1.78
AT5G67480	BT4	BTB and TAZ domain protein 4	-1.04	1.03	-3.25	-3.03
AT1G71030	MYBL2	putative myb family transcription factor	-1.04	1.34	-3.14	-2.25
		Biological process: Response to jasmonate				
AT1G19180	JAZ1	jasmonate-zim-domain protein 1	-1.38	1.07	-3.20	-2.18
AT1G18570	MYB51	myb domain protein 51	-1.34	1.26	-3.34	-1.98
AT4G35770	SEN1	senescence-associated protein DIN1	-1.33	4.41	-16.12	-2.77
AT1G72450	JAZ6	jasmonate-zim-domain protein 6	-1.22	1.02	-1.83	-1.47
AT3G15500	NAC3	ATAF-like NAC-domain transcription factor	-1.20	2.83	-7.08	-2.08
AT1G71030	MYBL2	putative myb family transcription factor	-1.04	1.34	-3.14	-2.25
AT5G46050	PTR3	peptide transporter 3	1.05	2.58	-1.29	1.90
		Biological process: Response to wounding				
AT1G80840	WRKY40	putative WRKY transcription factor 40	-1.73	1.39	-20.76	-8.61
AT5G20230	BCB	blue-copper-binding protein	-1.67	1.68	-19.15	-6.80
AT4G35770	SEN1	senescence-associated protein DIN1	-1.33	4.41	-16.12	-2.77
AT1G72450	JAZ6	jasmonate-zim-domain protein 6	-1.22	1.01	-1.86	-1.51
AT3G45640	MPK3	mitogen-activated protein kinase 3	-1.20	1.21	-2.50	-1.73
AT5G54170	AT5G54170	lipid-binding START domain-containing protein	-1.07	1.01	-1.84	-1.71
AT3G61060	PP2-A13	phloem protein 2-A13	1.03	1.27	-3.11	-2.41
AT1G73500	MKK9	MAP kinase kinase 9	1.03	1.27	-2.94	-2.28
AT5G46050	PTR3	peptide transporter 3	1.05	2.58	-1.29	1.90
AT2G37040	PAL1	phenylalanine ammonia-lyase 1	1.13	1.56	-1.06	1.30

Table A.2. Genes belonging to the biological processes overrepresented (FatiGO, P<0.05) in the microarray previous Z score transformation. DEG were filtered by a false discovery rate (FDR) lower than 1% and 1.5-fold change (log$_2$ |1.5|).

		FC			
Locus	Description	*copt5* +Cu /WT +Cu	*copt5* -Cu /WT -Cu	WT -Cu /WT +Cu	*copt5* -Cu /*copt5* +Cu
	Glucosinolate metabolism processes				
AT5G25980	Glucoside glucohydrolase 2	-2.73	-4.29	-1.32	-2.07
AT1G54040	Epithiospecifier protein	-2.47	-20.96	-1.01	-8.52
AT1G65860	Flavin-monooxygenase glucosinolate S-oxygenase 1	-1.43	-3.88	1.07	-2.53
AT5G23010	Methylthioalkylmalate synthase 1	-1.34	-2.14	-1.05	-1.68
AT1G62540	Flavin-monooxygenase glucosinolate S-oxygenase 2	-1.28	-1.67	1.48	1.13
AT4G39940	APS-kinase 2	-1.28	-2.13	-1.05	-1.75
AT1G62560	Flavin-monooxygenase glucosinolate S-oxygenase 3	-1.22	-3.48	1.26	-2.27
AT5G07690	Myb domain protein 29	-1.18	-2.84	1.31	-1.83
AT1G16410	Cytochrome p450 79f1	-1.18	-3.40	1.23	-2.34
AT5G60890	Myb domain protein 34	-1.16	-1.56	1.72	1.28
AT1G24100	UDP-glucosyl transferase 74B1	-1.12	-1.60	1.08	-1.32
	Cell recognition				
AT2G28830	PLANT U-BOX 12	-1.42	3.10	-1.33	3.30
AT1G11300	Protein serine/threonine kinase	-1.21	-1.21	1.78	1.78
AT1G11330	S-locus lectin protein kinase family protein	-1.12	1.67	-1.11	1.69
AT4G27300	S-locus lectin protein kinase family protein	-1.04	2.42	-1.32	1.91
AT1G61380	S-domain-1 29	-1.01	1.47	1.15	1.71
	Response to oxidative stress				
AT2G38470	WRKY DNA-binding protein 33	-1.58	1.09	-8.20	-4.78
AT5G62470	Myb domain protein 96	-1.38	-1.23	-2.59	-2.30
AT4G12720	MutT/nudix family protein	-1.38	1.03	-2.49	-1.75
AT1G18570	Myb domain protein 51	-1.34	1.26	-3.34	-1.98
AT1G08830	Copper/zinc superoxide dismutase 1	-1.24	-1.52	-22.99	-28.11
AT3G57530	Calcium-dependent protein kinase 32	-1.23	-1.02	-3.12	-2.57
AT4G12720	MutT/nudix family protein	-1.20	1.03	-2.65	-2.15
AT3G45640	Mitogen-activated protein kinase 3	-1.20	1.21	-2.50	-1.73
AT3G08720	Serine/threonine protein kinase 2	-1.20	1.13	-2.19	-1.62
AT5G20010	RAS-related nuclear protein-1	-1.19	-1.19	-1.95	-1.95
AT1G28380	MAC/Perforin domain-containing protein	-1.16	1.01	-1.60	-1.36
AT5G67300	Myb domain protein r1	-1.14	-1.01	-2.94	-2.61

		FC			
Locus	**Description**	*copt5* +Cu /WT +Cu	*copt5* -Cu /WT -Cu	WT -Cu /WT +Cu	*copt5* -Cu /*copt5* +Cu
AT3G21780	UDP-glucosyl transferase 71B6	-1.09	1.94	-1.64	1.28
AT1G71030	MYB-like 2	-1.04	1.34	-3.14	-2.25
AT5G67300	Myb domain protein r1	-1.03	1.29	-3.67	-2.76
AT3G02140	AFP2 (ABI five-binding protein 2) family protein	-1.03	1.46	-2.69	-1.79
AT2G23290	Myb domain protein 70	-1.01	-1.01	-3.58	-3.59
AT1G73500	MAP kinase kinase 9	1.03	1.29	-2.99	-2.40
AT4G37260	Myb domain protein 73	1.04	-1.03	-4.84	-5.19
AT5G59780	Myb domain protein 59	1.15	-1.03	-1.70	-2.01
AT3G50060	Myb domain protein 77	1.25	-1.67	-6.75	-14.15
AT5G07440	Glutamate dehydrogenase 2	1.35	2.62	-2.23	-1.14
AT5G64750	Integrase-type DNA-binding superfamily protein	1.62	1.82	-3.13	-2.78
	Response to ABA				
AT5G27420	Carbon/nitrogen insensitive 1	-1.47	-1.10	-3.36	-2.51
AT5G62470	Myb domain protein 96	-1.38	-1.23	-2.59	-2.30
AT1G18570	Myb domain protein 51	-1.34	1.26	-3.34	-1.98
AT5G37770	EF hand calcium-binding protein family	-1.32	-1.64	-2.25	-2.80
AT3G57530	Calcium-dependent protein kinase 32	-1.23	-1.02	-3.12	-2.57
AT3G14050	RELA/SPOT homolog 2	-1.23	1.84	-1.89	1.20
AT3G45640	Mitogen-activated protein kinase 3	-1.20	1.21	-2.50	-1.73
AT4G34390	Extra-large GTP-binding protein 2	-1.20	-1.03	-1.81	-1.56
AT4G09570	Calcium-dependent protein kinase 4	-1.15	1.09	-1.67	-1.33
AT3G02850	STELAR K+ outward rectifier	-1.14	-1.22	-1.81	-1.94
AT5G67300	Myb domain protein r1	-1.14	-1.01	-2.94	-2.61
AT3G20310	Ethylene response factor 7	-1.13	-1.38	-2.53	-3.09
AT3G21780	UDP-glucosyl transferase 71B6	-1.09	1.94	-1.64	1.28
AT1G71030	MYB-like 2	-1.04	1.34	-3.14	-2.25
AT5G67300	Myb domain protein r1	-1.03	1.29	-3.67	-2.76
AT3G02140	AFP2 (ABI five-binding protein 2) family protein	-1.03	1.46	-2.69	-1.79
AT4G18010	Myo-inositol polyphosphate 5-phosphatase 2	1.01	1.66	-2.63	-1.60
AT4G37260	Myb domain protein 73	1.04	-1.03	-4.84	-5.19
AT5G01810	CBL-interacting protein kinase 15	1.06	1.27	-2.19	-1.82
AT4G27410	NAC (No Apical Meristem) domain transcriptional Regulator superfamily protein	1.08	1.56	-5.82	-4.03
AT3G50060	Myb domain protein 77	1.25	-1.67	-6.75	-14.15
AT5G64750	Integrase-type DNA-binding superfamily protein	1.62	1.82	-3.13	-2.78

FC

Locus	Description	*copt5* +Cu /WT +Cu	*copt5* -Cu /WT -Cu	WT -Cu /WT +Cu	*copt5* -Cu /*copt5* +Cu
	Response to brassinosteroid				
AT2G44080	ARGOS-like	-1.16	3.20	-2.14	1.74
AT4G08950	Phosphate-responsive 1 family protein	-1.09	1.05	-7.08	-6.21
AT5G57560	Xyloglucan endotransglucosylase/hydrolase family protein	-1.05	-1.27	-18.84	-22.89
AT5G65430	General regulatory factor 8	1.11	1.12	-1.95	-1.92
AT1G13260	Related to ABI3/VP1 1	1.13	1.17	-4.67	-4.53
AT4G08950	Phosphate-responsive 1 family protein	1.17	1.16	-6.03	-6.08
AT5G54380	Protein kinase family protein	1.22	-1.23	-1.68	-2.53
	Response to ethylene				
AT1G68840	Related to ABI3/VP1 2	-1.12	1.89	-5.14	-2.44
AT3G23240	Ethylene response factor 1	1.01	2.06	-3.10	-1.53
AT1G70560	Tryptophan aminotransferase of Arabidopsis 1	1.03	1.62	1.26	1.99
AT1G21910	Integrase-type DNA-binding superfamily protein	1.05	1.81	-8.60	-4.97
AT1G25560	AP2/B3 transcription factor family protein	1.07	2.06	-4.00	-2.06
AT1G43160	Related to AP2 6	1.08	3.04	-5.00	-1.77
AT4G06746	Related to AP2 9	1.08	2.11	-1.38	1.41
AT5G61590	Integrase-type DNA-binding superfamily protein	1.08	1.50	-2.94	-2.12
AT1G79700	Integrase-type DNA-binding superfamily protein	1.14	1.80	-2.64	-1.67
AT3G25730	Ethylene response DNA binding factor 3	1.15	2.06	-1.73	1.04
AT5G13330	Related to AP2 6l	1.18	2.54	-1.31	1.64
AT3G23150	Signal transduction histidine kinase, hybrid-type, ethylene Sensor	1.19	2.47	-1.26	1.63
AT2G40940	Ethylene response sensor 1	1.21	1.61	-1.22	1.09
AT3G23150	Signal transduction histidine kinase, hybrid-type, ethylene Sensor	1.22	2.88	-1.45	1.63
AT5G25190	Integrase-type DNA-binding superfamily protein	1.23	2.50	-4.01	-1.97
AT1G68840	Related to ABI3/VP1 2	1.27	2.10	-4.15	-2.50
AT5G25350	EIN3-binding F box protein 2	1.29	1.82	-1.17	1.21
AT5G25350	EIN3-binding F box protein 2	1.34	1.90	-1.16	1.22
AT1G36060	Integrase-type DNA-binding superfamily protein	1.38	2.38	-2.29	-1.32
AT2G47520	Integrase-type DNA-binding superfamily protein	1.45	3.33	1.62	3.71
AT1G04310	Ethylene response sensor 2	1.55	1.98	-1.16	1.10
AT5G64750	Integrase-type DNA-binding superfamily protein	1.62	1.82	-3.13	-2.78
	Regulation of ethylene activation signalling pathway				
AT2G40940	Ethylene response sensor 1	1.21	1.61	-1.22	1.09
AT3G23150	Signal transduction histidine kinase, hybrid-type, ethylene Sensor	1.22	2.88	-1.45	1.63
AT5G25350	EIN3-binding F box protein 2	1.34	1.90	-1.16	1.22

| | | *FC* | | | |
Locus	Description	*copt5* +Cu /WT +Cu	*copt5* -Cu /WT -Cu	WT -Cu /WT +Cu	*copt5* -Cu /*copt5* +Cu
AT1G04310	Ethylene response sensor 2	1.55	1.98	-1.16	1.10
	Ethylene binding				
AT2G40940	Ethylene response sensor 1	1.21	1.61	-1.22	1.09
AT3G23150	Signal transduction histidine kinase, hybrid-type, ethylene sensor	1.22	2.88	-1.45	1.63
AT1G04310	Ethylene response sensor 2	1.55	1.98	-1.16	1.10
	Circadian rhythm				
AT4G25100	Fe superoxide dismutase 1	-1.15	-1.40	17.42	14.21
AT5G60100	Pseudo-response regulator 3	-1.06	-1.24	1.58	1.36
AT1G22770	Gigantea protein (GI)	1.01	1.02	2.08	2.11
AT5G24470	Pseudo-response regulator 5	1.15	1.16	1.52	1.53
AT4G18020	CheY-like two-component responsive regulator family protein	1.20	1.07	1.53	1.38
AT2G21660	cold, circadian rhythm, and rna binding 2	2.24	1.19	2.43	1.29
	Transition ion metal transport				
AT1G62280	SLAC1 homologue 1	-1.31	1.12	1.55	2.28
AT1G55910	Zinc transporter 11 precursor	-1.20	1.18	1.45	2.06
AT5G67330	natural resistance associated macrophage protein 4	-1.14	1.86	1.27	2.69
AT4G16370	oligopeptide transporter	-1.13	2.00	1.26	2.83
AT1G26230	TCP-1/cpn60 chaperonin family protein	-1.08	-1.04	1.46	1.51
AT3G56240	copper chaperone	-1.08	1.25	2.84	3.84
AT1G55910	zinc transporter 11 precursor	-1.07	1.11	1.44	1.70
AT3G46900	copper transporter 2	-1.06	1.08	7.66	8.76
AT3G46900	copper transporter 2	-1.05	1.12	3.27	3.85
AT2G32390	glutamate receptor 3.5	-1.04	1.28	1.44	1.94
AT4G30110	heavy metal atpase 2	1.05	1.35	2.16	2.77
AT3G51860	cation exchanger 3	1.05	1.51	1.46	2.10
AT5G59030	copper transporter 1	1.06	1.36	1.25	1.60
AT5G24380	YELLOW STRIPE like 2	1.13	1.23	7.97	8.71
AT5G53550	YELLOW STRIPE like 3	1.14	1.37	2.09	2.52
	Lipid binding				
AT4G23600	Tyrosine transaminase family protein	-2.98	-2.14	1.26	1.76
AT4G23600	Tyrosine transaminase family protein	-2.85	-2.60	1.41	1.54
AT2G37870	Bifunctional inhibitor/lipid-transfer protein/seed storage 2S albumin superfamily protein	-1.50	2.30	1.62	5.58

FC

Locus	Description	*copt5* +Cu /WT +Cu	*copt5* -Cu /WT -Cu	WT -Cu /WT +Cu	*copt5* -Cu /*copt5* +Cu
AT2G27550	centroradialis	-1.43	1.07	1.81	2.77
AT4G33550	Bifunctional inhibitor/lipid-transfer protein/seed storage 2S albumin superfamily protein	-1.41	1.24	1.28	2.24
AT5G01870	Bifunctional inhibitor/lipid-transfer protein/seed storage 2S albumin superfamily protein	-1.35	1.21	1.51	2.47
AT5G59320	lipid transfer protein 3	-1.26	1.28	3.11	5.02
AT3G08860	PYRIMIDINE 4	1.00	1.32	2.52	3.34
AT5G19550	aspartate aminotransferase 2	1.01	1.46	1.09	1.57
AT4G33010	glycine decarboxylase P-protein 1	1.02	1.13	1.50	1.66
AT1G70560	tryptophan aminotransferase of Arabidopsis 1	1.03	1.62	1.26	1.99
AT3G46970	alpha-glucan phosphorylase 2	1.09	1.10	2.22	2.24
AT3G05630	phospholipase D P2	1.55	1.84	1.96	2.32
AT3G22120	cell wall-plasma membrane linker protein	1.63	2.16	1.28	1.70
AT5G57240	OSBP(oxysterol binding protein)-related protein 4C	1.69	3.87	1.39	3.17
AT3G22120	cell wall-plasma membrane linker protein	1.99	1.90	1.30	1.24
AT4G12490	Bifunctional inhibitor/lipid-transfer protein/seed storage 2S albumin superfamily protein	3.27	6.32	39.68	76.71
AT4G22470	protease inhibitor/seed storage/lipid transfer protein (LTP) family protein	4.23	2.97	2.65	1.86

PUBLICATIONS

The results obtained in the present thesis, have been published in several articles during the research period under the following references:

- **Carrió-Seguí A**, Garcia-Molina A, Sanz A and Peñarrubia L, "Defective copper transport in the *copt5* mutant affects cadmium tolerance" Plant Cell Physiol. 2015 Mar; 56(3): 442–454. DOI: 10.1093/pcp/pcu180. (IF=4.931)

- Peñarrubia L, Romero P, **Carrió-Seguí A**, Andrés-Bordería A, Moreno M and Sanz A, "Temporal aspects of copper homeostasis and its crosstalk with hormones" Front Plant Sci. 2015 Apr 17; 6:255. DOI: 10.3389/fpls.2015.00255. (IF=3.9)

- **Carrió-Seguí A***, Romero P*, Sanz A and Peñarrubia L, "Interaction between ABA signaling and copper homeostasis in *Arabidopsis thaliana*" Plant Cell Physiol. 2016 Jul; 57(7):1568-1582. DOI: 10.1093/pcp/pcw087 (IF=4.319)
  *These authors contributed equally to this work.

- **Carrió-Seguí A**, Romero P, Curie C, Mari S and Peñarrubia L, "The vacuolar copper transporter COPT5 participates in iron deficiency signaling in *Arabidopsis*", in draft.

REFERENCES

Abdel-Ghany, S.E., Burkhead, J.L., Gogolin, K.A., Andrés-Colás, N., Bodecker, J.R., Puig, S., *et al.* (2005a) AtCCS is a functional homolog of the yeast copper chaperone Ccs1/Lys7. *FEBS Lett* 579: 2307–2312.

Abdel-Ghany, S.E., Müller-Moulé, P., Niyogi, K.K., Pilon, M. and Shikanai, T. (2005b) Two P-type ATPases are required for copper delivery in *Arabidopsis thaliana* chloroplass. *Plant Cell* 17: 1233–1251.

Abdel-Ghany, S.E. and Pilon, M. (2008) MicroRNA-mediated systemic down-regulation of copper protein expression in response to low copper availability in *Arabidopsis*. *J Biol Chem* 283: 15932–15945.

Abreu, I.A. and Cabelli, D.E. (2010) Superoxide dismutases-a review of the metal-associated mechanistic variations. *Biochim Biophys Acta - Proteins Proteomics* 1804: 263–274.

Van Aken, O., Zhang, B., Law, S., Narsai, R. and Whelan, J. (2013) AtWRKY40 and AtWRKY63 modulate the expression of stress-responsive nuclear genes encoding mitochondrial and chloroplast proteins. *Plant Physiol* 162: 254–271.

Al-Shahrour, F., Díaz-Uriarte, R. and Dopazo, J. (2004) FatiGO: A web tool for finding significant associations of Gene Ontology terms with groups of genes. *Bioinformatics* 20: 578–580.

Alonso, J.M., Hirayama, T., Roman, G., Nourizadeh, S. and Ecker, J.R. (1999) EIN2, a bifunctional transducer of ethylene and stress responses in *Arabidopsis*. *Science* 284: 2148–2152.

Andreini, C., Bertini, I. and Rosato, A. (2004) A hint to search for metalloproteins in gene banks. *Bioinformatics* 20: 1373–1380.

Andrés-Colás, N., Perea-García, A., Mayo de Andrés, S., García-Molina, A., Dorcey, E., Rodríguez-Navarro, S., *et al.* (2013) Comparison of global responses to mild deficiency and excess copper levels in Arabidopsis seedlings. *Metallomics* 5: 1234–1246.

Andrés-Colás, N., Perea-García, A., Puig, S. and Peñarrubia, L. (2010) Deregulated copper transport affects *Arabidopsis* development especially in the absence of environmental cycles. *Plant Physiol* 153: 170–184.

Andrés-Colás, N., Sancenón, V., Rodríguez-Navarro, S., Mayo, S., Thiele, D.J., Ecker, J.R., *et al.* (2006) The *Arabidopsis* heavy metal P-type ATPase HMA5 interacts with metallochaperones and functions in copper detoxification of roots. *Plant J* 45: 225–236.

Andrews, N.C. (2001) Mining copper transport genes. *Proc Natl Acad Sci U S A* 98: 6543–6545.

Andriankaja, M.E., Danisman, S., Mignolet-Spruyt, L.F., Claeys, H., Kochanke, I., Vermeersch, M., *et al.* (2014) Transcriptional coordination between leaf cell differentiation and chloroplast development established by TCP20 and the subgroup Ib bHLH transcription factors. *Plant Mol Biol* 85: 233–245.

Arnon, D.I. (1949) Copper enzymes in isolated chloroplasts. Polyphenoloxidase in *Beta vulgaris*. *Plant Physiol* 24: 1–15.

Arteca, R.N. and Arteca, J.M. (2007) Heavy-metal-induced ethylene production in *Arabidopsis* thaliana. *J Plant Physiol* 164: 1480–1488.

Asada, K. (2006) Production and scavenging of reactive oxygen species in chloroplasts and their functions. *Plant Physiol* 141: 391–396.

Attallah, C. V., Welchen, E., Martin, A.P., Spinelli, S. V., Bonnard, G., Palatnik, J.F., *et al.* (2011) Plants contain two SCO proteins that are differentially involved in cytochrome c oxidase function and copper and redox homeostasis. *J Exp Bot* 62: 4281–4294.

Attallah, C. V., Welchen, E., Pujol, C., Bonnard, G. and Gonzalez, D.H. (2007) Characterization of *Arabidopsis thaliana* genes encoding functional homologues of the yeast metal chaperone Cox19p, involved in cytochrome c oxidase biogenesis. *Plant Mol Biol* 65: 343–355.

Balandin, T. and Castresana, C. (2002) AtCOX17, an *Arabidopsis homolog* of the yeast copper chaperone COX17. *Plant Physiol* 129: 1852–1857.

Barrero, J.M., Rodríguez, P.L., Quesada, V., Piqueras, P., Ponce, M.R. and Micol, J.L. (2006) Both abscisic acid (ABA)-dependent and ABA-independent pathways govern the induction of NCED3, AAO3 and ABA1 in response to salt stress. *Plant, Cell Environ* 29: 2000–2008.

Bashir, K., Rasheed, S., Kobayashi, T., Seki, M. and Nishizawa, N.K. (2016) Regulating subcellular metal homeostasis: the key to crop improvement. *Front Plant Sci* 7: 1–9.

Beauchamp, C. and Fridovich, I. (1971) Superoxide dismutase: Improved assays and an assay applicable to acrylamide gels. *Anal Biochem* 44: 276–287.

Bernal, M., Casero, D., Singh, V., Wilson, G.T., Grande, A., Yang, H., *et al.* (2012) Transcriptome sequencing identifies SPL7-regulated copper acquisition genes FRO4/FRO5 and the copper dependence of iron homeostasis in *Arabidopsis*. *Plant Cell* 24: 738–761.

Billard, V., Ourry, A., Maillard, A., Garnica, M., Coquet, L., Jouenne, T., *et al.* (2014) Copper-deficiency in *Brassica napus* induces copper remobilization, molybdenum accumulation and modification of the expression of chloroplastic proteins. *PLoS One* 9.

Binder, B.M., Rodríguez, F.I. and Bleecker, A.B. (2010) The copper transporter RAN1 is essential for biogenesis of ethylene receptors in *Arabidopsis*. *J Biol Chem* 285: 37263–37270.

Binder, B.M., Rodriguez, F.I., Bleecker, A.B. and Patterson, S.E. (2007) The effects of Group 11 transition metals, including gold, on ethylene binding to the ETR1 receptor and growth of *Arabidopsis thaliana*. *FEBS Lett* 581: 5105–5109.

Bisson, M.M.A. and Groth, G. (2014) Ethylene in Plants. In *Ethylene in Plants*. pp. 223–244 Springer, London (UK).

Blaby-Haas, C.E. and Merchant, S.S. (2014) Lysosome-related organelles as mediators of metal homeostasis. *J Biol Chem* 289: 28129–28136.

Blaby-Haas, C.E., Padilla-Benavides, T., Stübe, R., Argüello, J.M. and Merchant, S.S. (2014) Evolution of a plant-specific copper chaperone family for chloroplast copper homeostasis. *Proc Natl Acad Sci U S A* 111: 5480–5487.

Boursiac, Y., Léran, S., Corratgé-Faillie, C., Gojon, A., Krouk, G. and Lacombe, B. (2013) ABA transport and transporters. *Trends Plant Sci* 18: 325–333.

Bradford, M.M. (1976) A rapid and sensitive method for the quantitation of microgram quantities of protein utilizing the principle of protein-dye binding. *Anal Biochem* 72: 248–254.

Brumbarova, T., Bauer, P. and Ivanov, R. (2015) Molecular mechanisms governing *Arabidopsis* iron uptake. *Trends Plant Sci* 20: 124–133.

Bull, P.C. and Cox, D.W. (1994) Wilson disease and Menkes disease: new handles on heavy-metal transport. *Trends Genet* 10: 246–252.

Burkhead, J.L., Gogolin Reynolds, K.A., Abdel-Ghany, S.E., Cohu, C.M. and Pilon, M. (2009) Copper homeostasis. *New Phytol* 182: 799–816.

Bürstenbinder, K. and Sauter, M. (2012) Early events in the ethylene biosynthetic pathway - regulation of the pools of methionine and s-adenosylmethionine. In *The Plant Hormone Ethylene*. pp. 19–52 Wiley, Oxford, UK.

Chen, C.-C., Chen, Y.-Y., Tang, I.-C., Liang, H.-M., Lai, C.-C., Chiou, J.-M., *et al.* (2011a) *Arabidopsis* SUMO E3 ligase SIZ1 is involved in excess copper tolerance. *Plant Physiol* 156: 2225–2234.

Chen, C.-C., Chen, Y.-Y. and Yeh, K.-C. (2011b) Effect of Cu content on the activity of Cu/ZnSOD1 in the Arabidopsis SUMO E3 ligase siz1 mutant. *Plant Signal Behav* 6: 1428–1430.

Chen, C., Twito, S. and Miller, G. (2014) New cross talk between ROS, ABA and auxin controlling seed maturation and germination unraveled in APX6 deficient *Arabidopsis* seeds. *Plant Signal Behav* 9: e976489.

Chen, H., Lai, Z., Shi, J., Xiao, Y., Chen, Z. and Xu, X. (2010) Roles of arabidopsis WRKY18, WRKY40 and WRKY60 transcription factors in plant responses to abscisic acid and abiotic stress. *BMC Plant Biol* 10: 281.

Chen, H., Zhang, J., Neff, M.M., Hong, S.-W., Zhang, H., Deng, X.-W., *et al.* (2008) Integration of light and abscisic acid signaling during seed germination and early seedling development. *Proc Natl Acad Sci U S A* 105: 4495–4500.

Cheng, W.-H., Endo, A. and Zhou, L. (2002) A unique short-chain dehydrogenase/reductase in *Arabidopsis* glucose signalling and abscisic acid biosynthesis and functions. *Plant Cell* 14: 2723–2743.

Clemens, S. (2006) Toxic metal accumulation, responses to exposure and mechanisms of tolerance in plants. *Biochimie* 88: 1707–1719.

Clemens, S., Aarts, M.G.M., Thomine, S. and Verbruggen, N. (2013) Plant science: The key to preventing slow cadmium poisoning. *Trends Plant Sci* 18: 92–99.

Cobbett, C. and Goldsbrough, P. (2002) Phytochelatins and metallothioneins: roles in heavy metal detoxification and homeostasis. *Annu Rev Plant Biol* 53: 159–182.

Cohu, C.M. and Pilon, M. (2007) Regulation of superoxide dismutase expression by copper

availability. *Physiol Plant* 129: 747–755.

Colangelo, E.P. and Guerinot, M. Lou (2004) The essential basic helix-loop-helix protein FIT1 is required for the iron deficiency response. *Plant Cell* 16: 3400–3412.

Colvin, R. a, Holmes, W.R., Fontaine, C.P. and Maret, W. (2010) Cytosolic zinc buffering and muffling: their role in intracellular zinc homeostasis. *Metallomics* 2: 306–317.

Connolly, E.L., Campbell, N.H., Grotz, N., Prichard, C.L. and Guerinot, M. Lou (2003) Overexpression of the FRO2 ferric chelate reductase confers tolerance to growth on low ron and uncovers posttranscriptional control. *Plant Physiol* 133: 1102–1110.

Crichton, R.R. and Pierre, J.L. (2001) Old iron, young copper: from Mars to Venus. *BioMetals* 14: 99–112.

Curie, C. and Briat, J.-F. (2003) Iron transport and signalign in plants. *Annu Rev Plant Biol* 54: 183–206.

Curie, C., Cassin, G., Couch, D., Divol, F., Higuchi, K., Le Jean, M., *et al.* (2009) Metal movement within the plant: contribution of nicotianamine and yellow stripe 1-like transporters. *Ann Bot* 103: 1–11.

Cutler, S.R., Rodríguez, P.L., Finkelstein, R.R. and Abrams, S.R. (2010) Abscisic acid: emergence of a core signaling network. *Annu Rev Plant Biol* 61: 651–679.

Cuypers, A., Karen, S., Jos, R., Kelly, O., Els, K., Tony, R., *et al.* (2011) The cellular redox state as a modulator in cadmium and copper responses in *Arabidopsis thaliana* seedlings. *J Plant Physiol* 168: 309–316.

Cuypers, A., Plusquin, M., Remans, T., Jozefczak, M., Keunen, E., Gielen, H., *et al.* (2010) Cadmium stress: An oxidative challenge. *BioMetals* 23: 927–940.

Dancis, A., Haile, D., Yuan, D. and Klausner, R. (1994a) The *Saccharomyces cerevisiae* copper transpor protein (Ctr1p). *J Biol Chem* 269: 25660–25667.

Dancis, A., Yuan, D.S., Haile, D., Askwith, C., Eide, D., Moehle, C., *et al.* (1994b) Molecular characterization of a copper transport protein in *S. cerevisiae*: An unexpected role for copper in iron transport. *Cell* 76: 393–402.

Darbani, B., Briat, J.-F., Holm, P.B., Husted, S., Noeparvar, S. and Borg, S. (2013) Dissecting plant iron homeostasis under short and long-term iron fluctuations. *Biotechnol Adv* 31: 1292–1307.

Davies, N.T. and Mertz, W. (1987) Trace elements in human and animal nutrition, 5th ed. Academic Press, San Diego, California.

Davin, L.B. and Lewis, N.G. (2005) Lignin primary structures and dirigent sites. *Curr Opin Biotechnol* 16: 407–415.

Deinlein, U., Weber, M., Schmidt, H., Rensch, S., Trampczynska, A., Hansen, T.H., *et al.* (2012) Elevated nicotinamine levels in *Arabidopsis halleri* roots play a key role in zinc hyperaccumulation. *Plant Cell* 24: 708–723.

Dobermann, A. and Fairhurst, T. (2000) Rice: nutrient disorders & nutrient management p. 191 Potash & Phosphate Institute (PPI), Potash & Phosphate Institue of Canada (PPIC) and International Rice Research Institute (IRRI), Los Banos (Philipines).

Edgar, R., Domrachev, M. and Lash, A.E. (2002) Gene Expression Omnibus: NCBI gene expression and hybridization array data repository. *Nucleic Acids Res* 30: 207–210.

Elbaz-Alon, Y., Rosenfeld-Gur, E., Shinder, V., Futerman, A.H., Geiger, T. and Schuldiner, M. (2014) A dynamic interface between vacuoles and mitochondria in yeast. *Dev Cell* 30: 95–102.

Ellis, M.J., Grossmann, J.G., Eady, R.R. and Hasnain, S.S. (2007) Genomic analysis reveals widespread occurrence of new classes of copper nitrite reductases. *J Biol Inorg Chem* 12: 1119–1127.

Endo, A., Okamoto, M. and Koshiba, T. (2014) Abscisic acid: metabolism, transport and signaling. In Edited by Zhang, D.-P. pp. 21–46 Springer, London.

Engle, T.E. (2011) Copper and lipid metabolism in beef cattle: A review. *J Anim Sci* 89: 591–596.

Eulgem, T., Rushton, P.J., Robatzek, S. and Somssich, I.E. (2000) The WRKY superfamily of plant transcription factors. *Trends Plant Sci* 5: 199–206.

Fargašová, A. (2001) Phytotoxic effects of Cs, Zn, Pb, Cu and Fe on Sinapis alba L. seedlings and their accumulation in roots and shoots. *Biol Plant* 44: 471–473.

Finkelstein, R. (2013) Abscisic Acid synthesis and response. *Arabidopsis Book* 11: e0166.

Foster, A.W., Osman, D. and Robinson, N.J. (2014) Metal preferences and metallation. *J Biol Chem* 289: 28095–28103.

Franchin, C., Fossati, T., Pasquini, E., Lingua, G., Castiglione, S., Torrigiani, P., *et al.* (2007) High concentrations of zinc and copper induce differential polyamine responses in micropropagated white poplar (*Populus alba*). *Physiol Plant* 130: 77–90.

Froschauer, E.M., Schweyen, R.J. and Wiesenberger, G. (2009) The yeast mitochondrial carrier proteins Mrs3p/Mrs4p mediate iron transport across the inner mitochondrial membrane. *Biochim Biophys Acta - Biomembr* 1788: 1044–1050.

Fujita, Y., Fujita, M., Shinozaki, K. and Yamaguchi-Shinozaki, K. (2011) ABA-mediated transcriptional regulation in response to osmotic stress in plants. *J Plant Res* 124: 509–525.

García-Molina, A., Andrés-Colás, N., Perea-García, A., Del Valle-Tascõn, S., Peñarrubia, L. and Puig, S. (2011) The intracellular *Arabidopsis* COPT5 transport protein is required for photosynthetic electron transport under severe copper deficiency. *Plant J* 65: 848–860.

García-Molina, A., Xing, S. and Huijser, P. (2014a) A conserved KIN17 curved DNA-binding domain protein assembles with SQUAMOSA PROMOTER-BINDING PROTEIN-LIKE7 to adapt *Arabidopsis* growth and development to limiting copper availability. *Plant Physiol* 164: 828–840.

García-Molina, A., Xing, S. and Huijser, P. (2014b) Functional characterisation of *Arabidopsis*

SPL7 conserved protein domains suggests novel regulatory mechanisms in the Cu deficiency response. *BMC Plant Biol* 14: 231.

Garcia, L., Welchen, E. and Gonzalez, D.H. (2014) Mitochondria and copper homeostasis in plants. *Mitochondrion* 19: 269–274.

Gayomba, S.R., Jung, H., Yan, J., Danku, J., Rutzke, M. a, Bernal, M., *et al.* (2013) The CTR/COPT-dependent copper uptake and SPL7-dependent copper deficiency responses are required for basal cadmium tolerance in *A. thaliana*. *Metallomics* 5: 1262–75.

Gilroy, S., Suzuki, N., Miller, G., Choi, W.G., Toyota, M., Devireddy, A.R., *et al.* (2014) A tidal wave of signals: Calcium and ROS at the forefront of rapid systemic signaling. *Trends Plant Sci* 19: 623–630.

Goldhaber, S.B. (2003) Trace element risk assessment: essentiality vs. toxicity. *Regul Toxicol Pharmacol* 38: 232–242.

González-Guzmán, M., Apostolova, N., Bellés, J.M., Barrero, J.M., Piqueras, P., Ponce, M.R., *et al.* (2002) The short-chain alcohol dehydrogenase ABA2 catalyzes the conversion of xanthoxin to abscisic aldehyde. *Plant Cell* 14: 1833–46.

Van Gossum, A. and Neve, J. (1998) Trace element deficiency and toxicity. *Curr Opin Clin Nutr Metab Care* 1: 499–507.

Gulec, S. and Collins, J.F. (2014) Molecular mediators governing iron-copper interactions. *Annu Rev Nutr* 34: 95–116.

Guzmán, P. and Ecker, J.R. (1990) Exploiting the triple response of *Arabidopsis* to identify ethylene-related mutants. *Society* 2: 513–523.

Halliwell, B. and Gutteridget, J.M.C. (1984) Oxygen toxicity, oxygen radicals, transition metals and disease. *Biochem J* 219: 1–14.

Hanikenne, M., Talke, I.N., Haydon, M.J., Lanz, C., Nolte, A., Motte, P., *et al.* (2008) Evolution of metal hyperaccumulation required cis-regulatory changes and triplication of HMA4. *Nature* 453: 391–395.

Haraguchi, H. (2004) Metallomics as integrated biometal science. *J Anal At Spectrom* 19: 5.

Harris, D. (1991) Copper transport: an overview. *Exp Biol Med* 196: 130–140.

Hartwig, A. (2001) Zinc finger proteins as potential targets for toxic metal ions: differential effects on structure and function. *Antioxid Redox Signal* 3: 804–813.

Hassett, R. and Kosman, D.J. (1995) Evidence for Cu(II) reduction as a component of copper uptake by Saccharomyces cerevisiae. *J Biol Chem* 270: 128–134.

Hawkesford, M.J. and Barraclough, P. (2011) The molecular and physiological basis of nutrient use efficiency in crops, 1rst Ed. ed. Wiley-Blackwell, Oxford (UK).

Haydon, M.J., Bell, L.J. and Webb, A.A.R. (2011) Interactions between plant circadian clocks and solute transport. *J Exp Bot* 62: 2333–2348.

Haydon, M.J., Hearn, T.J., Bell, L.J., Hannah, M.A. and Webb, A.A.R. (2013) Metabolic regulation of circadian clocks. *Semin Cell Dev Biol* 24: 414–421.

Heo, D.H., Baek, I.J., Kang, H.J., Kim, J.H., Chang, M., Kang, C.M., *et al.* (2012) Cd $^{2+}$ binds to Atx1 and affects the physical interaction between Atx1 and Ccc2 in *Saccharomyces cerevisiae*. *Biotechnol Lett* 34: 303–307.

Herbette, S., Taconnat, L., Hugouvieux, V., Piette, L., Magniette, M.L.M., Cuine, S., *et al.* (2006) Genome-wide transcriptome profiling of the early cadmium response of *Arabidopsis* roots and shoots. *Biochimie* 88: 1751–1765.

Hermans, C. and Verbruggen, N. (2005) Physiological characterization of Mg deficiency in *Arabidopsis thaliana*. *J Exp Bot* 56: 2153–2161.

Hirayama, T., Kieber, J.J., Hirayama, N., Kogan, M., Guzmán, P., Nourizadeh, S., *et al.* (1999) RESPONSIVE-TO-ANTAGONIST1, a Menkes/Wilson disease-related copper transporter, is required for ethylene signaling in *Arabidopsis*. *Cell* 97: 383–393.

Hoagland, D.R. and Arnon, D.I. (1950) The water-culture method for growing plants without soil. *Calif Agric Exp Stn Circ* 347: 1–32.

Hobo, T., Asada, M., Kowyama, Y. and Hattori, T. (1999) ACGT-containing abscisic acid response element (ABRE) and coupling element 3 (CE3) are functionally equivalent. *Plant J* 19: 679–689.

Hong-Hermesdorf, A., Miethke, M., Gallaher, S.D., Kropat, J., Dodani, S.C., Chan, J., *et al.* (2014) Sub-cellular metal imaging identifies dynamic sites of Cu accumulation in Chlamydomonas. *Nat Chem Biol* 10: 1034–1042.

Iqbal, N., Trivellini, A., Masood, A., Ferrante, A. and Khan, N.A. (2013) Current understanding on ethylene signaling in plants: the influence of nutrient availability. *Plant Physiol Biochem* 73: 128–138.

Jefferson, R.A., Kavanagh, T.A. and Bevan, M.W. (1987) GUS fusions: Beta-glucuronidase as a sensitive and versatile gene fusion marker in higher plants. *EMBO J* 6: 3901–7.

Jiang, C., Belfield, E.J., Cao, Y., Smith, J.A.C. and Harberd, N.P. (2013) An *Arabidopsis* soil-salinity-tolerance mutation confers ethylene-mediated enhancement of sodium/potassium homeostasis. *Plant Cell* 25: 3535–3552.

Jones, A.M., Xuan, Y., Xu, M., Wang, R.-S., Ho, C.-H., Lalonde, S., *et al.* (2014) Border control-a membrane-linked interactome of *Arabidopsis*. *Science* 344: 711–716.

Jouvin, D., Weiss, D.J., Mason, T.F.M., Bravin, M.N., Louvat, P., Zhao, F., *et al.* (2012) Stable isotopes of Cu and Zn in higher plants: evidence for Cu reduction at the root surface and two conceptual models for isotopic fractionation processes. *Environ Sci Technol* 46: 2652–2660.

Kazan, K. (2013) Auxin and the integration of environmental signals into plant root development. *Ann Bot* 112: 1655–1665.

Kende, H. (1993) Ethylene biosynthesis. *Annu Rev Plant Physiol Plant Mol Biol* 44: 283–307.

Keunen, E., Remans, T., Opdenakker, K., Jozefczak, M., Gielen, H., Guisez, Y., *et al.* (2013) A mutant of the *Arabidopsis thaliana* LIPOXYGENASE1 gene shows altered signalling and oxidative stress related responses after cadmium exposure. *Plant Physiol Biochem* 63: 272–280.

Keunen, E., Schellingen, K., Vangronsveld, J. and Cuypers, A. (2016) Ethylene and metal stress: Small molecule, big impact. *Front Plant Sci* 7: 23.

Kieselbach, T., Hagman, Å., Andersson, B. and Schröder, W.P. (1998) The thylakoid lumen of chloroplasts. Isolation and characterization. *J Biol Chem* 273: 6710–6716.

Kim, S.A., Punshon, T., Lanzirotti, A., Li, L., Alonso, J.M., Ecker, J.R., *et al.* (2006) Localization of iron in *Arabidopsis* seed requires the vacuolar membrane transporter VIT1. *Science* 314: 1295–8.

Kim, Y.-H., Khan, A.L., Kim, D.-H., Lee, S.-Y., Kim, K.-M., Waqas, M., *et al.* (2014) Silicon mitigates heavy metal stress by regulating P-type heavy metal ATPases, *Oryza sativa* low silicon genes, and endogenous phytohormones. *BMC Plant Biol* 14: 13.

Klaumann, S., Nickolaus, S.D., Fürst, S.H., Starck, S., Schneider, S., Ekkehard Neuhaus, H., *et al.* (2011) The tonoplast copper transporter COPT5 acts as an exporter and is required for interorgan allocation of copper in *Arabidopsis thaliana*. *New Phytol* 192: 393–404.

Klomp, A.E.M., Juijn, J.A., van der Gun, L.T.M., van den Berg, I.E.T., Berger, R. and Klomp, L.W.J. (2003) The N-terminus of the human copper transporter 1 (hCTR1) is localized extracellularly, and interacts with itself. *Biochem J* 370: 881–889.

Ko, G.Y.P., Shi, L. and Ko, M.L. (2009) Circadian regulation of ion channels and their functions. *J Neurochem* 110: 1150–1169.

Kobayashi, T., Nagasaka, S., Senoura, T., Itai, R.N., Nakanishi, H. and Nishizawa, N.K. (2013) Iron-binding haemerythrin RING ubiquitin ligases regulate plant iron responses and accumulation. *Nat Commun* 4: 2792–2804.

Kobayashi, T. and Nishizawa, N.K. (2012) Iron uptake, translocation, and regulation in higher plants. *Annu Rev Plant Biol* 63: 131–152.

Kobayashi, Y., Kuroda, K., Kimura, K., Southron-Francis, J., Furuzawa, A., Kimura, K., *et al.* (2008) Amino acid polymorphisms in strictly conserved domains of a P-type ATPase HMA5 are involved in the mechanism of copper tolerance variation in *Arabidopsis*. *Plant Physiol* 148: 969–980.

Kosman, D.J. (2010) Multicopper oxidases: A workshop on copper coordination chemistry, electron transfer, and metallophysiology. *J Biol Inorg Chem* 15: 15–28.

Krämer, U. (2010) Metal hyperaccumulation in plants. *Annu Rev Plant Biol* 61: 517–34.

Kuo, Y.M., Zhou, B., Cosco, D. and Gitschier, J. (2001) The copper transporter CTR1 provides an essential function in mammalian embryonic development. *Proc Natl Acad Sci U S A* 98: 6836–41.

Kuper, J., Llamas, A., Hecht, H.-J., Mendel, R.R. and Schwarz, G. (2004) Structure of the

molybdopterin-bound Cnx1G domain links molybdenum and copper metabolism. *Nature* 430: 803–6.

Küpper, H., Šetlík, I., Spiller, M., Küpper, F.C. and Prášil, O. (2002) Heavy metal-induced inhibition of photosynthesis: Targets of in vivo heavy metal chlorophyll formation. *J Phycol* 38: 429–441.

Kwak, J.M., Mori, I.C., Pei, Z.M., Leonhard, N., Angel Torres, M., Dangl, J.L., *et al.* (2003) NADPH oxidase *AtrbohD* and *AtrbohF* genes function in ROS-dependent ABA signaling in *Arabidopsis*. *EMBO J* 22: 2623–2633.

Lanquar, V., Lelièvre, F., Bolte, S., Hamès, C., Alcon, C., Neumann, D., *et al.* (2005) Mobilization of vacuolar iron by AtNRAMP3 and AtNRAMP4 is essential for seed germination on low iron. *EMBO J* 24: 4041–4051.

Lanquar, V., Ramos, M.S., Lelièvre, F., Barbier-Brygoo, H., Krieger-Liszkay, A., Krämer, U., *et al.* (2010) Export of vacuolar manganese by AtNRAMP3 and AtNRAMP4 is required for optimal photosynthesis and growth under manganese deficiency. *Plant Physiol* 152: 1986–99.

Lau, O.S. and Deng, X.W. (2010) Plant hormone signaling lightens up: integrators of light and hormones. *Curr Opin Plant Biol* 13: 571–577.

Lee, J., Prohaska, J.R. and Thiele, D.J. (2001) Essential role for mammalian copper transporter Ctr1 in copper homeostasis and embryonic development. *Proc Natl Acad Sci* 98: 6842–6847.

Lei, G.J., Zhu, X.F., Wang, Z.W., Dong, F., Dong, N.Y. and Zheng, S.J. (2014) Abscisic acid alleviates iron deficiency by promoting root iron reutilization and transport from root to shoot in *Arabidopsis*. *Plant, Cell Environ* 37: 852–863.

Lequeux, H., Hermans, C., Lutts, S. and Verbruggen, N. (2010) Response to copper excess in *Arabidopsis thaliana*: impact on the root system architecture, hormone distribution, lignin accumulation and mineral profile. *Plant Physiol Biochem* 48: 673–682.

Li, L. and Kaplan, J. (2004) A mitochondrial-vacuolar signaling pathway in yeast that affects iron and copper metabolism. *J Biol Chem* 279: 33653–33661.

Li, L., Murdock, G., Bagley, D., Jia, X., Ward, D.M. and Kaplan, J. (2010) Genetic dissection of a mitochondria-vacuole signaling pathway in yeast reveals a link between chronic oxidative stress and vacuolar iron transport. *J Biol Chem* 285: 10232–10242.

Lin, Y.F. and Aarts, M.G.M. (2012) The molecular mechanism of zinc and cadmium stress response in plants. *Cell Mol Life Sci* 69: 3187–3206.

Lingam, S., Mohrbacher, J., Brumbarova, T., Potuschak, T., Fink-Straube, C., Blondet, E., *et al.* (2011) Interaction between the bHLH transcription factor FIT and ETHYLENE INSENSITIVE3/ETHYLENE INSENSITIVE3-LIKE1 reveals molecular linkage between the regulation of iron acquisition and ethylene signaling in *Arabidopsis*. *Plant Cell* 23: 1815–1829.

Lippard, S.J. and Berg, J.M. (1994) Principles of bioinorganic chemistry. University Science Books,

New York, USA.

Livak, K.J. and Schmittgen, T.D. (2001) Analysis of relative gene expression data using real-time quantitative PCR and. *Methods* 25: 402–408.

Llamas, A., Ullrich, C.I. and Sanz, A. (2000) Cd^{2+} effects on transmembrane electrical potential difference, respiration and membrane permeability of rice (*Oryza sativa* L.) roots. *Plant Soil* 219: 21–28.

Lloyd, R. V, Hanna, P.M. and Mason, R.P. (1997) The origin of the hydroxyl radical oxygen in the Fenton reaction. *Free Radic Biol Med* 22: 885–888.

Loladze, I. (2014) Hidden shift of the ionome of plants exposed to elevated CO_2 depletes minerals at the base of human nutrition. *Elife* 2014: 1–29.

López-Bucio, J., Cruz-Ramírez, A. and Herrera-Estrella, L. (2003) The role of nutrient availability in regulating root architecture. *Curr Opin Plant Biol* 6: 280–287.

López-Molina, L. and Chua, N. (2000) A null mutation in a bZIP factor confers ABA-insensitivity in *Arabidopsis thaliana*. *Plant Cell Physiol* 41: 541–547.

Lu, W.P. and Kirkham, M.B. (1991) Genotypic tolerance to metals as indicated by ethylene production. *Water Air Soil Pollut* 605–615.

Lucena, C., Romera, F.J., García, M.J., Alcántara, E. and Pérez-Vicente, R. (2015) Ethylene participates in the regulation of Fe deficiency responses in strategy I plants and in rice. *Front Plant Sci* 6: 1056.

Lux, A., Martinka, M., Vaculík, M. and White, P.J. (2011) Root responses to cadmium in the rhizosphere: a review. *J Exp Bot* 62: 21–37.

Maksymiec, W., Wójcik, M. and Krupa, Z. (2007) Variation in oxidative stress and photochemical activity in *Arabidopsis thaliana* leaves subjected to cadmium and excess copper in the presence or absence of jasmonate and ascorbate. *Chemosphere* 66: 421–427.

Marcotte, W.R., Russell, S.H. and Quatrano, R.S. (1989) Abscisic acid-responsive sequences from the em gene of wheat. *Plant Cell* 1: 969–976.

Marschner, P. (2011) The role of the rhizosphere in nutrient use efficiency in crops. In *The Molecular and Physiological Basis of Nutrient Use Efficiency in Crops*. pp. 47–63 Wiley-Blackwell, Harpenden, Hertfordshire, UK.

Marschner, P. (2012) Mineral nutrition of higher plants, 3rd ed. Elsevier Academic Press, Amsterdam (Netherlands).

Martínez-Pastor, M.T., de Llanos, R., Romero, A.M. and Puig, S. (2013) Post-transcriptional regulation of iron homeostasis in *Saccharomyces cerevisiae*. *Int J Mol Sci* 14: 15785–15809.

Martínez-Peñalver, A., Graña, E., Reigosa, M.J. and Sánchez-Moreiras, A.M. (2012) The early response of *Arabidopsis thaliana* to cadmium- and copper-induced stress. *Environ Exp Bot* 78: 1–9.

Maruyama-Nakashita, A., Nakamura, Y., Watanabe-Takahashi, A., Inoue, E., Yamaya, T. and Takahashi, H. (2005) Identification of a novel cis-acting element conferring sulfur deficiency response in *Arabidopsis* roots. *Plant J* 42: 305–314.

Mary, V., Schnell Ramos, M., Gillet, C., Socha, A.L., Giraudat, J., Agorio, A., *et al.* (2015) Bypassing iron storage in endodermal vacuoles rescues the iron mobilization defect in the natural resistance associated-macrophage protein3natural resistance associated-macrophage protein4 double mutant. *Plant Physiol* 169: 748–759.

Masood, A., Iqbal, N. and Khan, N.A. (2012) Role of ethylene in alleviation of cadmium-induced photosynthetic capacity inhibition by sulphur in mustard. *Plant, Cell Environ* 35: 524–533.

Mayer, A.M. (2006) Polyphenol oxidases in plants and fungi: going places? A review. *Phytochemistry* 67: 2318–2331.

Mendel, R.R. and Kruse, T. (2012) Cell biology of molybdenum in plants and humans. *Biochim Biophys Acta - Mol Cell Res* 1823: 1568–1579.

Mertens, J., Vangronsveld, J., Van Der Straeten, D. and Van Poucke, M. (1999) Effects of copper and zinc on the ethylene production of *Arabidopsis thaliana*. In *Biology and Biotechnology of the Plant Hormone Ethylene II*. Edited by Kanellis, A.K., Chang, C., Klee, H., Bleecker, A.B., Pech, J.C., and Grierson, D. pp. 333–338 Springer Netherlands, Dordrecht.

Mertz, W. (1998) Review of the scientific basis for establishing the essentiality of trace elements. *Biol Trace Elem Res* 66: 185–191.

Mira, H., Martínez-García, F. and Peñarrubia, L. (2001) Evidence for the plant-specific intercellular transport of the *Arabidopsis* copper chaperone CCH. *Plant J* 25: 521–528.

Molins, H., Michelet, L., Lanquar, V., Agorio, A., Giraudat, J., Roach, T., *et al.* (2013) Mutants impaired in vacuolar metal mobilization identify chloroplasts as a target for cadmium hypersensitivity in *Arabidopsis thaliana*. *Plant, Cell Environ* 36: 804–817.

Murashige, T. and Skoog, F. (1962) A revised medium for rapid growth and bioassays with tobacco tissue cultures. *Physiol Plant* 15: 473–497.

Myers, S.S., Zanobetti, A., Kloog, I., Huybers, P., Leakey, A.D.B., Bloom, A.J., *et al.* (2014) Increasing CO2 threatens human nutrition. *Nature* 510: 139–42.

Nakano, T., Suzuki, K., Ohtsuki, N., Tsujimoto, Y., Fujimura, T. and Shinshi, H. (2006) Identification of genes of the plant-specific transcription-factor families cooperatively regulated by ethylene and jasmonate in *Arabidopsis thaliana*. *J Plant Res* 119: 407–413.

Nakashima, K., Fujita, Y., Katsura, K., Maruyama, K., Narusaka, Y., Seki, M., *et al.* (2006) Transcriptional regulation of ABI3- and ABA-responsive genes including RD29B and RD29A in seeds, germinating embryos, and seedlings of *Arabidopsis*. *Plant Mol Biol* 60: 51–68.

Nakashima, K., Yamaguchi-Shinozaki, K. and Shinozaki, K. (2014) The transcriptional regulatory network in the drought response and its crosstalk in abiotic stress responses including drought, cold, and heat. *Front Plant Sci* 5: 170.

Nambara, E. and Marion-Poll, A. (2005) Abscisic acid biosynthesis and catabolism. *Annu Rev*

Plant Biol 56: 165–185.

Nersissian, A.M., Immoos, C., Hill, M.G., Hart, P.J., Williams, G., Herrmann, R.G., *et al.* (1998) Uclacyanins, stellacyanins, and plantacyanins are distinct subfamilies of phytocyanins: plant-specific mononuclear blue copper proteins. *Protein Sci* 7: 1915–1929.

Nishiuchi, T., Shinshi, H. and Suzuki, K. (2004) Rapid and transient activation of transcription of the ERF3 gene by wounding in tobacco leaves: Possible involvement of NtWRKYs and autorepression. *J Biol Chem* 279: 55355–55361.

O'Halloran, T. V. and Culotta, V.C. (2000) Metallochaperones, an intracellular shuttle service for metal ions. *J Biol Chem* 275: 25057–25060.

Ogawa, M. and Hanada, A. (2003) Gibberellin biosynthesis and response during *Arabidopsis* seed germination. *Plant Cell* 15: 1591–1604.

Oldenkamp, L. and Smilde, K.W. (1966) Copper deficiency in Douglas fir (*Pseudotsuga menziesii* (Mirb.) Franco). *Plant Soil* 25: 150–152.

Peña, M.M., Lee, J. and Thiele, D.J. (1999) A delicate balance: homeostatic control of copper uptake and distribution. *J Nutr* 129: 1251–1260.

Perea-García, A., Andrés-Bordería, A., Mayo De Andrés, S., Sanz, A., Davis, A.M., Davis, S.J., *et al.* (2016) Modulation of copper deficiency responses by diurnal and circadian rhythms in *Arabidopsis thaliana*. *J Exp Bot* 67: 391–403.

Perea-García, A., García-Molina, A., Andrés-Colás, N., Vera-Sirera, F., Pérez-Amador, M.A., Puig, S., *et al.* (2013) *Arabidopsis* copper transport protein COPT2 participates in the cross talk between iron deficiency responses and low-phosphate signaling. *Plant Physiol* 162: 180–94.

Pilon, M. (2016) The copper microRNAs. *New Phytol* 213: 1030–1035.

Pourcel, L., Routaboul, J.M., Kerhoas, L., Caboche, M., Lepiniec, L. and Debeaujon, I. (2005) Transparent testa10 encodes a laccase-like enzyme involved in oxidative polymerization of flavonoids in *Arabidopsis* seed coat. *Plant Cell* 17: 2966–2980.

Printz, B., Lutts, S., Hausman, J.-F. and Sergeant, K. (2016) Copper trafficking in plants and its implication on cell wall dynamics. *Front Plant Sci* 7: 601.

Puig, S. (2014) Function and regulation of the plant COPT family of high-affinity copper transport proteins. *Adv Bot* 2014: 1–9.

Puig, S., Andrés-Colás, N., García-Molina, A. and Peñarrubia, L. (2007) Copper and iron homeostasis in *Arabidopsis*: Responses to metal deficiencies, interactions and biotechnological applications. *Plant, Cell Environ* 30: 271–290.

Puig, S. and Thiele, D.J. (2002) Molecular mechanisms of copper uptake and distribution. *Curr Opin Chem Biol* 6: 171–180.

Rae, T.D., Schmidt, P.J., Pufahl, R.A., Culotta, V.C. and O'Halloran, T. V. (1999) Undetectable intracellular free copper: The requirement of a copper chaperone for superoxide
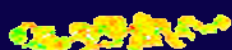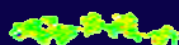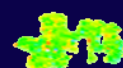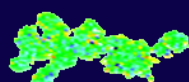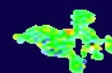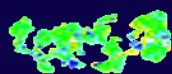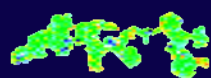
dismutase. *Science* 284: 805–808.

Ravet, K. and Pilon, M. (2013) Copper and iron homeostasis in plants: the challenges of oxidative stress. *Antioxid Redox Signal* 19: 919–32.

Ridge, P.G., Zhang, Y. and Gladyshev, V.N. (2008) Comparative genomic analyses of copper transporters and cuproproteomes reveal evolutionary dynamics of copper utilization and its link to oxygen. *PLoS One* 3: e1378.

Riva, S. (2006) Laccases: blue enzymes for green chemistry. *Trends Biotechnol* 24: 219–226.

Robinson, N.J. and Winge, D.R. (2010) Copper metallochaperones. *Annu Rev Biochem* 79: 537–562.

Rodrigo-Moreno, A., Andrés-Colás, N., Poschenrieder, C., Gunsé, B., Peñarrubia, L. and Shabala, S. (2013) Calcium- and potassium-permeable plasma membrane transporters are activated by copper in *Arabidopsis* root tips: Linking copper transport with cytosolic hydroxyl radical production. *Plant, Cell Environ* 36: 844–855.

Rodríguez-Serrano, M., Romero-Puertas, M.C., Pazmiño, D.M., Testillano, P.S., Risueño, M.C., Río, L.A. del, *et al.* (2009) Cellular response of pea plants to cadmium toxicity: cross talk between reactive oxygen species, nitric oxide, and calcium. *Plant Physiol* 150: 229–243.

Rodriguez, F.I., Esch, J.J., Hall, A.E., Binder, B.M., Schaller, G.E. and Bleecker, A.B. (1999) A copper cofactor for the ethylene receptor ETR1 from *Arabidopsis*. *Science* 283: 996–998.

Romero, P., Rodrigo, M.J., Alférez, F., Ballester, A.R., González-Candelas, L., Zacarías, L., *et al.* (2012) Unravelling molecular responses to moderate dehydration in harvested fruit of sweet orange (*Citrus sinensis* L. Osbeck) using a fruit-specific ABA-deficient mutant. *J Exp Bot* 63: 2753–2767.

Roschzttardtz, H., Conéjéro, G., Curie, C. and Mari, S. (2009) Identification of the endodermal vacuole as the iron storage compartment in the *Arabidopsis* embryo. *Plant Physiol* 151: 1329–38.

Rubio, M.I., Escrig, I., Martínez-Cortina, C., López-Benet, F.J. and Sanz, A. (1994) Cadmium and nickel accumulation in rice plants. Effects on mineral nutrition and possible interactions of abscisic and gibberellic acids. *Plant Growth Regul* 14: 151–157.

Rubio, V., Bustos, R., Irigoyen, M.L., Cardona-López, X., Rojas-Triana, M. and Paz-Ares, J. (2009) Plant hormones and nutrient signaling. *Plant Mol Biol* 69: 361–373.

Ryan, B.M., Kirby, J.K., Degryse, F., Harris, H., Mclaughlin, M.J. and Scheiderich, K. (2013) Copper speciation and isotopic fractionation in plants: uptake and translocation mechanisms. *New Phytol* 199: 367–378.

Saez, A., Robert, N., Maktabi, M.H., Schroeder, J.I., Serrano, R. and Rodríguez, P.L. (2006) Enhancement of abscisic acid sensitivity and reduction of water consumption in *Arabidopsis* by combined inactivation of the protein phosphatases type 2C ABI1 and HAB1. *Plant Physiol* 141: 1389–99.

Sancenón, V., Puig, S., Mira, H., Thiele, D.J. and Peñarrubia, L. (2003) Identification of a copper

transporter family in *Arabidopsis thaliana*. *Plant Mol Biol* 51: 577–587.

Sanchez, A., Shin, J. and Davis, S.J. (2011) Abiotic stress and the plant circadian clock. *Plant Signal Behav* 6: 223–231.

Sandalio, L.M., Rodríguez-Serrano, M., del Rio, L.A. and Romero-Puertas, M. (2009) Reactive oxygen species and signaling in cadmium toxicity pp. 175–189 Springer, London (UK).

Santi, S. and Schmidt, W. (2009) Dissecting iron deficiency-induced proton extrusion in *Arabidopsis* roots. *New Phytol* 183: 1072–1084.

Sanz, A., Llamas, A. and Ullrich, C.I. (2009) Distinctive phytotoxic effects of Cd and Ni on membrane functionality. *Plant Signal Behav* 4: 980–982.

Schellingen, K., Van Der Straeten, D., Vandenbussche, F., Prinsen, E., Remans, T., Vangronsveld, J., *et al.* (2014) Cadmium-induced ethylene production and responses in *Arabidopsis thaliana* rely on ACS2 and ACS6 gene expression. *BMC Plant Biol* 14: 1–14.

Schlagnhaufer, C.D., Arteca, R.N. and Pell, E.J. (1997) Sequential expression of two 1-aminocyclopropane-1-carboxylate synthase genes in response to biotic and abiotic stresses in potato (*Solanum tuberosum* L.) leaves. *Plant Mol Biol* 35: 683–688.

Schwartz, S.H., Léon-Kloosterziel, K.M., Koornneef, M. and Zeevaart, J.A. (1997) Biochemical characterization of the *aba2* and *aba3* mutants in *Arabidopsis thaliana*. *Plant Physiol* 114: 161–6.

Schwarz, G. and Mendel, R.R. (2006) Molybdenum cofactor biosynthesis and molybdenum enzymes. *Annu Rev Plant Biol* 57: 623–647.

Shang, Y., Yan, L., Liu, Z.-Q., Cao, Z., Mei, C., Xin, Q., *et al.* (2010) The Mg-chelatase H subunit of *Arabidopsis* antagonizes a group of WRKY transcription repressors to relieve ABA-responsive genes of inhibition. *Plant Cell* 22: 1909–1935.

Shi, W.G., Li, H., Liu, T.X., Polle, A., Peng, C.H. and Luo, Z. Bin (2015) Exogenous abscisic acid alleviates zinc uptake and accumulation in *Populus×canescens* exposed to excess zinc. *Plant, Cell Environ* 38: 207–223.

Shikanai, T. and Fujii, S. (2013) Function of PPR proteins in plastid gene expression. *RNA Biol* 10: 1446–1456.

Simpson, S.D., Nakashima, K., Narusaka, Y., Seki, M., Shinozaki, K. and Yamaguchi-Shinozaki, K. (2003) Two different novel cis-acting elements of erd1, a clpA homologous *Arabidopsis* gene function in induction by dehydration stress and dark-induced senescence. *Plant J* 33: 259–270.

Sivitz, A.B., Hermand, V., Curie, C. and Vert, G. (2012) *Arabidopsis* bHLH100 and bHLH101 control iron homeostasis via a FIT-independent pathway. *PLoS One* 7.

Smeets, K., Opdenakker, K., Remans, T., Forzani, C., Hirt, H., Vangronsveld, J., *et al.* (2013) The role of the kinase OXI1 in cadmium- and copper-induced molecular responses in *Arabidopsis thaliana*. *Plant, Cell Environ* 36: 1228–1238.

Smeets, K., Opdenakker, K., Remans, T., Van Sanden, S., Van Belleghem, F., Semane, B., *et al.* (2009) Oxidative stress-related responses at transcriptional and enzymatic levels after exposure to Cd or Cu in a multipollution context. *J Plant Physiol* 166: 1982–1992.

Sommer, F., Kropat, J., Malasarn, D., Grossoehme, N.E., Chen, X., Giedroc, D.P., *et al.* (2010) The CRR1 nutritional copper sensor in *Chlamydomonas* contains two distinct metal-responsive domains. *Plant Cell* 22: 4098–4113.

Stacey, M.G., Patel, A., McClain, W.E., Mathieu, M., Remley, M., Rogers, E.E., *et al.* (2008) The *Arabidopsis* AtOPT3 protein functions in metal homeostasis and movement of iron to developing seeds. *Plant Physiol* 146: 589–601.

Tapken, W., Kim, J., Nishimura, K., van Wijk, K.J. and Pilon, M. (2015) The Clp protease system is required for copper ion-dependent turnover of the PAA2/HMA8 copper transporter in chloroplasts. *New Phytol* 205: 511–517.

Tejada-Jiménez, M., Chamizo-Ampudia, A., Galván, A., Fernández, E. and Llamas, Á. (2013) Molybdenum metabolism in plants. *Metallomics* 5: 1191–1203.

Thompson, J.S., Harlow, R.L. and Whitney, J.F. (1983) Copper (I) - olefin complexes. Support for the proposed role of copper in the ethylene effect in plants. *J Am Chem Soc* 105: 3522–3527.

Thordal-Christensen, H., Zhang, Z., Wei, Y. and Collinge, D.B. (1997) Subcellular localization of H2O2 in plants. H2O2 accumulation in papillae and hypersensitive response during the barley-powdery mildew interaction. *Plant J* 11: 1187–1194.

Tsyganov, V.E., Belimov, A.A., Borisov, A.Y., Safronova, V.I., Georgi, M., Dietz, K.J., *et al.* (2007) A chemically induced new pea (*Pisum sativum*) mutant SGECdt with increased tolerance to, and accumulation of, cadmium. *Ann Bot* 99: 227–237.

Umezawa, T., Sugiyama, N., Mizoguchi, M., Hayashi, S., Myouga, F., Yamaguchi-Shinozaki, K., *et al.* (2009) Type 2C protein phosphatases directly regulate abscisic acid-activated protein kinases in *Arabidopsis*. *Proc Natl Acad Sci U S A* 106: 17588–17593.

Uraguchi, S., Mori, S., Kuramata, M., Kawasaki, A., Arao, T. and Ishikawa, S. (2009) Root-to-shoot Cd translocation via the xylem is the major process determining shoot and grain cadmium accumulation in rice. *J Exp Bot* 60: 2677–2688.

Valentovičová, K., Mistrík, I., Zelinová, V. and Tamás, L. (2012) How cobalt facilitates cadmium- and ethylene precursor-induced growth inhibition and radial cell expansion in barley root tips. *Cent Eur J Biol* 7: 551–558.

Valko, M., Morris, H. and Cronin, M.T.D. (2005) Metals, toxicity and oxidative stress. *Curr Top Med Chem* 12: 1161–1208.

Vasconcelos, M.W., Gruissem, W. and Bhullar, N.K. (2017) Iron biofortification in the 21st century: setting realistic targets, overcoming obstacles, and new strategies for healthy nutrition. *Curr Opin Biotechnol* 44: 8–15.

Vert, G., Briat, J.-F. and Curie, C. (2003) Dual regulation of the Arabidopsis high-affinity root iron

uptake system by local and long-distance signals. *Plant Physiol* 132: 796–804.

Vest, K.E., Wang, J., Gammon, M.G., Maynard, M.K., White, O.L., Cobine, J.A., *et al.* (2016) Overlap of copper and iron uptake systems in mitochondria in *Saccharomyces cerevisiae*. *Open Biol* 6: 150223.

Vigani, G. and Briat, J.-F. (2016) Impairment of respiratory chain under nutrient deficiency in plants: does it play a role in the regulation of iron and sulfur responsive genes? *Front Plant Sci* 6: 1185.

Vysotskaya, L.B., Korobova, A. V. and Kudoyarova, G.R. (2008) Abscisic acid accumulation in the roots of nutrient-limited plants: Its impact on the differential growth of roots and shoots. *J Plant Physiol* 165: 1274–1279.

Waadt, R., Hitomi, K., Nishimura, N., Hitomi, C., Adams, S.R., Getzoff, E.D., *et al.* (2014) FRET-based reporters for the direct visualization of abscisic acid concentration changes and distribution in Arabidopsis. *Elife* 1–28.

Wang, H.Y., Klatte, M., Jakoby, M., Bäumlein, H., Weisshaar, B. and Bauer, P. (2007) Iron deficiency-mediated stress regulation of four subgroup Ib BHLH genes in *Arabidopsis thaliana*. *Planta* 226: 897–908.

Wang, K.L., Li, H. and Ecker, J.R. (2002) Ethylene biosynthesis and signaling networks. *Plant Cell* 14: 131–152.

Wasilewska, A., Vlad, F., Sirichandra, C., Redko, Y., Jammes, F., Valon, C., *et al.* (2008) An update on abscisic acid signaling in plants and more... *Mol Plant* 1: 198–217.

Wastl, J., Bendall, D.S. and Howe, C.J. (2002) Higher plants contain a modified cytochrome c6. *Trends Plant Sci* 7: 244–245.

Waters, B.M., McInturf, S.A. and Stein, R.J. (2012) Rosette iron deficiency transcript and microRNA profiling reveals links between copper and iron homeostasis in *Arabidopsis thaliana*. *J Exp Bot* 63: 5903–5918.

Weigel, M., Varotto, C., Pesaresi, P., Finazzi, G., Rappaport, F., Salamini, F., *et al.* (2003) Plastocyanin is indispensable for photosynthetic electron flow in *Arabidopsis thaliana*. *J Biol Chem* 278: 31286–31289.

Weiss, D. and Ori, N. (2007) Mechanisms of cross talk between gibberellin and other hormones. *Plant Physiol* 144: 1240–1246.

Weng, J.-K. and Chapple, C. (2010) The origin and evolution of lignin biosynthesis. *New Phytol* 187: 273–285.

Wilkinson, S. and Davies, W.J. (2010) Drought, ozone, ABA and ethylene: new insights from cell to plant to community. *Plant, Cell Environ* 33: 510–525.

Wintz, H., Fox, T., Wu, Y.Y., Feng, V., Chen, W., Chang, H.S., *et al.* (2003) Expression profiles of *Arabidopsis thaliana* in mineral deficiencies reveal novel transporters involved in metal homeostasis. *J Biol Chem* 278: 47644–47653.

Wu, Y., Zhang, D., Chu, J.Y., Boyle, P., Wang, Y., Brindle, I.D., *et al.* (2012) The Arabidopsis NPR1 protein is a receptor for the plant defense hormone salicylic acid. *Cell Rep* 1: 639–647.

Xie, Z., Zhang, Z.-L., Zou, X., JIe, H., Ruas, P., Thompson, D., *et al.* (2005) Annotations and functional analyses of the rice WRKY gene superfamily reveal positive and negative regulators of abscisic acid signaling in aleruone cells. *Plant Physiol* 137: 176–189.

Yamaguchi, H., Fukuoka, H., Arao, T., Ohyama, A., Nunome, T., Miyatake, K., *et al.* (2010) Gene expression analysis in cadmium-stressed roots of a low cadmium-accumulating solanaceous plant, *Solanum torvum*. *J Exp Bot* 61: 423–437.

Yamasaki, H., Abdel-Ghany, S.E., Cohu, C.M., Kobayashi, Y., Shikanai, T. and Pilon, M. (2007) Regulation of copper homeostasis by micro-RNA in *Arabidopsis*. *J Biol Chem* 282: 16369–16378.

Yamasaki, H., Hayashi, M., Fukazawa, M., Kobayashi, Y. and Shikanai, T. (2009) SQUAMOSA promoter binding protein-like7 is a central regulator for copper homeostasis in *Arabidopsis*. *Plant Cell* 21: 347–361.

Yan, S. and Dong, X. (2014) Perception of the plant inmmune signal salicylic acid. *Curr Opin Plant Biol* 0: 64–68.

Yang, S.F. and Hoffman, N.E. (1984) Ethylene biosynthesis and its regulation in higher plants. *Plant Physiol* 35: 155–189.

Ye, N., Li, H., Zhu, G., Liu, Y., Liu, R., Xu, W., *et al.* (2014) Copper suppresses abscisic acid catabolism and catalase activity, and inhibits seed germination of rice. *Plant Cell Physiol* 55: 2008–2016.

Yruela, I. (2013) Transition metals in plant photosynthesis. *Metallomics* 5: 1090–109.

Yuan, H.M., Xu, H.H., Liu, W.C. and Lu, Y.T. (2013) Copper regulates primary root elongation through PIN1-mediated auxin redistribution. *Plant Cell Physiol* 54: 766–778.

Yuan, Y., Wu, H., Wang, N., Li, J., Zhao, W., Du, J., *et al.* (2008) FIT interacts with AtbHLH38 and AtbHLH39 in regulating iron uptake gene expression for iron homeostasis in *Arabidopsis*. *Cell Res* 18: 385–397.

Zaman, M., Kurepin, L. V., Catto, W. and Pharis, R.P. (2015) Enhancing crop yield with the use of N-based fertilizers co-applied with plant hormones or growth regulators. *J Sci Food Agric* 95: 1777–1785.

Zhang, H., Zhao, X., Li, J., Cai, H., Deng, X.W. and Li, L. (2014) MicroRNA408 is critical for the HY5-SPL7 gene network that mediates the coordinated response to light and copper. *Plant Cell* 26: 4933–4953.

Zhang, Y. and Gladyshev, V.N. (2010) General trends in trace element utilization revealed by comparative genomic analyses of Co, Cu, Mo, Ni, and Se. *J Biol Chem* 285: 3393–3405.